

Upper Rhine Graben: Quantitative aspects of
rifting and syn-rift sedimentation
with focus on
the Palaeogene series in the southern part

Inauguraldissertation

zur
Erlangung der Würde eines Doktors der Philosophie
vorgelegt
der Philosophisch-Naturwissenschaftlichen Fakultät
der Universität Basel¹

von
Sebastian Hinsken

aus
Deutschland

Basel, Mai 2010

¹Originaldokument gespeichert auf dem Dokumentenserver der Universität Basel edoc.unibas.ch. Dieses Werk ist unter dem Vertrag "Creative Commons Namensnennung-Keine kommerzielle Nutzung-Keine Bearbeitung 2.5 Schweiz" lizenziert. Die vollständige Lizenz kann unter creativecommons.org/licenses/by-nc-nd/2.5/ch eingesehen werden.

Genehmigt von der Philosophisch-Naturwissenschaftlichen Fakultät auf Antrag
von:
Prof. Dr. Andreas Wetzel
(Institut für Geologie und Paläontologie, Universität Basel)

Prof. Dr. Andreas Wetzel
(Fakultätsverantwortlicher)
Basel, den 24. Juni 2008

Prof. Dr. Hans-Peter Hauri
(Dekan der Philosophisch-Naturwissenschaftlichen Fakultät)

Creative Commons Namensnennung-Keine kommerzielle Nutzung-Keine Bearbeitung 2.5 Schweiz

Sie dürfen:

das Werk vervielfältigen, verbreiten und öffentlich zugänglich machen Zu den folgenden Bedingungen:

Namensnennung. Sie müssen den Namen des Autors/Rechteinhabers in der von ihm festgelegten Weise nennen (wodurch aber nicht der Eindruck entstehen darf, Sie oder die Nutzung des Werkes durch Sie würden entlohnt).

Keine kommerzielle Nutzung. Dieses Werk darf nicht für kommerzielle Zwecke verwendet werden.

Keine Bearbeitung. Dieses Werk darf nicht bearbeitet oder in anderer Weise verändert werden.

- Im Falle einer Verbreitung müssen Sie anderen die Lizenzbedingungen, unter welche dieses Werk fällt, mitteilen. Am Einfachsten ist es, einen Link auf diese Seite einzubinden.
- Jede der vorgenannten Bedingungen kann aufgehoben werden, sofern Sie die Einwilligung des Rechteinhabers dazu erhalten.
- Diese Lizenz lässt die Urheberpersönlichkeitsrechte unberührt

Quelle: <http://creativecommons.org/licenses/by-nc-nd/2.5/ch/> Datum: 3.4.2009

Die gesetzlichen Schranken des Urheberrechts bleiben hiervon unberührt. Die Commons Deed ist eine Zusammenfassung des Lizenzvertrags in allgemeinverständlicher Sprache:

<http://creativecommons.org/licenses/by-nc-nd/2.5/ch/legalcode.de>

Haftungsausschluss: Die Commons Deed ist kein Lizenzvertrag. Sie ist lediglich ein Referenztext, der den zugrundeliegenden Lizenzvertrag übersichtlich und in allgemeinverständlicher Sprache wiedergibt. Die Deed selbst entfaltet keine juristische Wirkung und erscheint im eigentlichen Lizenzvertrag nicht. Creative Commons ist keine Rechtsanwalts-gesellschaft und leistet keine Rechtsberatung. Die Weitergabe und Verlinkung des Commons Deeds führt zu keinem Mandatsverhältnis.

Danksagungen

Dank gilt neben Kathrin meiner Familie und meinen Freunden, allen die in irgendeiner Form an dieser Arbeit beteiligt waren oder mich die Jahre in Basel begleitet haben.

Liebe Kolleginnen und Kollegen, habt vielen Dank !!! - Es war eine wunderbare Zeit und ich habe Euch alle als liebenswürdige Menschen kennen und schätzen gelernt.

Namentlich hervorheben möchte ich meinen langjährigen Betreuer Prof. Dr. Andreas Wetzel, und Prof. Dr. Peter Ziegler, unseren Ehrenvorsitzenden des Eucor Urgent Projektes, die mir stets als kompetente und hilfsbereite Ansprechpartner zur Seite standen. Ebenso unterstützten mich Prof. Dr. Daniel Bernoulli, Dr. Pierre Dèzes und Prof. Dr. Stefan Schmid. Ausserdem möchte ich meinen Ko-Referenten und Mitautoren für Ihren Einsatz und Ihre Kooperation danken: Dr. Stefan Schmalholz, PD Dr. Christian A. Meyer, Dr. Kamil M. Ustaszewski, Prof. Dr. Jean-Pierre Berger Andrea Storni und Dr. Torsten Wappler. Schliesslich noch ein Dankeschön an meine Kollegen Herfried Madritsch, Marielle Faeffel, Stephane Kock und meinen Büronachbar Rüdiger Kilian für die gute Zeit. Ebenso ein Dank an alle weiteren und ehemaligen PhD-Kollegen, sowie an die Belegschaft des GPI und MPI.

Contents

1	Introduction	7
1.1	Research objectives and motivation	7
1.2	Overview	8
1.3	Previous studies and general approach	10
1.3.1	Previous studies	11
1.4	Thesis organisation	13
2	Palaeoecology and depositional environment of Early Oligocene insect-bearing laminites (Rupelian; Zone Fossilifère, Upper Rhine Graben; Altkirch; France)	15
2.1	Abstract	16
2.2	Introduction	17
2.3	Geological context	17
2.3.1	Studied section	19
2.4	Materials and Methods	20
2.5	Sedimentology	20
2.6	Sedimentological Interpretation	23
2.7	Fossil Record	24
2.7.1	Aquatic Fauna	24
2.7.2	Semiaquatic insects	26
2.7.3	Terrestrial Fauna	28
2.7.4	Micro Fossils	30
2.8	Palaeoecology	30
2.8.1	Modern counterparts of discovered taxa	30
2.8.2	Population dynamics and community palaeoecology	33
2.8.3	Insect taphonomy	35
2.8.4	Synopsis	39
2.9	Discussion	39
2.10	Conclusions	42
3	A fossil sawfly of the genus <i>Athalia</i> (Hymenoptera: Tenthredinidae) from the Eocene-Oligocene boundary of Altkirch, France	44
3.1	Abstract	45
3.2	Introduction	46

3.3	Geographical and geological setting	47
3.3.1	Geological framework	47
3.3.2	Age constraints	48
3.3.3	Sample location	48
3.4	Material	49
3.5	Systematic palaeontology	49
3.6	Discussion of taxonomy	53
3.7	Palaeoenvironmental implications	55
4	Graben width controlling syn-rift sedimentation: The Palaeo- gene southern Upper Rhine Graben as an example	58
4.1	Abstract	59
4.2	Introduction	60
4.3	Geological context	61
4.3.1	Study area	61
4.3.2	Graben evolution	65
4.4	Syn-rift sedimentation	69
4.4.1	Lithofacies associations	70
4.4.2	Basin-fill architecture	72
4.4.3	Palaeogeography	77
4.4.4	Flank uplift	79
4.4.5	Sediment source	79
4.4.6	Sediment partitioning and A/S-ratio	80
4.4.7	Age constraints	81
4.4.8	Sedimentary dynamics and base-level fluctuations	82
4.4.9	Tectonic implications	83
4.5	Formation of the southern Upper Rhine Graben	84
4.5.1	Basin geometry	84
4.5.2	Extension, graben width and subsidence	84
4.5.3	Extension in the URG	86
4.5.4	Rift basin formation	87
4.6	Discussion and conclusions	91
4.7	Acknowledgements:	92
5	Thermo-Tectono-Stratigraphic Forward Modeling of the Upper Rhine Graben in reference to geometrical balancing: brittle crustal extension on a high viscous mantle	93
5.1	Abstract	94
5.2	Introduction	95
5.3	Evolution of the Upper Rhine Graben	97
5.3.1	Pre-rift evolution	97
5.3.2	Syn-rift evolution	98
5.3.3	Basement configuration and deep structures	100
5.4	Material and Methods	103
5.4.1	Theory	103
5.4.2	Analyzed cross-sections	107

5.4.3	Modeling Approach and TTSF-Modeling input parameters	109
5.4.4	Set up	110
5.5	Results	110
5.6	Interpretation and Discussion	115
5.6.1	Position and meaning of necking level	115
5.6.2	Time-extension paths	118
5.7	Conclusions	119
5.8	Acknowledgements	120
6	Elastic plate bending and shoulder uplift in the (southern) Upper Rhine Graben: new evidence from the sedimentary record and flexural Isostasy modeling	121
6.1	Abstract	122
6.2	Introduction	123
6.3	Geologic evidence for elastic plate bending in the URG and North Alpine Foreland	126
6.3.1	Geological context	126
6.3.2	Reconstruction of graben shoulder uplift in the southern URG	131
6.3.3	Discussion and interpretation of Palaeogene uplift and subsidence	133
6.4	Numerical modeling of flexural rock uplift	137
6.4.1	Material and Methods	139
6.4.2	Set up	140
6.4.3	modelling approach	142
6.4.4	Results	142
6.4.5	Discussion and interpretation of modeling results and the Neogene rise of VBFA	143
6.5	Final Conclusions	147
7	Summary and Conclusions: UPPER RHINE GRABEN; new evidences from the sedimentary record and numerical modeling	148
7.1	Palaeogene syn-rift Sedimentation in the southern URG	148
7.2	Extension and basin subsidence	152
7.3	Necking level and lithospheric strength	153
7.4	Rift-shoulder uplift and elastic plate bending	154

Chapter 1

Introduction

1.1 Research objectives and motivation

This Phd-thesis is a contribution to the Eucor Urgent Project, that was funded to investigate the Upper Rhine Graben Evolution and Neotectonics. It is the result of a self-defined research project that arose from the conclusions of my diploma thesis (Hinsken, 2003). The thesis follows the concept of generating new insights into the evolution of the Upper Rhine Graben by investigating its sedimentary record.

During the diploma thesis Palaeogene syn-rift sediments were studied along a transect from the graben margin to the graben center. Thereby the marginal facies (inter fingering conglomerate fans) were studied in context of the diploma mapping project. In a further step proximal to distal facies architecture was studied in the few existing outcrops and in the basin center sedimentology and palaeoecology of these deposits were investigated.

It was concluded that there was a strong relationships between tectonics and sedimentation and therefore that tectonic signals are preserved in the sedimentary record.

1. differential syn-tectonic block movements led to rapid facies and thickness changes.
2. uplifting graben shoulders protected the graben itself from external clastic supply and resulted in under filling and re-sedimentation of graben shoulder derived material within the sedimentary basin.
3. depositional environments were therefore restricted to enclosed which was also reflected in the preserved fauna.

Although the biotic conditions and depositional environments are strongly influenced by the exogene dynamics, it appeared possible that further studying of the Palaeogene syn-rift deposits might allow separation of endogene and exogene signals encrypted in the sedimentary record from each other and therefore to

generate new evidence about the tectonic processes that resulted in graben formation. In this sense and with respect to the focus of the Eucor Urgent Project on recent crustal deformation the current thesis can be most simply understood as an inversion of the uniformitarianism principle saying that the present is the key to the past: 'The past is the key to the present'.

1.2 Overview

The Upper Rhine Graben forms a major rift basin within Central Europe (Fig. 1.1). It developed during the Cenozoic contemporaneous with the Alpine orogeny and is part of a number of extensional structures, referred to as Cenozoic European Rift System (ECRIS) Ziegler (1992) The Cenozoic European Rift System (CERS) follows a pre-rift thinned weak zone within the European lithosphere between the Mediterranean and the North Sea (Fig.1, Dèzes et al., 2004). Rift basin evolution involved the reactivation of major crustal discontinuities (inherited structures) that already date back to the Palaeozoic such as the Rhenish Lineament (e.g. Wetzel et al., 2003). The temporal and spatial relation with the Alps, in particular the Cenozoic orogeny of the Western Alps (e.g. Schmid et al., 2004) and the development of the CERIS suggest a causal link between both processes and indeed most authors regard the development of ECRIS related to the Alpine orogeny (e.g. Illies and Greiner, 1978; Ziegler, 1992; Merle, 2001; Rotstein et al., 2005), however a few authors (e.g. Neugebauer, 1978) suggested active rifting to account for the development of the URG. With respect to the law of cause and effect, rifting is therefore regarded to be Alpine induced passive rifting (e.g. Illies and Greiner, 1978; Ziegler, 1992; Schumacher, 2002; Michon and Merle, 2001; Merle, 2001).

Development of such passive rifts that are found in many forelands go hand in hand with the collision of continental plates and the subduction of oceanic lithosphere. Active rifts in contrast initiate continental break up and the creation of oceans. This spectacle of dying and reincarnating oceans forming the backbone of the plate tectonics theory is expressed in the Wilson Cycle 1.2.

Evolution of the URG During the Late Palaeozoic, The Variscan orogeny led to continental collision between Gondwana and Laurasia and several derivative terranes. Decay of this orogen at the end of the Palaeozoic, due to erosion and tans-tensional rifting that was associated with magmatism, extensional basin formation resulted in crustal re-equilibration and formation of the basement as it is today exposed on the graben shoulders of the URG.

Subsequent thermal subsidence led to the deposition of a 'pre-rift sequence' with about 1km thickness.

A new Wilson-Cycle between Europe and Africa led to formation of the Neothetys-ocean followed by the evolution of the (Western-)Alps (Cenozoic; e.g. Schmid et al., 2004). Continental collision in the Middle Eocene initiated the evolution of the URG (chapter 5; Dèzes et al., 2005).

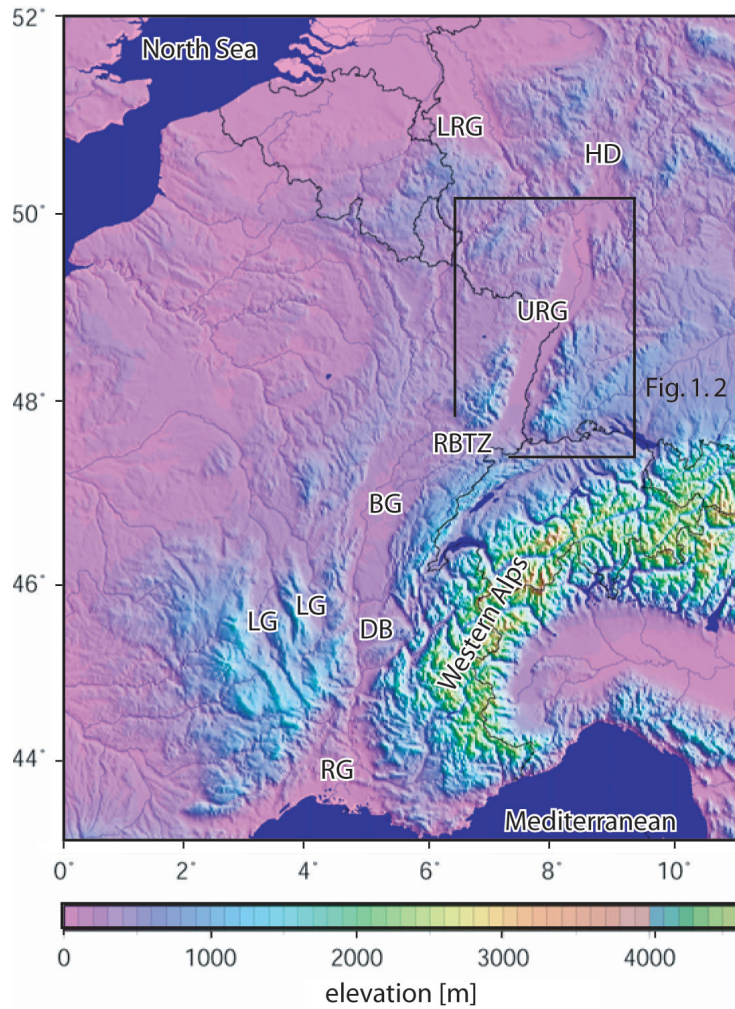


Figure 1.1: Digital elevation Map on western Central Europe showing the alignment of the rift basins of the CERS and their spatial relation to the Western Alps. LRG Lower Rhine Graben, HD Hessian Depression, URG Upper Rhine Graben, RBTZ Rhine Bresse Transfer Zone, BG Bresse Graben, DB Dauphiné Basin, LG Limagne Grabens, RG Rhone Grabens

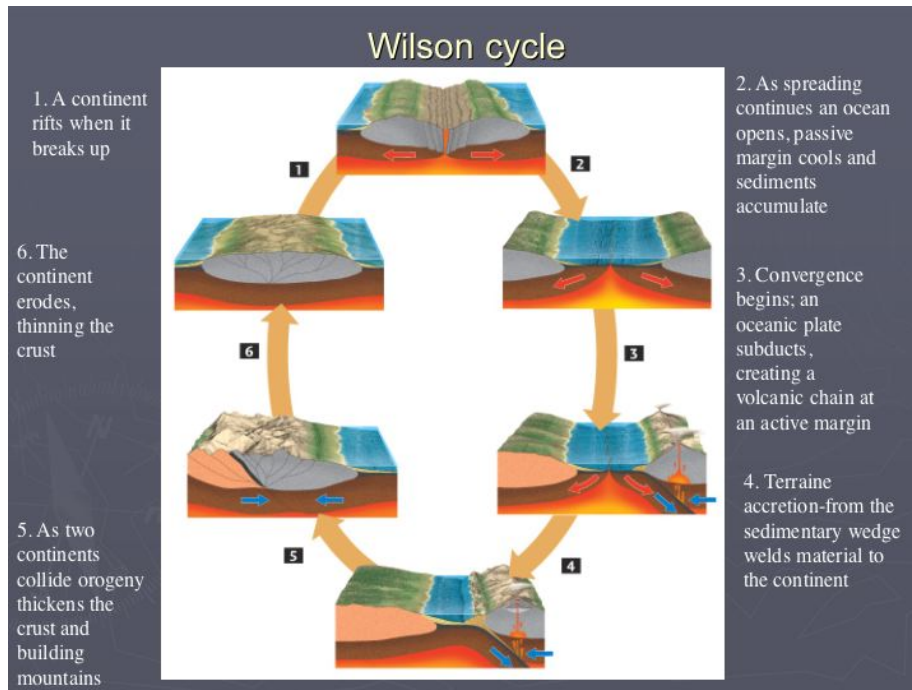


Figure 1.2: The Wilson-Cycle illustrating the basic concept of Plate Tectonics.(from: www.gly.fsu.edu)

The URG forms an symmetrical graben with elevated graben shoulders. vertical offset between Graben and shoulders amounts to more than 4 km (Fig.1.3). The southern part of the URG is much higher elevated than the northern part. Uplift that occurred during the Neogene caused uplift and erosion. Hence Early in the southernmost URG and along the basin margins early stage syn-rift deposits became exposed and can be investigated in the field.

1.3 Previous studies and general approach

For the Upper Rhine Graben various mechanisms of graben formation as well as kinematics and timing of rifting have been proposed so far and are still under discussion (e.g. Michon and Merle, 2005; Dèzes et al., 2005). The interpretations range from orthogonal to oblique rifting (e.g. Illies, 1967; Behrmann et al., 2003), simple shear and pure shear rifting (e.g. Brun et al., 1992; Illies, 1967).

Basically graben formation is the response of the continental lithosphere to extension leading to localized stretching and thinning (e.g. Allen and Allen, 2005). Thinning of the crust leads to tectonic subsidence, that may be followed by thermal subsidence. Isostatic readjustment in response to resulting changes lithospheric static loading may result in additional regional uplift or subsidence

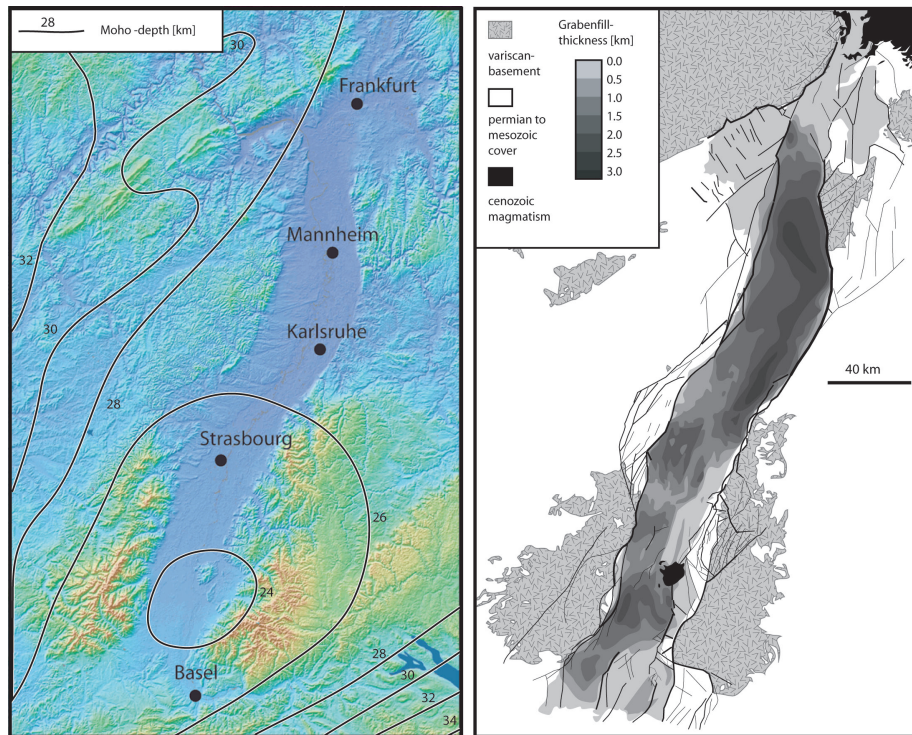


Figure 1.3: overview of the URG: Left DEM image superimposed with iso-hypes of Moho-topography, right simplified geological map.

(e.g. Wernicke, 1985; Kooi and Cloetingh, 1992). Consequently the basin will subside below the global base-level and accommodation space for syn-rift sediments will be generated. In contrast it is very likely that rift shoulders will experience uplift and become subsequently eroded. Rift shoulders, thus, act as areas of sedimentary supply but also form a barrier against external input of sediments and water. Understanding a basin as a geodynamic entity requires therefore an appreciation of the coupling between mantle, lithosphere, oceans and atmosphere (e.g. Allen and Allen, 2005).

Nonetheless most interpretations or models of rift basin formation, however, rely on deciphering the sedimentary record of the syn-rift deposits. A detailed study focusing on the syn-rift sediments, thus, can provide important hints about subsidence and uplift in space and time and therefore contributes to quantitative data about rifting.

1.3.1 Previous studies

For the Upper Rhine Graben, Schumacher (2002) as well as Michon and Merle (2000) have stated, the evolution and distribution of depot-centers to reflect

the kinematic evolution of the rift. Nevertheless both studies come to different results; five different tectonic stages, including three Palaeogene deformation phases have been distinguished by Schumacher (2002) in reference to 'Palaeo-stress' data (Bergerat, 1987), whereas Michon and Merle (2005) conclude a constant ESE-WNW extension direction during the Palaeogene according to results from analogue modeling.

A detailed basin analysis, however, addresses not only the thicknesses of sedimentary units, it also integrates facies and its distribution, diagenesis and thermo-chronological data into a model (Allen and Allen, 2005).

For instance in the Upper Rhine Graben 'coastal conglomerates' Kessler (1909) of the Palaeogene Salt Formation (*Formation Salifere, Salzfolge*) that occur along the graben margins represent alluvial fan delta deposits that formed in response to rift-shoulder uplift (Düringer, 1988) and therefore they are highly suggestive for syn-tectonic deposition (Schäfer, 2005). In addition the complex facies pattern of the Salt Formation documents syn-depositional tectonic movements, deposition in relation to growth faults and tilted blocks was recently described by Derer et al. (2003) for contemporaneous deposits from the northern URG (see also 1.1). Next to exposure in the southern and proximal parts of the basin, mining for Potassium salts (MDPA), the search for Petroleum and deep heat mining have led to a large data sets about the stratigraphy in the southernmost part of the URG.

Therefore, the Salt Formation in the southern Upper Rhine Graben represents an ideal area to study the interrelations of sedimentation and tectonics. For this purpose, the concept of genetic stratigraphy (e.g. Cross and Lessenger, 1998) was chosen as a principal method, because it relates aspects of sedimentation, like sedimentary supply, accommodation space, base-level and sediment volume partitioning quantitatively to each other. Before applying the concepts of genetic stratigraphy depositional environments and palaeo-geography need to be understood to a certain extend.

A further approach to understand basin evolution is numerical modeling. It helps to quantify and to test concepts that have been developed during basin analysis. It could be seen as a final step in basin analysis when qualitative formulated models get quantified. However there are different approaches and numerical basin modeling can result in new aspects that will require further Basin analysis. One way of numerical modeling ties to involves all related variables and processes and aims to reproduce the real world as accurate as possible, however in many cases when to little is known a 'simplistic' approach concentrating on a single aspect and a strongly simplified model and tries to evaluate its impact on the real world.

These general concepts forms the backbone of the present thesis, consisting of seven Chapters.

1.4 Thesis organisation

This cumulative PhD-Thesis consists of five research chapters, next to a final conclusion (Chapter 7) and this introduction (**Chapter 1**). Two Chapters have been published in peer-reviewed International Journals. The remaining three are supposed to be published with or without slightly modifications. Chapter two and three encompass results from the precedent diploma study that were suitable for publication. However as some results were published before the conclusions may have been slightly modified

Chapter 2 focuses on depositional environments and palaeogeography of fossiliferous Early Oligocene laminites (Salt Formation) in the southern Upper Rhine Graben. An sedimentological-palaeontological investigation was done during the authors Master thesis in the Rebberg quarry of Altkirch - the interpretation of the data was finalized and the manuscript was written in context of this PhD-thesis. Majority of work was done by S. Hinsken. Micro-palaeontology and Palaeo-botanics were contributed by A. Storni and J.-P. Berger (University of Fribourg). Elaboration of the Manuscript was done in co-operation with the Co-Authors. The investigation is supposed to be published in *Palaios*.

Chapter 3 is a palaeontological study on two fossil sawfly specimen discovered in the Rebberg quarry of Altkirch that was performed in a co-authorship with Dr. T. Wappler (Bonn). Discovery of the fossils was done by J.J. Brocks and the S.Hinsken. Taxonomy was done by T. Wappler. Description of Geology was by S. Hinsken. The work was published in the *C.R.Palevol* of the Academie des Sciences, Paris, in 2005.

Chapter 4 investigates 3D facies geometries and spatio-temporary subsidence patterns of the Eo-Oligocene Salt Formation in the southern URG by applying the concepts of genetic stratigraphy. The stratigraphic subdivision was refined and a new 'tectonic' rift basin model was proposed according to the results from the sedimentary study. The sedimentological part was done S. Hinsken. The tectonic part was supported by K. Ustaszewski, who provided next to mental and written contribution a geological cross-section and line length extension measurements. The Article was published in the *International Journal of Earth Sciences* in 2007.

Chapter 5 focuses on the extension history in the Upper Rhine Graben. Thermo Tectono Stratigraphic Forward Modeling of cross-sections in the central northern part of the URG was done in reference to geometrical balancing. New evidence on the lithospheric strength and a time/extension path for the rifting in the URG resulted from this study and the new rift basin model was further validated. The work was done in Team work with S. M. Schmalhoz who provided software and modeling knowledge and P. A. Ziegler who supported interpret-

ing the data and writing of the manuscript. The work has been submitted to Tectonophysics.

Chapter 6 focuses on flexural isostasy and flexural foreland bending, as a possible reason for rift shoulder uplift in the southern part of the URG. The study combines simplistic modeling of flexural isostasy with evidence from the sedimentary record. This work is still in progress and is planned in parts to be published later.

Chapter 7 represents a summary and conclusion of the previous five chapters and focuses on the evolution of the URG in context of the Alpine orogeny.

Chapter 2

Palaeoecology and depositional environment of Early Oligocene insect-bearing laminites (Rupelian; Zone Fossilifère, Upper Rhine Graben; Altkirch; France)

Sebastian Hinsken¹, Andrea Storni², Andreas Wetzel¹, Christian A. Meyer¹ and
Jean-Pierre Berger²

1) Geologisch-Paläontologisches Institut, Universität Basel, Switzerland

2) Geologisches Institut, Universität Fribourg, Switzerland

Manuscript is submitted to *Palaios*

2.1 Abstract

A combined sedimentological and palaeoecological investigation of Early Oligocene fossiliferous laminites (Zone Fossilifère) exposed in the 'Rebberg Quarry' near Altkirch (France) was carried out to better understand the depositional dynamics and palaeogeography the southern end of the Upper Rhine Graben (URG) at that time. These laminites yield a well preserved fauna with fishes, crustaceans, mollusks, insects and insect larvae, additionally plant remains, bryozoans, ostracods, foraminifers, coccoliths and dinoflagellates and bird feathers were found. The aquatic fauna is characterized by low diversity and monospecific mass-occurrences of opportunistic taxa which are limited to certain horizons. Terrestrial fossils are less frequent, but more diverse and more uniformly distributed throughout the section. Most of the extant relatives of the aquatic fossils show a high tolerance against salinity changes; today they are omnipresent in marginal marine and freshwater settings. A few taxa indicating fully marine conditions and corresponding with the fauna known in the Middle Pechelbronn Beds occur in the lower part of the section, whereas the taxa in the upper part (insect larvae and a general absence of 'marine' macro-organisms) suggest a more lacustrine environment. Similar faunal associations have been described from modern coastal lakes which are characterized by strong seasonal salinity changes. Insect taphonomy indicates pelagic deposition in a huge lake. Therefore, we propose a new model for the laminites of the Zone Fossilifère and suggest a deposition within a restricted to isolated, temporarily marine-influenced lacustrine setting that experienced rapid lake-level changes and salinity fluctuations. For most of the time, the water column was stratified however, short-term mixing events caused biotic crises. Rapidly changing physiochemical conditions led to the demise of the present population and provided new habitats for the rapid spreading of opportunistic taxa. The recurrent high frequency changes in salinity level resulted from fluctuating humidity and sea level, and were enhanced by the physiography of the rift basin.

2.2 Introduction

The Cenozoic Upper Rhine Graben (URG) is a part of the ECRIS (European Cenozoic Rift System) (e.g. Ziegler, 1992). It preserves a continuous sedimentary record ranging from the Middle Eocene to the Late Oligocene in the south and from the Middle Eocene to the Recent in the northern part (e.g. Grimm, 2005a; Berger et al., 2005b). The fill architecture of the URG is fairly well known from seismic investigations and industrial exploration wells (e.g. Doebel, 1967, 1970; Blanc-Valleron and Schuler, 1997; Lutz and Cleintuar, 1999; Derer et al., 2003; Le Carlier de Velsud et al., 2005; Hinsken et al., 2007; Roussé, 2006). Nonetheless detailed insights into the sedimentary record are limited. Outcrops are sparse because of widespread Quaternary cover (Fig 2.1). Therefore many aspects concerning the depositional history, the age and palaeogeography remain unclear or are still a matter of debate (e.g. Hinsken et al., 2007). During the early stage of rifting (Middle Eocene to the Early Oligocene) a thick evaporite-bearing sequence, including terrestrial, lacustrine and brackish-water deposits accumulated in the southern URG. Marly laminites constitute a common lithofacies type (Laminite Lithofacies Association, (sensu Hinsken et al., 2007). These laminites are extremely fossiliferous and are often associated with evaporites. First descriptions of these laminites and their fossil record, called 'Plattige Steinmergel' from outcrops in the area south and east of Mulhouse date back more than 100 years. In reference to a comparable stratigraphic level in Pechelbronn area ('Middle Pechelbronn Beds'), the term 'Zone Fossilifère' ('Versteinerungsreiche Zone') was later coined for fossiliferous laminites that occur in the uppermost part of the Middle Salt Sub-Formation. 'Zone Salifère moyenne' (e.g. Vonderschmitt, 1942). Despite its richness for fossils, the palaeogeographical setting under which the laminites accumulated is still a matter of debate; reconstructions vary between a marginal marine environment (e.g. Berger et al., 2005a) local lagoon deposits (e.g. Fischer, 1969) and a lacustrine setting (e.g. Braun, 1914; Fontes et al., 1991; Hinsken et al., 2007).

Earliest Oligocene fossiliferous laminated carbonates and marls of the Zone Fossilifère are well exposed in the 'Rebberg-quarry' near Altkirch (France), located in the central, southern most part of the URG (Fig. 2.1).

It is the aim of this study to analyze the Zone Fossilifère in the southern Upper Rhine Graben integrating palaeocological and sedimentological aspects of the outcrop 'Rebberg'. The presented model helps to understand similar lagerstätten situated in other extensional basins (e.g. Cérèste; Lutz, 1984a) in a broader context.

2.3 Geological context

The Salt Formation (Zone Salifère, Salzfolge) in the southern Upper Rhine Graben comprises evaporite-bearing Lutetian to middle Rupelian early syn-rift deposits (Fig. 2.2). It has been subdivided into the Lower-, Middle-, and Upper Salt Sub-Fm. (Hinsken et al., 2007). In the central and northern segment of the

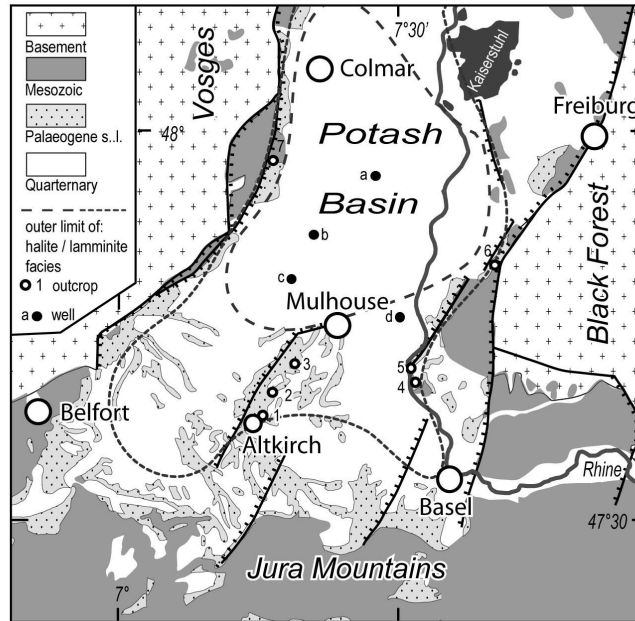


Figure 2.1: Geological overview and location of the Rebberg Quarry in the southern URG. Palaeogene syn-rift deposits are exposed on the Mulhouse Horst (MH) in the Dannemarie Basin (DB), on the Istein Block (IK) and along the Graben margins, while the Potash Basin forming the depot-centre of the southern URG is covered entirely with Quaternary deposits. Palaeontological descriptions of Fossiliferous laminites exist from outcrops: 1 this study 2 Tagolsheim 3 Brunstatt 4 Kleinkems (Kalkwerk) 5 Kleinkems (Russgraben) 6 Britzingen 7 Rouffach and drillings: a-d

URG, where the Lutetian to middle Rupelian strata are less rich in evaporites, there the Lower Salt Member is equivalent to the Green Marl Formation and the Middle Salt Member to the Lower and Middle Pechelbronn Beds, while the Upper Salt Member corresponds to the Upper Pechelbronn Beds (e.g. Berger et al., 2005b). The Salt Formation rests on Eocene residual clays and lacustrine limestones. It is overlain by marine deposits of the Grey Marl Formation (middle Rupelian to Chattian), that in turn grades into Chattian brackish-water and Late Chattian freshwater deposits (e.g. Berger et al., 2005a,b). During the Neogene the area of the southern URG was uplifted and the Palaeogene succession was partially removed by erosion (e.g. Hinsken et al., 2007).

The Salt Formation consists of thick, prevailing continental deposits. In the depot-center within the southern URG, the so-called Potash Basin, comprises 2 km of marls alternating with evaporites. Toward the margins lacustrine limestones, marls and sandstones dominate, while alluvial fans formed along the basin margins (e.g. Düringer, 1988; Hinsken et al., 2007). Deposition of the

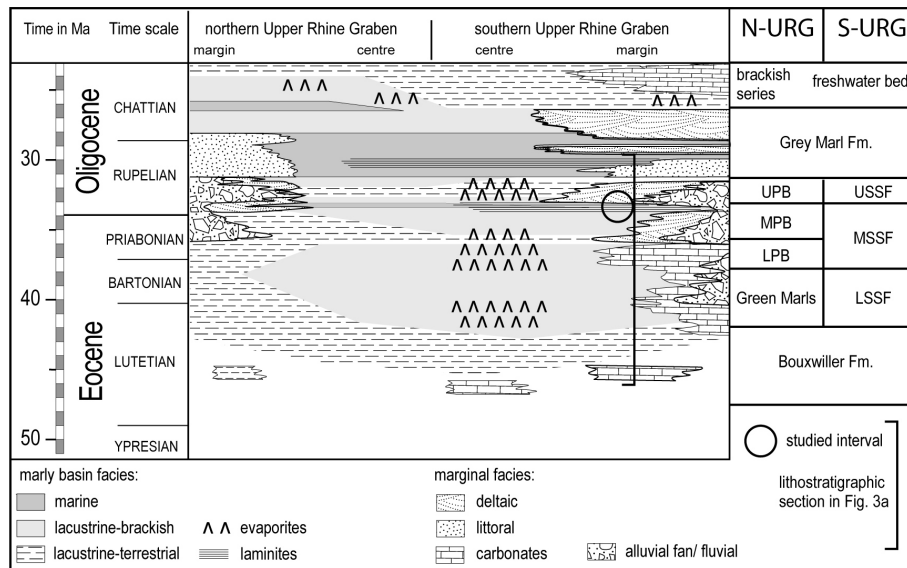


Figure 2.2: Simplified stratigraphical chart of the Palaeogene series in the URG showing correlation of chronostratigraphy lithostratigraphy and facies as well as the position of the reference section and studied interval that are shown in fig. 2.3 (modified from Grimm, 2005a; Berger et al., 2005a,b; Hinsken et al., 2007).

Salt Formation was controlled by clastic supply from the graben shoulders and accommodation space made available by differential tectonic subsidence. Base-level fluctuations within the under filled basin caused sediment partitioning and led to several orders of cyclic deposition (e.g. Hinsken et al., 2007). Each of the tree members of the Salt Formation represents a major base-level cycle corresponding to an episode of intensified evaporite sedimentation (low base-level). A shift toward brackish or even freshwater conditions (high base-level) marks the end of a Member (Hinsken et al., 2007).

The so-called Zone Fossilifère forms a distinct stratigraphic interval within the top of the Middle Salt Sub-Formation consisting of marls, laminated marls, lithographic limestones and intercalated gypsum layers. The Zone Fossilifère forms a deposit rich in exorbitant-preserved fossils containing completely articulated fishes, crustaceans and insects as well as mollusks and plant fossils known from a number of localities (fig. 2.1). Most of them, however, are no longer accessible.

2.3.1 Studied section

The studied section in the Reberg Quarry ($N47^{\circ}36'03''$, $E7^{\circ}14'37''$) is located on the crest line of the E-ward tilted Altkirch block (Rotstein et al., 2005; Hinsken et al., 2007) that forms part of the so-called Mulhouse Horst. There the syn-rift deposits of the Salt Formation are thin ($\approx 500\text{m}$) and a swell-

like facies is developed in some intervals of the Salt Formation such as the 'Melanienkalk' and the 'Haustein', while to the west and to the east the strata thicken (Fig. 2.3A, Vonderschmitt, 1942; Le Carlier de Velsud et al., 2005; Rotstein et al., 2005; Hinsken et al., 2007). Therefore, the Mulhouse Horst formed an intra-basinal elevation, at least for some time during rifting (Hinsken et al., 2007). The studied section in the Rebberg Quarry exposes the uppermost part of the Middle Salt Member represented by grey gypsiferous marls and the carbonaceous laminites of the Zone Fossilifère, as well as the basal and middle part of the Upper Salt Member (Fig. 2.3B) consisting of shallow-water carbonates of the Haustein (e.g. Düringer, 1988; Wappler et al., 2005; Hinsken et al., 2007). This section can easily be correlated with the Hirzbach Wells located a few kilometers to the south which completely penetrate the graben fill (Fig. 2.3, Vonderschmitt, 1942).

2.4 Materials and Methods

Distinct horizons of the Zone Fossilifère in the Rebberg Quarry were semi-quantitatively investigated for their fossil content by splitting blocks and recording the specimens. Fossil-rich layers were studied on an area of several tens of square-metres. The high abundance of fossils provided information about the relative frequency of individual species within the investigated layers. All fossils are stored in the collection of the Museum of Natural History in Basel (access no. 19'206).

2.5 Sedimentology

The Zone Fossilifère comprises a 5 m thick succession of laminated marls and lithographic limestones rich in fossils (Fig. 2.4). Below and above grey gypsiferous marls are exposed (Fig. 2.3b). Bryozoans occur in a massive gypsum layer at the base of the studied section. The section comprises the following litho-facies types:

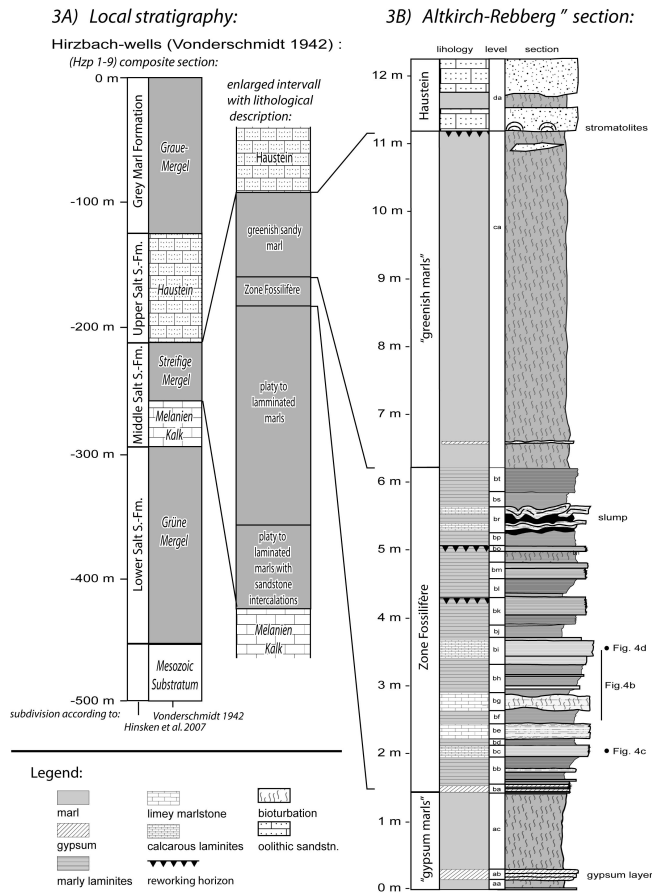
Marl: Grey to greenish homogenous marls rich in pyrite and with abundant burrows. Mass occurrence of pyritised hydrobids and ostracods in single layers.

Gypsum: A laminated gypsum-layer occurs at the base of the section, having fragmented bryozoans on top. Further fine gypsum layers are intercalated into marly laminites. One gypsum arenite with HCS structures occurs in the grey marls covering the Zone Fossilifère.

Limey marls: Grey platy limey homogenous marls containing distinct intervals of pyritised gammarids and biodeformational structures.

Figure 2.3:

Lithostratigraphical correlation of the studied section with the Hirzbach wells (Vonderschmitt, 1942) located a few km to the south. The Zone Fossilifère represents the highest part of the so-called Streifige Mergel Member that build up the Middle Salt Sub Formation together with the Melanien Kalk Member. It is bordered by several metres of greenish marls (here assigned to the Middle Salt Member) from the covering Hausteine Member that is assigned to the Upper Salt Member. The trilogy of Melanien Limestone Member, Streifige Mergel Member and Hausteine Member in the southernmost URG is more or less equivalent to the Lower -, Middle- and Upper Pechelbronn Beds in the middle and northern part of the URG.



Calcareous laminites: Greyish to yellowish fossiliferous calcareous laminites containing insects, isopods and plant remains. Millimetre-scale varve-like lamination consists of micritic layers and detrital carbonaceous material. Microturbidites may occur (Düringer, 1988).

Marly laminites: Greyish fossiliferous laminites with insects, crustaceans and plant remains show millimetre-scale alternation of calcareous layers and marly detrital layers.

Organic-rich marly laminites: Millimetre-scale lamination of shaly, marly and carbonaceous layers. Dark grey colour is caused by relative high organic

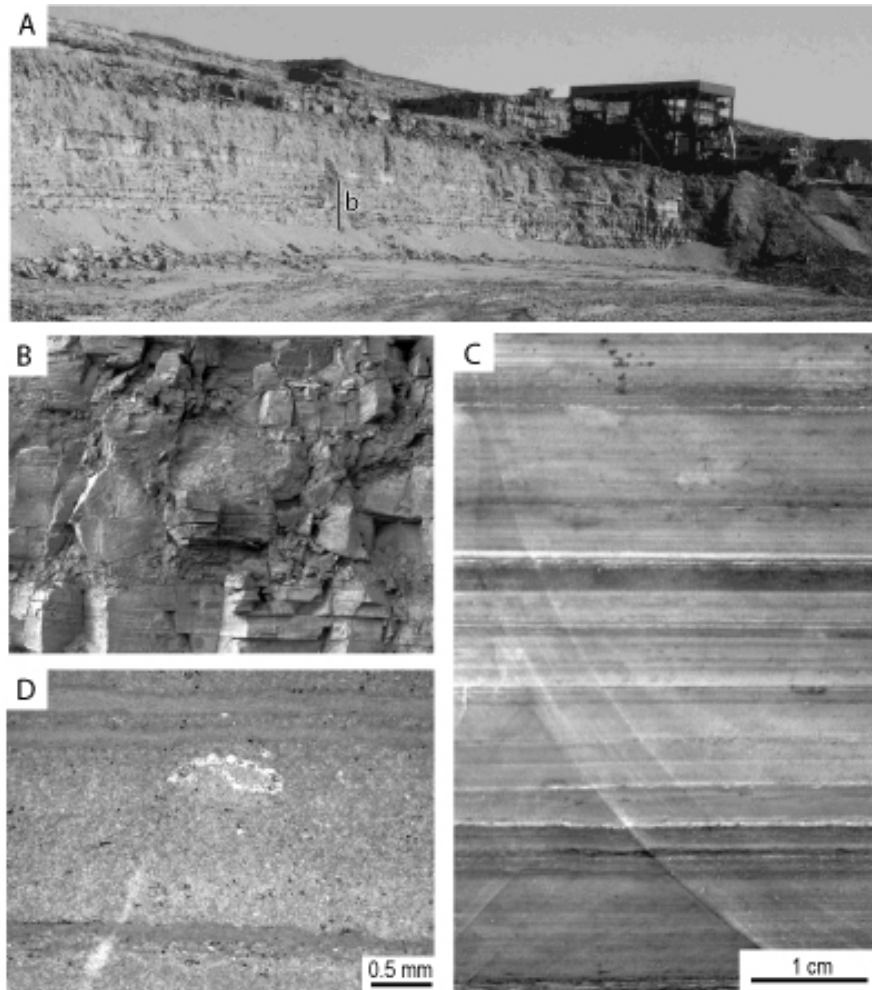


Figure 2.4: A Exposure of the Zone Fossilifère (level *ba-bt*) in the 'Rebberg Quarry' are covered by grey marls (level *ca*, wall height ~ 11 m) and by light pedogenetically overprinted shallow water carbonates and marls of the Haustein (background). B Intercalation of palty to laminated marls and lithographic limestones (level *bf-bi*) showing boudinage-like soft sedimentary deformation (level *bc*, image height ~ 1 m). C millimetric scale lamination in lithographic limestone, darker layers due to enrichment of framboidal pyrite. D Lamination consists of varve like alternations of detritic layers (including chara-stem remain) and thin micritic layers interpreted as microbial mat.

matter content >1% and finely dispersed pyrite. Fishes, mollusks, insects and crustaceans were found.

The distinct lithological intervals are between 1-40 cm thick and some layers show syn-depositional deformation like slumping and boudinage (Fig 2.4B). The layers can be followed within the whole outcrop for about 100 m and even single laminae can be traced throughout.

The lamination is about 1 mm thick (Fig. 2.4C) and consists of alternations of micritic layers and detrital layers of silt-sized material embedded within a marly matrix (Fig. 2.4D). The marly layers contain reasonable amounts of quartz, some white mica, as well as sometimes pollen, plant remains and rare microfossils (ostracods, foraminifers). Further up the laminites contain framboidal pyrite that is concentrated layerwise leading to dark-coloured stripes. Based on the sedimentary structure the micritic layers have been interpreted as microbial mats (Fig. 2.4D; Düringer, 1988). Articulated skeletons of arthropods and fishes are generally preserved within the micritic 'microbial mat' layers.

2.6 Sedimentological Interpretation

The laminites of the Zone Fossilifère were deposited under stagnant conditions. Slumps and microturbidites but also lamination suggest a rather deep environment located below the wave base. An anoxic environment is indicated by lamination, excellent fossil preservation and occurrence of framboidal pyrite. However, occurrence biodeformational structures in several layers as well as two minor reworking horizons (top level *bk* and *bo*) indicate temporal oxygenation and mixing of the bottom waters. Gypsum and carbonate precipitation under stagnant conditions indicates supersaturation of the bottom waters with respect to these phases. Marls accumulated in the basin centre and carbonates on swells and along the margins. Therefore, the lithographic limestones are thought to have accumulated in relative shallow water while the laminated marls might have formed in deeper water. Consequently, the waterdepth fluctuated as suggested by the alteration of intervals dominated by lithographic limestones and laminated marls and the inverse relation of TOC to carbonate (Hinsken, 2003). Lacustrine laminites imply a stratified waterbody (Wetzel, 1991; Lutz, 1997). Thereby the surface waters are oxygenated due to mixing by wind and waves (mixolimnion), while the bottom water is stagnant (monolimnion). Stratification of the waterbody results from the density difference between the surface and bottom waters either due to temperature or salinity, or both (e.g. Talbot and Allen, 1998). For the deposition of TOC-rich laminites within the lowest part of the Upper Salt Member (Salt IV sensu Blanc-Valleron and Schuler, 1997) of the Potash Basin, haline water stratification was assumed by Hofmann et al. (e.g. 1993). Rhythmic bedding of laminites has been interpreted to represent annual cycles (Düringer, 1988; Hofmann et al., 1993; Storni, 2002). With an average lamina thickness of 1mm, the 5m section of laminites, would, therefore provide insight into a time interval of about 5000 years.

The Hausteine Member covering the Zone Fossilifère consists of marls, cal-

careous sandstones, lacustrine limestones and lignite layers. It formed in a marginal lacustrine or marine setting documented by HCS-bedding, oolites and widespread stromatolite growth. Pedogenic overprint like root traces, karstification along roots or calcrete crusts are present in almost every layer, indicating recurrent exposure and lake level fluctuations. A similar facies has been encountered at the basin margin interfingering with the Zone Fossilifère. Therefore the Zone Fossilifère and the Haustein Member appear to be genetically related.

2.7 Fossil Record

Among the fossil taxa that have been found in the studied section (Fig. 2.5, 2.6 and 2.7) four major groups can be distinguished; (1) autochthonous aquatic macro-fauna (2) semiaquatic insects including their full aquatic reproduction cycle, (3) allochthonous terrestrial fauna and flora and (4) Microfauna and flora. The distribution of species in the section is shown in Fig. 2.9.

2.7.1 Aquatic Fauna

Fishes

Aquatic taxa include 2 species of fish; *Enoploptalamus alsaticus* (Fig. 2.5A), *Notogoneus cf. cuvieri*; that have been described from the locality by Gaudant and Burkhardt (1984), and also a third species, *?Dapaloides sp.* which was not found during our study. The specimens of *E. alsaticus* show skin impression due to enrichment of framboidal pyrite (Fig. 2.5A), while the incomplete specimens of *Notogoneus sp.* are preserved including the ctenoid scales. Some specimens of *E. alsaticus* were found partially disarticulated and some specimens are fragmented into numerous pieces while some others occur enrolled. In the upper part of level *bo* many disarticulated fishbones of *Notogoneus sp.* can be observed. *Notogoneus sp.* is also known from the Rustenhardt well (Gaudant and Burkhardt, 1984).

Crustaceans

The aquatic isopod *Eosphaeroma obstusum* (Martini, 1972) occurs very frequent in the investigated section and in other localities of the Zone Fossilifère. It was described among others from the Zone Fossilifère of Brunstatt, Tagolsheim, Kleinkems and several wells (Förster, 1892, 1913; Stucky, 2005). Amphipods were found in several levels of the section. In level *be* mass occurrences occur (Fig. 2.5B). Specimens from this level were determined to belong to the Gammaridea (W. Etter pers. comm.). It is very likely that more than one genus is present, as some bigger specimens (up to 2cm body length) appear in level *bk*, but due to complex and high order taxonomy (Hessler, 1969) it was not possible to distinguish the different genera. Förster (1892) described the genus *Gammarus sp.* from Brunstatt and Lümschweiler and Maikovsky (1941) described *Gammarus retzi* and *Melita palmata* from the wells Schönensteinbach

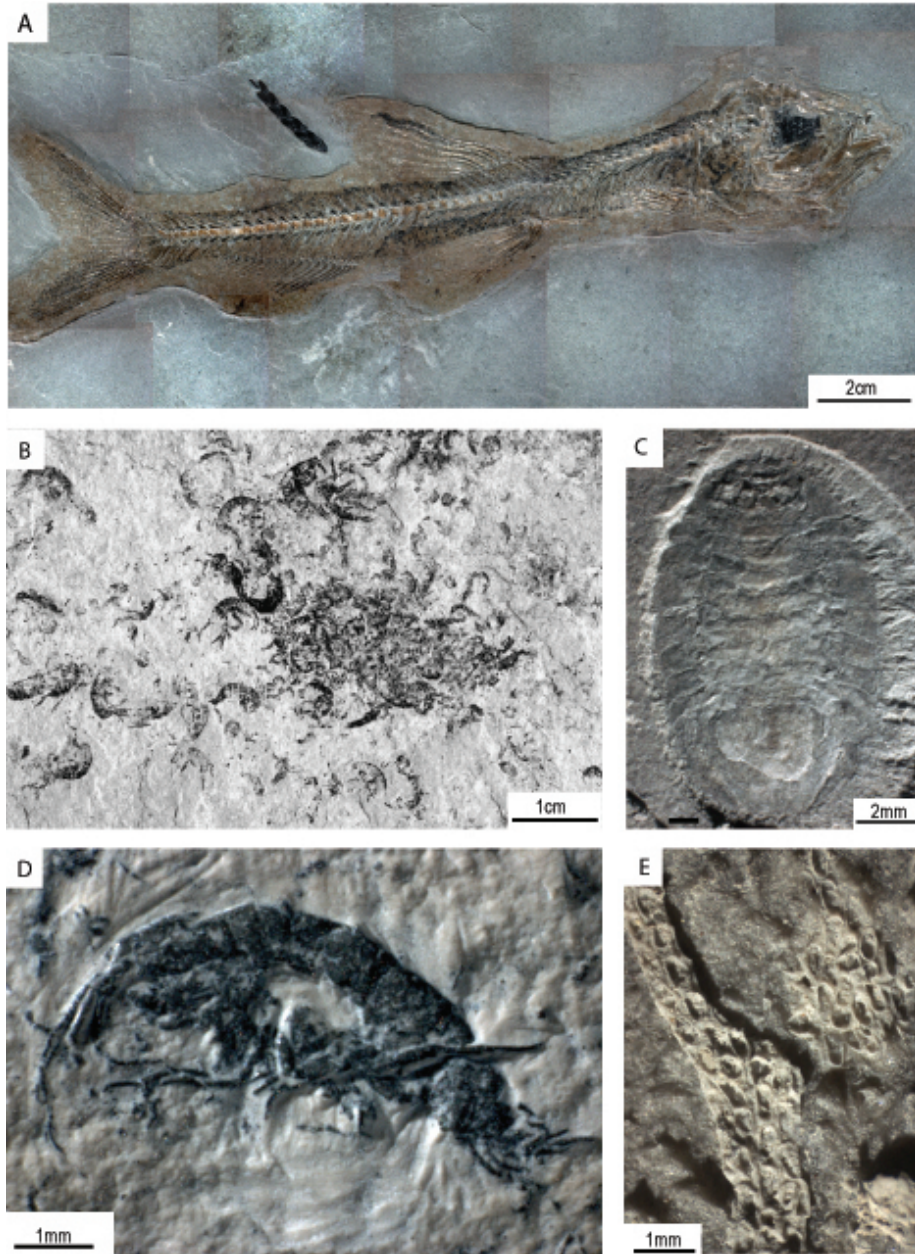


Figure 2.5: Autochthonous aquatic fossils: A) *Enoploptalamus alsaticus*. B) monospecific mass assemblage of pyritised Gammaridae. C) pyritised Gammaridae. D) *?Elektra monostachys*.

and Homburg. Crustaceans are either preserved chitinous; some amphipods (level *bk*) and *Eosphaeroma*, or they are preserved three dimensional in pyrite, as the amphipods in level *be*.

Molluscs

Small gastropods that are attributed to the genus *Hydrobia sp.*, and small bivalves that most likely belong to the Corbiculacea. Hydrobids are very common in the Zone Fossilifère, however due to preservation a taxon determination is mostly not possible. Bivalves could be assigned to the Corbiculacea, because of hinge preservation and small body size. These bivalves were previously determined to belong to the group of *Cyrena* (e.g. Förster, 1892; Gaudant and Burkhardt, 1984). Additionally, Düringer (1988) and Gaudant (1988) described *Mytilus faujasy* from the investigated section, but these finds, that are very common in other localities of the Zone Fossilifère, could not be confirmed. Mollusks are preserved with chalky shell remains, *Hydrobia* in level *ac*, however, are preserved in pyrite. Corbiculaceans in highest part of level *bk* were discovered in unstable position (sensu Allen and Allen, 2005, ;47 out of 48 specimen) and even in live position, indicating that they lived autochthonous.

Bryozoans

In the gypsum layer below the Zone Fossilifère fractured remains of a single bryozoan species form a distinct shill layer (e.g. Düringer, 1988). These bryozoans appear to be closely related to the recent genera *Electra monostachys* (Vavra, written comm.), but a revision of all bryozoans from the 'Zone Fossilifère' (with *Electra* and *Nellia*) and the 'Middle Pechelbronn beds' (with *Nellia*, *Alderina* and *Penemia*) is actually in progress (Th. Lavoyer, oral comm.).

2.7.2 Semiaquatic insects

In several levels of the investigated section, culicids (mosquitoes) including their entire larval cycle occur in large quantities reaching more than 10 000 specimen/m²: larvae head capsules (Fig. 2.6B), pupae (Fig. 2.6C) and imagoes (Fig. 2.6D) are very common and even egg floats (Fig. 2.6A) were found. Size range of head capsules indicates the presence of 4 larval stages. The finds are very similar to those from the Early Oligocene of Céreste (SE-France) reported by Lutz (1985a). In level *bi* Trichoptera remains are very common including imagoes, larval caddies, larval remains and pupae. However some of these remains might also be ascribed to Lepidoptera (Wichard, written comm.). Chironomids including one larva and several specimens of Odonata, have been discovered (Fig. 2.6H, Gaudant and Burkhardt, 1984). Although single insect larvae were described from other localities in the Zone Fossilifère (Théobald, 1937), the large quantities of semiaquatic insects including their larval stages discovered in the investigated section clearly suggest, that the insect larvae are autochthonous.

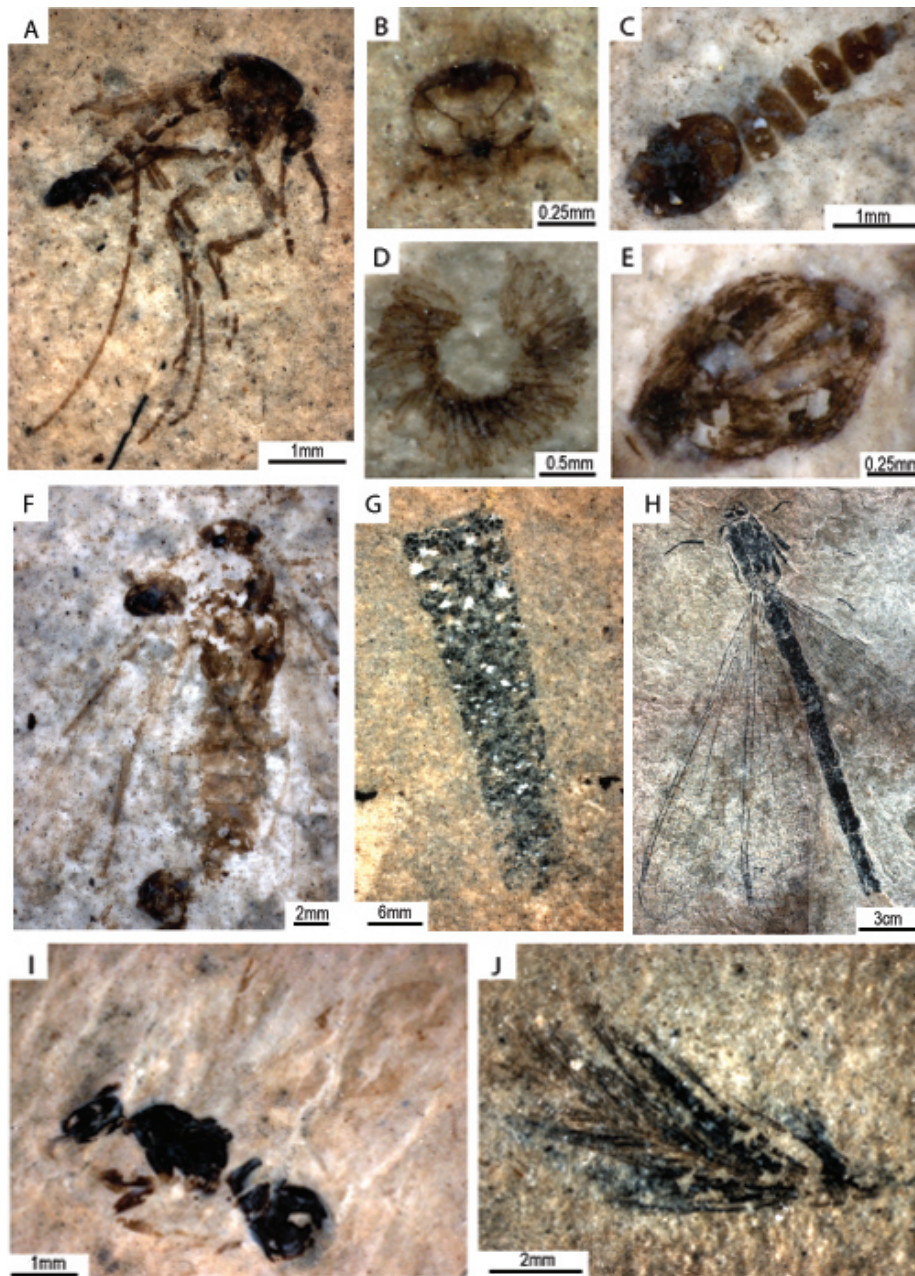


Figure 2.6: Semiaquatic insects and terrestrial fossils: A Imago of Culicidae B Head capsule of culicid-larvae C Culicid pupae D enrolled culicid-eggfloat consisting of laterally pill-shaped eggs E transparent head capsule of culicid-pupae, showing evolving imago F Amphiesmenopteran imago (?Trichoptera) G Trichopteran larval-caddy H Dragonfly I ?Formicinae J bird feather.

2.7.3 Terrestrial Fauna

Terrestrial insects include the orders Diptera, Hymenoptera (Fig. 2.6I), Coleoptera, Hemiptera, Lepidoptera and Cicadomorpha. Most of them could not be determined. However *Athalia vettuecclesia* (Wappler et al., 2005) probably represents the oldest representative of a sawfly genus. Very similar insect finds were described from the Zone Fossilifère of Brunstatt and Kleinkems (Förster, 1891; Mieg et al., 1892; Théobald, 1937). However, they are in need of revision (J. Rust pers. comm). Insects occur as compressed skeletons on bedding planes. Normally they are bound within the micritic 'microbial mat' layer. Chitinous preservation is documented by ?Lepidopteran wing scales discovered under the SEM (Fig. 2.7A (compare with; Grimaldi and Engel, 2005, Fig. 13.27, p. 569) . The insect bodies are mainly articulated including fragile details like bristles or facet eyes. However, slight disarticulation, like for instance loss of legs is common especially among the bigger specimen. Disarticulated insect remains such as legs and wings regularly appear on the bedding planes. A specific layer within level *bi* is characterized by enrichment of brownish wings that appear at first sight very similar to fossilized leaves and most probably belong to representants of the Cicadomorpha group (Wappler 2004, pers comm). Moreover remains of bird feathers (Fig. 2.6J) were found in level *bi*, from where they were also reported by Gaudant and Burkhardt (1984).

Terrestrial plant remains comprise next to fractured plant material; leaves, seeds, and flower-remains. Among the leaves 'Cinnamomum' morphotype leaves are common, next to a number of small roundish leaves with presumably unruffled leaf-margins. Among the conifers taxodiaceous remains like *Glyptostrobus* and/or *Sequoia* are common. Cupressaceae are principally represented by *Calocedrus* (Fig. 2.7 I). *Sequoia* remains were discovered in level *bt* and palm leaf remains were discovered in level *bi*. Comparable plant remains were described from other localities of the Zone Fossilifère (e.g. Förster, 1892). According to Schuler (1990) palynological investigations indicate a humid warm forest dominated by Pinaceae, Palms, Juglandaceae and Myricaceae under a humid subtropical palaeoclimate with temperate influences . Our palynological assemblages found in 2 samples (level *br* and *ca*) are very distinct: in sample *br*, the palynomorphs are essentially represented by spores and pollens, whereas sample *ca* contains a high percentage of dinoflagellates with *Phtamoperidinium*, *Heteraulacysta* and *Deflandrea*. Schuler (1990) also recorded several events with marine dinoflagellates occurrences during the Middle Salt Formation, the Middle Pechelbronn beds and within the Zone fossilifère (for example wells Reiningue, Roggenhouse, Bollwiler, Entzheim, Ebersheim).

Moreover remains of bird feathers (Fig. 2.5J) were found in level *bi*, from where they were also reported by Gaudant and Burkhardt (1984).

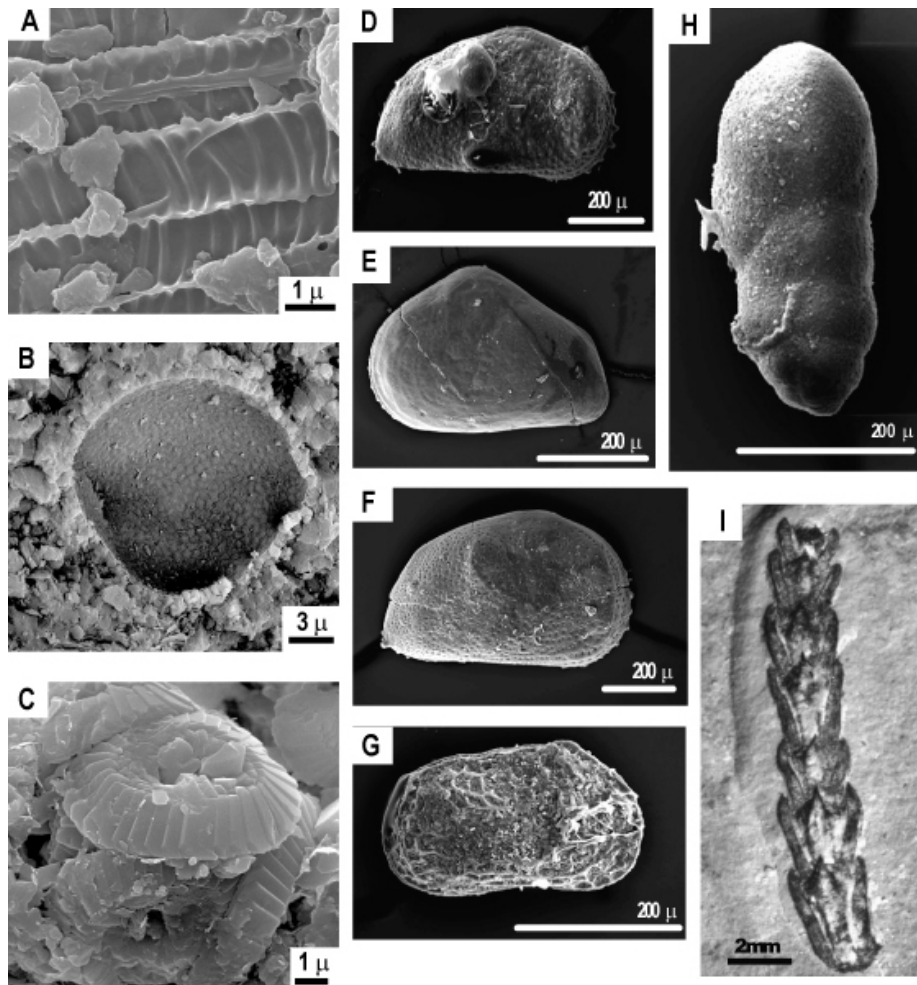


Figure 2.7: SEM-images of Micro- and Nanno fossils. A) ?lepidopteran wing scale. B) dinoflagellate cyst. C) Coccusphere of *Coccolithus pelagicus*. D)+E) *Cytheridea pechelbronnensis*. F *Hemicyprideis trigonella*. G) *Cytheromorpha* ex gr. *Zinndorfii*. H) *Praeglobulimina coprolithoides*. I) *Glyptostrobus*

2.7.4 Micro Fossils

The microfauna and flora- / and flora is principally represented by brackish to marine Ostracods (*Cytheridea pechelbronensis*, Fig.2.7 D and E, *Hemicyprideis trigonella*, Fig.2.7F, *Cytheromorpha ex gr. Zinndorfii*, Fig.2.7G) and foraminifers , with polymorphinidae, rotaliidae and buliminidae (*Praeglobobulimina coprolithoides*, Fig. 2.7H). Nannofossils (with *Ismolithus recurvus* and *Coccolithos pelagicus* Fig. 2.7C) have been found at the base of the section (level ac). They indicate an age between NP19 and Middle NP22.

2.8 Palaeoecology

The fossil assemblages of the Zone Fossilifère have been interpreted using three palaeoecological methods. A uniformitarian approach is applied for the discovered species assessing the ecology of their extant counterparts. Second, the frequency of fossils in the section was interpreted in terms of population dynamics and community palaeoecology. Third, the insect assemblage was interpreted in terms of taphonomic filters.

2.8.1 Modern counterparts of discovered taxa

Almost all species discovered in the Zone Fossilifère have modern relatives. Therefore a uniformitarian approach has been used to interpret the faunal associations. Among the preserved fishes, smelts (*Osmerus*) are anadromous. Several species (e.g. *Osmerus eperlanus eperlanus*) have populations in large inland lakes (McAllister, 1984). In costal lakes smelts can develop huge populations and mass death events have been reported from Lake Washington (USA, Frodge and Li, 1997) and the Kurisches Haff (Poland/Russia, Juengst, 1938). Smelts live nektonic, predate on small fishes and crustaceans. Like all salmonids they prefer highly oxygenated water and represent, therefore, a cold water species. *Notogoneus* sp. represents a fossil genus reported from the Palaeogene of Europe as typical brackish-water species by Gaudant (1988). However, *Notogoneus* sp. appears in the lacustrine deposits of the Green River Shales (USA) too. According to Gaudant (1981) the fish fauna of the Zone Fossilifère points to a feebly brackish-water environment. Similar fish associations have been described from Oligocene and Neogene deposits of the northern URG that accumulated under lacustrine to brackish conditions (e.g. Reichenbacher, 2000).

Among the Amphipoda, the suborder Gammaridea is the only one having non-marine representatives. Gammarids occur in marine, brackish and freshwater habitats, some species have even adapted to a terrestrial habitat. Gammaridea are generally herbivorous. Most genera are benthic, but have the ability to swim (Hessler, 1969). Amphipod associations are commonly soft-ground communities in brackish habitats like estuaries, but in freshwater they are very frequent too (Etter, 1994). Aquatic isopods of the order Sphaeromidae live nektonic or benthic and settle in environments ranging from marine to fluvial

(Hessler, 1969) while some species are aquatic troglodytes (e.g. *Sphaeroma raymondii*). The bryozoan of the family Electridae form an euryhaline group that occurs today in marine, as well as in marginal-marine lagoons. They tolerate salinities changes down to 10‰, some species in the Baltic Sea even down to 2‰. *Electra monostachys* is often found in marginal-marine settings close to river-mouths (Barnes 1994).

Only a few mollusc taxa were found in the Zone Fossilifère. Corbiculids occur in a wide range of habitats from shallow marine to fluviatil. They are endobenthic and are either detritus and/or suspension feeder. Due to their short reproduction cycles (about 3/a) they can rapidly colonize a habitat. For instance, the fluvial neozoan *Corbicula fluminea* succeeded in the colonisation of the four major river basins in France during the last 20 years.. Mytilids (*Mytilus faujasi*) appear frequently in more marginal settings of the Zone Fossilifère (eg. Kleinkems, Rouffach), but are also known from the Zone Fossilifère at Altkirch (Düringer, 1988; Gaudant and Burkhardt, 1984). Mytilids represent an euryhaline group, tolerating salinity down to 2‰ (Barnes, 1994), while the related genus *Dreissena* sp. lives in freshwater. Hydrobiid gastropods are a cosmopolitan group that occurs frequently in brackish and freshwater habitats . They may reach very high population densities in brackish water (up to 300'000 specimens/m²). Apart from hydrobiids single cerithid gastropods have been observed in the Zone Fossilifère (Förster, 1892). Culicids are cosmopolitans and may develop large populations in sub-polar and tropical regions. They are able to breed in small stretches of water and their aquatic larval stage may last less than two weeks (e.g. Lutz, 1997). They can tolerate increased salinity and some species even occur in marginal marine settings (Ward, 1991). Mass occurrences appear during rainy seasons in flooded areas or costal lakes. The nectonic larvae hang upside-down below the water surface as they breath on air with an abdominal tube. Therefore they are an easy prey for fish. Thus, if fishes are present, culicid larvae are normally very sparse or even absent. Trichoptera larvae are omnivorous feeders and are typical representatives of benthic communities in freshwater ecosystems. However several species can tolerate increased salinities up to 10‰ (e.g. Barnes, 1994).

The ostracods *H. trigonella* and *C. pechelbronnensis* are considered as marine species, whereas *C. zinndorfii* was probably a brackish species (Pirkenseer, 2007). The presence of marine benthic foraminifers (i.e. Buliminidae) as well as marine dinoflagellates (Deflandrea) could be also seen as indicators for increasing salinity.

Plant remains indicate a subtropical palaeoclimate with temperate influences (Schuler, 1990).

The salinity tolerance has been estimated for the organism groups present in the Zone Fossilifère (Fig. 2.8). All discovered species belong to euryhaline groups. The microfauna and species from the grey marls above and below the Zone Fossilifère (level *ac* and *ca*) suggest higher salinities (20-30‰) than the macrofauna from the laminites of the Zone Fossilifère (0-20‰).

The ecological significance of single species encountered in the Zone Fossilifère is limited, because most taxa occur in various settings, ranging from

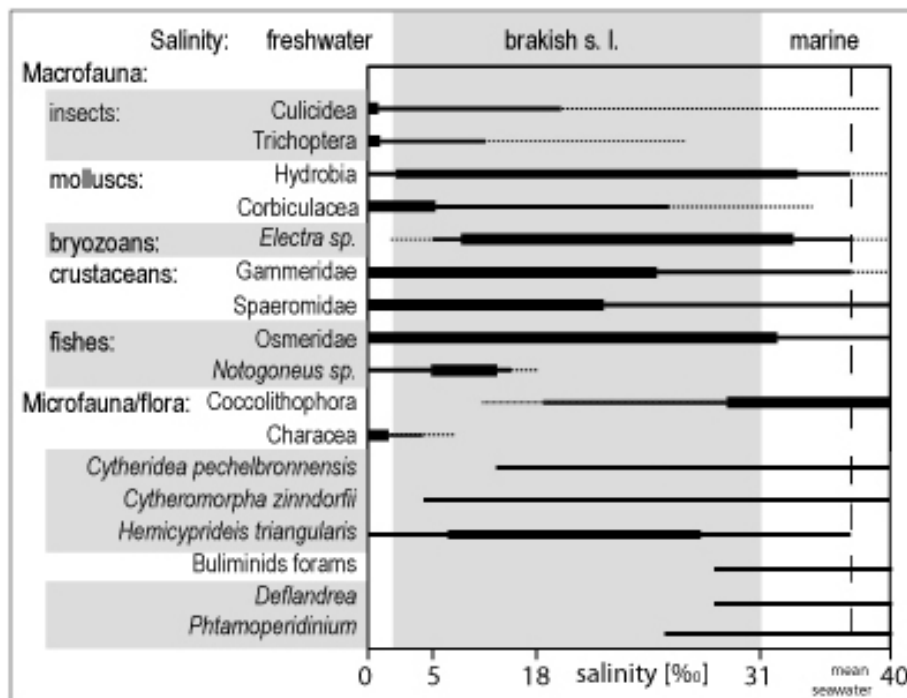


Figure 2.8: Salinity tolerance estimated for the aquatic and semiaquatic species discovered in the Zone Fossilifère. The Zone Fossilifère preserves a euryhaline Fauna.

fluviatile to marginal-marine environments. Therefore, the ecologic signature of the whole faunal association is of special interest and might provide further evidence. A similar Recent macro-faunal association has been described from Lake Clifton, a coastal lake in SW-Australia that has become known for extant stromatolite growth (Moore and Burne, 1994). The elongate interdunal lake ($\approx 0.7 * 20\text{km}$) is shallow and hydrologically isolated. It is fed by groundwater from a carstic aquifer as well as by infiltrating marine waters. Due to seasonal rainfall, the lake level fluctuates by several metres and salinity varies from 15 ‰ to 35 ‰. Moore and Burne (1994) describes the following macrofauna (with potential to be fossilized) from Lake Clifton:

The chordata comprise 3 species of fish 2 Gobiade (*Pseudogobius olorum*, *Favonigobius suppositus*) and 1 Atherinidae (*Atherisoma* sp.) and the aquatic turtle *Chelonida oblonga*. The crustacea include 1 unident Anostraca species, three Amphipoda species (*Melita zeylancia*, *Talorchestia* sp., *Paracorophium excavatum*), a Sphaeromid isopod (*Sphaeroma* sp) and two decapoda species (*Palaemonetes australis*, *Cherax plebejus*) as well as an ostracod belonging to the Cyprididae. One Gymnolaematan bryozoan species (*Conopeum aciculata*) one bivalve (*Arthritica semen*) and two hydrobid gastropods (*Coxiella striatula*, *Potamopyrgus* sp.) occur. Moreover aquatic insects; 1 trichoptera species (?*Symph-*

toneura wheeleri) and two 2 coleoptera, 1 Hydrophilidae species and 1 Tabanidae larvae are reported.

The striking similarities in terms of (bio-) diversity and faunal composition between the Zone Fossilifère and the Lake Clifton, as well as intense stromatolite growth along the lake margins are strongly suggestive of similar hydrological conditions, especially strong seasonal changes in salinity and a high calcium carbonate saturation (necessary for algal calcite precipitation, see Merz-Preiss and Riding, 1999). This deduction is supported by the fact that the majority of aquatic species found in the Zone Fossilifère and Recent Lake Clifton tolerate wide ranges of salinity from freshwater to seawater (see Fig.2.8).

2.8.2 Population dynamics and community palaeoecology

The Zone Fossilifère is characterized by an extremely low diverse aquatic fauna showing monospecific mass occurrences in distinct layers 2.9.

Aquatic and semiaquatic taxa are distributed much less uniform than the terrestrial taxa. This might indicate that the occurrence pattern was controlled rather by population dynamics than by taphonomic processes. Fish and Trichopteran remains are restricted to a specific level where they occur frequently. Crustaceans, culicids and molluscs are preserved in a few distinct levels where they are very frequent and appear more or less monospecific. There they reach densities of more than 10'000 specimen per m². Among the aquatic and semi-aquatic taxa the co-ocurrence of fossils suggests to group them under the following communities (Fig. 2.9):

Culiscid-Eosphaeroma assemblage : Insect larvae, especially culicids, occur together with other insects and the aquatic isopod Eosphaeroma, but they are absent in the layers with fish.

Fish-mollusc assemblage : Fishes co-occur with corbiculid clams and sometimes with hydrobids and gammarids. Marine ostracods have been principally found in the 3 first meters of the section, whereas foraminifers occur rarely, sporadically and irregularly along the profile.

Layerwise monospecific mass occurrences are typical for opportunistic species respectively r-strategists (Hallam, 1972). Indeed most aquatic species show features of r-strategy, like high reproduction rates, high population densities, small body size, as well as tolerance to changing ecologic conditions. r-strategists are the dominant species in physiochemical controlled settings, where recurrent biotic crises may cause mass mortality (Etter, 1994). Further indications about the depositional environment arise from community palaeoecology . The antagonism of fish (fish-mollusc community) and insect larva (insect-Eosphaeroma community) points to a predator prey relationship. Because fish feed on culicidae larvae, they are absent or very sparse in most ecologically balanced freshwater ecosystems. Therefore the absence of culicids in the fish layers can be explained by predation. Vice versa, the mass occurrence of culicids, including the full reproduction cycle as well as the high abundance of Eosphaeroma

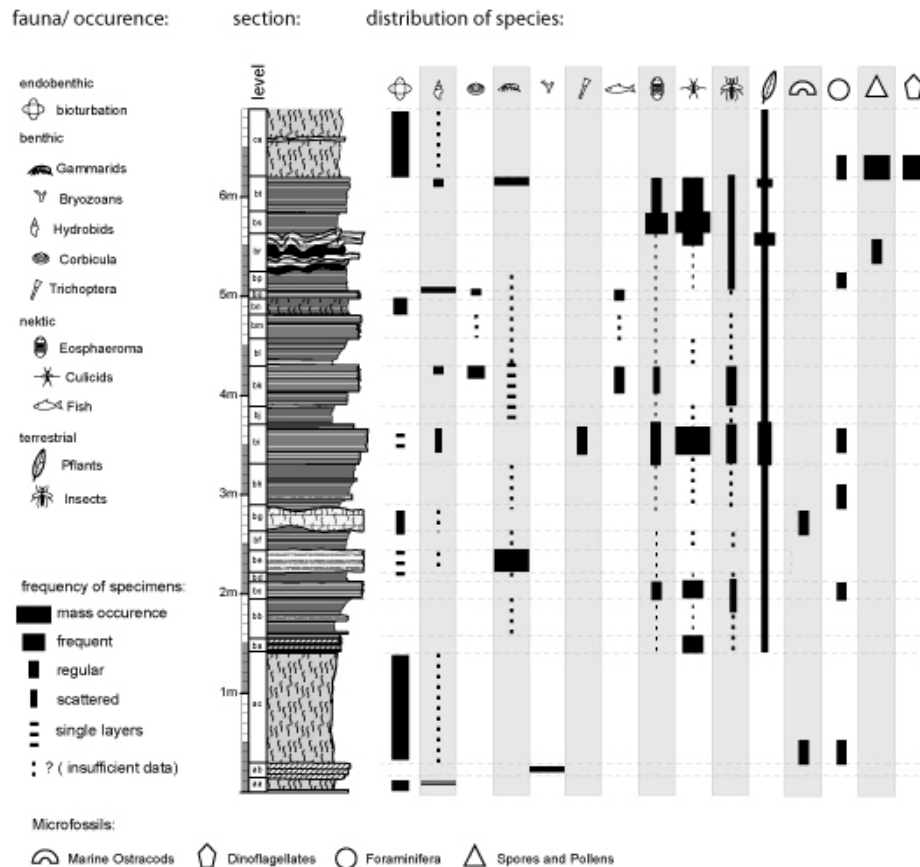


Figure 2.9: Distribution and frequency of macro-fossils in the investigated section. Terrestrial plants and insects are relatively homogenously distributed within the section, while aquatic species are limited to distinct levels where they appear very frequent and more or less monospecific. Gammarids hydrobids and culicids including the entire aquatic reproduction cycle appear in large quantities up to 10'000 individuals per m².

provides strong evidence for the absence of fish during these time intervals. Although there is no direct evidence for absence of fish within the basin during such times, the mass occurrence of culicid larvae within pelagic sediments clearly indicates a strong ecological disturbance. Such an ecological impact is best explained with a biotic crisis and hydrological isolation that prevents recolonisation. In contrast the fish mollusc assemblage points to open hydrological conditions otherwise the presence of anadromous fish (smelts) cannot be explained. Also the co-occurrence of corbiculid clams can be explained with fish or other migrating (semi-) aquatic organisms being used by the larvae as a vector as the rapid settlement of recent *Corbicula fluminea* within many European freshwater ecosystems during the last decades has been discussed in this way

(e.g. Prezant and Chalermwat, 1984).

2.8.3 Insect taphonomy

The high abundance of fossil insects in the Zone Fossilifère is the most outstanding characteristic. The preservation of insects moreover contributes to decipher the palaeo-environmental setting. Insect bearing aquatic sediments are frequently located within the Cenozoic Central European Rift System and related volcanic fields (Fig.2.10; sites according to Lutz (1997) and Théobald (1937)). Most of the insect bearing deposits are either formed in tectonic basins or in maar-lakes. In contrast insects have been rarely discovered yet in aquatic sediments of the large Cenozoic basins like the North Alpine Foreland Basin, the Paris Basin or the Aquitaine Basin.

Basin settings seem therefore to be a major factor controlling insect fossilization within aquatic sediments. Basins hosting insect bearing aquatic deposits generally exhibit a high ratio of depth to width, low clastic supply and, hence, reasonable water-depths not too far from the shoreline. Most of these basins remained hydrological isolated for some time and evaporation phases are often indicated (e.g. Lutz, 1997). Reasonable water-depth and/or dissolved salts may cause water-stratification and the formation of stagnant bottom waters, conditions that favour insects to fossilize.

Among the different basin types characteristic insect taphocoenosis occur (see below), most probably, because taphonomic filters strongly influence the preservation in aquatic sediments. Insect assemblages within aquatic sediments do, therefore, not reflect the original bio-diversity (e.g. Wilson, 1980, 1982, 1988a,b; Lutz, 1997). Taphonomic processes leading to concentration or depletion of some insect groups within subaquatic deposits have been assigned to (1) ability to fly (e.g. Wilson, 1988b; Rust, 2000), (2) flow segregation (e.g. Lutz, 1997; Martínez-Delclós and Martinell, 1993), (3) predation or 'microbial' disintegration (e.g. Lutz, 1984a; Tischlinger, 2001; Duncan, 2003) and (4) physiochemical composition of the watercolumn (e.g. Lutz, 1997). Among these factors flow segregation appears to be a factor of major importance; due to low weight and large body surface, insect bodies are fixed on the water surface because of water surface tension and they can float for a long time before settling. The ability to float depends largely on the anatomy and therefore is different among the different insect orders, but is also dependent on the body size (e.g. Lutz, 1997; Martínez-Delclós and Martinell, 1993). Experiments have shown rapidly settling taxa like beetles (Coleoptera) and bugs (Heteroptera) start to sink soon after having fallen into the water, while very long-floating species like butterflies (Lepidoptera), caddflies (Trichoptera), or dragonflies (Odonata) respectively very small specimen can float for several weeks (Martínez-Delclós and Martinell, 1993; Lutz, 1997). However there are still only few data available and detailed studies about settling behavior of the different groups do not exist. Settling often occurs due to waves and/or rain drops that help floating insect bodies to overcome surface tension. Sinking is then influenced by boundary layers within the water column, like haloclines or thermoclines along which density

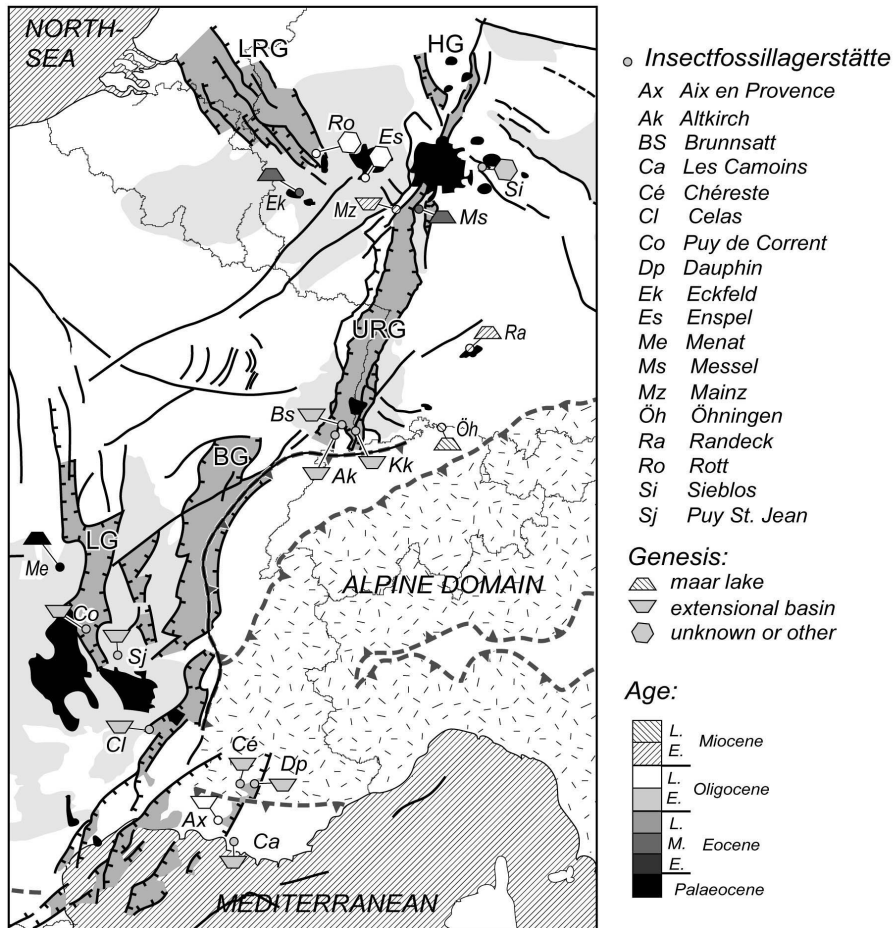


Figure 2.10: Insect bearing aquatic deposits of Cenozoic age in Central Europe occur frequently in spatial relation with the European Cenozoic Rift System. Majority of insect sites found in deposits from maar lakes or extensional basins, while insect sites from the larger basins have not been described yet.

increases. Such levels might prevent insect bodies from further settling (Lutz, 1997). The occurrence of insect-orders in some insect sites is shown in Figure 11 and is sorted according to the frequency of coleopterans (Lutz unpublished data).

Three groups are distinguished:

Group 1 : Righthand the deposits Eckfeld, Sieblos, Messel, and Orappa are dominated by Coleoptera. Hymenoptera and Diptera are seldom in these deposits and Ampisomenoptera respectively Odonata are only represented by single finds

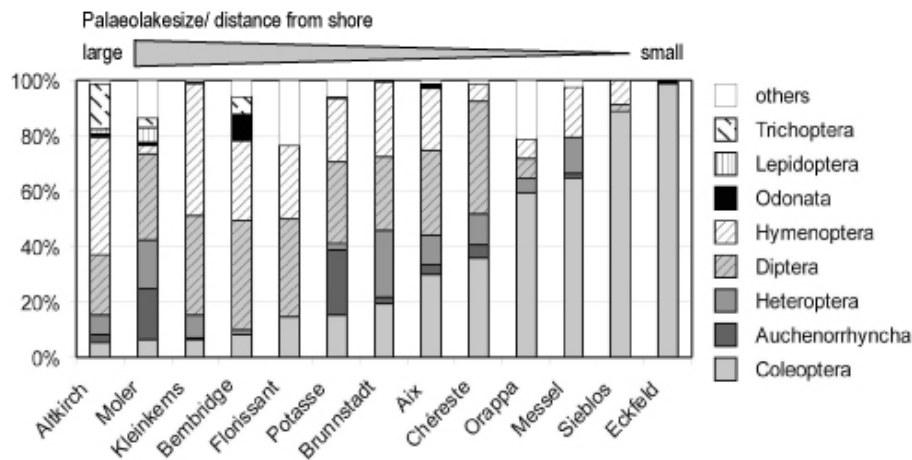


Figure 2.11: Insect taphocoenosis from different aquatic fossilagerstätten: Deposits of small lakes (righthand) are characterized by concentration of rapid settling groups like coleoptera, while intermediate and large lake deposits are typically dominated by Hymenoptera and Diptera. In large lake or marine deposits additional very long drifting taxa such as Odonata or Amphiesmenoptera occur frequently too. The taphocoenosis of Altkirch is therefore compatible with off-shore deposition in a huge lake.

Group 2 : In the other sites Diptera and Hymnoptera are very frequent ranging from 30% (Moler) to more than 70% (Kleinkems). Coleopterans are much less frequent than in group 1 (35%-5%), while Ampismenopterans respectively Odonata are in average more common than in group 1.

Group 3 : In the third group is rather a subgroup of group 2. It is characterized by relative high frequency of amphiesmenopterans and Odonata are exceeding a total of 5%. Altkirch, Bembridge and Moler. In contrast Coleoptera only accounts for less than 10% of the finds.

Eckfeld, Messel and Orappa are Maar deposits. These maar lakes did hardly exceed more than one kilometre in diameter. The same lake size is indicated for Sieblos as it forms a very local deposit. The dominance of Coleoptera can be best explained with rapid settling of these taxa while long floating species might have been rafted to the lake shore where preservation is impossible. The occurrence of Trichoptera in the Eocene Messel and Eckfeld deposits (both sites have more than 1000 reported insect finds), for instance, has been proven by frequent finds of larval caddisflies (e.g. Lutz, 1997; Wappler, 2003a). However an imago or any other representative of the Amphiesmenoptera has not been found yet.

Group two includes the lacustrine deposits that formed in extensional basins of the European rift System and other deposits of medium to large sized lakes. Aix and Céreste are located in extensional basins of the Rhône Graben while

Brunnstatt and Kleinkems are sites of the 'Zone Fossilifère' in the southern Upper Rhine Graben. All deposits from the Southern URG have higher percentages of Dipterans and Hymenoptera but lower percentages of coleopteran than those from the Rhône Graben. Compared to the deposits in the southern URG those from the Rhône Graben are inferred to have formed in smaller basins. It appears that they represented medium sized lakes of several kilometers to a few tens of kilometers in diameter, while the deposits of the southern URG point to a palaeolakesize covering almost the entire URG.

Group 3 forming a subgroup of Group 2 host high frequencies of Amphipoda and Odonata and is only represented by Altkirch, Bembridge limestone and the open marine deposits from Moler. A positive relation of these groups to lake size was postulated by Lutz and Uwe (2006), and indeed long floating time, but also high ability to fly (Rust, 1999) might lead to concentration of these groups in off shore deposits.

New investigations have shown that the Lepidoptera are even much more frequent in Moler than assumed afore. As the majority of specimens is strongly disintegrated these specimens might have been overlooked (Rust, 2000). Therefore microbial disintegration might be an additional factor limiting the occurrence of these very long floating species too.

In relation to palaeogeography both, depletion of coleoptera and enrichment of long floating species appear to correlate positively with distance from shore and consequently palaeo lake size. Therefore the investigated deposit Altkirch appears to have formed in a large lake and far from shore. This assumption is moreover supported by the palaeogeographic setting. Preserved facies belts suggest the palaeoshoreline in the southern URG during deposition of the Zone Fossilifère was almost equivalent to the present-day graben margin (see Fig. 2.1). Therefore an off shore distance of >10 km's must be assumed. Moreover the small size of leaves indicates size sorting due to rafting that is in agreement with results from Roth and Dilcher (1987). Altkirch and Kleinkems show a relatively similar insect taphocenosis among the sites of the Salt Formation within the southern Upper Rhine Graben. The higher percentage of long floating taxa in Altkirch might be explained with larger distance from shore. However the deposit Potasse d' Alsace and Brunstatt show a contradictory pattern. Being located more distally with respect to the present day graben margin, they host more coleoptera and less long floating taxa. A possible explanation is, that they do not reflect the same stratigraphic level and were deposited during times of lower lake level and hence smaller lake size. This is indicated by the deposit Brunstatt represents the basal part of the Streifige Mergel Member as it rests only a few metres above a paraconformity to the laying Melanien Kalk (see Fig. 2.3, Förster, 1892). Therefore it might have formed in an early transgressive stage and it does not represent the Zone Fossilifère in the stratigraphical sense of Vonderschmitt (1942, ;see Fig.2.3).

2.8.4 Synopsis

Based on the sedimentological and palaeoecological observations a marine influenced lake setting is postulated for the Zone Fossilifère (Fig. 2.12). Intervals with a molluscs fish assemblage appear to have formed during an open lake stage while the levels with predominately culicid-Eospharoma assemblage probably accumulated within a closed lake stage very likely without the presence of fishes. The studied section provides strong evidence for temporal stratification of the water column and deposition below or above a pycno- and/or chemocline, respectively. Lamination of sediments and preservation of fossils indicates stagnant conditions and a moniolimnion, while repeated appearance of biodeformational structures and layerwise occurrence of benthos point to deposition in the mixolimnion. Some layers suggest mass mortality events such as those rich in gammarids, hydrobids or bryozoans, but also the high frequency of smelts might be related to mass mortality events. Recurrent biotic crises are further evidenced by the opportunistic characteristics of the fauna and very low species diversity. Mass mortality of benthic organisms might be explained by a rapidly rising chemocline. However, biotic crisis in such environments are most likely due to turnover of the entire waterbody that might lead to poisoning of the fauna. Within the Laminites of the Zone Fossilifère a gradual trend toward decreased salinity is evident from the fossil assemblage but the salinity might have decreased only in the mixolimnion, while brines very likely formed in the deeper parts of the lake. Based on the observation a dynamic depositional model is proposed for the accumulation of the Zone Fossilifère laminites (Fig. 2.12):

The water body was haline stratified. The mixolimnion consisted of light oxygenated 'freshwater' and has been colonized by a 'lacustrine fauna' (Fig. 2.12A). The moniolimnion consists of highly saline water which was oxygen deficient to euxinic. Toxic substances like H_2S were dissolved. Marl was deposited in the mixolimnion and colonized by benthic organisms, while laminites were deposited in the moniolimnion and served as 'konservatfalle'. Evaporation increased salinity and the density of mixolimnion and prohibited the settling of freshwater organisms. Increasing salinity/density contemporaneous with lake level due to evaporation might have destabilized the chemocline.

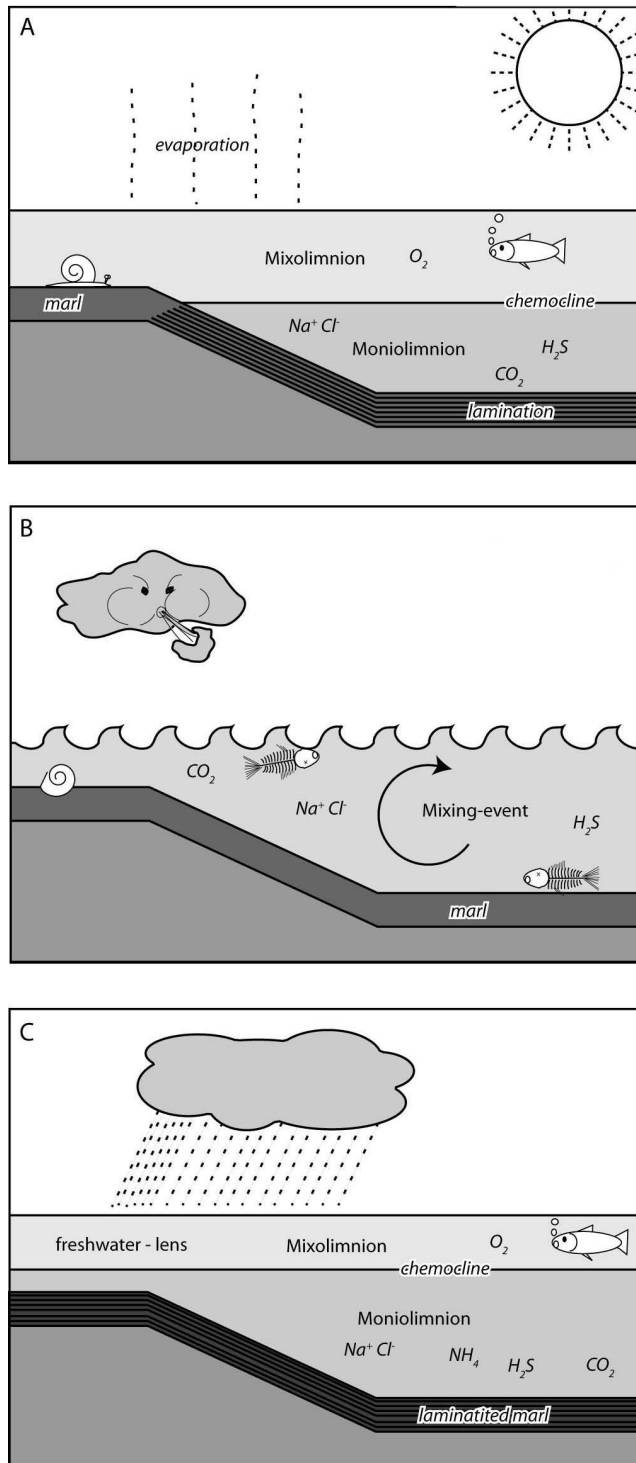
Stormevents, but also periodical sea-water inflow might have resulted in mixing events (Fig. 2.12B), During which the whole water body was mixed poisoned by remobilized H_2S of the moniolimnion. A following freshwater overflow (Fig. 2.12C) led to a stratification of water body and surviving opportunistic species were able to fill the empty niches rapidly.

2.9 Discussion

The ecological significance of discovered species has its weakness in the inaccurate taxonomic identification and the fact that species may adapt to changing environmental conditions during their evolution. Within this respect the Palaeogeography of the Zone Fossilifère has been discussed to represent either a lake

Figure 2.12:

Depositional model for deposition of the Zone Fossilifère in the southern Upper Rhine Graben: A) Water column is stratified. The saline and euxinic monolimnion overlies the mixolimnion, that is settled by an euryhaline lacustrine fauna. Evaporation reduces the mixolimnion and increases salinity. Therefore the mixolimnion gets unstable. B) finally a mixing event occurs - for instance in relation to a thunder-storm. Mixing leads to poisoning of the mixolimnion due to dissolved ions and fluids. C) finally freshwater overflow establishes a chemocline again and provides a habitat rapidly settled by opportunistic taxa.



or a sea (e.g. Düringer, 1988; Schuler, 1990; Fontes et al., 1991; Hinsken et al., 2007) The fauna of the Zone Fossilifère clearly indicates brackish water and has been described, therefore, as a marginal marine habitat by some former workers (e.g. Förster, 1892; Berger et al., 2005b). This interpretation is supported by the occurrence of a few marine taxa described above and by the paleogeographic correlation with the marine episodes during the Middle Pechelbronn beds, which are clearly marked by several short marine incursions in the Mainz Basin and the Pechelbronn area (see Martini and Radtke, 2007; Berger et al., 2005a; Hottenrott and Pross, 2007; Griessemer et al., 2007) as well as in the Southern URG (Pirkenseer, 2007).

However, this interpretation is questioned by the following reasons: (1) Many species typical for marine brackish water habitats, for instance, decapods, hermit crabs or oysters have never been encountered in the Zone Fossilifère. (2) In contrast some species like the aquatic insect larvae clearly indicate a lacustrine setting. (3) Compared to the large number of species described from Recent brackish water habitats of Europe (e.g. Barnes, 1994) or the diversity of ancient brackish lakes (Magyar, 2002), the species-diversity is much too low to be explained by the brackish water alone. This question and the discussions on the palaeogeography most probably reflect the very complex and instable ecosystem developed during the deposition of the Middle Pechelbronn beds and the Zone Fossilifère. The salinity probably changed rapidly from freshwater to marine, and vice-versa, depending of the seasonal precipitation regime, eustasy and the geodynamic/palaeogeographic context.

The ecological significance of population dynamics and community paleoecology is limited due to incomplete knowledge about the taphonomic processes that might have distorted the picture of the past (e.g. Wilson, 1988b). The majority of studies on konservat lagerstätten do not consider taphonomic sorting processes in stagnant deposits and come to the result that about 70% of the aquatic fauna will be preserved (e.g. Etter, 1994). Contradictory Wilson (1988b) described biases in the terrestrial and aquatic faunas that occur due to distance from shore and or seasonal variability. Recent studies have shown the preservation potential of vertebrates is restricted due to the water-depth (Reisdorf personal com.). The knowledge about the taphonomic processes can provide further indications about the depositional environment as demonstrated with the autochthonous terrestrial assemblage. In contrast, combining several paleoecological methods has the advantage that the results of each method can be compared and independently be tested. In this sense, the results of this study are self consistent. The high tolerance against salinity changes of the discovered organism groups is substantiated by the distribution of fossils in the section indicating opportunism. The comparison with a potential modern counterpart shows that composition and diversity are similar in both cases.

The insect taphonomy implies pelagic deposition within a large basin as evidenced by the facies distribution too: The palaeo-shoreline was close to the graben margins during deposition of the Zone Fossilifère.

In the basin centre strong salinity changes are further indicated by cyclic occurrence of evaporite layers in the Salt Formation. In contrast temporal fresh-

water inflow is documented by flashflood deposits in the marginal alluvial fan conglomerates, while there is no evidence of large tributaries in the area of the southern URG. Episodic inflow of freshwater in a saline lake favours water stratification and, subsequently, stagnant bottom water conditions and finally formation of laminites. A very similar depositional model including temporal marine incursions was suggested for the marls associated with evaporites of the Upper Salt Member covering the Zone Fossilifère (Hofmann et al., 1993).

The fossil association within the Zone Fossilifère indicates that fully marine conditions rarely established and conditions changed between paralic to lacustrine. However, restricted marine conditions are very likely for the grey marls and gypsum horizons at the base of the section (level a). Microfossils indicative of a marine transgression have been found in several levels of the upper part of the Middle Salt Formation (Martini, 1995; Pirkenseer, 2007) and they are also known from the equivalent Middle Pechelbronn Beds (Berger et al., 2005a; Martini and Radtke, 2007).

However the studied section only comprises the uppermost part of the Middle Salt Member, and therefore reflects already a regressive cycle. A trend towards lacustrine conditions was also described from the highest levels of the Middle Pechelbronn beds in the N-URG (Griessemer et al., 2007).

Palaeogeographic reconstructions indicate marine incursions during deposition of the Middle Pechelbronn Beds and the upper part of the Middle Salt Member that are assigned to the first Rupelian transgression which entered the URG from the North Sea Basin via the Hessian Depression (Berger et al., 2005a; Griessemer et al., 2007). Thereby a number of palaeogeographic swells might have formed barriers that were only temporally flooded during short term high stands. Such swells have been described from the northern URG; like the Frankfurt Swell and Oppenheim swell (Grimm and Grimm, 2003) and the Stockstadt swell on which the Middle Pechelbronn Beds are not preserved (Derer et al., 2003). In response to these swells the basin of the URG is inferred to have changed repeatedly between marine influenced and lacustrine conditions. Consequently depositional dynamics were triggered by global sea-level and climate change both are very likely to have fluctuated around the Eo-Oligocene transition (development of Antarctic ice). On the other hand accumulation of evaporites does not depend only on climate but was also controlled by Basin-physiography, catchment to lake size ratio and probably reworking of Triassic evaporites from the graben shoulders (Hinsken et al., 2007).

2.10 Conclusions

Early Oligocene laminites of the Zone Fossilifère in the southern Upper Rhine Graben accumulated under restricted conditions, within a temporary marine influenced off-shore lake environment. Depositional dynamics was characterized by strong fluctuations of lake level and salinity that came along with brine formation and related haline stratification of the water column. Biotic crisis, most probably due to mixing events and rapid salinity changes, limited the environ-

ment to an euryhaline opportunistic fauna. Next to a seasonal dry subtropical climate, sedimentary dynamics were controlled by the basin physiography. Elevated rift shoulders surrounding the graben protected the basin against external sediment and water supply. Small drainage area of the tributaries and quick tectonic subsidence led to an underfilled basin that favored the accumulation of evaporites, but also the preservation of fossils.

Aknowledgements

This study resulted from the MSC and PhD thesis of the first and second author and involved the cooperation with a number of experts that we wish to thank for their crucial commitments. Thorsten Wappler Jes Rust and Wilfried Wichard (Bonn), Herbert Lutz (Mainz) and Cesare Baroni-Umbarni (Basel) are thanked for help and support with handling fossil bugs, Norbert Varva (Vienna) for a close look to Bryozoans and Walter Etter an Burkhard Engesser(Basel) for help with the crustaceans respectively Mamalian Biostrat () A Reisdorf (Basel) is thanked for stimulating discussions, and two anonymous reviewers for their constructive corrections.

Chapter 3

A fossil sawfly of the genus *Athalia* (Hymenoptera: Tenthredinidae) from the Eocene-Oligocene boundary of Altkirch, France

Torsten Wappler, Sebastian Hinsken, Jochen J. Brocks, Andreas Wetzel,
Christian A. Meyer

a) Hessisches Landesmuseum, Darmstadt, Germany

b) Geological & Paleontological Institute, University, Basel, Switzerland

c) Department of Organismic and Evolutionary Biology, Harvard University,
USA

d) Museum of Natural History Basel, Basel, Switzerland

Article published (2005) in: C. R. Palevol 4:7-16

3.1 Abstract

A new species of coleseed sawfly (Tenthredinidae: Athaliini) is described and figured from the Eocene-Oligocene 'Rebberg'-quarry within the Fossiliferous Zone, a member of the Middle Salt Formation. *Athalia vetuecclesiae* n. sp. is the first representative of the *Athalia*-group from the geological record. The new species is most similar to members of the *A. vollenhoveni*-group represented by only six species from Africa, but can be distinguished by details of antennal structure and length of spurs of the hind tibia. The phylogenetic position of the fossil within the Tenthredinidae*, its palaeoenvironmental implication, and the geological setting of the quarry are briefly discussed.

3.2 Introduction

In spite of its incompleteness, the hymenopteran record is rich enough to represent as many as 51 out of 54 extant families (Rasnitsyn and Quicke, 2002). As many as 38 of these families are known at least since the Mesozoic, a time during that in many high-level phylogenetic events occurred, and 20 additional families are known to be extinct (mostly since the Mesozoic; Rasnitsyn and Martínez-Delclòs, 2000; Rasnitsyn and Quicke, 2002). The ecological diversity of the hymenopterans increased during the Early Cretaceous due to the appearance of indisputably phyllophagous Tenthredinidae (Rasnitsyn and Quicke, 2002). Within the large symphytan family Tenthredinidae, *Athalia* is a member of the subfamily Allantinae, tribe Athaliini. The tribe is divided into four genera (three of them are monotypic). The genus *Athalia* represents a primitive form of hymenopteran insects. Therefore, in particular the relationships to other tenthredinid taxa are not always clearly cut. Apart from that, *Athalia* is considered as a sister-group of all other Tenthredinoidea s.s. (Schulmeister, 2003a,b; Vilhelmsen, 2001). *Athalia* contains in all 73 species with seven subspecies and occurs mostly in the Palaearctic region, but also extends into the Indo-Malayan and Ethiopian regions (Abe, 1988; Benson, 1962). The host plants of the genus *Athalia* are restricted to herbaceous species in the families Compositae, Crassulaceae, Cruciferae, Labiatae, Plantaginaceae, and Scrophulariaceae (Abe, 1988; Benson, 1962). One of the mostly commonly encountered species in Europe is *Athalia rosae* and it is from this species that most biological information is known (many species are unknown for their biology and so might be different from *A. rosae*). *Athalia rosae* predominantly feeds on several glucosinolate-containing plants and sequesters the glucosinolates of different hosts. Some examples of host plants include *Barbarea stricta*, *Sinapis alba*, and *Brassica nigra* (pers. commun. Dr. M. S. Engel). Fossils of the genus *Athalia* are rare and as such their palaeontological history is poorly understood. Earlier 'coleseed sawfly' fossils were variously assigned to different genera. Cockerell (1906) described *Eriocampa wheeleri*, a fossil from the Eocene-Oligocene of Florissant, Colorado. Later, Cockerell (1927) assigned four new species to the Tenthredinidae (*Tæniurites*, *Tenthredella*, and *Dineura*) and a second specimen of *Eriocampa wheeleri*. The latter were removed from the genus *Eriocampa* by Zhelochovtzev and Rasnitsyn (1972) who considered the specimens probably belonging to, or near to, the genus *Athalia*. These fossils are best to considered *incertae sedis* because their generic assignment is doubtful (as done by Carpenter (1992)). Therefore, discovery of well-preserved and almost complete coleseed sawflies is particularly significant. The specimens described below are the first fossil representatives of the *Athalia*-group and, thus, the oldest known members of a major branch of Hymenoptera (Fig. 6). In addition to the palaeontological importance of the found sawflies, these specimens have palaeoecological implications.

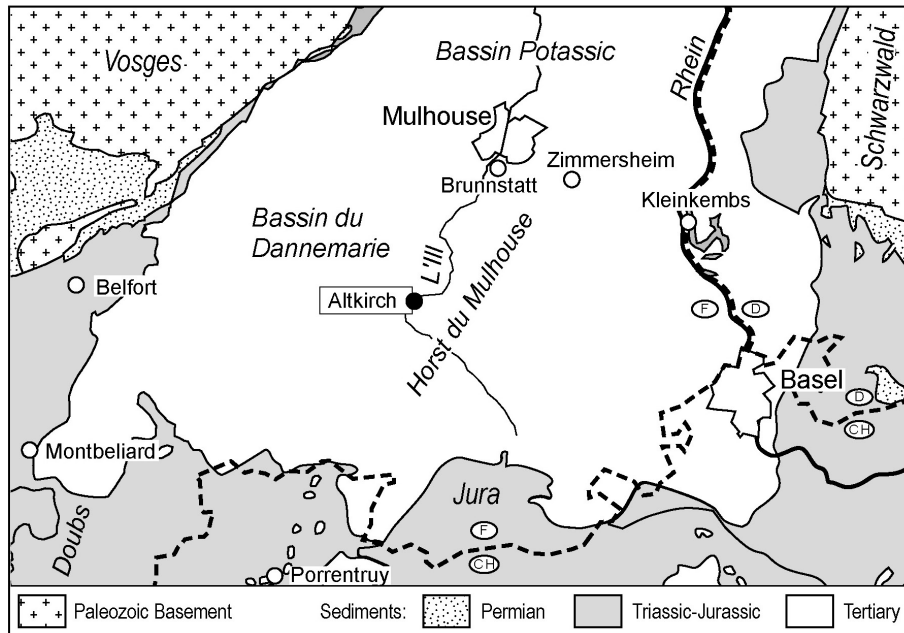


Figure 3.1: Simplified geological map of the study area.

3.3 Geographical and geological setting

3.3.1 Geological framework

The Upper Rhinegraben belongs to a major rift system within central Europe which started to develop during the Early Tertiary (Pflug, 1982; Ziegler, 1990). During the early rift stages in the Eocene, local depot-centres formed, which became interconnected during the further development (Schumacher, 2002). One of these basins is the so-called Potassic Basin in the southern Rhine Graben (Fig. 1).

In the Potassic Basin, up to 1600-m-thick marls and evaporites accumulated during the Late Eocene-Early Oligocene (Salt-Formation) (Blanc-Valleron and Schuler, 1997). The marginal parts of the basin and its southernmost part contain brackish, lacustrine, fluvial and terrestrial sediments. The basin border is characterized by fluvial conglomerates, which have been interpreted as alluvial fan deposits (Düringer, 1988), which formed in response to the uplift of the graben flanks. The Cenozoic sedimentary record in the Potassic Basin starts above a residual red, iron-rich soil (*'Sidérolithique'*) with Lutetian freshwater limestones (*'Calcaire à Planorbes'*). This is overlain by the Salt Formation, which is formed during the main rift phase during the Eocene-Oligocene (Schumacher, 2002). The Salt Formation has been subdivided into the Lower Salt Formation (Lower Lacustrine Marls, Salt I, Upper Lacustrine Marls, Salt II),

the Middle Salt Formation (Salt III, Fossiliferous Zone) and Upper Salt Formation Salt IV, Marls without Salt) (Fig. 2). Further up, the Members of the Grey Marl Formation, Foraminifera Marls, Fish Shales, Meletta Shales and Cyrenea Shales, which are covered by freshwater beds (Blanc-Valleron and Schuler, 1997; Düringer, 1988). Due to the abundance of fossils and the generally articulated preservation of fish and insect skeletons, the Fossiliferous Zone of the Middle Salt Formation can be described as a Fossilagerstätte. Like many other comparable Palaeogene insect-bearing deposits in central Europe e.g., Céreste/France (Lutz, 1984a, 1985a,b; Nel, 1991; Nel et al., 1993; Pfretzschner, 1998; Wappler, 2004); Rott/Germany (Gaudant, 1988; Lutz, 1985a, 1996; Mai, 1995), the environmental conditions under which the host sediments formed are still a matter of debate. Some authors postulate a lagoonal, marine-influenced setting (Blanc-Valleron and Schuler, 1997; Hofmann et al., 1993; Lutz, 1997; Wagner, 1924) others favor a saline lake (Braun, 1914; Düringer, 1988; Fontes et al., 1991) similar to the Lower Eocene Green River Formation (Wyoming, USA) as interpreted by Eugster and Surdam (1973) or Boyer (1982).

3.3.2 Age constraints

In spite of abundant fossils, index fossils are rare and, hence, the stratigraphical position of the Salt Formation members has not been totally clarified yet. The most authors regard the Fossiliferous Zone as Earliest Oligocene (Martini, 1972). Schuler (1990) postulates the lower part of the member to be Latest Eocene in age. A biostratigraphical age based on mammals in the hanging Haustein member (Upper Salt Formation) of the 'Rebberg' quarry about 35 m above the horizon of discovery covers the time interval of the Mammal Reference Level MP21 and corresponds to the Lower Stampian and Upper Priabonian, thus coinciding with Stöcklin's 'Grande coupure' (Stöcklin, 1909). So the stratigraphical position of the Fossiliferous Zone member seems to be close to the Eocene-Oligocene boundary (Fig. 2).

3.3.3 Sample location

Deposits of the Fossiliferous Zone were studied in the Rebberg quarry, near Altkirch (47°62'34" N/ 7°23'92" E; Fig. 1). This location is currently the only well exposed outcrop of the Fossiliferous Zone in the southernmost Upper Rhine Graben. The laminated marls, platy marls and lithographical limestones of the Fossiliferous Zone have been reported from many drill cores, quarries and outcrops in the southern Upper Rhine Graben. It reaches a maximum thickness of approximately 75 m in the Potassic Basin (Blanc-Valleron and Schuler, 1997) and contains a typical brackish fossil assemblage (Düringer, 1988; Förster, 1891; Gaudant, 1979; Gaudant and Burkhardt, 1984; Gaudant, 1984). The Fossiliferous Zone seems to be correlative within the whole basin except along margins where it interfingers with fluvial conglomerates (Gaudant, 1988). To date, a total of some hundred insect specimens have been collected, most of them in no longer existing outcrops near Kleinkems (D), Brunstatt (F) and Zimmersheim

(F) (Fig. 1). The first descriptions of fossil insects date back to the late 19th century (Förster, 1891; Mieg et al., 1892) and the latest revision of the insect fauna was written by Théobald (1937). Therefore, an updated review, including the insects from the Rebberg quarry in Altkirch (Gaudant and Burkhardt, 1984), is urgently required (pers. commun. Prof. Dr. Rust).

3.4 Material

The two specimens described in this study were discovered in the quarry 'Rebberg' (Figs. 1 and 2) within the Fossiliferous Zone, a member of the Middle Salt Formation. They were found in an approximately 40-cm-thick horizon of lithographical limestone, which can be correlated with the Horizon No. 6 of Gaudant and Burkhardt (1984). The fossil insects from Altkirch are preserved chitinous (SEM) and are fixed in calcareous biolaminae. Preparation is not needed, but the specimens were covered with Laumin resin. The specimens studied are stored in the Naturhistorisches Museum Basel under the access number NHMB: Alt:Hy-01 and Alt:Hy-02.

3.5 Systematic palaeontology

Order: Hymenoptera Linneus, 1758

Suborder: 'Symphyta' Gerstaecker, 1867

Family: Tenthredinidae Latreille, 1804-1805

Subfamily: Allantinae Panzer, 1801

Tribe: Athaliini Benson, 1962

Genus: *Athalia* Leach, 1817

Type species: *Tenthredo rosae* Linnaeus, 1758 (= *T. spinarum* Fabricius, 1787).

Diagnosis: (modified after Benson, 1962) (1) Antennae 13-9-segmented, third segment prolonged, (2) flagellum subclavate, (2) C and Sc+R swollen as almost to obliterate cell C, (3) origin of M in fore wings from Rs+M after the latter has left Sc+R, (4) abscissa of Rs short (5) 2m-cu present, (6) anal cell complete with oblique cross vein, (7) cell 1M angular anteriorly, and (8) tarsal claw simple. *Athalia vetueclesiae* n. sp.

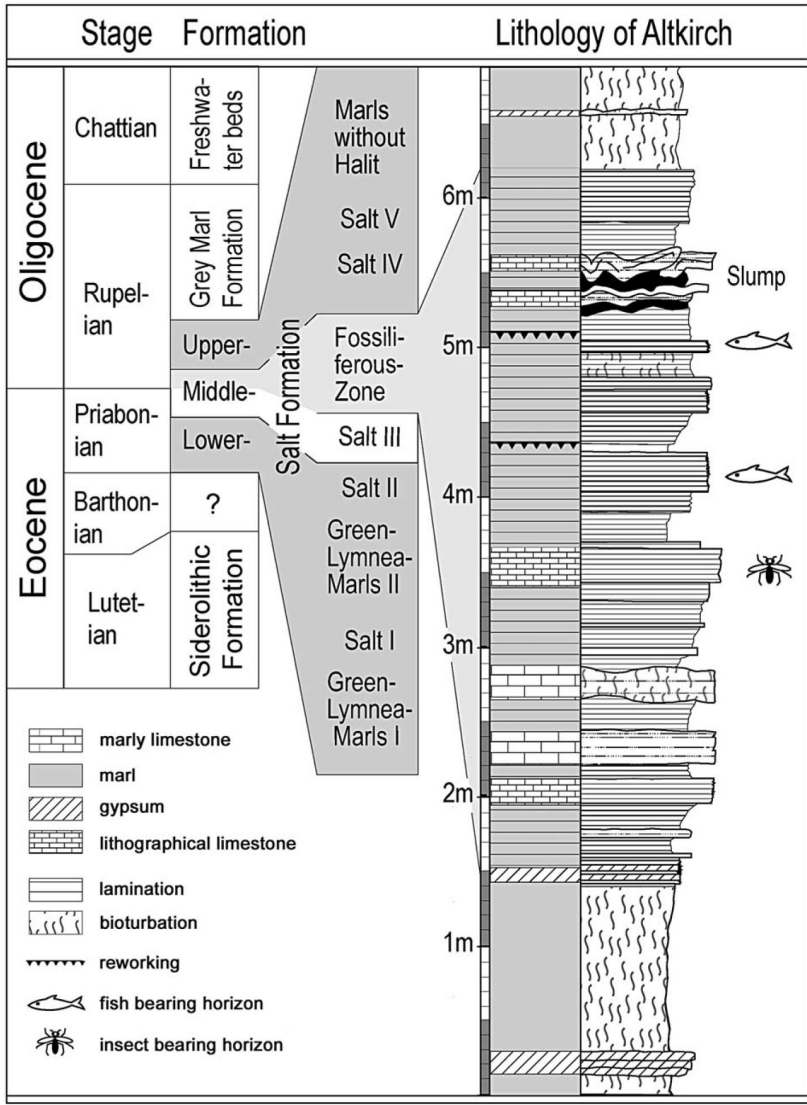


Figure 3.2: Fig. 2. Stratigraphical position of the *Athalia vetuecclesiae* n. sp. specimens. Left: chronostratigraphical correlation with Mediterranean Stages. Middle: Rhine Graben syn-rift Formations with close-up of the main stratigraphical subunits of the Salt Formation in the Potassic Basin. Right: close-up of the outcrop of the Fossiliferous Zone in the Reberg quarry/ Altkirch including meter scale, lithology and observed section. Stratigraphy according to Blanc-Valleron and Schuler (1997).

Etymology: From Latin for 'old' and 'church', in reference to the type-locality Altkirch.

Holotype: Alt:Hb-02, probably ♀, leg. J. J. Brocks at the Altkirch locality, 'Rebberg' quarry /Holcim AG, 'Zone fossilifère', x = 7°14'50"/y = 47°37'75", France.

Referred material: Alt:Hb-01, leg. S. Hinsken at the Altkirch locality, [see above], France.

Type locality and horizon: Altkirch locality, ['Rebberg' quarry /Holcim AG, 'Zone fossilifère', 7°14'50" E/ 47°37'75"N, France. Middle Salt Formation, 'Zone fossilifère', which can be correlated with the Horizon No. 6 of Gaudant and Burkhardt (1984).

Diagnosis: This species is most similar to the *Athalia vollenhoveni*-group. *A. vetuecclesiae* n. sp., however, can be distinguished by (1) extended labrum, (2) medially excised clypeus, and (3) 6th flagellomere prolonged.

Dimensions (in mm): Total body length 6.92, head length 1.02, head width 1.92, interocular space 1.92, diameter of antennae socket 0.15, length of flagellomere III-VIII: 0.38, 0.15, 0.17, 0.27, 0.17, 0.16, length of inner hind tibial spur 0.2, length of tarsal segment I-V: 0.97, 0.33, 0.25, 0.1, 0.24, wing length 6.76.

Description (Figs. 3-5): Head more or less rectangular. Compound eyes strongly converging below and emarginated. Ocelli not enlarged. Antennal sockets near base of clypeus, separated by less than antennal socket diameter. Malar space shorter than basal mandibular width. Mandible with strong apical tooth. Labrum elongated, covering apical edge of mandibles. Clypeus medially shorter than distance between antennal sockets, apical margin doubly arcuate (Fig. 4B), supraclypeal area, face, and vertex smooth. Antennae probably composed of nine segments, scarcely longer than width of head. Sixth segment prolonged and from the seventh segment onwards longer than broad (Fig. 4E). Last two segments fused to a small club. Wings strongly infuscated; stigma and venation black. Basal vein straight and strongly basal to cu-a. First abscissa of Rs short, cells R and 1R barely touching. Cell 1M angular anteriorly. Marginal cell apex slightly bent away from anterior wing margin. 2rs originating beyond midpoint of pterostigma. 3rs-m entering marginal cell in its apical half. 2m-cu slightly arched and distad 2rs-m by three times vein width. Posterior anal vein fused to anterior anal vein in the middle of anal cell, not reaching hind wing margin. Mesonotum black. Inner hind tibial spur shorter than apical width of tibia (Fig. 4H). Tibiae and tarsal segments of hind legs broadly ringed with black. Claws simple.

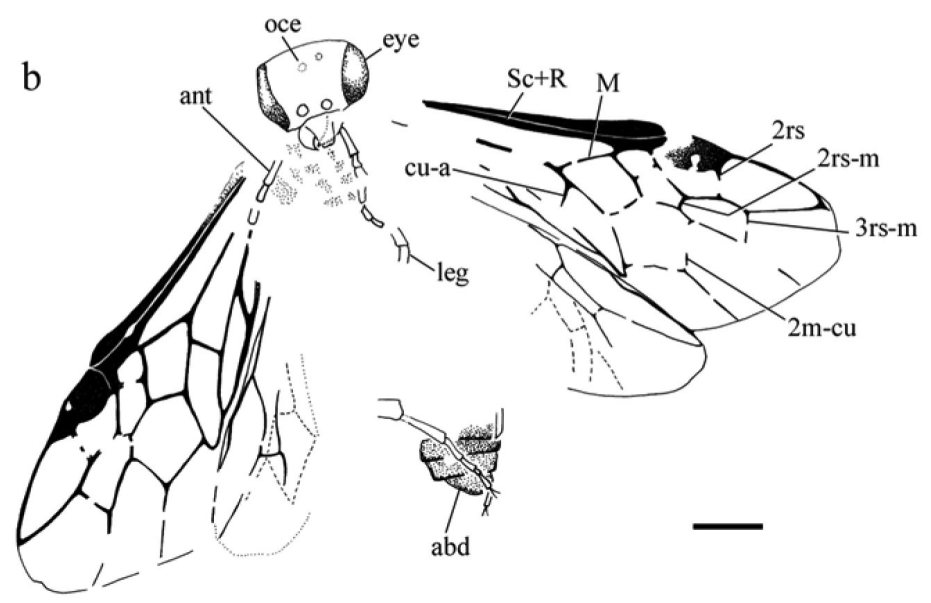
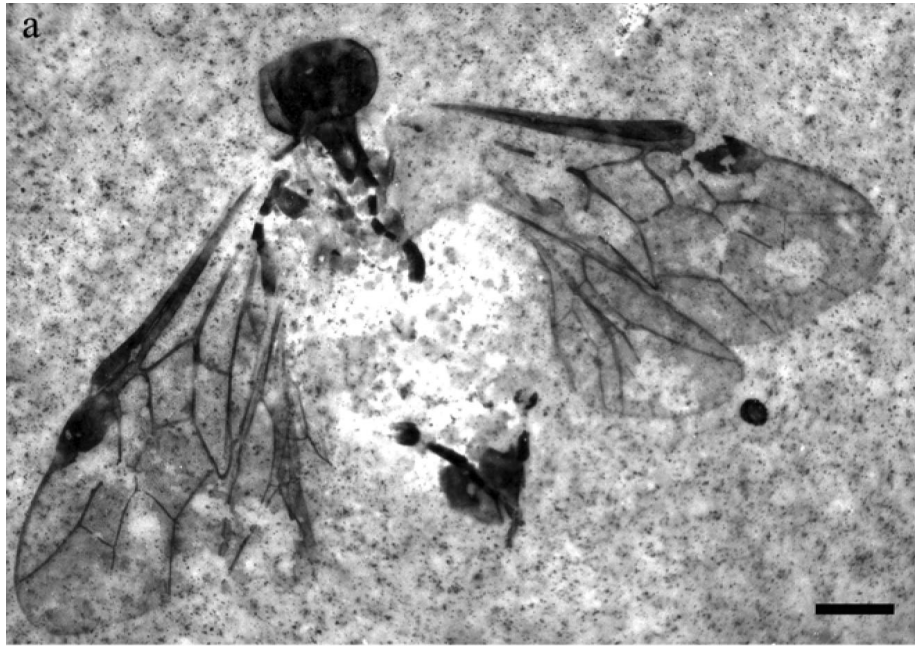
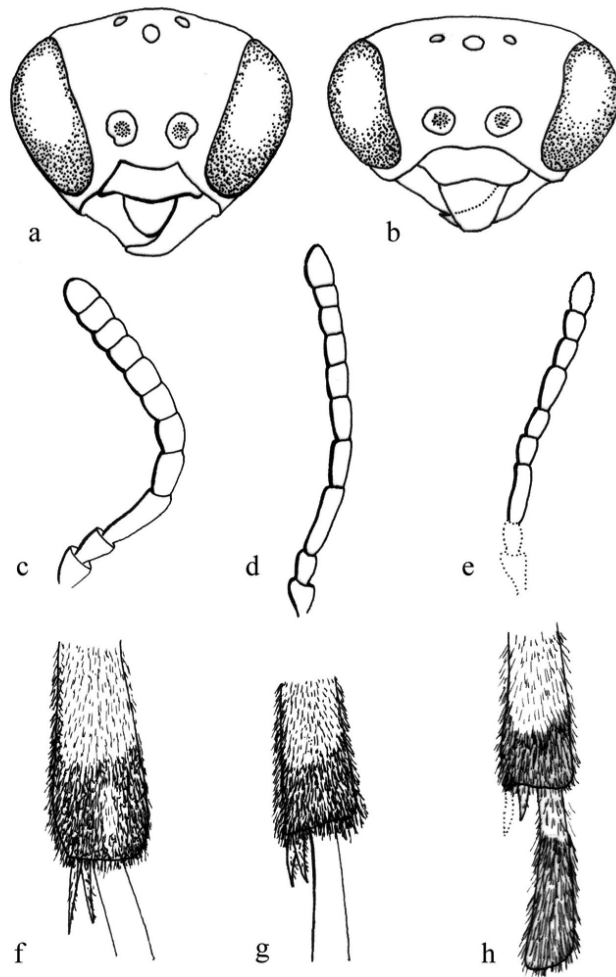


Figure 3.3: *Athalia vetuecclesiae* n. sp. (A) Photomicrograph of holotype specimen (Hb-02); (B) Camera lucida drawing of holotype specimen (Hb-02)

Figure 3.4: Face without antennae, antennae, and apex of hind tibia of different *Athalia* specimens. (A, F) *A. rosae* (4). (C) *A. glabricollis* (4). (D) *A. lugens* (4). (B, E, H) *A. vetuecclesiae* n. sp. (reconstruction).



3.6 Discussion of taxonomy

Although not complete, the fossils are well preserved and show all characteristic features such as head structure, antennae and wing venation, necessary to admit a determination on generic level. An important character to distinguish the Tenthredinidae from most other families of the Tenthredinoidea s.s. is the 9-segmented antenna. This type of antenna is found in the diverse genera of the subfamilies Selandriinae, Tenthredininae, Nematinae, Allantinae. In particular members of the Athaliini show a progressive reduction in antennal segments from 18-21 of *Hennedyia* and *Hennedyella* to 10(9)-13 of *Hypsathalia* and *Athalia* (Benson, 1962). However, the antennae are distinctly more apomorphically developed in *Athalia* than in the other members of the Athaliini (i.e., antennae have more segments in the former). Fig. 3. *Athalia vetueccle-*

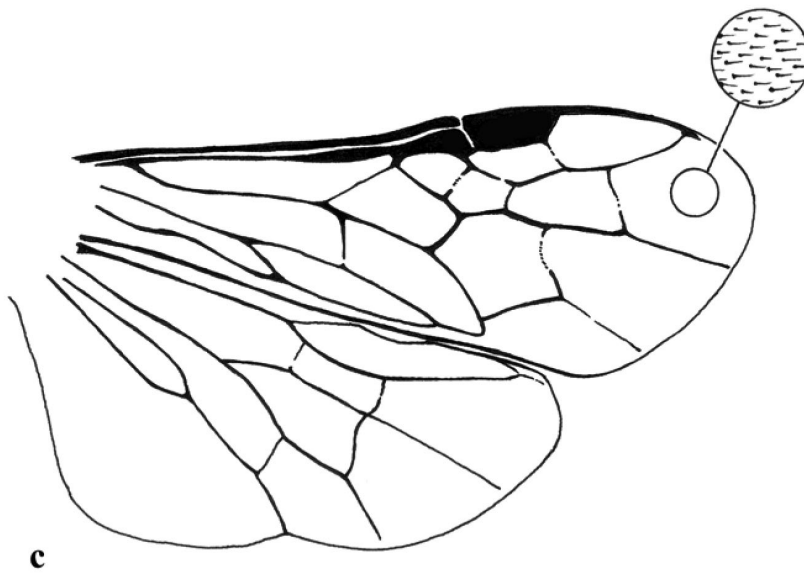
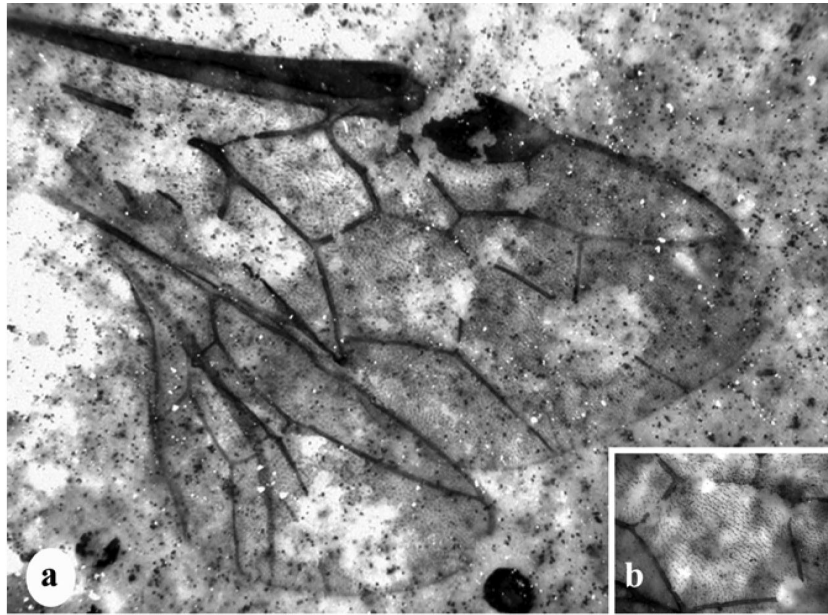


Figure 3.5: *Athalia vetuecclesiae* n. sp. (A) Photomicrograph of left fore and hind wing (Hb-02). (B) Enlarged photomicrograph of the strongly infuscated wing membrane (Hb-02). (C) Reconstruction of wing venation of *A. vetuecclesiae* n. sp.

siae n. sp. (A) Photomicrograph of holotype specimen (Hb-02); (B) Camera lucida drawing of holotype specimen (Hb-02). The wing venation of the fossil specimens excludes the Selandriinae, Tenthredininae and Nematinae as possible candidates, but it is highly similar to representatives of the Allantinae. Within Allantinae, preserved details of the fossil wings suggest membership to the genus *Athalia* within the tribe Athaliini (Fig. 3). Characteristic for Athaliini, and also observed in the fossil specimens, is the presence of the first abscissa of Rs (Fig. 3; MacGillivray, 1906; Schulmeister, 2003b; Vilhelmsen, 2001). Moreover, in addition to the previous character, C and Sc+R are swollen as almost to obliterate cell C, and the third flagellomere is prolonged, a combination of characteristics solely known from *Athalia* (pers. commun. Dr. S. Schulmeister). The fossil *Athalia* specimens show even more a mosaic of characters common to different *Athalia*-groups. Interestingly, this species appears most similar in respect to the clypeus structure and to the infuscated wings (Fig. 5b) to the extremely rare *A. vollenhoveni*-group represented by only six species from Africa (Benson, 1962). Both, the new species and the representatives of the vollenhoveni-group, have a clypeus with an apical doubly arcuate margin. Aside from the characters given above, the new species can be distinguished from the members of the *A. vollenhoveni*-group by the antennal structure and the length of spurs of the hind tibia. Exceptional long spurs occur in *A. armata* of the *A. furvipennis*-group (Benson, 1962). In *A. vetuecclesiae*, the antennal segments are from the seventh segment onwards only inconspicuously longer than broad. In contrast, in the *A. vollenhoveni*-group, all flagellar segments are longer than broad. Moreover, the spurs of the hind tibia are longer than the width of tibia in the *A. vollenhoveni*-group, but shorter in *A. vetuecclesiae*. Regarding the form of the elongated labrum in the *A. vollenhoveni*-group, the new species is most comparable to representatives of the *A. bicolor*-group (in particular *A. bicolor* mainly distributed in southeastern Europe and the eastern Mediterranean) and the *A. furvipennis*-group (in particular *A. mellis* only known from Africa) (Benson, 1962). The fossil species presented herein is most similar to the *A. vollenhoveni*-group and is presumably the basal most taxa of *Athalia* and thereby of the Tenthredinidae* sensu Schulmeister (Schulmeister, 2003a,b) as a whole (Fig. 6). For these reasons it may be advisable to place *Athalia vetuecclesiae* n. sp. near members of the *A. vollenhoveni*-group once a cladistic analysis of the Tenthredinidae* has been finalized. It does seem reasonable, however, that the Tenthredinidae* as a whole must be quite ancient. Each of the major representatives of the Tenthredinoidea s.l. probably arose and became differentiated rapidly at the end of the Cretaceous, with subsequent diversification within each lineages progressing from that time on (Rasnitsyn and Quicke, 2002; Zhelochovtzev and Rasnitsyn, 1972).

3.7 Palaeoenvironmental implications

Fossil insects are often good palaeoclimatic indicators. As insects are poikilotherm, their metabolism is closely adjusted to the thermal conditions of their

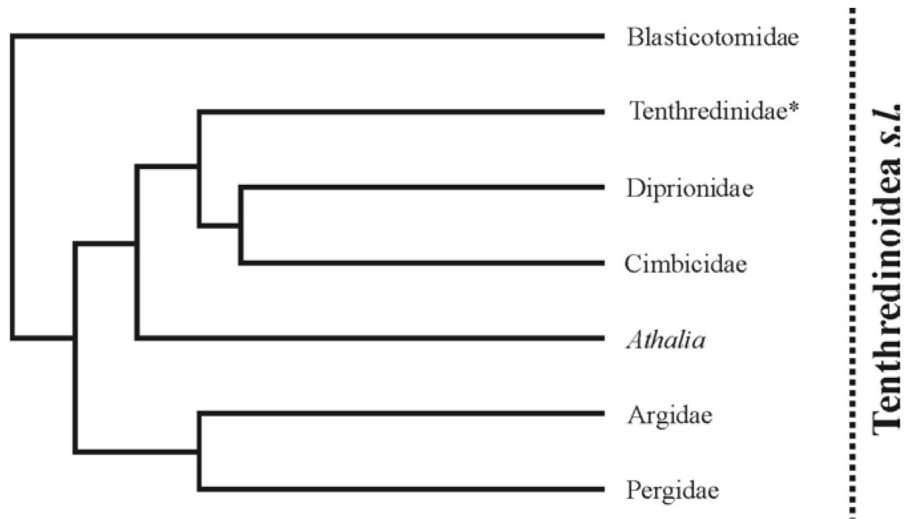


Figure 3.6: Phylogeny of the Tenthredinoidea s.l. (modified after Schulmeister, 2003a). Tenthredinidae are still indicated as a paraphyletic grade, with respect to the remaining Tenthredinoidea

habitat. Therefore, single species, and often also higher taxa, are restricted to a specific climatic realm. Moreover, insect species and genera have a particularly long geological life-span, commonly many million years (Lutz, 1990; Rust, 1999; Wappler, 2003a,b). Fossil insects have proven to be a useful and reliable indicator for reconstructing ancient climate and environment ('nearest-living-relative method'). They are sensitive indicators of climate, and they could be, in a sense, a thermometer of the past. Although physiological aspects are not preserved in fossils, it is possible to examine morphological characters that show strong correlations with climate. From these clues, the occurrence of *Athalia sp.* in deposits of the basal Oligocene could be regarded as an implication for climatic change in the Palaeogene of Central Europe coherent to the global Eocene-Oligocene boundary 34 Myr ago (Collinson, 1992; Prothero, 1994; Wolfe, 1992). Nevertheless, the vegetation distribution indicates a gradual trend from the Eocene paratropical/subtropical evergreen forest vegetation through vegetation, with an increasing proportion of temperate deciduous elements resulting in the Oligocene in establishments of broad-leaved mixed deciduous and evergreen forests across Eurasia between about palaeolatitudes 55° and 40° north (Collinson, 1992). Further evidence from leaf floras, palynology and sedimentology seems to indicate that the belt with common sclerophylls in southern Europe was, at least in places, a vegetation adapted to a humid warm temperate climate but with a slighter drier interval, probably in winter (Collinson, 1992; Mai, 1995; Prothero, 1994). These trends are also identical in the ecological diversity pattern of mammals. In particular, the mammalian ecological diversity is suggestive for drier and more open habitats in southern France

(Franzen, 1968; Hooker, 1992). Evidence from the palaeoecology of mammals for drier more open habitats in the Oligocene has been put forward for Europe. In western Europe, the transition is more gradual with the loss of paratropical elements and incoming of deciduous elements from the late Middle Eocene (Collinson, 1992). Typical leaf floras of the Late Eocene have been interpreted as evergreen to semi-evergreen mesophilic, e.g., Célas, France (leaf assemblage illustrated by Mai (1995)). Similarly, an 'aridisation' is also reflected in the highly diverse insect palaeofaunas from Céreste (Lutz, 1984a, 1985a; Nel, 1991; Schmidt-Kittler and Storch, 1985) or Florissant (Meyer, 2003). The abundance of distinctly specialized insect taxa that as far as known primarily inhabit open meadows to fairly dry rangelands does well correspond with the climatic change at the Eocene/Oligocene transition and supports this theory (Collinson, 1992; Nel et al., 1993; Pfretzschner, 1998; Wappler, 2004). If the climatic requirements of *A. vetuecclesiae* n. sp. were comparable to its very close and distinctly specialized living relatives, then the appearance of this insect confirms that the shift to a 'cooler' climate had already occurred when the laminated carbonates of the Fossiliferous Zone were deposited. This interpretation is also supported by other plant and animal fossils recovered at the Altkirch locality. The dominance of conifer remains (Schuler, 1990) and the occurrence of salmonid fishes (smelts: Gaudant and Burkhardt, 1984), are typical for temperate zones. Clearly, the nearest-living-relative method for estimating palaeoclimate, whether used with plants or insects, present contradictions (Meyer, 2003; Nel, 1997). Nevertheless, the climate shift from the Eocene to the Oligocene opened a probably vast new habitat for *Athalia* in the Palaearctic region and might mark the onset of a major radiation of the genus. So *Athalia* probably dispersed to, or persisted in higher latitudes, where most of their descendants remain today.

Acknowledgements

We are indebted to Dr S. Schulmeister (New York), Dr M.S. Engel (Lawrence) for providing valuable advices to the Tenthredinidae, and two anonymous reviewers for comments on the manuscript. In particular, we would like to thank Dr R. Güsten (Darmstadt) for the loan of several pinned *Athalia* specimens from the collection of the HLMD (Hessisches Landesmuseum Darmstadt). We are also grateful to Prof. Dr. J. Rust (Bonn) for providing valuable advice. This work would not have been possible without the generous support of M. Moser, Director of Holcim AG Altkirch, who provided access to the quarry and supported S. Hinsken during work on his Masters thesis. We also greatly appreciate the technical support of the miners.

Chapter 4

Graben width controlling syn-rift sedimentation: The Palaeogene southern Upper Rhine Graben as an example

Sebastian Hinsken, Kamil Ustaszewski, Andreas Wetzel

Geologisch-Paläontologisches Institut , Universität Basel, Switzerland

Article published (2007) in: International Journal of Earth Sciences 96:979-1002

4.1 Abstract

Eocene to Early Oligocene syn-rift deposits of the southern Upper Rhine Graben (URG) accumulated in restricted environments. Sedimentation was controlled by local clastic supply from the graben flanks, as well as by strong intra-basinal variations in accommodation space due to differential tectonic subsidence, that in turn led to pronounced lateral variations in depositional environment. Three large-scale cycles of intensified evaporite sedimentation were interrupted by temporary changes towards brackish or freshwater conditions. They form three major base level cycles that can be traced throughout the basin, each of them representing a stratigraphic sub-unit. A relatively constant amount of horizontal extension (ΔL) in the range of 4 to 5 km has been estimated for the URG from numerous cross-sections. The width of the rift (L_f), however, varies between 35 and more than 60 km, resulting in a variable crustal stretching factor (β) between the bounding masterfaults. Apart from block tilting, tectonic subsidence was, therefore, largely controlled by changes in the initial rift width (L_0). The along-strike variations of the graben width are responsible for the development of a deep, trough-like evaporite basin (Potash Basin) in the narrowest part of the southern URG, adjacent to shallow areas in the wider parts of the rift such as the Colmar Swell in the north and the Rhine Bresse Transfer Zone (RBTZ) that delimits the URG to the south. Under a constant amount of extension, the along-strike variation in rift width is the principal factor controlling depot-centre development in extensional basins.

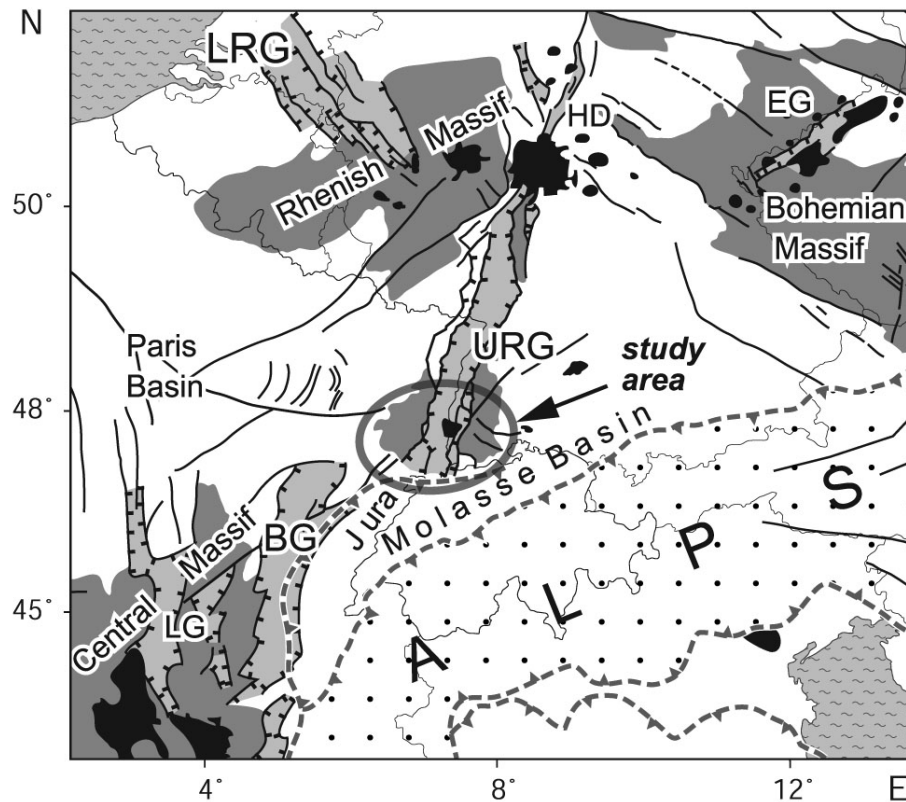


Figure 4.1: The southern part of the URG (encircled) occupies a central position within the Central European Rift System. Rift basins (light grey): URG Upper Rhine Graben, HD Hessian Depression, EG Eger Graben, BG Bresse Graben, LRG Lower Rhine Graben; Cenozoic volcanics (black); the Variscan massifs (dark grey) are bounded by inherited faults (black lines) and rifts (modified from Dèzes et al., 2004).

4.2 Introduction

The Upper Rhine Graben (URG) forms the central part of the Cenozoic Central European Rift System, traversing Europe from the Mediterranean to the North Sea (e.g. Dèzes et al., 2004, Fig. 7.1). Graben formation is thought to have resulted from uniform crustal extension, involving the reactivation of numerous pre-existing faults under a temporally changing stress regime (Illies and Greiner, 1978; Schumacher, 2002). However, the URG comprises several sub-basins showing distinct differences in terms of amount and timing of subsidence, and hence of sediment fill (Sittler, 1969; Sissingh, 1998).

In the URG intense exploration for hydrocarbons and potash salts has yielded a large data set (drillings, seismic lines) that has become accessible during the last decade. Due to Neogene uplift and erosion, the rift flanks and marginal

parts of the basin are exposed and accessible for field investigations. Numerous recent studies have provided new insights into the basin architecture and graben evolution (e.g. Schumacher, 2002; Derer et al., 2003; Berger et al., 2005a,b; ?; Rotstein et al., 2005; Ustaszewski et al., 2005a). Nonetheless, the URG is lacking 3D seismic coverage and many aspects concerning the age and timing of crustal movements, the palaeogeography and the thermal history are still a matter of debate.

In the light of newly available data the sedimentary record of the URG has been reviewed applying the new concept of genetic stratigraphy (*sensu* Cross and Lessenger, 1998). Since such investigations address quantitative aspects of sedimentation, they may provide important information about tectonic graben development. Additionally, graben volume, extension and crustal stretching factors have been estimated using two new cross-sections, located in different parts of the area, and some published cross-sections across the northern URG have been re-evaluated. A detailed basin analysis can elucidate how sedimentation was affected by "syn-rift" tectonic movements and thus contributes valuable information on rifting dynamics (e.g. Leeder and Gathrope, 2002).

The purpose of this study is to outline the tectono-sedimentary basin evolution of the southern URG during the late Middle Eocene to Early Oligocene main rifting phase. Special attention is paid to the along-strike variations in the crustal stretching factor β and to the basic relationships between sedimentation and tectonics during extensional basin development.

4.3 Geological context

4.3.1 Study area

The study area comprises the southern part of the URG, between the Colmar Swell in the north and the Jura Mountains in the south (Figs. 2-4). Today the area is an elevated zone that covers the watersheds between the North Sea (Rhine) and the Black Sea (Danube) as well as the North Sea and the Mediterranean (Doubs) (Fig. 7.3). This regional topographic dome coincides with a decreased crustal thickness of 24 km below the Mulhouse Potash Salt Basin (Potash Basin).

The eastern and western parts of the southern URG show a slight asymmetry. The western part represents an elongated half graben, while the eastern part is dissected into a number of antithetic blocks (Fig. 7.4). The Vosges to the west and the Black Forest to the east form the graben shoulders of the southern URG; on both sides the crystalline basement is exposed. Towards the south the graben is delimited by the frontal folds of the Jura Mountains. Within the study area four structural domains are distinguished (Fig. 7.2):

Potash Basin (e.g. Courtot et al., 1972; Blanc-Valleron and Schuler, 1997, Fig. 7.4); it represents the depo-centre of the southern URG. There, up to 1800 m thick evaporites and marls accumulated during the late Middle Eocene to Early

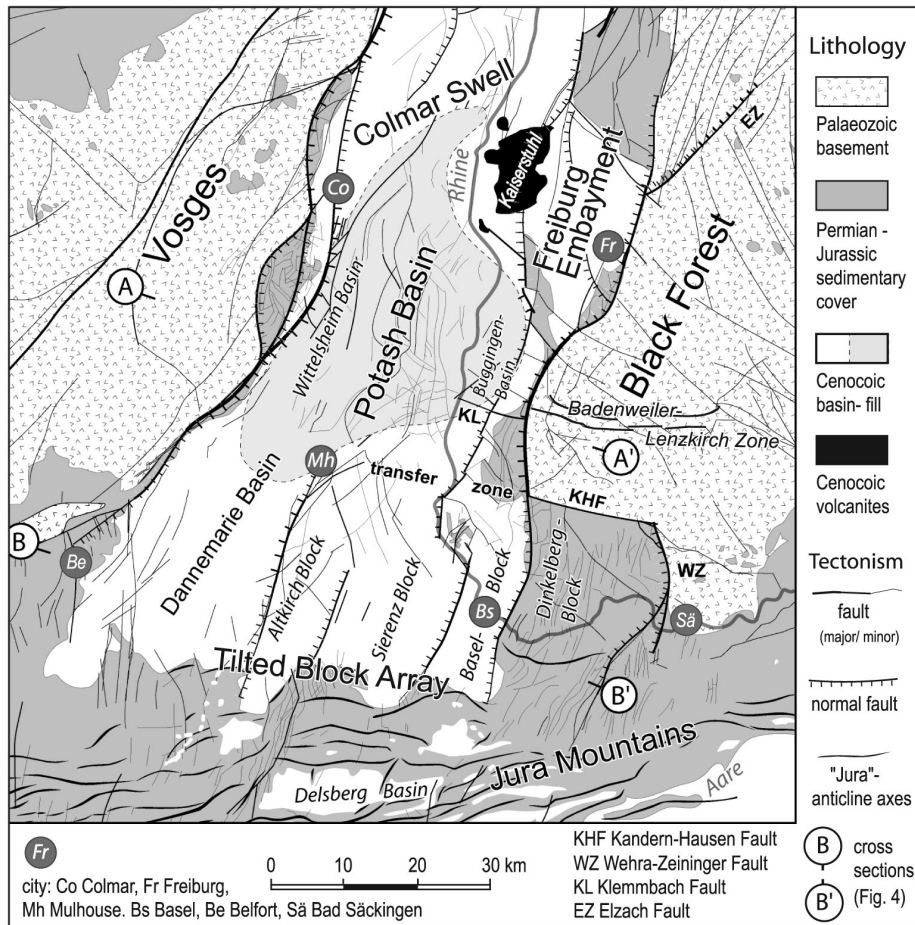


Figure 4.2: Schematic geological map of the southern URG. The depot-centre of the Mulhouse Potash Salt Basin (Potash Basin) is located in the narrowest part of the graben that is flanked by the highest mountains of the Vosges and Black Forest. Towards the south the graben widens considerably where it is bordered by the Jura Mountains.

Oligocene main rifting stage. The salt partly forms diapirs and the basin fill is overprinted by salt tectonics resulting in shallow, listric low-angle detachments as well as block tilting and bending of incompetent layers (see Blanc-Valleron, 1991; Lutz and Cleintuar, 1999). The Potash Basin is bordered to the east and west by major normal fault zones with up to several 1000 m throw. In the basin interior the throw on normal faults is usually less than a few hundred metres (e.g. Bertrand et al., 2005). Two major sub-basins, one in the west and one in the east, represent the hanging-wall half grabens of the large border faults. The Wittelsheim Sub-Basin to the west extends for about 40 km in N-S direction between Colmar and Mulhouse. The Buggingen Sub-Basin to the east extends

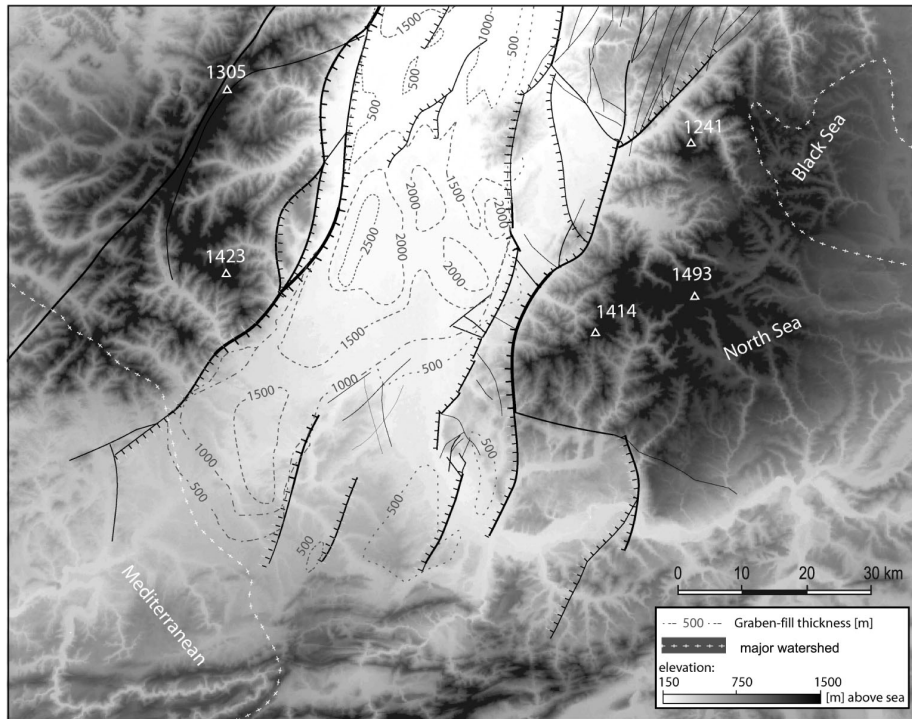


Figure 4.3: Digital elevation map of the study area on which a simplified fault grid and isopaches of graben fill (broken lines; thickness in m) have been superimposed. This part of the graben was strongly uplifted and exposed during the Neogene. The area forms an intra-continental high, gathering the watersheds between the North Sea, the Black Sea and the Mediterranean.

for about 15 km in N-S direction between the Freiburg Embayment and the Klemmbach Fault (Fig. 7.2).

Colmar Swell and *Freiburg Embayment* delimit the Potash Basin to the north. They are characterized by relatively thin syn-rift deposits. The Colmar Swell forms an elevation, crossing the URG obliquely between Colmar and north of the Kaiserstuhl, where it passes into the northern part of the Freiburg Embayment.

Tilted Block Array between Belfort and Bad Säckingen (Figs. 7.2, 7.4b); it is located at the southern end of the URG. The transfer zone between Mulhouse and the Wehra-Zeiningen Fault marks the transition to the Potash Basin (Fig. 7.2). The Dannemarie Basin forms the southern prolongation of the Wittelsheim Sub-Basin (e.g. Wagner, 1938) and contains the thickest syn-rift deposits of the southernmost graben domain. This basin changes from a symmetrical graben in the north to a half graben in the south. The Tilted Block Array rises progressively towards the eastern graben shoulder.

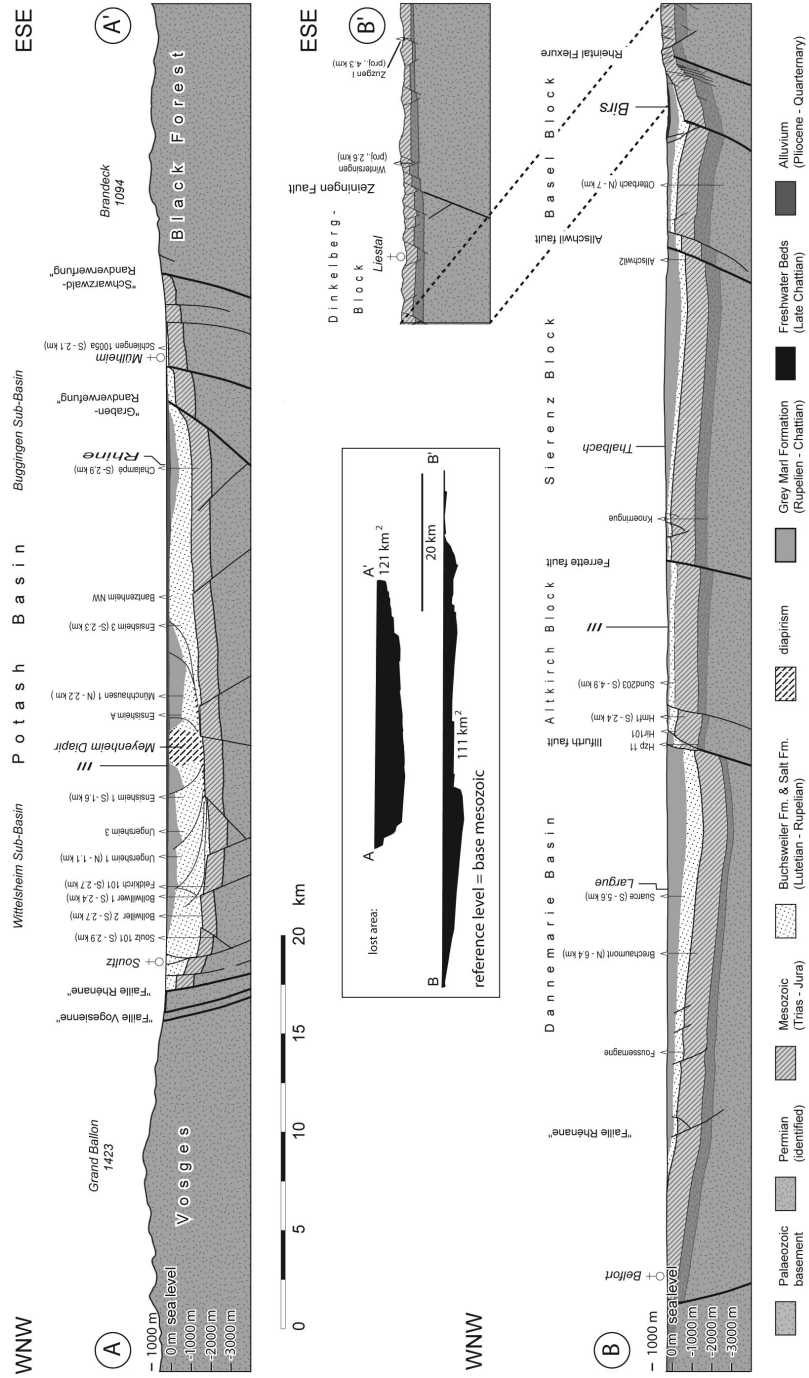


Figure 4.4: Cross-sections through the Potash basin (A-A') and the southern end of the URG (B-B') based on compilations of subsurface data. The narrow Potash Basin (A-A') hosts thick syn-rift deposits (marls and evaporites) and was partly affected by salt tectonism. It is bordered by normal faults with some kilometres throw. The southernmost graben compartment (B-B') is much wider and comprises several E-dipping tilted blocks. Extension measured by length balancing gave 4.6 km (A-A') respectively 4.2 km (B-B'). Lost area (A_{lost}) of A-A' yields 121 km², of B-B' 111 km² (centre). For location of cross-sections see Figure 7.2.

It comprises from W to E the southern Dannemarie Basin (?), Altkirch Block, Sierentz Block (Rotstein et al., 2005), Basel Block and Dinkelberg Block. In map view, the hanging wall half grabens of these blocks appear as Tertiary filled embayments that encroach onto the front of the Jura Mountains (Fig 7.2). A mosaic of small fault blocks occupies the western part of the Mulhouse-Wehra Transfer Zone. In the east, however, this zone is represented by a distinct dextral tear fault, the Kandern-Hausen Fault. This fault juxtaposes the Dinkelberg Block against the Black Forest and forms the connection between the Black Forest Border Fault and the Wehra-Zeiningen Fault.

Jura Mountains ; they consist of Mesozoic pre-rift series and contain several small Tertiary basins, such as the Laufen Basin and the Delsberg Basin (e.g. Laubscher, 1998; Berger et al., 2005a). During the Palaeogene these basins were occasionally connected to the southern URG and/or to the Molasse Basin (e.g. Berger et al., 2005a). Palaeogene deposits onlap onto monoclines of pre-rift series at the southern end of the graben and hence document its stable position since that time (Ustaszewski et al., 2005a). The southern end of the URG forms part of the so-called Rhine Bresse Transfer Zone (RBTZ), along which crustal extension across the URG was transferred via a diffuse zone to the Bresse Graben (e.g. Laubscher, 1970; Illies, 1981; Ustaszewski et al., 2005b).

4.3.2 Graben evolution

Palaeozoic basement configuration

The basement below the URG is part of the Variscan internides comprising several terranes (e.g. Franke, 1989). Pre-existing faults within the crystalline basement were reactivated during the formation of the URG (e.g. Schumacher, 2002). They had originally developed during the late phases of the Variscan orogeny (e.g. Cloos, 1939), as well as during Late Palaeozoic wrench tectonics that led to the development of several transtensional intramontane basins, the so-called Permo-Carboniferous Troughs (e.g. Ziegler, 1990; Wetzel et al., 2003) and fault zones, including the NNE-trending "Rhenish Lineament" (Boigk and Schöneich, 1970).

The Permo-Carboniferous Burgundy Trough (e.g. Boigk and Schöneich, 1970) underlies the area of the RBTZ, the northern Jura Mountains and the adjacent part of the southern URG (Ustaszewski et al., 2005a). In many instances, Cenozoic graben structures and Palaeozoic basement structures coincide spatially. The Potash Basin, for instance, is bordered to the SE by the Klemmbach Fault (Schnarrenberger, 1925), forming the prolongation of the E-W striking Badenweiler-Lenzkirch Zone (Wagner, 1938). This zone has been interpreted as a Variscan suture (Löschke et al., 1998). To the NE, the boundary of the Potash Basin coincides with a NW-trending dike swarm within the basement of the Black Forest (see Metz, 1970). The Dinkelberg Block, as a further example, is juxtaposed against the Black Forest along Late Palaeozoic shear zones (Echtler and Chauvet, 1992).

Mesozoic pre-rift sedimentation

During the Triassic and Jurassic the study area belonged to the southern part of the epicontinental Germanic Basin, where about 1.2 to 1.5 km of sediments accumulated (e.g. Geyer and Gwinner, 1986). Lateral facies and thickness changes of the Mesozoic sediments point to the reactivation of Palaeozoic basement structures (Wetzels et al., 2003; Ziegler et al., 2004b).

During the Triassic depositional environments changed repeatedly between continental and restricted shallow marine conditions. Evaporites formed during the Middle and Late Triassic (e.g. Geyer and Gwinner, 1986). During the Jurassic predominantly shales and carbonates accumulated in a subtropical epicontinental sea. Carbonate platforms developed during the Middle Dogger and the Malm (e.g. Ziegler, 1990). Cretaceous sediments are lacking in the URG area, because of non-deposition or erosion. Therefore, the area is considered a lowland close to base level during the Late Cretaceous, but this is still a matter of debate (e.g. Ziegler, 1990; Mueller et al., 2002; Timar-Geng et al., 2006).

The earliest hint of rift-related activity is minor volcanism during the Paleocene about 60 Ma ago (Keller et al., 2002). Prior to rift-induced subsidence, palaeosols on top of the pre-rift sediments document weathering and denudation before Early to Middle Eocene times. Below this erosional unconformity the stratigraphic age of the Mesozoic subcrop increases generally towards the north with superimposed local domes and depressions (e.g. Sittler, 1969, Fig. 4.5). This implies a general southward tilt of an undulating pre-rift land surface.

The oldest known syn-rift sediments in the southern URG are red iron-pisolite-bearing (feralitic) palaeosols (Siderolite Formation) and freshwater limestones (Buchweiler Formation). Mammalian remains found therein provided a Late Lutetian age (Schmidt-Kittler, 1987). The onset of lacustrine sedimentation in the basin interior, as well as the local accumulation of residual clays in wedge-shaped grabens along the main border faults (Hinsken, 2003) and within the adjacent Jura (Laubscher, 2004) clearly indicate the onset of tectonic movements by the Middle Eocene at the latest.

Increased rifting during the late Middle Eocene to Early Oligocene (Lutetian-Rupelian) led to the formation of several evaporitic sub-basins, within the central and the southern URG including the Potash Basin (e.g. Blanc-Valleron and Schuler, 1997). In these sub-basins the environment changed repeatedly between terrestrial, fluvial, lacustrine, brackish and evaporitic (e.g. Düringer, 1988).

In the northern and central URG, deposits of that time are subdivided in the (basal) Green Marl Formation (*Lymnaeenmergel*) and (up-section) the Pechelbronn Beds (*Pechelbronn Schichten*), whereas in the southern URG deposits of that time constitute the Salt Formation (*Salzfolge*). The Salt-Formation represents the majority of graben-fill in the southern URG, in particular in the Potash Basin, where it contains large amounts of evaporites. Fault-related distribution of facies and thickness implies that the Salt Formation represents syn-rift sedimentation (Düringer, 1988; Hauber, 1991; Rotstein et al., 2005). Therefore it is the centre of interest in this study.

During the Middle Oligocene (Late Rupelian), a marine transgression flooded

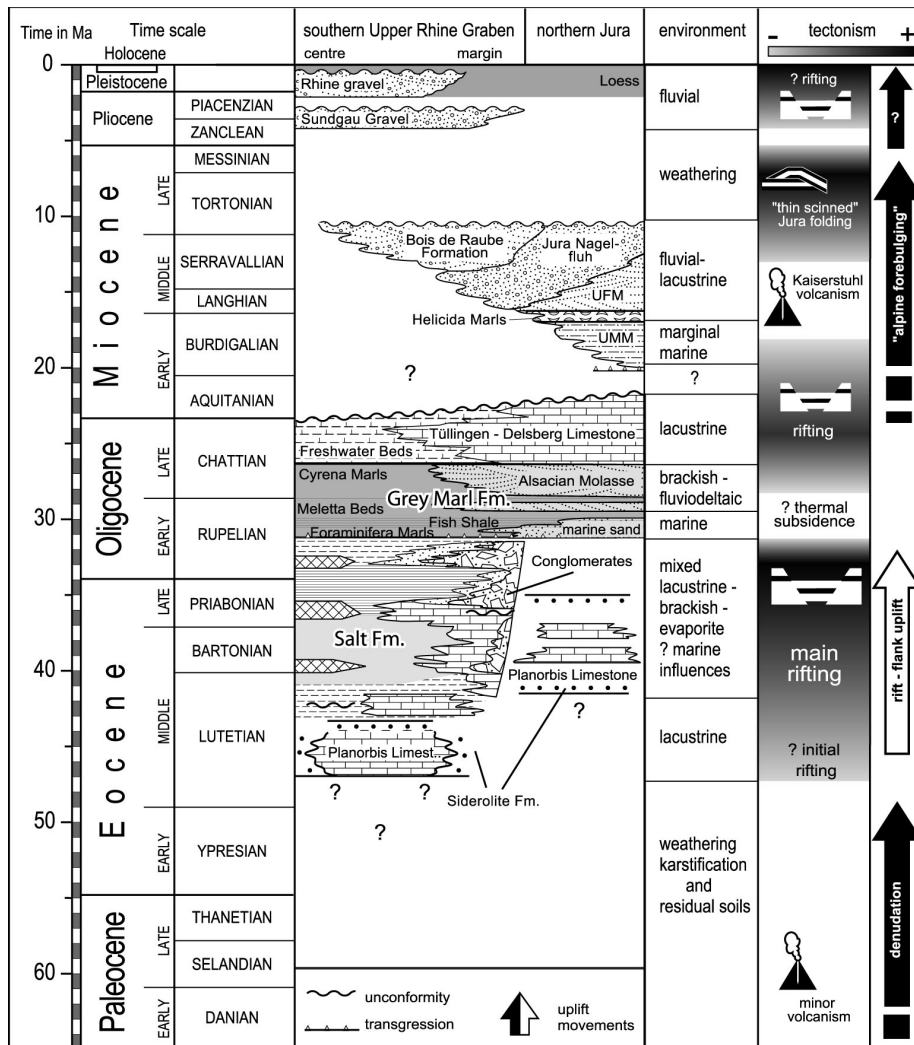


Figure 4.5: Stratigraphic chart illustrating the Cenozoic evolution of the southern URG and northern Jura Mountains modified after Giamboni et al. (2004) and own observations; numerical ages after Gradstein et al. (2004). The Salt Formation forming the majority of graben fill in the southern URG represents the syn-rift sediments.

the URG and the area to the south. Grey muds and sands that constitute the Grey Marl Formation (*Graue Schichtenfolge*) were deposited. Minor displacements along faults occurred when the Grey Marl Formation formed (Hauber, 1991; Rotstein et al., 2005), while the coastline was shifted onto the graben shoulders and the northern Jura (Wittmann, 1952; Ustaszewski et al., 2005a). This suggests decreased rifting and the onset of increased thermal subsidence (Hinsken, 2003; Rotstein et al., 2005). The Foraminifera Marl Member (*Foraminiferenmergel*) at the base is overlain by the black shales of the Fish Shale Member (*Fischschiefer*). Laterally both pass into calcarenites of local origin at the southern end of the graben, the Marine Sand Member, interpreted as littoral facies (*Meeressand*; (Fischer, 1969)). A rich fauna indicates open marine conditions and water depths of more than 200 m (Huber, 1994). Up-section, the Meletta Shale Member (*Melettaschichten*) contains, particularly in its lower part, Alpine-derived Molasse-type sandstones, implying a connection with the "overfilled" Molasse Basin (Kuhleemann et al., 1999). Decreased faunal diversity implies prevailing deposition under brackish-marine conditions, but still with water depths of about 100 m (Huber 1994). The overlying Cyrena Marl Member (*Cyrenenmergel*) accumulated under marine, brackish and freshwater conditions. Towards the Jura it interfingers with fluvio-deltaic Molasse-type sandstones of the Alsacian Molasse Member (*Elsässer Molasse*), which are correlated with the Lower Freshwater Molasse (Kuhleemann et al. 1999).

Freshwater sedimentation prevailed inside the URG until the end of the Oligocene (Rollier, 1911). Relicts of these almost completely eroded deposits have been described from the Potash Basin, the SE part of the graben (Tüllingen Beds; *Tüllinger Schichten*) and the Jura Mountains (Delsberg Limestone; *Calcaires Délemontiens*); there, deposition continued until the Early Miocene (Berger et al., 2005a).

Sediments of Early Miocene age have not been found in the southern part of the URG, whereas approximately 1 km thick brackish deposits are preserved in the northern URG implying increased subsidence there (Derer et al., 2003). It is still a matter of debate, to which extent the lack of sediments younger than Early Aquitanian in the southern URG is due to non-deposition (discussed by Schumacher, 2002) and/or major erosion after the Early Miocene (e.g. Sissingh, 1998; Lutz and Cleintuar, 1999). However, major sediment accumulation after the Early Miocene is highly unlikely for the following reasons:

1. The (Burdigalian) Upper Marine Molasse of the Alpine foreland basin wedges out towards the north within the Jura Mountains (e.g. Berger et al., 2005a), suggesting that the southern URG was uplifted above the regional base level during this time.
2. The Middle Miocene volcanics of the Kaiserstuhl rest unconformably on faulted and deeply truncated Late Oligocene sediments (Wimmenauer, 1977).
3. Salt diapirs are restricted to the Lower Salt Sub-Formation (e.g. Larroque and Laurent, 1988; Blanc-Valleron and Schuler, 1997). As the development

of diapirs requires a considerable overburden, the lack of diapirism within the Upper Salt Sub-Formation implies that Neogene sediments did not accumulate in considerable thickness (>100 m).

4. High resolution reflection seismic data recorded on the river Rhine show a major erosional unconformity between the Plio-Pleistocene gravels and the Palaeogene graben fill sediments (P. Ziegler, pers. comm.).
5. Mean random vitrinite reflectance (%Rr) measured on Oligocene samples from the southernmost URG and the Delsberg Basin indicating low thermal maturity (Todorov et al., 1993).

During the Middle Miocene, the area of the southern URG was emergent due to lithosphere-scale folding contemporaneous with volcanic activity in the Kaiserstuhl (e.g. Ziegler et al., 2004b). The concomitant uplift and exhumation of the graben shoulders is documented by conglomerates of Middle Miocene age, the so-called "Jura Nagelfluh", which were transported southward into the northern Jura (e.g. Laubscher, 2001; Berger et al., 2005a). However, the lack of Early Miocene deposits in the southern URG implies that uplift could have already started in the Early Miocene (Schumacher, 2002).

During the Late Miocene to Early Pliocene the Jura was thrust and folded (Kälin, 1997; Becker, 2000; Giamboni et al., 2004). During the Early Pliocene (4.3 Ma), Alpine rivers entered the southern URG at its southeastern corner, flowed to the west and drained via Bresse and Rhone Grabens into the Mediterranean, depositing the so-called "Sundgau-Gravel" (Manz, 1934). During the Late Pliocene drainage changed to the modern pattern (Villinger, 1999; Giamboni et al., 2004).

4.4 Syn-rift sedimentation

The Salt Formation comprises the syn-rift sediments of the southern URG, whereas the overlying Grey Marls probably represent the late syn-rift or even the post-rift stage (e.g. Rotstein et al., 2005). The Salt Formation consists of three sub-formations and several members (Fig. 4.5; see also Fig. 4.12). Due to the rarity of fossils several stratigraphical subdivisions based on lithological criteria have been established (see Schuler, 1990). Strong intrabasinal variations of accommodation space, sediment supply as well as obvious base level fluctuations led to distinct facies changes and to the recurrent appearance of the same facies at several levels. Previous lithostratigraphical subdivisions remain, therefore, highly questionable and need to be revised. A sequential concept was developed by Düringer (1988) for the conglomerates and by Blanc-Valleron (1991) for the evaporites of the southern and middle URG. Derer et al. (2003) applied a genetic concept to the Late Eocene to Early Oligocene syn-rift deposits within the northern URG.

4.4.1 Lithofacies associations

Several lithofacies associations (LFAs) formed recurrently in the different domains of the southern URG during the late Middle Eocene to Early Oligocene (Fig. 4.6). The following LFAs are distinguished:

Conglomerate LFA (alluvial fan); it forms a belt of alluvial fans along the margins of the southern URG (Düringer, 1988). The conglomerates are mainly composed of Mesozoic limestone clasts that were eroded from the graben shoulders. Palaeocurrent directions imply transport towards the basin centre (Fig. 4.5). Continuous uplift and erosion of the graben flanks is documented by a stratigraphically inverse pebble petrography. The conglomerates interfinger with littoral sandstones and sometimes with variegated marls (Düringer, 1988).

Variegated Marl LFA (alluvial plain); variegated marls are widespread in the uppermost part of the Salt Formation. In the lower part they are restricted to the marginal areas of the basin; they are reddish in colour and interfinger with thin conglomerates and probably represent alluvial plain deposits. In the basin centre, greenish, greyish and brownish colours suggest poorly-drained conditions.

Calcareous sandstone LFA (marginal lacustrine); it occurs basinward of the conglomerate fans. The sandstones are interbedded with variegated marls, lacustrine limestones and sometimes lignites. These deposits are called "Haustein" (Förster, 1892); in this study the term "Haustein Facies" is used. It occurs along the margins of the basin, particularly in the southern graben domain. The depositional environments range from high-energy littoral settings, where cross-bedded, sometimes oolitic packstones are found, to low-energy deposits, including oncolites, stromatolites, fluvio-deltaic wackestones and reed remains (Düringer and Gall, 1994).

Lacustrine limestone LFA (mainly shallow lacustrine); it occurs predominantly in the southern part of the graben, where it dominates the lower parts of the Salt Formation ("Melania Limestone", "Planorbis Limestone"). It often formed in the vicinity of the Haustein Facies. Oncolites, stromatolites and remains of characeans and reeds document a shallow lake setting (Stucky, 2005). Often these deposits were pedogenetically overprinted (Stucky, 2005) and, hence, are assigned to a palustrine facies (*sensu* Wright and Platt, 1995). Towards the basin centre these limestones interfinger with grey to greenish marls.

Laminite LFA (moniolimnion of meromictic lake); it comprises rhythmically thin-bedded, laminated marls and lithographic limestones containing subordinate intercalations of grey, homogeneous marls. The laminites occur in the internal parts of the basin. Towards the basin margin, laminites interfinger with Haustein Facies (see below Fig. 4.8), as well as with lacustrine limestones (well

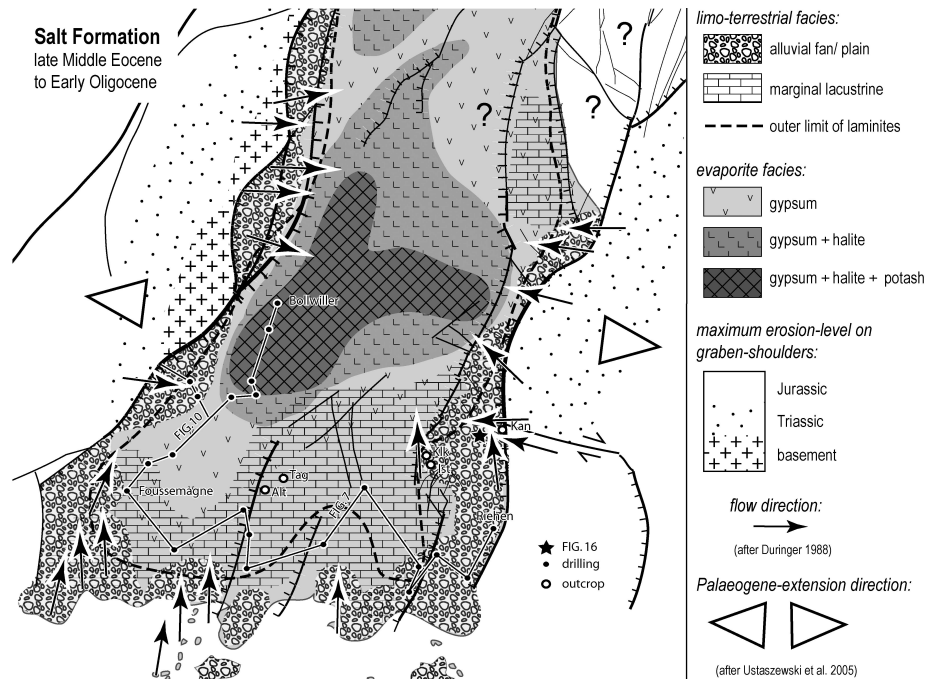


Figure 4.6: Palaeogeographic map illustrating late Middle Eocene to Early Oligocene syn-rift sedimentation within the southern URG modified from Düringer (1988); Blanc-Valleron (1991) and own observations. A limno-terrestrial facies is found in the southernmost part of the graben and in the Freiburg Embayment comprising fluvial to shallow-water sediments (Calcareous Sandstone LFA, Lacustrine Limestone LFA), whereas the basin centre yields a thick sequence of marls and evaporites. Erosion of the rift flanks is documented in alluvial fans, which formed along the graben margins. Crystalline basement had been exhumed along the crest of the masterfault footwall during the Early Oligocene. Outcrops: Kan, Kik Kleinkems, Ist Istein, Tag Tagolsheim, Alt Altkirch.

Heimersdorf 1901; Vonderschmitt, 1942). Several intervals contain monospecific mass occurrences of euryhaline taxa, insects and terrestrial plant remains (e.g. Förster, 1892; Wappler et al., 2005). Especially the "Fossiliferous Zone", in the upper part of the Middle Salt Sub-Formation, represents a marker horizon, that can be traced almost basin-wide (Wappler et al., 2005).

Because the laminites are closely associated with evaporites (Förster 1892), they are assigned to a saline facies. They are interpreted to have been deposited in an open-water environment during a meromictic lake stage, when stagnant, highly saline, oxygen-depleted waters filled the deep part of the basin (moniolimnion), overlain by an almost pure freshwater lens (mixolimnion, Hofmann et al., 1993; Hinsken, 2003). As permanent stratification of a water body requires a minimum water depth of several tens of metres (e.g. Wetzel, 1991; Talbot and Allen, 1998), the laminites are thought to represent a deepwater facies.

Grey and Green Marl LFA (e.g. open lake-brackish); it is the dominant lithology in the central part of the basin. It is interpreted as an open lake facies. However, it is not always possible to distinguish this facies from that of the Variegated Marl LFA in the sparse well-reports. Faunal remains indicate oscillations between an evaporitic and a freshwater environment (Blanc-Valleron and Schuler, 1997).

Evaporite LFA (salt lake); it occurs in the Potash Basin and consists of gypsum, anhydrite, halite, and some potash salts (Fig. 4.6), that are generally interbedded with marls. The evaporites of the Middle and Upper Salt Sub-Formations preserve depositional features (Sturmfels, 1943), whereas the evaporites of the Lower Salt Sub-Formation have been partly deformed by halokinesis (Blanc-Valleron and Schuler, 1997). The potassium salts occur only within some seams at the base of the Upper Salt Sub-Formation and are restricted to the deepest part of the Potash Basin (see below).

4.4.2 Basin-fill architecture

The distribution of the different LFAs in space and time is used to outline the basin fill architecture (Figs. 6-11). This is illustrated by a palaeogeographical map showing the distribution of characteristic lithofacies associations (Fig. 4.6), a few outcrop sections (Figs. 4.8a, 4.9), well sections (Figs. 4.9, 4.11) and cross-sections (Figs. 4.7, 4.8b, 4.10). The cross-sections shown in Fig. 4.7 and 4.10 are based on subsurface data.

Basin margin ; the graben margins are characterized by a sharp termination of the Salt Formation against growth faults or extensional flexures, whereas the Grey Marls seem to onlap the Dinkelberg Block (Fig. 4.7; well Riehen and well Reinach).

Conglomerates attributed to the Middle and Upper Salt Sub-Formations are exposed about 15 km to the north near Kandern (Fig. 4.8a), where they unconformably rest on Mesozoic sediments, that have been affected by an extensional flexure (Fig. 4.8b). Based on fossils these lower intervals are allocated to the "Fossiliferous Zone" (Hinsken, 2003; Stucky, 2005). The clastics are covered by the open marine Grey Marl Formation. At the top a major stratigraphic gap occurs which is overlain by Neogene gravels.

Basel Block and Sierentz Block ; sediment thickness of the individual stratigraphic units varies across faults implying sedimentation contemporaneous with faulting. Across these blocks sediment thickness increases towards the footwall testifying to a half graben setting, whereas the sedimentary facies on the individual blocks was quite uniform (Fig. 4.7). The separation of the Basel Block and Sierentz Block by the Allschwil Fault Zone probably occurred relatively late during the deposition of the Middle Salt Sub-Formation.

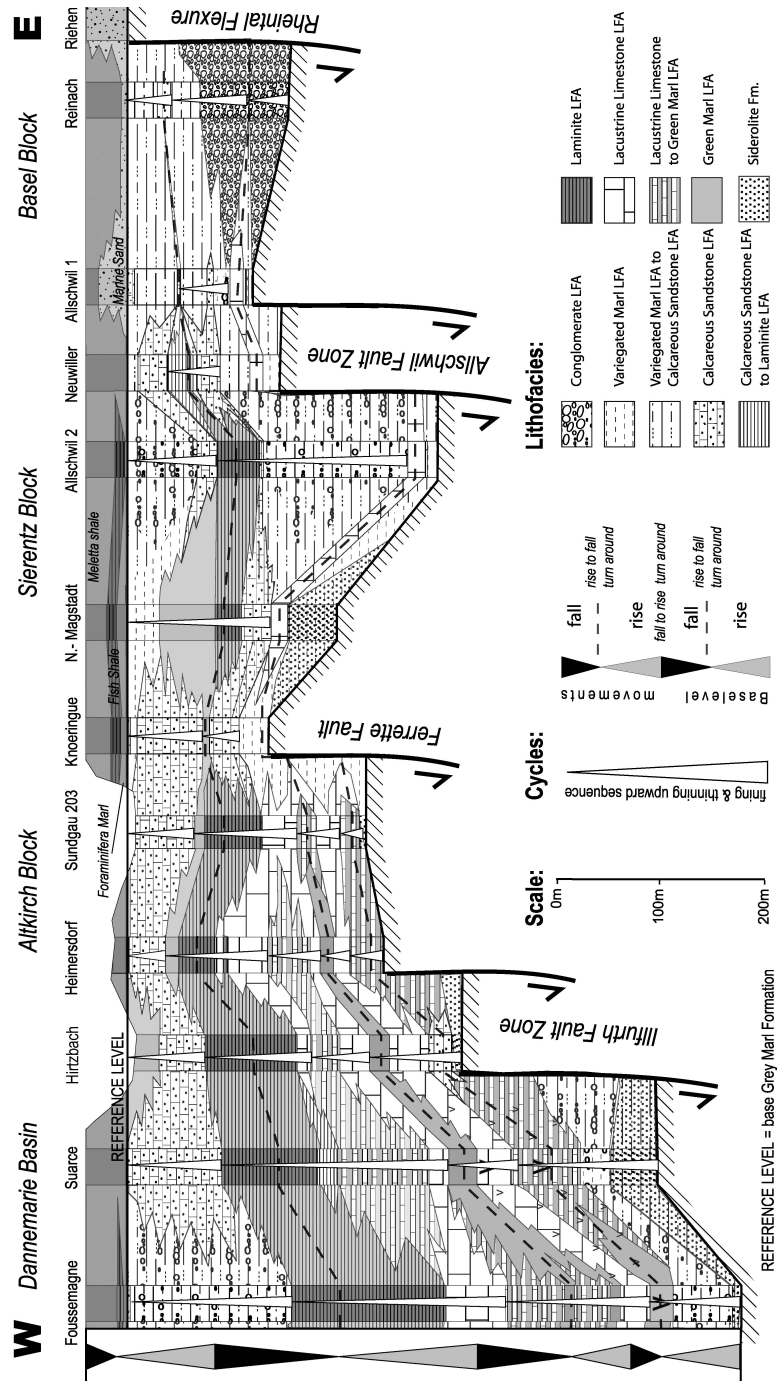


Figure 4.7: Basin fill architecture at the southern graben end reconstructed from lithological descriptions of drill holes (for location see Fig.4.6). Facies and thickness changes occur across fault zones and indicate deposition during active faulting.

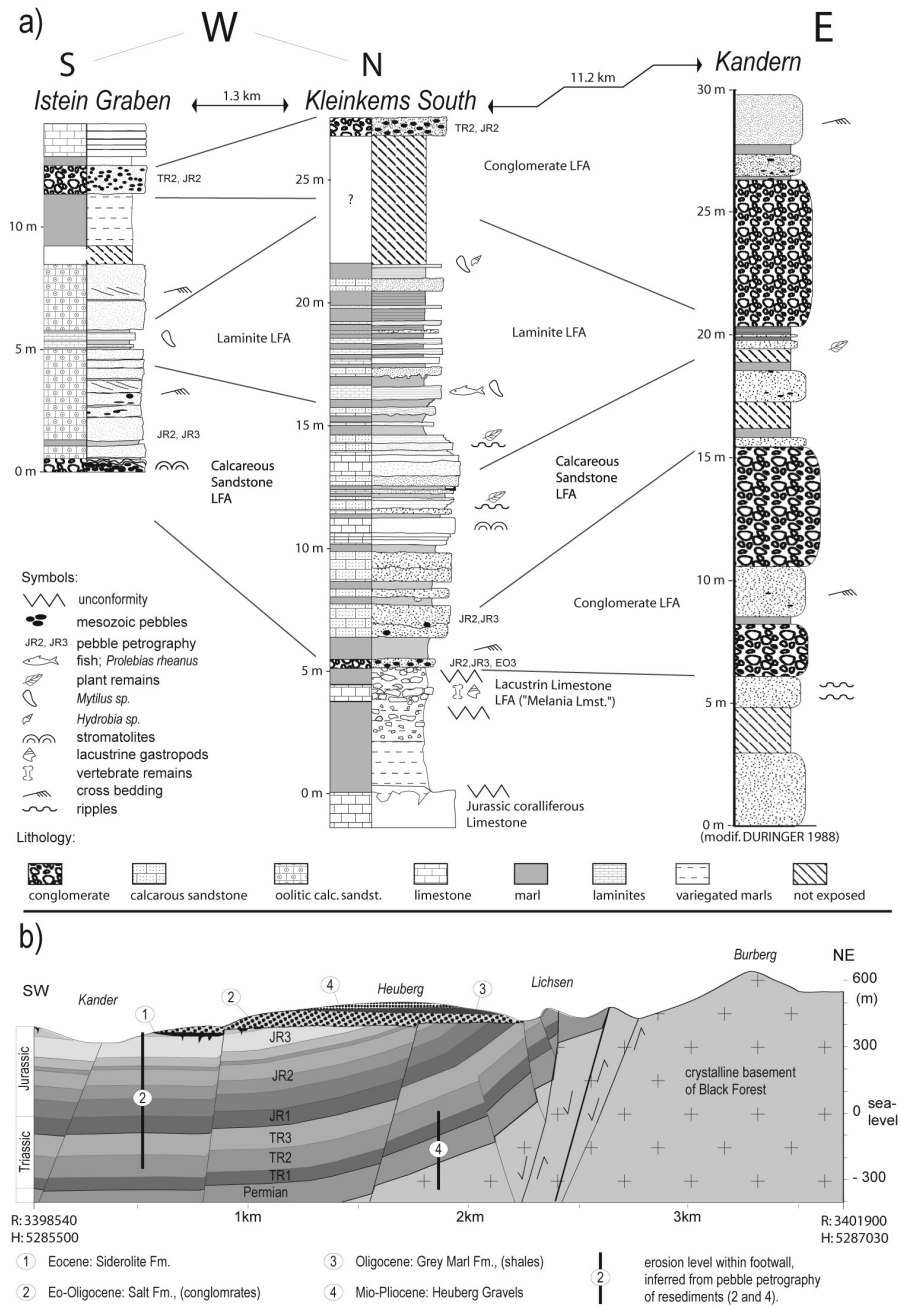


Figure 4.8: Geological situation in the marginal part of the basin illustrated by three sections (a) from the SE basin margin (location see Fig. 4.6). Coarse conglomerates at the graben margin prograde basinward into lacustrine deposits. At the borderfaults the conglomerates rest unconformably on an extensional flexure (b).

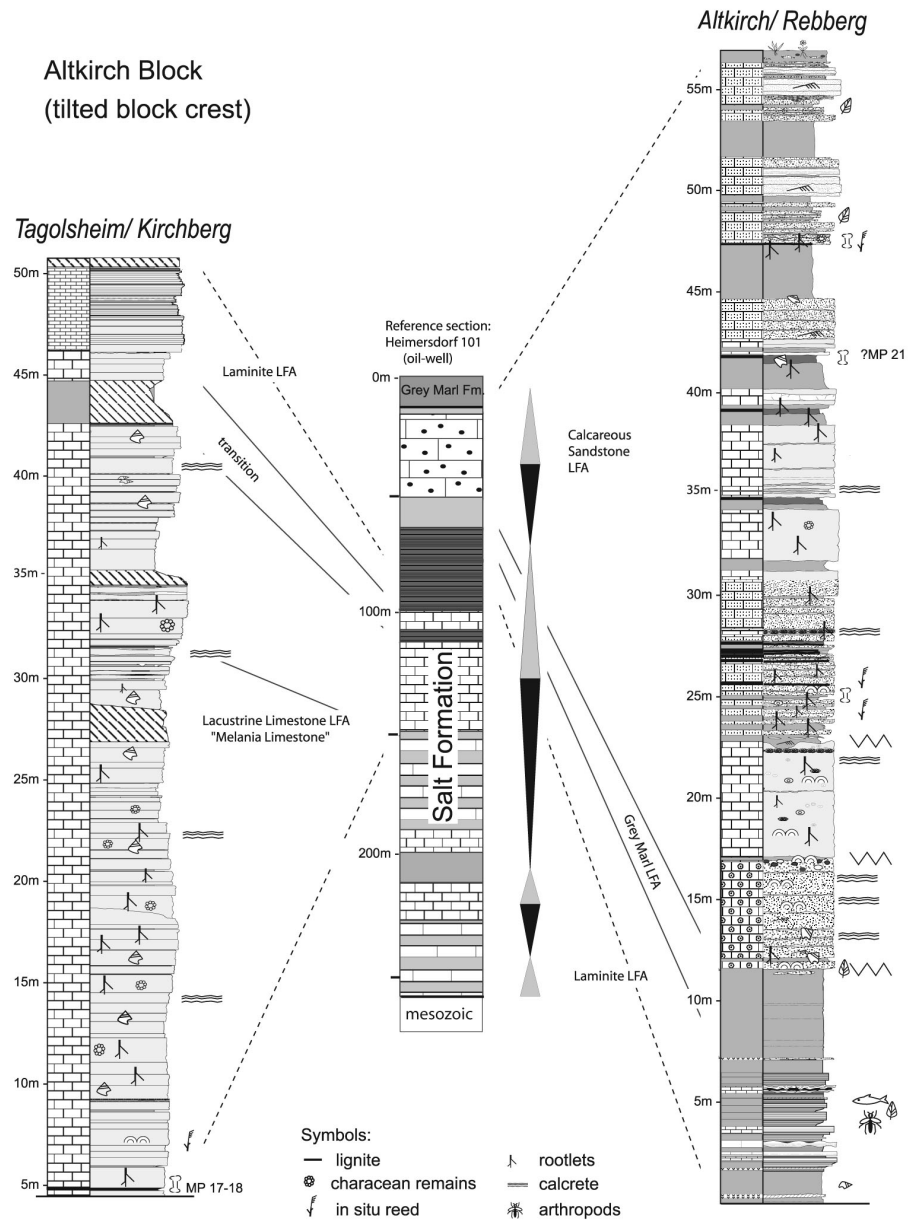


Figure 4.9: Sections exposed at the crest of the tilted Altkirch Block (for location see Fig. 4.6) correlated with the Heimersdorf well (Fig. 4.7). The Tagolsheim section (modified from Stucky, 2005) exposes the "Melania Limestone" of Middle-Late Eocene age. The Altkirch quarry exposes laminites and the "Haustein" (Calcareous Sand LFA) in the top. "Melania Limestone" and "Haustein" are marginal lacustrine sediments, that have been pedogenetically overprinted.

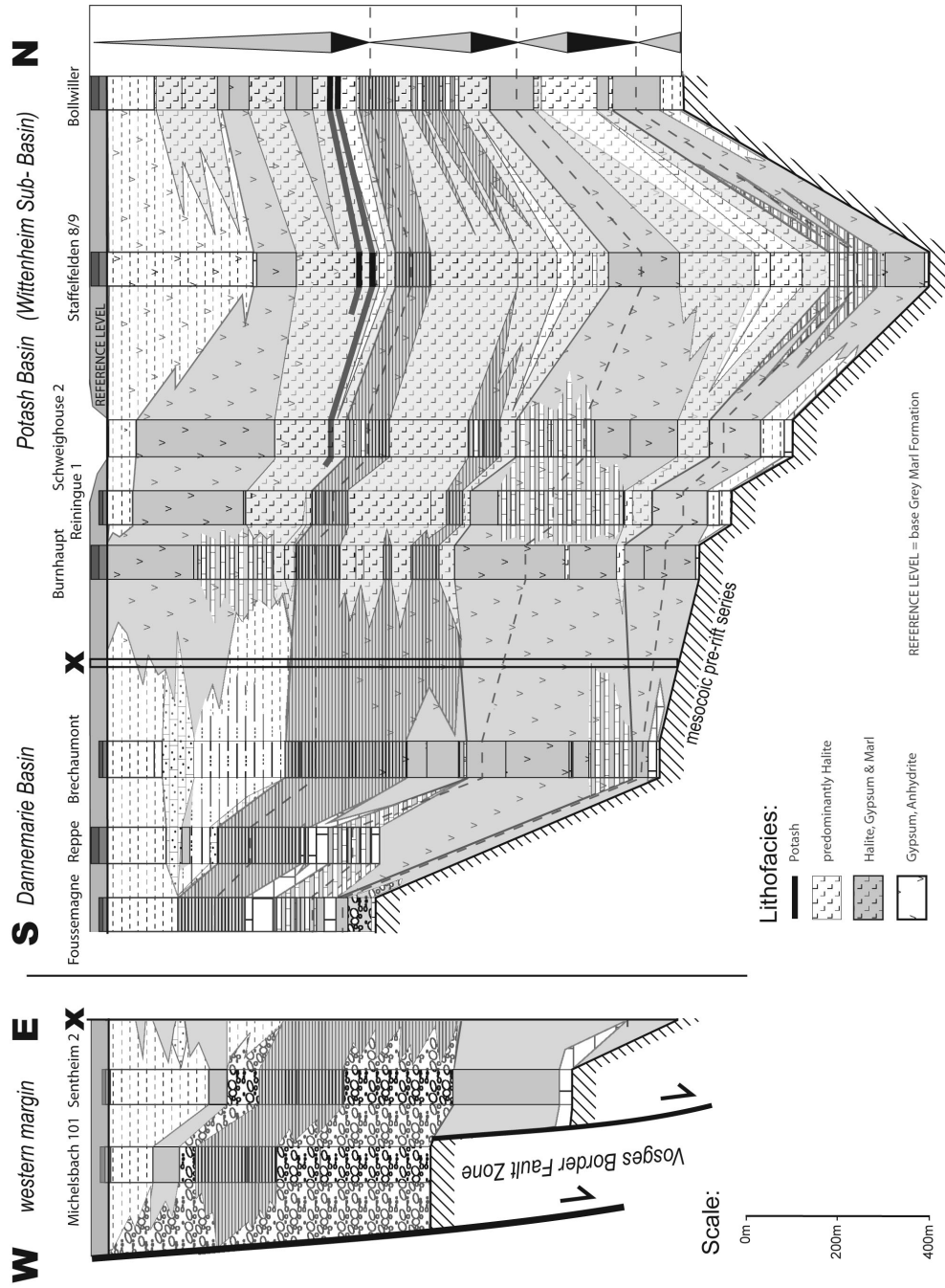


Figure 4.10: Basin fill architecture of the DanneMarie Basin and the Potash Basin reconstructed by lithological descriptions from drill holes (for location see Fig.4.6). Strongly increasing sediment thicknesses to the north coincide with the transition to an evaporitic environment.

This fault zone displaces a unit of Eocene lacustrine limestone that partly has been eroded on the footwall crest (well Allschwil 1, (Schmidt et al., 1924)). The crest area of the tilted Sierentz Block exhibits a shift towards a proximal facies and a drastically reduced sediment thickness (well Knoeringue). Further south, the Salt Formation is replaced by a hiatus ((Ustaszewski et al., 2005a); well Sundgau 201).

Two major sections expose the Altkirch Block footwall crest (Fig. 4.9): At Tagolsheim about 40 m pedogenetically modified lacustrine "Melania Limestone" are covered by the laminites of the "Fossiliferous Zone". At Altkirch the laminites of the "Fossiliferous Zone" are overlain by the "Haustein", which has been strongly affected by pedogenesis. The lowermost part of the Haustein shows an oolitic facies and includes intra- and extraformational pebbles.

Istein Block ; the facies changes observed on the Basel and the Sierentz Block in wells are exposed on the Istein Block (Fig. 4.8a). Conglomerates interfinger with sandstones, laminites and limestones. The "Istein Graben" locality (e.g. Wittmann, 1952) also exposes oolitic calcareous sandstones containing Mesozoic clasts, interbedded with conglomerates derived from Middle and Late Jurassic rocks and laminated carbonates preserving the characteristic fauna of the "Fossiliferous Zone". They are covered by variegated marls and conglomerates.

In the "Kleinkems South" section Late Jurassic limestones unconformably overlain by palaeosols are covered by variegated marls including reworked relicts of lacustrine "Melania Limestone". Conglomeratic calcareous sandstones follow above another erosional unconformity. They grade upward into the laminites of the "Fossiliferous Zone". The section ends with conglomerates.

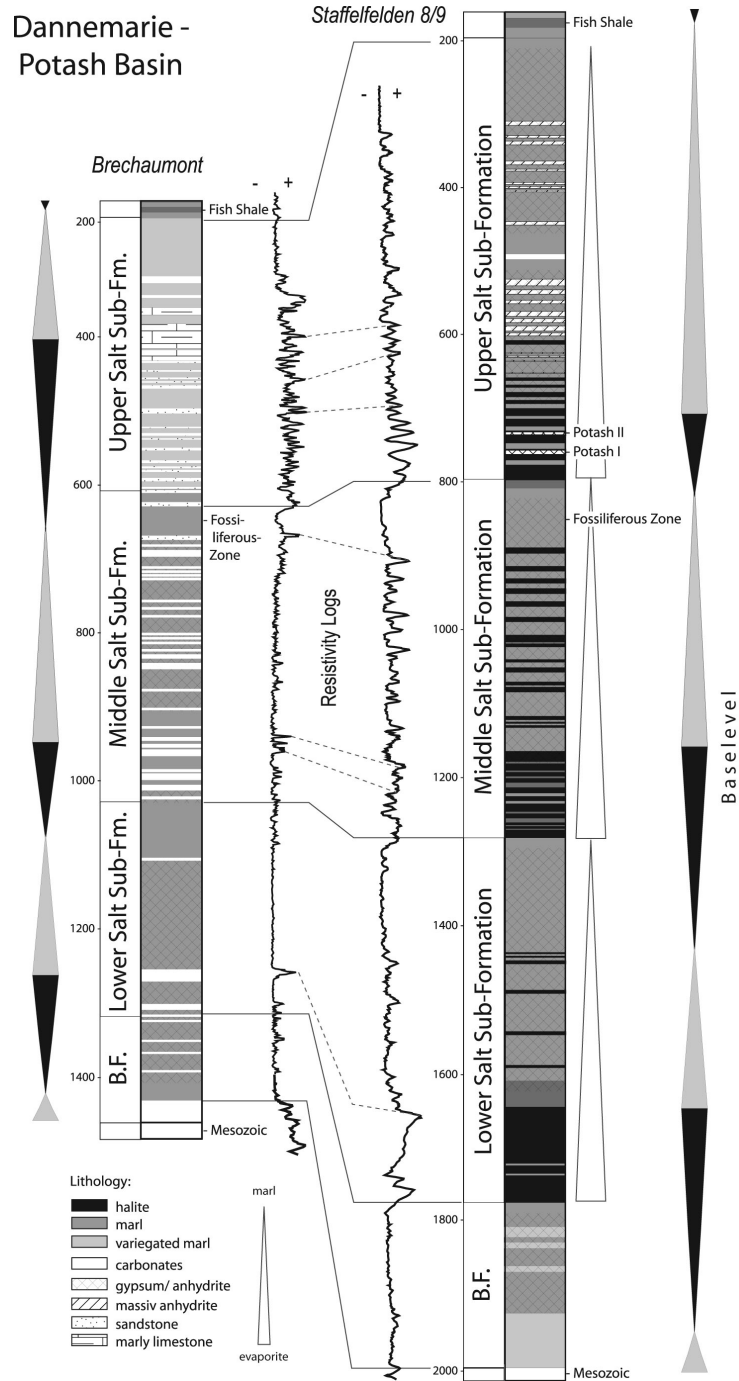
Dannemarie Basin ; at the south of the Dannemarie Basin the facies is similar to that on the Altkirch and the Sierentz Blocks (Fig. 4.7). Sediment thickness continuously increases towards the north (Fig. 4.10). Gypsiferous marls become the prominent lithology while lacustrine limestones and "Haustein Facies" are drastically reduced in thickness (Fig. 4.11; Brechaumont well).

Potash Basin ; further north, near Mulhouse, the facies changes abruptly. The occurrence of halite and potash salts characterizes the transition towards the Potash Basin. The fill of the central part of the Potash Basin is well documented (Fig. 4.11; well Staffelfelden 8/9). Three major evaporation cycles can be distinguished. The cycles show massive halite at the base, that is repeatedly interbedded with marls (2nd order cycles), that become prominent towards the top of a cycle.

4.4.3 Palaeogeography

The environmental setting in the southern URG changed repeatedly between lacustrine, brackish and evaporitic. It is still a matter of debate, whether the

Figure 4.11: Wells within the Dannemarie Basin and the Wittelsheim Sub-basin (for location see Figs. 4.6, 4.10) show the facies distribution in the internal graben domains. The Staffelfelden 8/9 well-log resembles the stratigraphical reference section of the Salt Formation and the underlying Middle Eocene. According to correlation by resistivity well-logs and application of a base-level concept, the major cycles can be traced throughout wide parts of the basin.



southern URG was connected to the ocean during deposition of the Salt Formation or not (e.g. Wappler et al., 2005). Benthic foraminifera, dinoflagellate cysts, nanoplankton and bryozoans in several intervals of the Middle Salt Sub-Formation imply a marine influence (Förster, 1892; Martini, 1995; Blanc-Valleron and Schuler, 1997). However, these taxa have been reported also from saline lakes (e.g. Tappan, 1980; Rauscher et al., 1988; Fontes et al., 1991; Pawlowski and Holzmann, 2002). The fauna is of low diversity and characterized by monospecific mass occurrences of opportunistic species indicating a rather restricted environment (Hinsken, 2003). In addition, no euhaline marine macrofossil has yet been found (Fontes et al., 1991). Furthermore, the continuous rim of fluvial conglomerates around the basin (Wagner, 1938; Düringer, 1988; Derer et al., 2003) contradict a fully marine setting. The facies association in the southern URG (Figs. 4.6, 4.7, 4.10) points to a typical continental evaporite basin with freshwater limestones surrounding the evaporites in the centre, as was described, for instance, in the Piceance Creek Basin (Green River Formation; Cole and Pickard, 1981). Consequently, facies distribution and palaeoecology support the interpretation that the Salt Formation was at least for its major part deposited in a restricted to enclosed environment in a continental setting.

4.4.4 Flank uplift

The amount of graben-shoulder uplift can be estimated from pebble petrography. The local changes of the pebble petrography within the Conglomerate LFA along the Vosges, Black Forest and Jura Mountains suggest differential uplift of the rift flanks (e.g. Düringer, 1988, Fig. 4.6). Strongest uplift occurred in the Vosges, where erosion reached the crystalline basement already during Early Oligocene (Upper Salt Sub-Formation). At the same time erosion in the Black Forest cut down to the Middle Triassic. In the northern Jura, erosion affected only Late Jurassic limestones. The uplift pattern derived from pebble composition is inverse to the subsidence pattern: in cross-section, the graben is deepest, where the flanks have been uplifted the most (deepest erosional truncation), like along the western rim of the Potash Basin.

4.4.5 Sediment source

Most of the graben-fill sediments were delivered from the graben flanks (e.g. Roll, 1979). Only little sediment was derived from the Jura representing the Alpine forebulge during the Late Eocene (Kempf and Pfiffner, 2004). However, sediment input from the north (e.g. Gaup and Nickel, 2001) might have occurred due to the erosion on the Rhenish Massif (see Ziegler, 1990). The southward increase of evaporites and the carbonate facies along the southernmost graben margins point to clastic supply from the north, rather than from the south.

The composition of the lacustrine deposits in the southern graben is largely controlled by the lithology in the catchment area (e.g. Talbot and Allen, 1998). The Mesozoic strata along the rift flanks probably supported carbonate sedimentation at the lake margins and marl accumulation in the open lake. Erosion

of Triassic evaporites is regarded to be the main source for the salts (e.g. Gale, 1920; Düringer, 1988; Fontes et al., 1991), as pebbles of the Triassic salt-bearing strata are frequently found within the Conglomerate LFA, and the amount of halite dissolved on the graben shoulders exceeded that deposited in the graben (Blanc-Valleron, 1991). Furthermore the isotopic composition of gypsum suggests a Triassic rather than a Tertiary marine origin (Fontes et al., 1991).

4.4.6 Sediment partitioning and A/S-ratio

The facies distribution within the southern URG was strongly affected by accommodation space as well as sediment supply (Figs. 4.6, 4.7, 4.10). As accommodation space was often filled up to the base level, especially at the margins of the basin, sediment partitioning played a major role during the filling of the basin. Therefore, the ratio of accommodation space (A) and sediment supply (S), the A/S-ratio, was the main factor controlling sediment partitioning and facies distribution.

Low A/S-ratio at graben margins ; high sediment supply from the rising flanks, but low subsidence led to the formation of wedge-shaped conglomerate and sandstone bodies along the graben borders. Locations of major sediment infill appear to be spatially related to active transfer zones and the intersection of reactivated lineaments (see below). A large fan delta system developed west of Mulhouse (e.g. well Michelsbach, well Guewenheim) between the Dannemarie Graben and the Wittelsheim Sub-Basin in front of the recent valley of the river Thur, which follows a major lineament.

The central Potash Basin was bordered by a conglomerate belt sometimes only a few hundreds of metres wide (e.g. Schreiner, 1977). This points to a low sediment input in front of the strongly uplifted footwalls along the margins of the Potash Basin. Intraformational pebbles of lacustrine limestones along the graben margins (e.g. Kiefer, 1928; Genser, 1959, Fig. 4.8a) point to sediment cannibalism during times of low base-level.

Medium A/S-ratio on intrabasinal swells ; low subsidence and low sediment input characterize the intra-basinal highs. Similarly, the crests of tilted blocks received little or no clastic sediment. At such sites carbonates dominate (Figs. 8-10) and sometimes even oolite shoals formed. Frequently, the deposits became exposed (during low base-level) and were subject to pedogenesis (Fig. 4.9).

High A/S-ratio in the Potash Basin ; in the Potash Basin at high subsidence rates the sediment input was on average low (Fig. 4.11). Evaporites formed during times of increased aridity and there was almost no terrigenous supply. Marls accumulated during relatively humid periods.

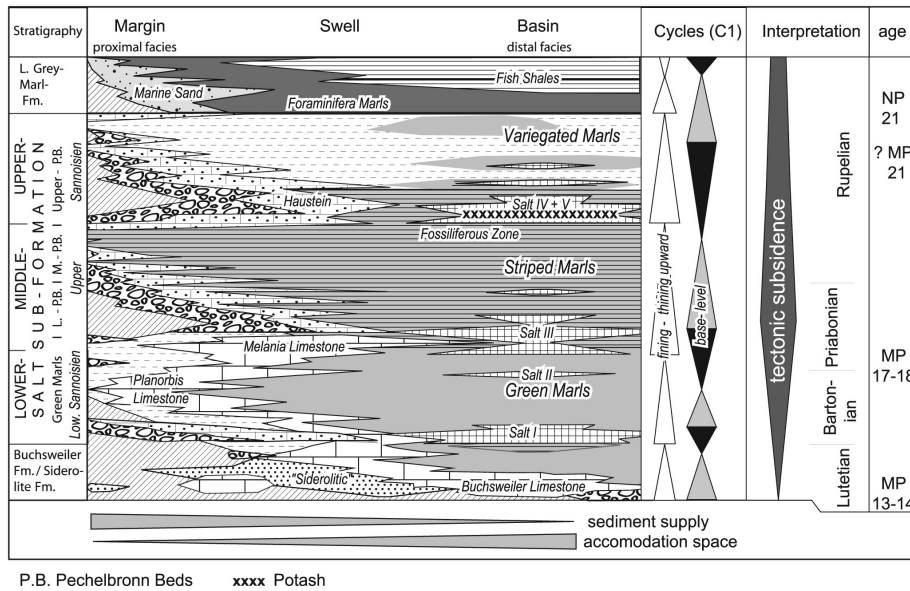


Figure 4.12: Facies diagram illustrating the interpreted basin-fill architecture and the major base-level cycles of the Eo-Oligocene syn-rift sediments in the southern URG.

4.4.7 Age constraints

The age of the members of the Salt Formation has not been well established yet because of sparse and equivocal biostratigraphical data (e.g. Berger et al., 2005b; Wappler et al., 2005, Fig. 4.12). A maximum age of the Lower Salt Sub-Formation can be estimated by the Lutetian age (zone MP13-14) of the basal Siderolite Formation and Buchsweiler Formation (e.g. Berger et al., 2005b). The gradual transition from the Siderolite Facies to the Green Marl Facies reported from many drill holes contradicts a postulated Bartonian unconformity within the southern URG (e.g. Sissingh, 1998; Schumacher, 2002). A mammalian fauna recently discovered in the lower part of the "Melania Limestone" at Tagolsheim (Stucky, 2005) has provided a preliminary age of stage MP 17-18 corresponding to the Early Priabonian (B. Engesser pers. com.). Thus, the oldest part of the Lower Salt Sub-Formation must be Bartonian or even Lutetian in age (see Fig. 4.9).

The low diverse, but abundant nanoplankton community within the upper part of the Middle Salt Sub-Formation in the "Fossiliferous Zone" can be correlated with the Middle Pechelbronn Beds and, hence, implies an Early Oligocene age (Martini, 1995). Mammalian remains from the "Haustein Member" at Altkirch provide an Early Oligocene age (MP 21; B. Engesser pers. com.). A maximum age of the Upper Salt Sub-Formation is given by the overlying Foraminifera Marls that belong to Nanoplankton Zone NP 21 (Gradstein et al., 2004, early Middle Oligocene;).

Further age estimates rely on the correlation with strata in the middle and northern URG. The Green Lymnea Marls (Middle Eocene) are seen as correlative with the Lower Salt Sub-Formation (e.g. Berger et al., 2005b). The Lower Pechelbronn Beds are correlated with the lower part of the Middle Salt Sub-Formation and represent the Late Eocene (e.g. Berger et al., 2005b). The Middle Pechelbronn Beds are regarded to have a Late Eocene to Early Oligocene age (Gaup and Nickel, 2001). The Upper Pechelbronn beds are correlated with the Upper Salt Sub-Formation and point to an Early Oligocene to Middle Oligocene age (Gaup and Nickel, 2001).

As the deposition of the Salt Formation appears to be climatically controlled, enhanced evaporation in neighbouring basins, in particular the Paris Basin, provide useful additional information (e.g. Blanc-Valleron, 1991). Based on the biostratigraphical results, Salt I might correspond to the Lutetian-Bartonian evaporation cycle in the Paris Basin, Salt II and Salt III to the Late Priabonian evaporation cycles during which the "Gypse de Montmartre" formed (see Rochy, 1997).

4.4.8 Sedimentary dynamics and base-level fluctuations

Tripartite lake model

Because of the great variability of environmental settings and the disputed connection to the ocean the base-level concept was chosen to subdivide the deposits of the Salt Formation. However, instead of the classic correlation of A/S-ratio cycles (*sensu* Cross and Lessenger, 1998) the base-level concept of a triple stage lake model was applied (Bohacs et al., 2000). This approach represents a slight modification of the classical base-level concept, which better fits the palaeogeographic conditions in the southern URG. The tripartite lake model (*sensu* Bohacs et al., 2000) distinguishes between overfilled, balanced and underfilled basin mode.

During an *overfilled basin mode* the base-level was high due to decreased subsidence or increased supply of water and sediment; a freshwater lake formed in the basin. Carbonates accumulated along the margins and marls in the central part.

During an underfilled basin mode base-level was low due to increased subsidence and/or decreased supply of water and sediment. Evaporites accumulated in the basin centre. Distinct alluvial fans developed on the graben margins, favoured by extended slopes. The marginal parts of the basin were characterized by deposition of variegated marls or the formation of palaeosols.

A *balanced basin mode* occurred during transitional periods. Water stratification resulted from superficial freshwater inflow onto a saline brine and led to a meromictic lake stage. Carbonate sedimentation dominated in shallow lake areas. A base-level fall resulted in fan delta progradation, while base level rise resulted in fan delta retreat (Düringer, 1988).

Cycles

Three major evaporation cycles formed in the Potash Basin (Figs. 4.11, 4.12). Each cycle starts with thick halite beds, which decrease in abundance and thickness towards the top, and finally grade into marls. They represent 1st order base-level rise cycles, which define the Lower, Middle and Upper Salt Sub-Formations. According to the stratigraphic age estimates, each cycle may have had a duration of approximately 3 My. Major fining-upward cycles at the graben borders are correlated with the base-level rise cycles of the sub-formations.

2nd order cycles are expressed by interbedding of single layers (e.g. halite, marl) and show a drastically reduced, probable allocyclically controlled frequency (Blanc-Valleron, 1991). Along the basin margins and on intra-basinal highs 1st order cycles are often asymmetrically developed and show dominantly base-level rise tendency, whereas base-level falls seem to be represented by an unconformity (Fig. 4.8). Cycles as well as facies along the margins of the basin are well correlatable with the strata of comparable thickness within the northern URG (see Derer et al., 2003). Towards the basin centre lower order cycles become increasingly pronounced. The subcycles exhibit a tendency towards symmetrical base-level cycles.

Although the three salt sub-formations are similar with respect to the general trends, they show considerable differences in their depositional style.

The *Lower Salt Sub-Formation* is characterized by greyish to greenish marls and evaporites in the basin centre as well as abundant limestones in the marginal parts. Lateral sediment supply was low. Laminites are restricted to the depocentres. A relatively low relief and moderate basin subsidence is suggested for the Lower Salt Sub-Formation.

The *Middle Salt Sub-Formation* is characterized by increased clastic supply from the graben shoulders, abundant carbonate sedimentation on swells and abundant "deep-water" laminites within the basin. All these features point to the formation of a distinct relief and thus to enhanced subsidence.

The *Upper Salt Sub-Formation* records a basinward progradation of clastic wedges in its lower part and a transition towards a fluvio-terrestrial environment in the higher parts. Both trends imply a transition towards an overfilled basin and indicate peneplainisation of the relief due to decreased rifting.

4.4.9 Tectonic implications

The spatial distribution of facies and sediment thicknesses provides some information about subsidence. Little shifting of syn-rift facies belts implies uniform subsidence and a pure extensional stress regime with a constant extension direction during such a period. However, in the southern graben a shift of the area of maximum subsidence from W to E is observed, which has been interpreted to have resulted from a transition from oblique to orthogonal extension

(Schumacher, 2002). Syn-rift sediment thicknesses and facies changes suggest that subsidence was strongest in the Potash Basin and decreased towards the southern and northern graben domains.

Long-term changes (several My) of the depositional setting are interpreted to be of tectonic origin. Theoretically, increased rifting results in distal facies in the basin centre and proximal facies along the borders. Decreased rifting leads to propagation of marginal facies basinwards (decrease in accommodation space). Therefore the Middle Salt Sub-Formation, characterized by deep-water environments in the basin interior and the onset of strong clastic supply from the graben shoulders, probably represents the climax of rifting.

4.5 Formation of the southern Upper Rhine Graben

4.5.1 Basin geometry

The width of the southern URG has been determined by locating its break-away faults and by measuring it parallel to the Palaeogene extension direction (Ustaszewski et al., 2005a, mean azimuth of 095°;), which is more or less perpendicular to the graben's strike (Fig. 4.6). The graben width varies between 63 km in its southernmost part near Basel, 35 km in the area of the Potash Basin to the north of Mulhouse, and about ≥ 50 km in the area of Colmar. This along-strike change in rift width is accompanied by a change of graben depth (Cloos, 1939), and sedimentary facies (Figs. 7.3, 4.6). Within this context it is important to recall that the development of the URG was pre-determined by (the reactivation of) pre-existing Late Palaeozoic crustal discontinuities.

4.5.2 Extension, graben width and subsidence

The amount of extensional displacement (ΔL) across the URG is in the order of 5 km, as estimated from several cross-sections (see below). This value appears to be constant along the entire graben (Sittler, 1969; Laubscher, 1970; Doehl and Teichmüller, 1979; Villemin et al., 1986; Durst, 1991; Brun et al., 1992). However, as the present day, "final" rift width (L_f) varies along strike, ΔL is partitioned over a variably wide zone in the different graben segments. Therefore, differences in the initial rift width (L_0) are responsible for variations in the crustal stretching factor (β), which mainly controls the extensional-basin subsidence (Allen and Allen, 2005).

β can be calculated from ΔL and is related to L_0 by:

$$\beta = \Delta L / L_0 + 1 \quad (4.1)$$

ΔL and observed L_f are related by:

$$L_0 = L_f - \Delta L \quad (4.2)$$

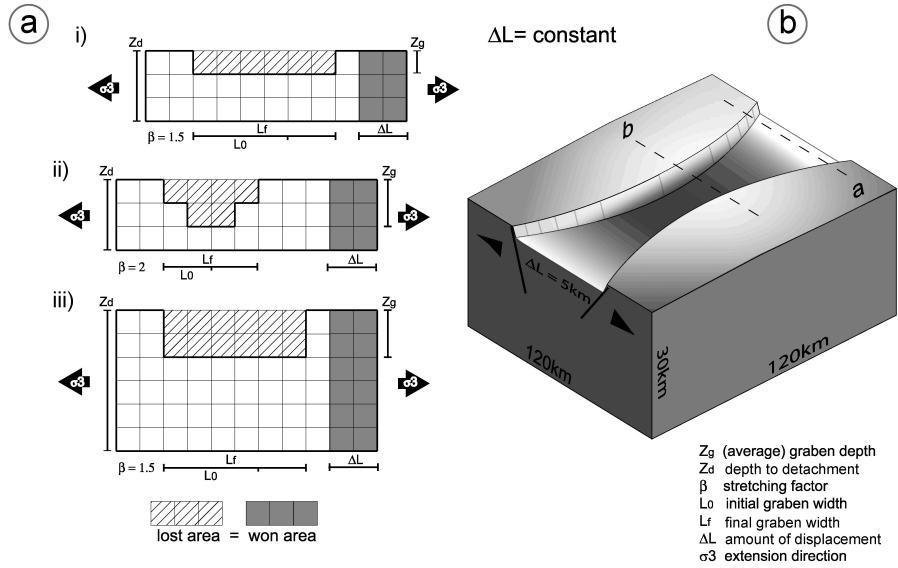


Figure 4.13: Effect of rock volume balance at constant extension ΔL . (a) Rift basin subsidence depends largely on graben width L_f (i versus ii) and depth to detachment Z_d (i versus iii). (b) Consequently an axial depo-centre develops in a narrow rift zone, if ΔL and Z_d are constant.

Substituting (2) into (1), β can be alternatively expressed as:

$$\beta = \Delta L / (L_f - \Delta L) + 1 \quad (4.3)$$

In this equation the direct dependence of β and the observed L_f can be shown, especially if ΔL stays constant along strike of the graben.

Moreover, graben-subsidence is related to the compensation depth of extensional faulting (Z_d ; depth to detachment *sensu* Groshong, 1996,), which is generally associated with the sole-out level of listric faults forming on a common detachment. This can be shown by rift volume balancing (Fig. 4.13a).

Rift volume balancing (e.g. Groshong, 1996) is another method to calculate ΔL independently from line length balancing (retro-deformation) of a cross-section (if Z_d is known), or to estimate Z_d (if ΔL is known) using the graben volume V_R (Fig. 4.13a). In cross-section, V_R is defined as the so-called "lost area" (A_{lost} ; Groshong 1996) between the pre-rift and the present position of a reference level (e.g. top of basement). If the rock volume did not change (i.e. if volcanism is excluded), the "lost area" equals the so-called 'won area', which compensates the displacement above Z_d .

Z_d and ΔL are related by:

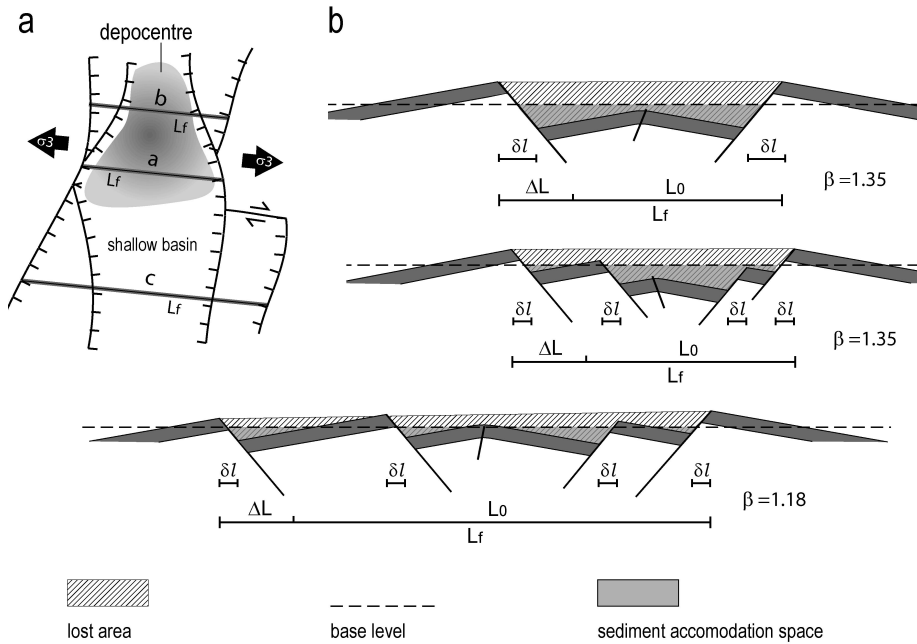


Figure 4.14: Effect of block tilting on extensional basin formation, where ΔL is partitioned among several normal faults (δl). A symmetrical tilt-block graben (a) of constant ΔL develops a local depo-centre and highest graben shoulder uplift in a narrow rift zone, especially if the graben opens splay-like. Thereby the graben volume and the dip of normal faults are almost constant (b).

$$Z_d = A_{lost}/\Delta L \quad (4.4)$$

Assuming that ΔL and Z_d (and thus A_{lost}) of the evolving graben remain constant along its strike, then depocentres evolve within narrow graben segments (small L_0 , high β), whereas shallow basins develop in the wide parts of the graben (large L_0 , low β ; Fig. 4.13b and 4.14a; equation (3)).

The same effect occurs in the case of block tilting (Fig. 4.14), which frequently occurs in lithospheric-scale extensional basins (e.g. Leeder and Gathrope, 2002) and that is generally regarded to be the surface expression of listric faulting, soling out on common detachment at Z_d . Block tilting therefore enables the rift volume to be balanced if ΔL is partitioned over a variable rift width and among a variable number of fault-bounded tilted blocks (Fig. 4.14b).

4.5.3 Extension in the URG

To test the hypothesis developed above, ΔL , A_{lost} and Z_d were estimated from two cross-sections in the study area (Fig. 7.4). ΔL was measured along the top of the pre-Mesozoic basement. A_{lost} was constructed using the same reference

level, and a top-line connecting both break-away faults at reference level, as is shown in Figure 14b. For section B-B', located in the shallow southernmost part of the URG (Figs. 7.3, 7.4), line-length balancing yielded a ΔL of 4.2 km (?). This value appears to be very reliable, because the reference horizon can be traced over most of this cross-section. For section A-A', the base of the Mesozoic was first extrapolated over the crests of the graben-shoulders, assuming negligible basement erosion there (in agreement with Paul, 1955). Line-length balancing for section A-A' yields a ΔL of about 4.5 km. Measurement of A_{lost} provides 111 km² in cross-section B-B', while it results in 121 km² for cross-section A-A'. Using equation (4), Z_d yields almost 27 km for both cross-sections. The values estimated for both cross-sections are in a reasonable agreement. However, ΔL and A_{lost} are about 10% in cross-section B-B'.

The calculated Z_d values are in a good agreement with the Moho-depth of about 26 km in the area adjacent to the URG (see Dèzes et al., 2004). This suggests that the whole crust was affected by brittle tectonics and the compensation depth of extensional faulting is located in the proximity of the Moho (in agreement with Groshong, 1996). Indeed, the crustal configuration of the URG (Brun et al., 1992) and the occurrence of earthquakes almost down to the Moho in its southern parts (Plenefisch and Bonjer, 1997) imply that the crust behaves in a brittle manner at present. The observed strong syn-rift uplift of the graben flanks is compatible with flexural rebound due to a very deep level of necking (see Kooi and Cloetingh, 1992) located within the upper mantle and proves the assumption that the entire crust was affected by brittle tectonics during Palaeogene extension.

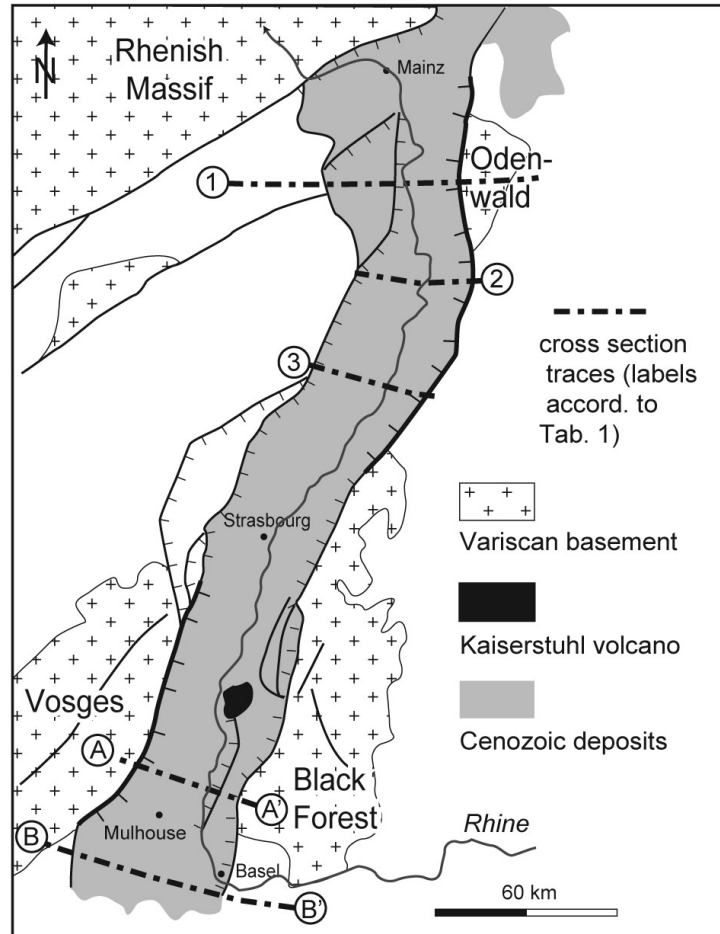
In order to get further information about extension in the URG A_{lost} was measured from several published cross-sections (Fig. 4.15; Tab. 1) and the calculated Z_d of 27 km was used to estimate ΔL (eq. (4)). All cross-sections show a similar A_{lost} of about 120 km² and point to a constant extension of about 4.5 km. However, isostatic flexural rebound affects A_{lost} and the measured values might be slightly underestimated (calculated ΔL too small). ΔL directly measured from seismic sections (line length balancing), may also be somewhat smaller than the actual value because small-scale faults are below the resolution and therefore not taken into account. The real ΔL may be marginally higher and a ΔL of 5km appears to be a realistic value for the Cenozoic URG.

4.5.4 Rift basin formation

Obviously, the Potash Basin is located in the deepest and narrowest part of the southern URG ($L_f \approx 35$ km) for which a high average stretching factor ($\beta \approx 1.14$) has been determined (section 3 in Figs. 4.15 and 4.16). This depo-centre was already bordered during the Palaeogene by strongly elevated rift flanks. Therefore, the Potash Basin is regarded as a narrow basin with a relatively high β value.

To the north, the Potash Basin shallows and narrows as the graben, including the shallow Freiburg Embayment, widens to $L_f \approx 43$ km ("2" in Fig. 4.16) near

Figure 4.15:
Location of cross-sections mentioned in Table 1. Section 1 from Wenzel et al. (1991), section 2 and 3 from Doebel and Teichmüller (1979), section A-A' this work, section B-B' from Ustaszewski (2004).



section	A_{lost} [km ²]	ΔL [km]
1	≥ 101	3.7
2	127.6	4.7
3	129.9	4.8
A-A'	121	4.5
B-B'	112	4.13

Table 4.1: Measured A_{lost} and calculated ΔL values for several published cross-sections in the URG applying volume balancing with a Z_d of 27 km. Location of the sections is shown in Figure 4.15. For section 1 an accurate A_{lost} value can not be given, because the base-Mesozoic reference-level has been eroded before rifting.

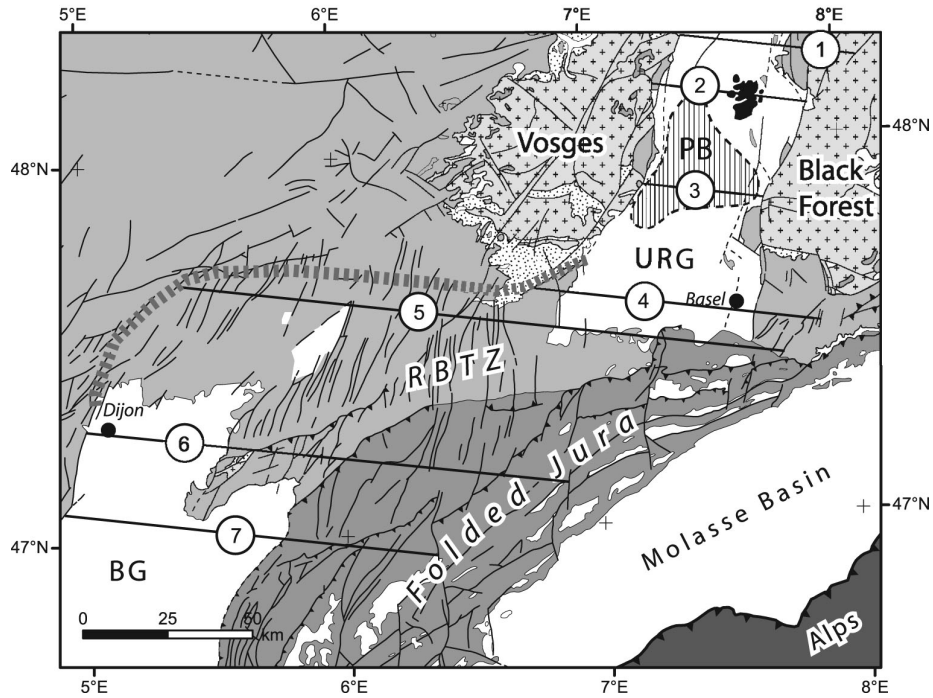


Figure 4.16: Tectonic interpretation of the Palaeogene southern URG and the Rhine-Bresse Transfer Zone. An almost constant total crustal extensional strain of about 5 km has been distributed within several graben domains of variable width (black bars). The orthogonally rifted Potash Basin, representing the narrowest part of the graben, experienced an average strain of about 14% extension, resulting in strong subsidence and pronounced graben shoulder uplift, whereas the obliquely rifted Rhine-Bresse Transfer Zone experienced only about 2% extensional strain, resulting in negligible subsidence and the formation of a swell, which acted as barrier towards the Molasse Basin and the Bresse Graben.

Freiburg. This suggests that in this area ΔL was partitioned over a wider zone and a larger number of faults than in the central parts of the Potash Basin. North of Freiburg, where the Elzach Fault branches off from the Black Forest Border Fault, the rift zone widens to $L_f \approx 55$ km (at N-end of Elzach Fault) whilst the URG shallows, forming the Colmar Swell ("1" in Fig. 4.16).

South of Mulhouse ("4" in Fig. 4.16), the URG widens from $L_f \approx 41$ km to $L_f \approx 63$ km across the Kandern-Hausen Fault. This increase in graben width coincides with a distinct decrease in the thickness of Palaeogene syn-rift sediments and a pronounced change from the Potash Basin deep-water and/or evaporite facies to the shallow-water and/or terrestrial facies domain of the southernmost URG. This part of the graben is characterized by an average stretching factor ($\beta \approx 1.07$) and is thus regarded as a low- β basin, consisting of several tilted blocks (Fig. 7.4b). South of the Kandern-Hausen Fault, the elevation of

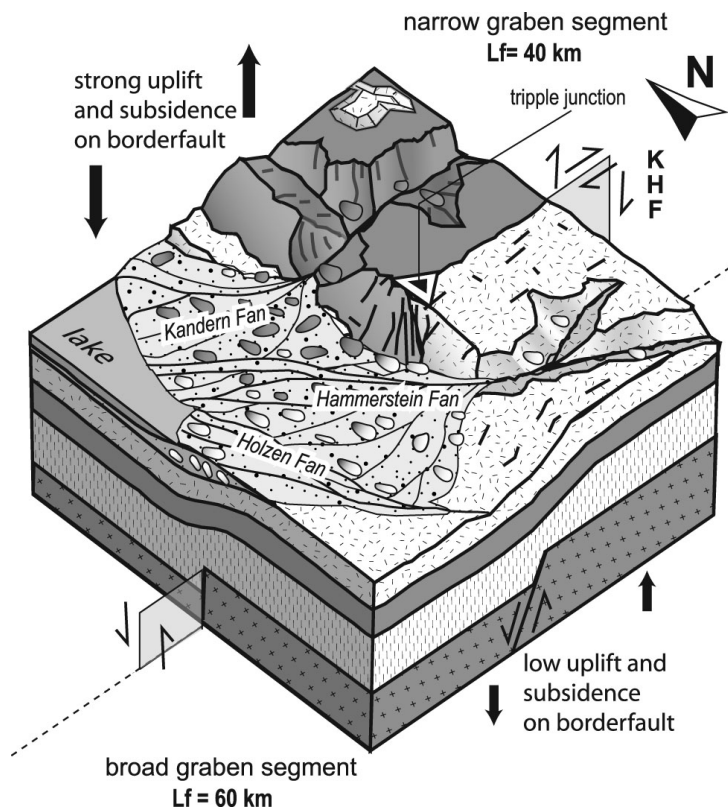


Figure 4.17: Alluvial fan configuration observed near Kandern (for location see Fig. 4.6) at the triple junction of the eastern main border fault and Kandern-Hausen Fault (KHF). The Kandern Fan prograded westward and the age of the pebbles ranges from Middle Jurassic to Middle Triassic. The Hammerstein Fan and the Holzen Fan prograded northwest/northward and include almost exclusively Late Jurassic limestone pebbles. The specific alluvial fan configuration points to greater throw on border fault in the narrow graben segment northern the KHF as well as decreased throw on normal faults south of the KHF, along which the graben broadens to the south by about 20 km.

the Black Forest rift flank decreased during the Palaeogene rifting phase, as evidenced by a change in the pebble petrography and the flow directions of alluvial fans in the Kandern area (Fig. 4.17). The Kandern Fan prograded westward and contains Middle Jurassic to Middle Triassic pebbles, reflecting strong uplift of the hinterland being located to the north of the Kandern-Hausen Fault. By contrast, the Holzen Fan and Hammerstein Fan prograded north- and northwestward and contain only Late Jurassic pebbles. This indicates decreased uplift of the hinterland, which was located south of the Kandern-Hausen Fault, and strong subsidence of the graben north of this fault.

Still further south, the diffuse sinistrally transtensive Rhine-Bresse Transfer Zone (RBTZ) (Laubscher, 1970; Illies, 1981; Lacombe et al., 1993; Ustaszewski et al., 2005b) extends from the Wehra-Zeiningen Fault Zone in the east to the northern part of the Bresse Graben near Dijon in the west and beyond into the Massif Central over a distance of more than 200 km ("5" in Fig. 4.16). This transfer zone is regarded as a very wide, obliquely rifted domain (Illies, 1981) that is characterized by a very low stretching factor ($\beta \approx 1.02$). This interpretation is compatible with the local occurrence of monocline-bounded basins (i.e. Delsberg Basin) containing only thin Late Eocene and Early Oligocene sediments within the domain of RBTZ (Laubscher, 1998; Berger et al., 2005a).

The RBTZ is superimposed onto a WSW-ENE trending, Permo-Carboniferous trough system; its faults were repeatedly reactivated during the evolution of the URG and the Bresse Graben (Ustaszewski et al., 2005b). Partial decoupling of the Mesozoic cover from the basement during their reactivation played an important role in the development of the N-S and NNE-SSW trending fault system that characterizes the RBTZ (Fig. 4.16).

4.6 Discussion and conclusions

The rift-related subsidence of the southern parts of the URG commenced during the Middle Eocene, increased during the Late Eocene-Earliest Oligocene and decreased considerably during the Middle Oligocene. Miocene termination of rift-subsidence of the southern parts of the URG and deep erosional truncation of their syn-rift sediments is related to lithospheric folding controlling rapid uplift of the Vosges-Black Forest Arch (Dèzes et al., 2004).

For the Palaeogene evolution of the southern parts of the URG, Chorowicz and Defontaines (1993), Schumacher (2002), Behrmann et al. (2003), Bertrand et al. (2005) and Schwarz and Henk (2005) postulated oblique rifting. However, there is no evidence for a temporal shift of facies belts during the Middle Eocene to Early Oligocene in the URG. Based on the presented results, Palaeogene extension across the southern URG was almost perpendicular to the rift axis and normal faulting occurred along its break-away faults. However, contemporaneous transtensional faulting occurred along transfer faults across which the initial rift width (L_o) increased/decreased (e.g. Kandern-Hausen Fault).

The Potash Basin is located in the deepest and narrowest part of the southern URG. Facies analyses indicate that this basin was under-filled most of the time during Early Bartonian, Priabonian and Early Oligocene times, when the Salt Formation accumulated. Evaporites formed in the central basin part and alluvial fans prograded from the rift flanks. Mechanisms controlling the development of the three 1st order evaporite depositional cycles are still a matter of dispute. Düringer (1988) attributed the development of these 1st order cycles to climatic controls. Although deposition of evaporites is obviously climatically controlled, almost all levels of the Salt Formation do indeed contain evaporitic layers that can be related to a 2nd order climatic cyclicity. For the Pechel-

bronn Beds in the northern parts of the URG, that are time equivalent to the Salt Formation, Derer et al. (2003) implied a eustatic signal. However, it has as yet to be unequivocally established that the URG was connected to marine realms during this time span. Our results strongly suggest tectonic controls on the development of accommodation space and therefore the observed 1st order cyclicity reflects tectonic cycles that governed the shift towards an underfilled basin mode in response to accelerated subsidence. Nonetheless, the factors leading to development of the observed 1st order cycles are still controversial.

As a first approximation the URG presumably represented during Middle Eocene to Early Oligocene times an enclosed depositional system that was affected by along-strike variations in accommodation space, which in turn was governed by changes in the initial graben width L_0 and local clastic supply from the uplifted rift flanks. The initial graben width largely resulted from pre-existing crustal discontinuities that were reactivated under the prevailing stress regime (Schumacher, 2002; Dèzes et al., 2004; Ustaszewski et al., 2005a).

Across the URG the total extensional displacement ΔL amounts to about 5 km and appears to be rather constant along strike, likewise Z_d , which appears to be located near the Moho. The constancy of ΔL and Z_d resulted in a graben volume $V_R (A_{lost})$ being almost constant along strike. However, the extensional displacement was partitioned over variably wide graben segments ($L_f \approx 35\text{-}65$ km) with narrow graben segments corresponding to relatively high- β basins (e.g. Potash Basin) and wide segments to relatively low- β basins (e.g. southernmost part of URG around Basel).

4.7 Acknowledgements:

This work was performed under the umbrella of the EUCOR-URGENT-PROJECT (<http://comp1.geol.unibas.ch>). We wish to thank Philippe Elsass (BRGM Strasbourg) and Peter Huggenberger (Basel) for providing access to unpublished well data. We are grateful to Peter Ziegler (Basel) and Daniel Bernoulli (Basel) for carefully reading the manuscript, and to our colleagues Stefan Schmid, Markus Schumacher, Pierre Dèzes, Horst Dresmann, James McKenzie, Achim Stucky and Silvio Lauer (all at Basel) for helpful discussions and/or for technical support. Constructive comments by Jan-Diederik van Wees (Utrecht) and Gerhard Greiner (Berlin) helped to improve the manuscript.

Chapter 5

Thermo-Tectono- Stratigraphic Forward Modeling of the Upper Rhine Graben in reference to geometrical balancing: brittle crustal extension on a high viscous mantle

Sebastian Hinsken¹, Stefan M. Schmalholz², Peter A. Ziegler¹, Andreas Wetzel¹

1) Geologisch-Paläontologisches Institut , Universität Basel, Switzerland

2) Geologisches Institut, ETH-Zürich, Switzerland

Manuscript submitted to Tectonophysics

5.1 Abstract

Four structural cross-sections across the central parts of the Upper Rhine Graben (URG) were balanced by means of Thermo-Tectono-Stratigraphic Forward Modeling (TTSF-Modeling) of the 'syn-rift' sediments. Results were compared to geometric retro-deformation of pre-rift reference horizons applying line length and area balancing methods. TTSF-Modeling with a deep level of necking (>20 km) and/or a high effective elastic lithospheric thickness (EET = 15 km) provided extension values compatible with those from geometric balancing, while modeling with shallower necking depths and/or low EET yielded unrealistic high extension values. A best-fit of geometric balancing, providing in average 5 km rift orthogonal extension, was reached by TTSF-Modeling with a EET of 15 km and a 'pre-rift' necking depth of 29 km coinciding with the Moho discontinuity. This outcome is compatible with the fact that the Moho does not shallow significantly beneath the central part of the URG and its uplifted shoulders, and that the seismically active part of the lithosphere is confined to the crust. The coincidence of the necking level and the Moho suggests that the compensation depth of crustal faults is located at the base of the brittle-deforming crust, which is underlain by a ductile-deforming highly viscous lithospheric mantle. Modeled extension-time paths imply rifting during Middle Eocene to Early Miocene times, a Late Miocene post-rift stage and renewed rifting during the Pliocene to recent. A northward migration of modeled extension in time can be explained by 'non rift-related' uplift and the development of a regional angular unconformities. Correcting for these 'uplift' effects, a very similar extension history is evident for the four modeled cross-sections, suggesting plane strain deformation at very low, strain rates of about $1.7 \times 10^{-16} \text{ s}^{-1}$. These results challenge the hypothesis of a poly-phase rifting stage and argue for a uniform rifting process affecting a brittle crust and a highly viscose upper lithospheric mantle.

Key words: Upper Rhine Graben, cross-section balancing, Thermo-Tectono-Stratigraphic Forward Modeling, necking level, rifting-process

5.2 Introduction

The Cenozoic Upper Rhine Graben (URG) is an intra-continental rifted basin that is located in a densely populated part of central Europe (Fig.5.1). It forms part of the European Cenozoic Rift System (ECRIS), a chain of kinematically linked extensional basins stretching from the Mediterranean to the North Sea, which opened more or less simultaneously (Ziegler, 1992, 1994; Prodehl et al., 1995). The URG has been intensely studied and explored for hydrocarbons and minerals and more recently also for geothermal energy. The structure and sedimentary fill of the URG is documented by numerous wells, surface geologic investigations and a dense grid of 2D industrial reflection-seismic lines (e.g. Wirth, 1962; Doebel, 1967, 1970; Bartz, 1974; Doebel and Teichmüller, 1979; Durst, 1991; Lutz and Cleintuar, 1999). Moreover, academic research projects have focused on its crustal and lithospheric configuration (e.g., DEKORP and ECORS; International Lithosphere Program), and its evolution (EUCOR-URGENT, EN-TEC). In this context large data sets have recently been compiled, providing overviews at regional and even super-regional scales (e.g. Dèzes et al., 2004; Rotstein et al., 2006; Berger et al., 2005a,b). For the evolution of the URG numerous models have been proposed and discussed in literature and are still debated (see Ziegler, 1994; Dèzes et al., 2004, 2005; Michon and Merle, 2005; Bourgeois et al., 2007). Most authors agree, however, that the URG evolved in the context of the Alpine orogeny and, therefore, assume that the build-up of far field stress induced passive rifting (Ziegler, 1994). This concept is supported by the absence of significant syn-rift thermal disturbance of the crust, as constrained by fission-track data modeling (Timar-Geng et al., 2006). A two-stage evolution of the URG with more or less orthogonal extension during the Paleogene and sinistral transtension during the Neogene has been advocated by Illies and Greiner (1978), Buchner (1981), Michon et al. (2003) and Dèzes et al. (2004). In contrast Schumacher (2002) proposed a five-stage evolutionary model for the URG, whilst Behrmann et al. (2003) and Lopes Cardozo and Behrmann (2006) advanced a model of continuous sinistral transtension. Hinsken et al. (2007) have shown for the southern parts of the URG that Paleogene syn-rift subsidence and sedimentation are consistent with pure shear orthogonal rifting and a deep level of lithospheric necking. Cross-section balancing is a standard technique that has been successfully applied to unravel the evolution of extensional sedimentary basins (e.g. Woodward et al., 1987; Buchanan and Nieuwland, 1996, and references therein). Geometric approaches to balancing of cross-section through rifted basins focus on retro-deformation of pre-rift reference horizons with the aim of quantifying the amount of extension. Combined with back stripping of the syn-rift sediments, the basin can be retro-deformed and extension-time paths determined. Alternatively, extension-time paths can be derived from quantitative subsidence analysis of the syn-rift sediment since development of accommodation space is directly related to the magnitude of crustal stretching described by the β -factor (e.g. McKenzie, 1978; Allen and Allen, 2005). However, as a number of non-linear processes are involved in extensional basin development, such as changes in heat flow and

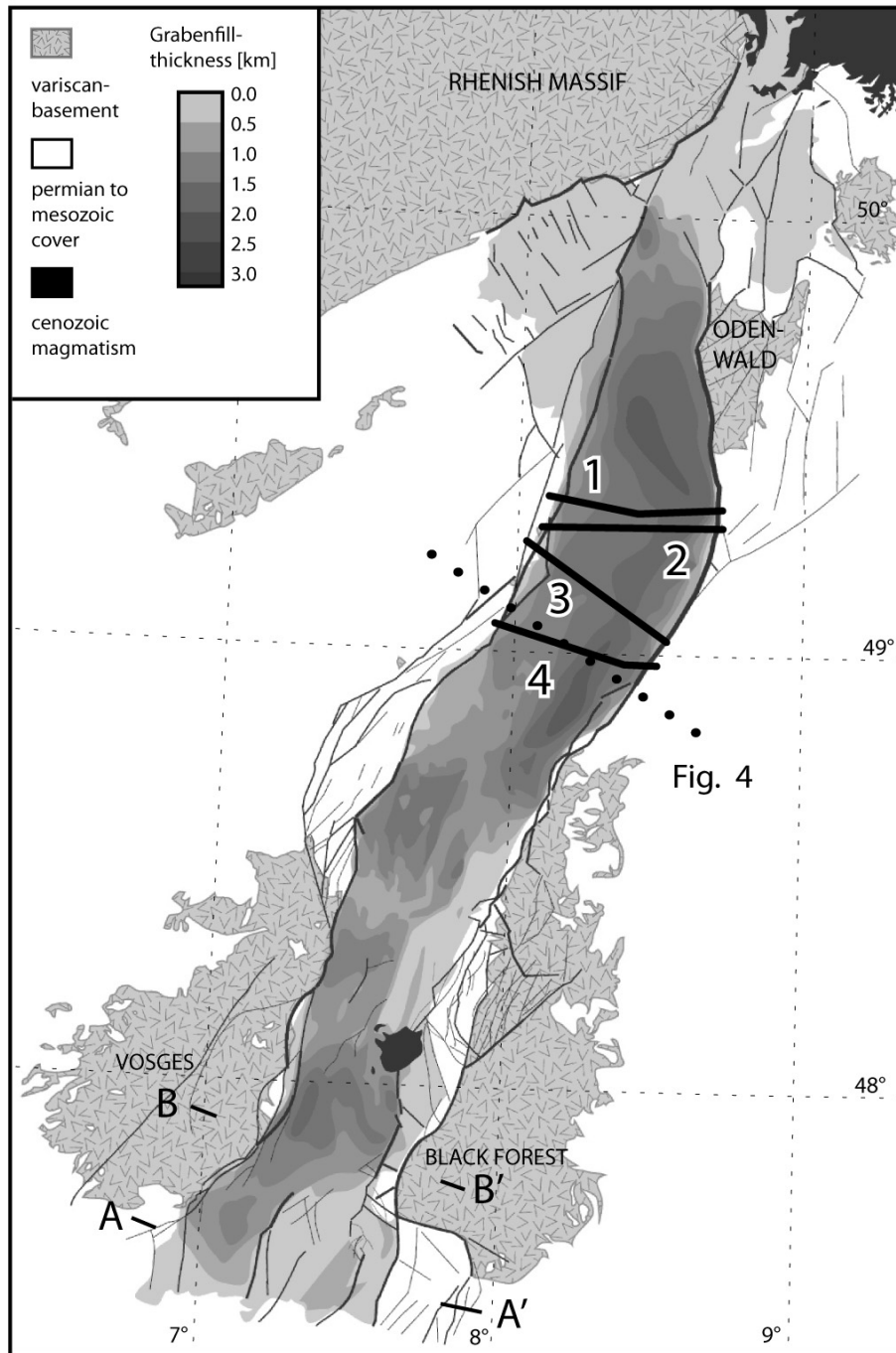


Figure 5.1: Simplified geological map of the URG, showing thickness of the Cenozoic graben fill and the location of studied cross-sections (1-4) in its central part.

Author	Method	Extension (ΔL)
Bourgeois et al. 2007	crustal thinning with $t_0 = 30\text{km}$	30% $\approx 12\text{ km}$
Hinsken et al. 2007	geometrical methods	5 km
Schwarz & Henk 2004	3D TTSMF with 2 borderfaults solving out at 15-16 km depth	8-8.5 km rift orth. ext. 3-4 km left lat. disp.
Brun et al. 1992	line length balancing crustal conuration	5-7 km 17 km
Meier & Eisbacher 1991	area balance with detachment at 15km	6-10km
Villemin et al. 1986	TTSMF	6 km
Illies 1967	geometrical methods	4.8 km

Table 5.1: Extension values for the URG from previous studies

isostatic compensation, a more advanced restoration of a rifted basin generally requires forward modeling. For this purpose special software has been developed that is also commercially used by the petroleum industry (e.g. Ruepke et al., 2008).

Despite numerous earlier approaches to assess the total amount of crustal extension across the URG (Tab. 5.1), detailed balancing of cross-sections, including back-stripping of the basin fill, has so far not yet been carried out. Forward modeling of a set of cross-sections across the URG may, however, help to improve the understanding of its evolution, specifically by permitting a comparison of extension-time paths derived from the individual cross-sections in an effort to assess the total amount of rift-related crustal extension as well as the rifting mode (orthogonal vs. oblique). Therefore, this study aimed at deciphering the extension history of the URG on the base of four geological cross-sections through its central part that were published by Doebl and Teichmüller (1979). The chosen methodology combined Thermo-Tectono-Stratigraphic-Forward modeling (TTSMF-Modeling, e.g., Ruepke et al., 2008) and geometric cross-section balancing. Applying different methodologies permitted to compare their results and to assess their validity. Nevertheless, the applicability of the chosen approach is limited to the northern, continuously subsiding parts of the URG whilst in its southern parts a major erosional hiatus spans Miocene and Pliocene times (e.g. Roll, 1979; Ziegler and Dèzes, 2007).

5.3 Evolution of the Upper Rhine Graben

5.3.1 Pre-rift evolution

The basement of the URG area was consolidated during the Late Paleozoic Variscan Orogeny and the subsequent latest Carboniferous-Early Permian phase of strike-slip deformation, magmatism and transtensional basin development (e.g. Ziegler et al., 2004b). During the Late Permian and Mesozoic re-equilibration of the lithosphere-asthenosphere system, the area of the URG was tectonically mainly quiescent, subsided and was incorporated into an intracratonic basin that extended from the Paris Basin on to the Franconian Platform (Ziegler et al.,

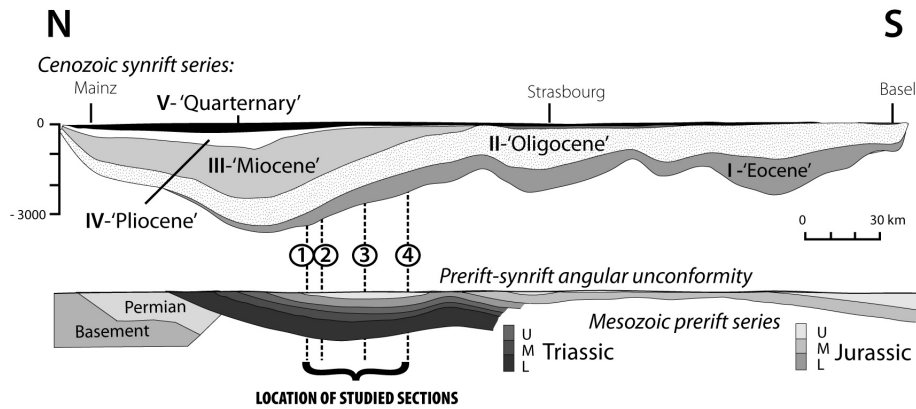


Figure 5.2: Longitudinal section through the URG showing northward shift of depocenters with time (after Von Eller and Sittler, 1974). Numbers refer to the location of analyzed cross-sections. (see Fig. 5.1)

2004b). In the URG area, a 1-1.5 km thick 'pre-rift' sedimentary sequence accumulated during the Triassic and Jurassic, locally affected by reactivation of Paleozoic crustal discontinuities (Wetzel et al., 2003; Allenbach and Wetzel, 2006). Zircon fission track ages from the basement exposed on the flanks of the URG indicate a significant Late Jurassic thermal event (Timar-Geng et al., 2006) that is still poorly understood. The extent to which the URG area was covered by Cretaceous deposits is uncertain (e.g. Ziegler, 1990). During the Latest Cretaceous and Paleocene the area of the future URG was affected by an important phase of Eo-Alpine, respectively Pyrenean collision-related intraplate compression, which caused buckling of the Mesozoic platform and its erosional truncation (Ziegler, 1990; Ziegler and Dèzes, 2007). These deformations, which controlled the subcrop pattern of pre-rift sediments beneath the syn-rift sedimentary fill of the URG (Fig. 5.2), were accompanied by the intrusion of scattered dykes reflecting very low degree partial melting of the lithospheric boundary layer (Keller et al., 2002; Dèzes et al., 2004; Ziegler and Dèzes, 2007).

5.3.2 Syn-rift evolution

Determining the onset of rift-related tectonic subsidence of the URG is difficult. The oldest syn-rift deposits occurring near the graben margins (lacustrine *Bouxwiler Fm.*) yield a Lutetian age of about 47 Ma (50-45 Ma; Berger et al., 2005b; Grimm and Hottenrott, 2005b). No biostratigraphic ages are, however, available from depocenters in which sedimentation may have started earlier. In the northern URG, in the area of the investigated cross-sections (Doebel and Teichmüller, 1979) erosion patterns of pre-rift series actually imply that the onset of rifting may have preceded the accumulation of syn-rift sediments (see be-

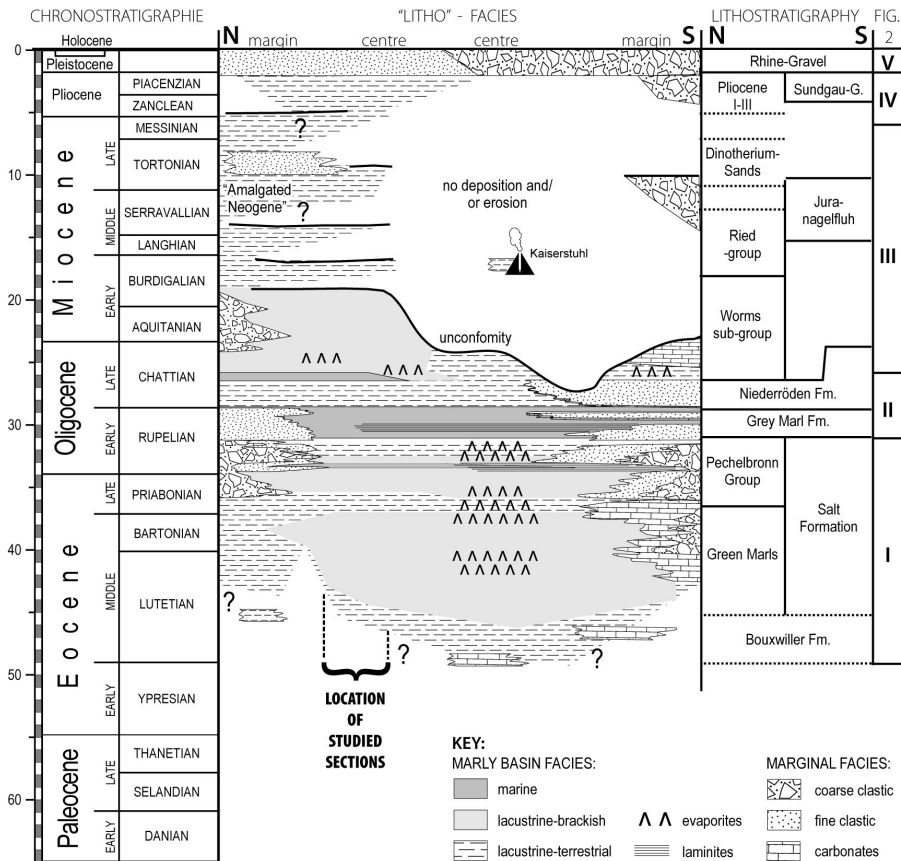


Figure 5.3: Stratigraphic chart of the Cenozoic URG fill. Roman numbers to the right refer to the stratigraphic subdivision shown in Fig.5.2.

low). A longitudinal profile through the fill of the URG indicates a progressive northward shift of depocentres with time (Fig. 5.2; Von Eller and Sittler, 1974). During the late Middle Eocene to Early Oligocene, subsidence of the URG accelerated and a thick succession of marls, including evaporites, accumulated in its axial part, while carbonates conglomerates and sandstones were deposited along its margins (Fig. 5.3); depositional environments changed repeatedly between fluvial, lacustrine, brackish and evaporitic (*Green Marl Fm.*, *Pechelbronn Gp.*; e.g., Düringer, 1988; Derer et al., 2003; Hinsken et al., 2007). Minor marine incursions from the north are indicated during the Early Oligocene Griessemer (*Middle Pechelbronn beds*; e.g., 2002); Pirkenseer (*Middle Pechelbronn beds*; e.g., 2007). During the Middle Oligocene the URG basin was flooded by a major transgression, establishing open marine conditions (*Grey Marls Fm.*). Subsequently a connection to the Paratethys realm was established (e.g., Roussé, 2006; Pirkenseer, 2007). Increased supply of sediments resulted in rapid infilling

of the basin (Huber, 1994) and a regression that led to a gradual shift towards brackish and finally fluvial-lacustrine conditions (*Niederröden Fm.*). Brackish to lacustrine conditions were re-established in the northern parts of the URG by the end of the Oligocene (*Worms Gp.*) and continued during the Early Burdigalian, while in the southern URG time-equivalent series are missing. From the Middle Burdigalian onward the northern URG was a continental domain with Middle Burdigalian to Pliocene fluvial and limnic deposits (*Ried Gp.*; Grimm and Hottenrott, 2005b). Reflection seismic profiles show that in the northern URG the Neogene succession was deposited in continuity with Oligocene series, thus suggesting continuous subsidence and sedimentation (Roll, 1979; Derer et al., 2005; Haimberger et al., 2005; Berger et al., 2005a; Ziegler and Dèzes, 2007). By contrast, uplift and erosion of the southern parts of the URG is evident by a regional angular unconformity that extends northward to the area between Karlsruhe and Speyer and against which the Middle and Late Miocene and Pliocene series of the northern URG progressively onlap (Fig. 5.2; Roll, 1979; Ziegler and Dèzes, 2007; Wirsing et al., 2007). Development of this unconformity is attributed to Mid-Burdigalian rapid uplift of the Vosges-Black Forest Arch, involving lithospheric folding in response to the buildup of Alpine collision-related intraplate compressional stresses (Ziegler et al., 2002; Dèzes et al., 2004; Bourgeois et al., 2007; Ziegler and Dèzes, 2007). From this arch coarse clastics were shed southward into the area of the future Jura Mountains where they interfinger with the Middle Miocene freshwater deposits of the Molasse Basin (e.g. Ziegler and Fraefel, 2009). This reflects large-scale erosional unroofing of the Vosges-Black Forest Arch and of the fill of the southern URG. Uplift of this arch was accompanied by a relatively short pulse of volcanic activity (Kaiserstuhl 18-16 Ma; Hegau 15-7 Ma, Urach, 16-11 Ma; Keller et al., 2002) that reflects low-percentage partial melting of a predominantly asthenospheric source in response to its adiabatic decompression (Ziegler and Dèzes, 2007). Whilst subsidence of the northern parts of the URG continued during Late Miocene, Pliocene and Quaternary times, accumulation of fluvial clastics in fault-controlled depressions resumed in its southern parts only during the Late Pliocene. The modern drainage system with the river Rhine passing through the URG on its way from the Alps to the North Sea was established around 2.8 Ma during the Late Pliocene (e.g. Ziegler and Dèzes, 2007; Ziegler and Fraefel, 2009). During the Quaternary up to 300 m thick, mainly Alpine derived coarse clastics (*Rhine gravels*) accumulated in fault-controlled depocentres in the southern and northern parts of the URG (e.g. Bartz, 1974; Roll, 1979; Haimberger et al., 2005; Hagedorn and Boenik, 2008; Kock et al., 2009a,b).

5.3.3 Basement configuration and deep structures

The URG is a more or less symmetric full graben that is 300 km long and on average 40 km wide. The graben is bounded by large normal faults with vertical displacements of up to 4 km, separating it from its variably elevated shoulders (e.g., Illies, 1970). A slight asymmetry of the URG is, however, evident from the alignment of its Cenozoic depocentres, which are associated with the west-

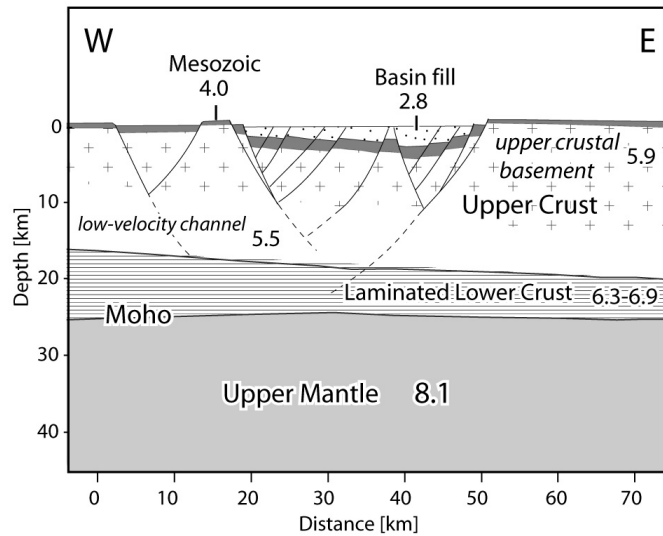


Figure 5.4: Crustal section through the central part of the northern URG re-interpreted from Taben Rodt seismic refraction line (Meissner et al., 1970).

ern master-fault in the south and the eastern master-fault in the north (Fig. 5.1). In the URG the inclination of normal faults ranges between 55° and 80° (Wirth, 1962), with 60° to 65° dominating (e.g., Dohr, 1957; Maurin, 1995). Tilting of individual fault blocks is common and testifies to the listric shape of their controlling normal faults (Behrmann et al., 2003; Rotstein et al., 2005). With increasing depth, the configuration of normal faults becomes, however, increasingly uncertain. Some authors interpreted normal faults to sole out at the base of the 'middle crust' into a common detachment horizon (Meier and Eisenbacher, 1991; Durst, 1991; Schwarz and Henk, 2005), whilst others traced them into shear zones that were interpreted to crosscut the crust-mantle boundary (Brun et al., 1992; Wenzel et al., 1991), suggesting simple shear rifting (sensu Wernicke, 1985). The deep seismic reflection lines published by Durst (1991), Brun et al. (1992, ; DEKORP-ECORS line south)) and Wenzel et al. (1991, DEKORP-ECORS line north) all show in the prolongation of the border faults oblique reflectors which can be traced at least down to the Moho. The relation of these reflectors to Cenozoic rifting is, however, not straight forward. Similar deep oblique reflectors occur also below the Black Forest and the Vosges, where they have been interpreted as being related to the Variscan basement fabric (e.g., Eisbacher et al., 1989).

Refraction seismic studies indicate that the crust of southern Germany and adjacent areas is characterized by a rather uniform structure and consists of two major layers (e.g., Zeis et al., 1990) as illustrated by a re-interpretation of the Taben-Rodt seismic refraction profile (Fig. 5.4). In the area of the URG the 'upper crust' (excluding the sedimentary cover) ranges in thickness between

16 to 20 km and is characterized by p-wave velocities of 5.9-6.0 km/s and a basal low velocity channel with p-wave velocities of 5.5-5.7 km/s. A distinct velocity contrast, identified as the Conrad Discontinuity, marks the top of the lower crust that has a thickness of about 10 km, p-wave velocities of 6.3-6.9 km/s and is characterized on reflection-seismic profiles by densely spaced anastomosing sub-horizontal reflectors which overprint the orogenic fabric (Eisbacher et al., 1989; Brun et al., 1992; Wenzel et al., 1991; Meissner and Kern, 2008). The thickness of this laminated lower crust, which directly overlies the Moho is, however, variable. Seismic velocities within the upper crust are compatible with a granitic composition (Mueller, 1977), whilst gravimetric and magnetic data modeling implies a relatively heavy ($\rho = 2.72\text{-}2.78 \text{ g/cm}^3$) and strongly magnetic basement in the central and northern parts of the URG, indicative for pelitic meta-sediments (Gutscher, 1995). The laminated lower crust reflects either amphibolitic and granulitic metamorphic layering or the presence of a network of mantle-derived sills and dykes (Ziegler et al., 2004b; Meissner and Kern, 2008). Gravity modeling indicates high densities ($\rho = 3 \text{ g/cm}^3$) for the lower crust. Xenoliths brought to surface by Cenozoic rift-related volcanics include high density/velocity lower crustal rocks, such as granulites, pyroxenitic and amphibolitic rocks. Nonetheless, a felsic composition is proposed for the upper as well as the lower crust with mafic material occurring only near the crust-mantle transition (Downes, 1993; Mengel, 1992; Wittenberg et al., 2000). Earlier interpretations, postulating the occurrence of a mantle diapir centered on the southern parts of the URG, are, however, not supported by more recent seismic tomography and refraction seismic studies (Prodehl et al., 1995; Achauer and Masson, 2002.). Observed gravity anomalies can be explained by a modest density contrast at the Moho due to the presence of a high-density lower crust (Gutscher (1995)). In the wider URG area the topography of the Moho discontinuity describes a broad dome. Its axes are aligned with the ENE trending Vosges-Black Forest Arch and the NNW-striking URG whilst its flanks extend far beyond the border faults of the URG (e.g. Ziegler and Dèzes, 2007). The uplift pattern of this dome is dominated by the Vosges-Black Forest Arch, the culmination of which is centered on the Kaiserstuhl volcanic complex in the southern parts of the URG where the Moho occurs at a depth of less than 24 km (Dèzes et al., 2004; Ziegler and Dèzes, 2007). With reference to the Moho topography below the rift-shoulders and their observed syn-rift uplift and erosion, a pre-rift crustal thickness of 28-30 km is postulated (Ziegler et al., 2004b). The URG area is characterized by an elevated heat flow that is related to a relatively thin thermally defined 90-100 km thick lithosphere (Achauer and Masson, 2002.; Tesauro et al., 2009b). Therefore the integrated compressional strength of the URG lithosphere is generally low (Cloetingh et al., 2005). Estimates of the effective elastic thickness (EET) of the lithosphere in the North Alpine Foreland are derived from flexural modeling of the North Alpine Foreland Basin, yielding EET values in the range 50-25 km. These values are reduced in the ECRIS area (e.g. Gutscher, 1995), with thermo-rheological modeling indicating EET values of 15-20 km in the wider UGR area (Tesauro et al., 2009a). However, the flexurally uplifted shoulders of the URG permit to determine the EET of the

lithosphere in the immediate vicinity of the graben,. The URG graben shoulders extend about 100 km to the east and west of the graben axis. Assuming that their symmetrical uplift reflects flexural isostatic rebound of the lithosphere in response to its extensional unloading in the URG, the EET of the lithosphere can be calculated from their width. Using an analytical solution for a thin-plate equation, the distance from the graben axis (seen as a negative line load) to the outer limit of the uplifted shoulders equals the 'deflection distance' X_0 that relates to the flexural parameter (Turcotte and Schubert, 2002).

$$X_0 = \frac{3\pi}{4}\alpha \quad (5.1)$$

The flexural parameter (α depends on the flexural rigidity (D) and the density (ρ) difference of the media replacing each other (in this case mantle replacing air):

$$\alpha = \frac{4D}{\rho_{mantle} - \rho_{air}} g^{-1/4} \quad (5.2)$$

The flexural rigidity is directly related to the thickness (h) representing the EET and its internal elastic properties, including the Youngs Modulus (E) and the Poisson's ratio (μ)

$$D = \frac{E * h^3}{12(1 - \mu)} \quad (5.3)$$

Assuming $X_o = 100$ km, $E = 8 * 10^{10}$ Pa (Gutscher, 1995), $\mu = 0.25$ and $\rho_{mantle} - \rho_{air} = 3300$ kg/m³ the EET of the URG lithosphere is about 15 km.

5.4 Material and Methods

5.4.1 Theory

Retro-deformation of cross-sections can only be successful if two basic requirements are fulfilled, namely plane strain deformation and orientation of the cross-section parallel to the direction of deformation. Whether and to what extent both requirements are fulfilled is often a matter of debate. Moreover, controls on the structural configuration of the to be restored cross-sections are often not optimal and leave room for multiple interpretations. For extensional basins, this pertains specifically to structural cross-sections that are based on industry-type reflection-seismic profiles imaging their sedimentary fill. In this context, it ought to be kept in mind that the reflection-seismic resolving power, particularly of faulting, decreases with increasing depth (Ziegler and Cloetingh, 2004a). Reflection-seismically constrained basin-scale cross-sections provide only approximate extension values and hence, multiple approaches are required to validate such values. Similarly, crustal-scale cross-sections, which are based on refraction- and/or deep reflection-seismic data, can give a measure of crustal extension, if the base of the syn-rift sediments is identified, the crust/mantle boundary is imaged, the velocity distribution within the crystalline crust

is determined with sufficient accuracy to permit reliable depth conversion of the data, a uniform pre-rift crustal thickness can be assumed and there is no evidence of syn-rift magmatic destabilization of the crust/mantle boundary. For these reasons, the magnitude of extension values derived from basin-scale as well as crustal-scale cross-sections needs to be qualified.

Geometrical methods

Line-length balancing. The magnitude of total extension across a rifted basin can be quantified by mapping on a cross-section that trends normal to the rift axis a pre-rift reference horizon (sedimentary or top basement) and by measuring and summing up the length of its fault-bounded segments. The difference between the total length of the measured reference horizon (L_0) and the distance between the endpoints of its occurrence on the cross-section (L_f) corresponds to the amount of extension (ΔL).

$$\Delta L = L_f - L_0 \quad (5.4)$$

Alternatively the horizontal displacement across individual normal faults (δx) can be directly measured and summed up along a cross-section.

$$\Delta L = \Sigma \delta x \quad (5.5)$$

In extensional basins, the offset on faults generally decreasing upward in syn-rift sediments. As the reflection-seismic resolution of such growth faults generally deteriorates with increasing depth it is often difficult to determine their geometries at depth (e.g. Behrmann et al., 2003). Moreover, the vertical offset (δZ) on normal faults is generally better known than the horizontal offset (δx). Extension can be roughly estimated from the (known) vertical offset by the tangential ratio of the average dip angle of faults (α) as observed in outcrops or derived from reflection-seismic data.

$$\Delta L = \Sigma \delta Z / \tan \alpha \quad (5.6)$$

Area balancing Volume balancing methods are based on the concept of constant rock volumes, approximated by the cross-sectional area, which is tectonically deformed or displaced. This method can be applied to less well-constrained data sets but requires additional knowledge about initial conditions or the deformation compensation depths. Normally the area balancing method compares the thickness of a layer after its extensional deformation (Z_f) with its initial thickness (Z_0).

$$\Delta L = L_f * (Z_f / Z_0) \quad (5.7)$$

Alternatively the 'lost area' method (Groshong, 1996; Hinsken et al., 2007) deals with the volume of the graben (A_{lost}), referred to as the 'lost area' that is compensated by stretching of a crustal unit by a defined length (ΔL) and

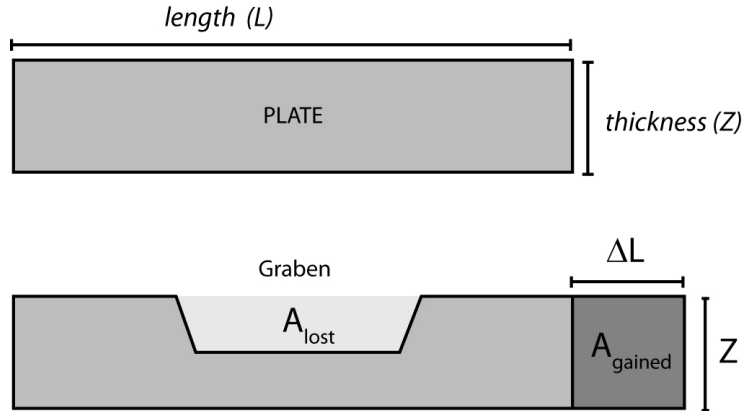


Figure 5.5: Area balancing of a plate with defined length and thickness. The 'lost area' equals the gained area compensating the extension.

thickness (Z). The 'lost area' equals the 'gained' area (A_{gained}), as a function of extension and volume conservation (Fig.5.5).

$$A_{lost} = A_{gained} \quad (5.8)$$

If (Z) is known, the amount of extension can be calculated:

$$\Delta L = A/Z \quad (5.9)$$

Transferred to a geological scenario, the thickness of the crustal unit (Z) represents the depth of the compensation level that may either represent the extensional detachment level (Fig. 5.6A; e.g. Groshong, 1996) or the necking level (Fig. 5.6B; e.g. Kooi and Cloetingh, 1992).

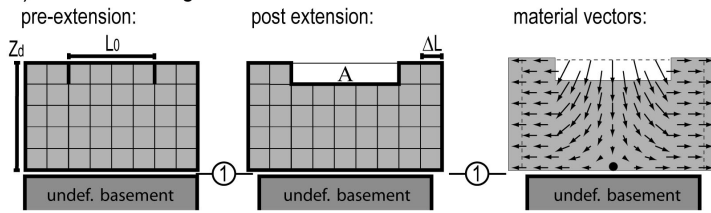
Both cases assume pure shear kinematics and virtual (material) points along the detachment level, respectively necking level, move only horizontally in response to crustal extension (Fig. 5.6 right-hand).

Theoretically, the necking level and detachment level are related to rock rheology. While detachment levels are generally located in rheologically weak zones (e.g. evaporites), the necking level is considered to represent the strongest interval of the lithosphere (Braun and Beaumont, 1989). The location of the necking level moreover accounts for rift related loading or unloading and the related flexural isostatic response. A deep level of necking will cause upward flexure of the rifted basin and its shoulders, while a shallow necking level will cause downward flexure (Kooi and Cloetingh, 1992). This flexural deformation has to be taken into account, when measuring the 'lost area'.

TTSF-Modeling

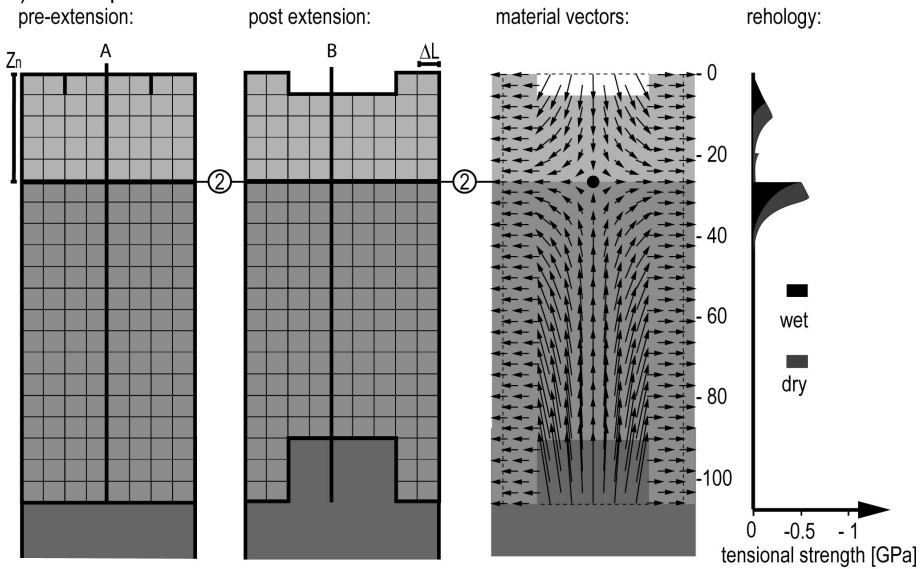
Various types of numerical models have been developed to reconstruct the evolution of sedimentary basins. These models have to contend with processes

1) Thin-skinned graben



① location of detachment-level

2) Lithospheric scale rift



② location of necking-level ■ "asthenosphere" ■ below neck ■ above neck

Figure 5.6: In a geological scenario the 'compensation depth' can be either a detachment 1) or 2) the necking level. At this depth material points only move in a horizontal direction (right).

such as flexural isostasy, transient heat conduction and sediment compaction that require, especially in two and three dimensions, a considerable amount of computing time. Two different types of numerical models are usually applied for basin reconstruction:

1. Backward models start with the present day configuration, calculate a retro-deformation including back-stripping of the sedimentary fill, and provide a precise mechanical solution. However, because transient heat conduction cannot be modeled backwards, inverse models are limited to mechanical basin evolution while their thermal evolution has to be calculated separately. This may lead to inconsistent results.
2. Forward models start with an initial rifting phase and calculate lithospheric thinning, sediment accumulation, compaction, temperature, and isostatic compensation forward in time. Such models require improved input data on the basin geometry, its sediment fill and assumptions on rifting processes.

The numerical algorithm applied in this study for two-dimensional TTSF-Modeling is based on the coupling of a forward model to an inverse scheme and does, in principle, not require any a priori information on paleo-bathymetry, fault locations, and stretching factors. Clearly, a priori information will improve the model and can be implemented in the forward model. The forward model accounts for sediment deposition, thermal blanketing, and compaction, as well as flexural isostasy, multiple thinning events of finite duration, thermal advection and conduction, and radiogenic heat production. The model simultaneously resolves lithospheric processes such as stretching, flexure, and heat conduction, and sedimentary processes such as sediment accumulation, compaction, and thermal maturation. The inverse scheme is based on an iterative optimization algorithm and automatically updates crustal- and mantle-thinning factors and paleo-water-depths until the input stratigraphy is fitted as closely as possible. The model employs 7 major units; (1) asthenosphere, (2) mantle lithosphere, (3) lower crust, (4) upper crust, (5) sediment, (6) water and (7) atmosphere. The sediment unit can be further subdivided into stratigraphic intervals, characterized by different lithologies. To all lithologies variable physical properties such as compaction coefficient or thermal conductivity can be attributed. The TTS-Modeling algorithm, as applied in the present study on the URG, was successfully tested in the northern Viking Graben by Ruepke et al. (2008) who provided a detailed description of the mathematical and numerical model

5.4.2 Analyzed cross-sections

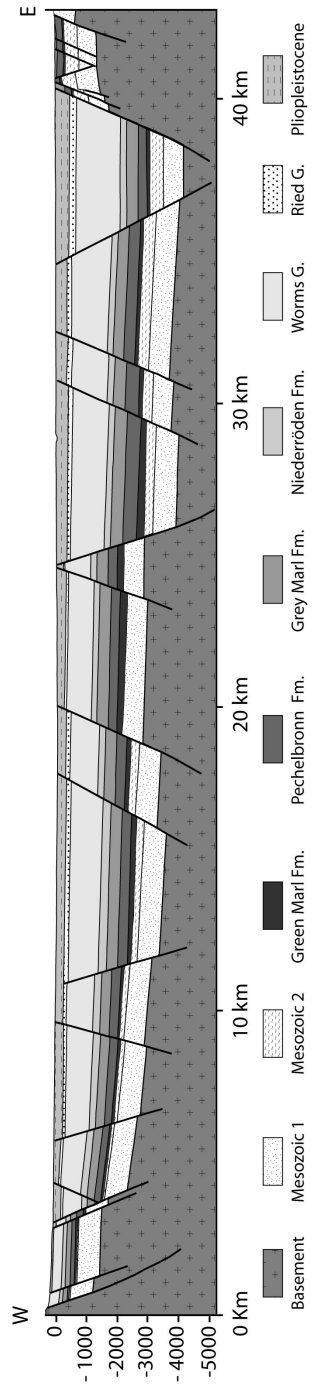


Figure 5.7: Re-evaluated cross-section (Line 2), redrawn from DoebI and Teichmüller (1979). Mesozoic 1 refers to the Early and Middle Triassic strata while Mesozoic 2 refers to the Late Triassic to Early Jurassic strata forming an angular unconformity and are not present on the central horst.

Lithology	ρ [kg/m ³]	α [10 ⁻⁶ k ⁻¹]	A [W/m ³]	k [Wm ⁻¹ k ⁻¹]	sPor. [%]	c.l. [km ⁻¹]
Sand& Shale	2405	0	1	2.56	56	0.39
Shale	2420	0	1	1.5	62	0.5
Granite	2750	2.4	2	3	0	0
Diabase	2900	2.4	2	3	0	0
Peridotit	3340	3.2	0	3.5	0	0

Table 5.2: Rock properties used for TTSTF-Modeling; ρ density, α thermal expansion, A radiogenic heat production, k conductivity, sPor surface porosity, c.l. compaction length

Our investigation focused on four published cross-sections through the URG between the cities of Karlsruhe and Speyer (for location see Fig. 5.1; Doebl and Teichmüller, 1979). These high-quality cross-sections are based on industry-type reflection-seismic data calibrated by wells (Fig. 5.7). In this part of the URG a fully developed Paleogene and Neogene syn-rift sequence rests on pre-rift sediments, part of which is also preserved on the rift flanks. By contrast published cross-sections through the southern URG are less suitable for modeling its evolution owing to the absence of Neogene deposits, partial erosion of the Paleogene syn-rift series, and the lack of a well-defined 'base Mesozoic' reference horizon on the elevated graben shoulders. The investigated segment of the URG is slightly asymmetric with a distinct Neogene depocentre adjacent to the eastern border fault (Fig. 5.7). All four cross-sections trend at a high angle to the graben axis (010°), with lines 1, 2 and 4 paralleling each other (90°-100°) and line 3 trending slightly obliquely (124°; Fig. 1). The sedimentary fill of the graben volume ('lost area') decreases from 95% in the north to about 85% in the south with the lowest fill values occurring in section 3, which crosses an intra-basinal swell. While sections 1 and 2 show an uninterrupted syn-rift sedimentary sequence, the Neogene *Ried Group* is only partly developed in section 3 and appears to be missing in section 4 owing to on-lap against the mid-Burdigalian unconformity. On the graben shoulders, erosion has reduced the thickness of the Mesozoic pre-rift sediments by about 700 m as compared to their thickness within the graben. It is, however, uncertain, whether this amount of erosion can be exclusively attributed to syn-rift shoulder uplift. The distribution of the truncated 'Mesozoic 2' (Upper Triassic and Lower Jurassic) within the graben (Fig. 5.7) reflects the geometry of the rift basin, and hence, suggests that in this area the graben may have started to subside prior to the onset of syn-rift sedimentation.

5.4.3 Modeling Approach and TTSTF-Modeling input parameters

Rock properties used for modeling are listed in Table 5.2.

The initial thickness of the lithosphere was set to 109 km (29 km crust and

90km lithospheric mantle) with a temperature of 1300°C at its base. An initial crustal thickness of 29 km was adopted, as presently seen beneath the rift shoulders, assuming that they were not affected by rift-related crustal thinning. The crust was subdivided into an upper unit (0-20 km) with a 'granitic' composition and a lower unit (20-28 km) with a 'diabase'-dominated composition. In the modeled scenario, rifting commenced around 47 Ma during the Middle Eocene. Assuming that the Mesozoic pre-rift sequence was down-faulted prior to the onset of syn-rift sedimentation, a 'pre-depositional unit' was modeled using 'Mesozoic 2' as a fully compacted sequence. The chronostratigraphy of the syn-rift sequences was updated according to the compilations by Berger et al. (2005a) and Grimm (2005a) (Fig. 5.3). The following eight intervals were modeled: (I) Pre-depositional Sequence (47-43.5 Ma), (II) Green Marls Formation (43.5-36.5 Ma), (III) Pechelbronn Group (36.5 -30.6 Ma), (IV) Grey Marls Formation (30.6-28 Ma), (V) Niederröden Formation (28-26.4 Ma), (VI) Worms Group (26.4-19.5 Ma), (VII) Ried Group (19.5-5 Ma), (VIII) Plio-Pleistocene (5-0 Ma). For modeling purposes the syn-rift sediments II-VIII were decompacted, assuming a shale-dominated lithology for the Green Marls Formation to Worms Group and a shale-sandstone mixture for the Ried Group and Plio-Pleistocene deposits.

5.4.4 Set up

In a first step the cross-sections were retro-deformed using the base Mesozoic as reference horizon. Extension was measured between the break-away faults of the graben by line-length balancing (equations 5.4,5.5 and 5.6) and by determining the volume of the 'lost area'. TTSF-Modeling of line 1 was then tested with variable input parameters, such as the necking depth and EET, and modeled Moho geometries compared with the geophysically mapped Moho topography. Furthermore, the crustal mass balance was investigated and the flexural isostatic response of the lithosphere to the extension-induced loading change was modeled using a 2D FFT solution of a thin-plate equation (eq. Jordan, 1981; Allen and Allen, 2005). Finally a best-fit of geometric balancing and TTSF-Modeling was evaluated and the most reasonable values chosen for TTSF-Modeling of the remaining cross-sections and for plotting time-extension paths.

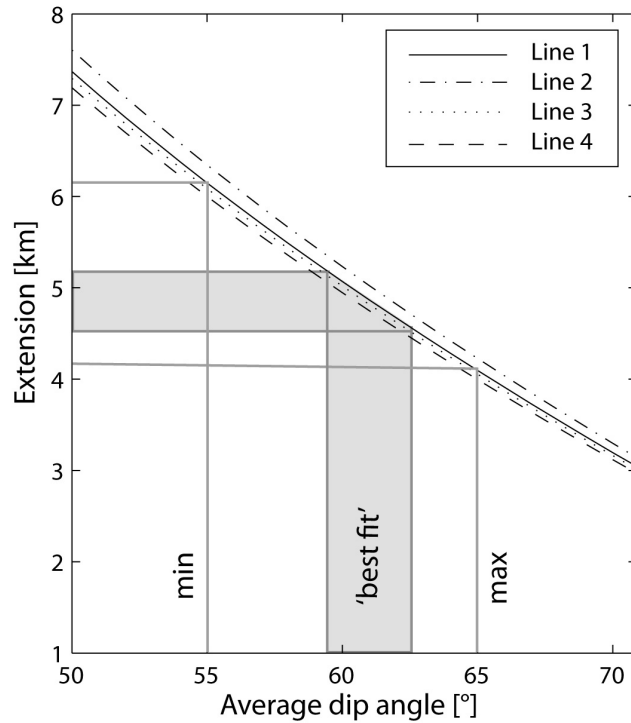
5.5 Results

For the four cross-sections extension values obtained by direct measurements of ΔL range between 3.0 km and 4.7 km (Tab. 5.3). Application of equation 5.4 gave 3.6 ± 0.5 km of extension, while equation 5.5 gave 4.3 ± 0.3 km. Extension values derived from equation 5.6, assuming that the dip angle of faults varies between 65°-55°, range from 4.1 to 6.1 km (Fig. 5.8). All results are very consistent between the four cross-sections. A best-fit angle of 60° in agreement with observations and theoretical assumptions (e.g., Heiskanen and Vening-Meinesz, 1958), yields an extension value of 5.1 ± 0.1 km. 'Lost area'

line No.	trend [°]	length [km]	'lost area' [km ²]	eq. 5.4 [km]	eq. 5.5 [km]	eq. 5.6 (60°) [km]	TTSFM (28km) [km]
1	095	41.9	126.5	3.43	4.07	5.07	5.2
2	089	42.3	120.3	3.45	4.28	5.23	5.38
3	124	42.4	116.3	4.29	4.7	5.02	4.69
4	103	40.0	128.2	3.04	4.26	4.95	4.81
mean	103	41.6	122.8	3.6	4.3	5.1	5.02
std	15	1.1	5.5	0.53	0.27	0.12	0.32

Table 5.3: Extension values ΔL obtained from line length balancing (equation 5.4,5.5,5.6) and TTSFM with T_e and neck at 29 km; std standard deviation.

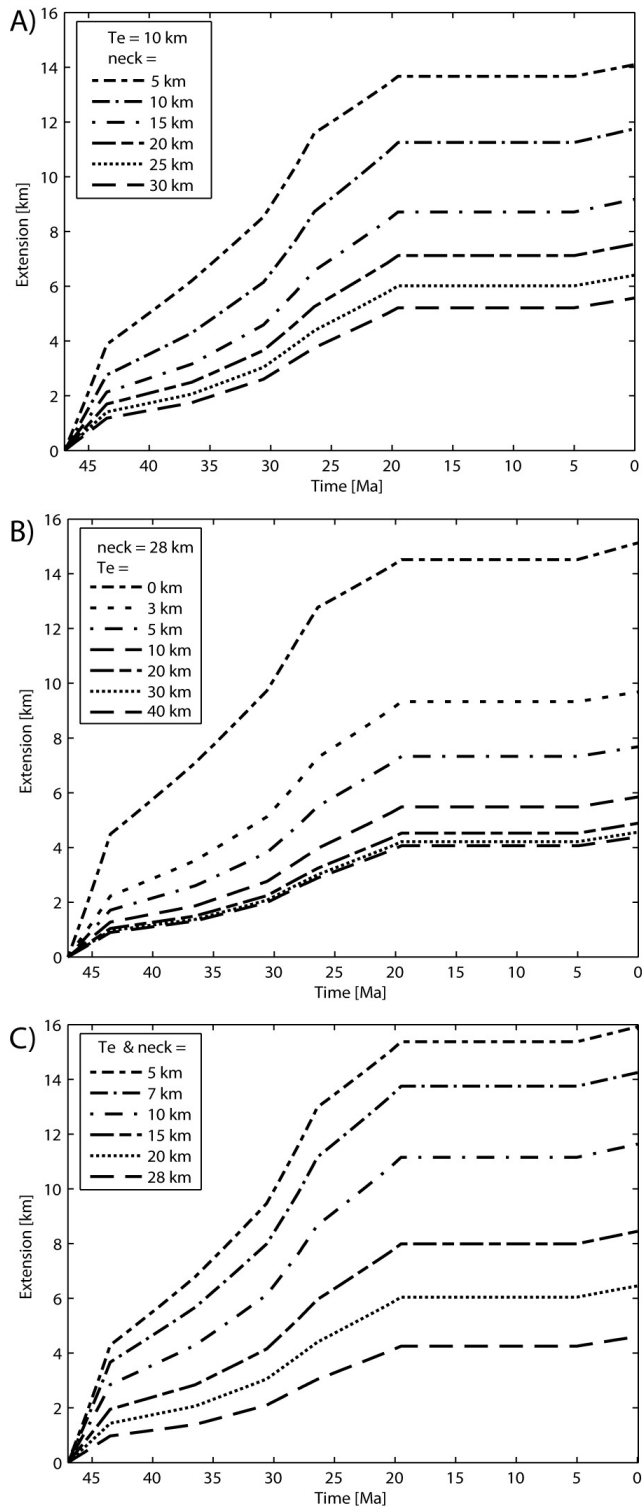
Figure 5.8: Relation between the extension values calculated from the heave and the (average) dip angle of the normal faults (eq. 5.6).



values are rather constant and range between 116 km² and 128 km². Using equation 5.9 the average values obtained by geometric crustal balancing indicate a necking level in the depth range of 20-34 km. TTSF-Modeling with necking depth varying between 5 and 35 km and a constant EET of 10 km yielded similar shaped time-extension paths and extension values ranging from 5 km to 14 km (Fig. 5.9A). TTSF-Modeling with a constant necking depth of 28 km and a EET varying between 0 and 40 km yielded similar shaped time-extension paths with extension values ranging between 4 and 15 km (Fig. 5.9B). As the necking depth and EET of the lithosphere are both related to its rheological structure and internal strength distribution, they are expected to be roughly correlative. A deep level of necking and a high EET is expected for a strong crust, while the opposite is expected for a weak crust. A possible range of extension values between 4.5 km and 16 km was modeled with the combined EET and necking depth varying between 28 km and 5 km (Fig. 5.9C). This sensitivity analysis shows that the EET and necking depth of the lithosphere inversely relate to the magnitude of the extension value (equation 5.8). For a EET of 15 km and a necking depth in the range of 20 - 30 km, the TTSF-modeled Moho topography (Fig. 5.10A) is very similar to the geophysically mapped Moho topography (Dèzes et al., 2004; Ziegler and Dèzes, 2006, Mechie, written com. 2008). The theoretical flexural isostatic flank uplift computed from the modeled scenarios is shown in Figure 5.10B. Flexural isostasy driven shoulder uplift can only be expected with a necking level deeper than 15 km. The modeled maximum shoulder uplift of about 200 m roughly equates the observed topographic elevation contrast between the alluvial plain of the graben and the average elevation of the rift flanks in the area under investigation. It is, however, important to note that this area is located where the SW-NE striking Mesozoic Nancy-Pirmasens-Kraichgau Depression crosses the URG (Boigk and Schöneich, 1970); to the north and south of it the elevation of graben shoulders is much more pronounced (Fig. 5.1). The best fit to results obtained by geometric section balancing suggests that the necking level coincides with the crust-mantle boundary, located at a depth of 29 km, while the observed graben shoulder width indicates an EET of about 15 km. TTSF-Modeling lines 1 to 4 using these values leads to a best fit between modeled and input stratigraphy when crustal stretching occurs during intervals I-VI and VIII (Fig. 5.11). Incorporating an additional stretching phase during interval VII (*Ried Group*) yields, however, unsatisfactory results.

The 'best fit' provides for all four cross-sections similar time-extension paths with 5.0 ± 0.3 km of rift orthogonal extension (Fig. 5.12, Tab. 5.3). This value is very close to the extension value of 5.1 ± 0.1 km that was derived from line-length balancing using average fault dips in the range of 60°, (equation 5.6; see Discussion). The time extension paths of the four modeled cross-sections show a similar development between 47 and 19.5 Ma. However, a shift in the modeled extension in time is evident - with the southern sections having the highest extension rates during the Eocene and the northern ones during the Early Miocene. TTSF-Modeling yields extension rates of about $1.4 \cdot 10^{-16} \text{ s}^{-1}$ for the Eocene to Mid-Miocene main rifting stage (47-19.5 Ma) and $7.4 \cdot 10^{-17}$

Figure 5.9: Impact on lithospheric strength on modeled time extension paths. A) Time-extension paths obtained from TTSF-Modeling with variable necking depth (2-35km) and a constant EET of 10km. B) Time-extension paths obtained from TTSF-Modeling with variable EET (0-40km) and a constant necking level at 28km depth. C) Time-extension paths obtained from TTSF-Modeling with same EET and necking level (5-28km).



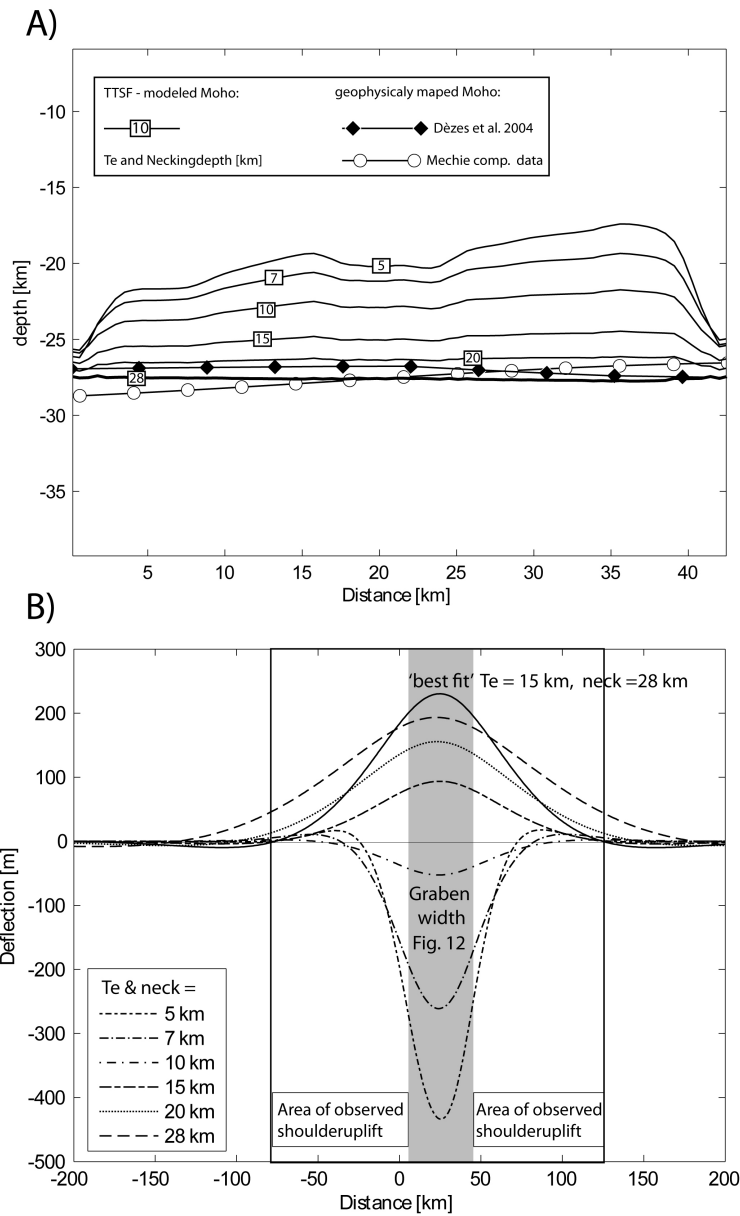


Figure 5.10: A) Moho-topography obtained from TTSF-Modeling with 15 km EET and necking level (5-28km) compared with geophysically mapped (interpolated) Moho topography. A deep level of necking between 20-28km would 'best fit' the observed Moho pattern. B) Effects of flexural isostatic rebound would lead to a 'steers-head' basin geometry with a shallow necking-level (≤ 10 km), while shoulder uplift can be expected with a necking depth ≥ 15 km. A EET of 15 km leads to a 'best fit' between the modeled and observed width of the graben shoulders.

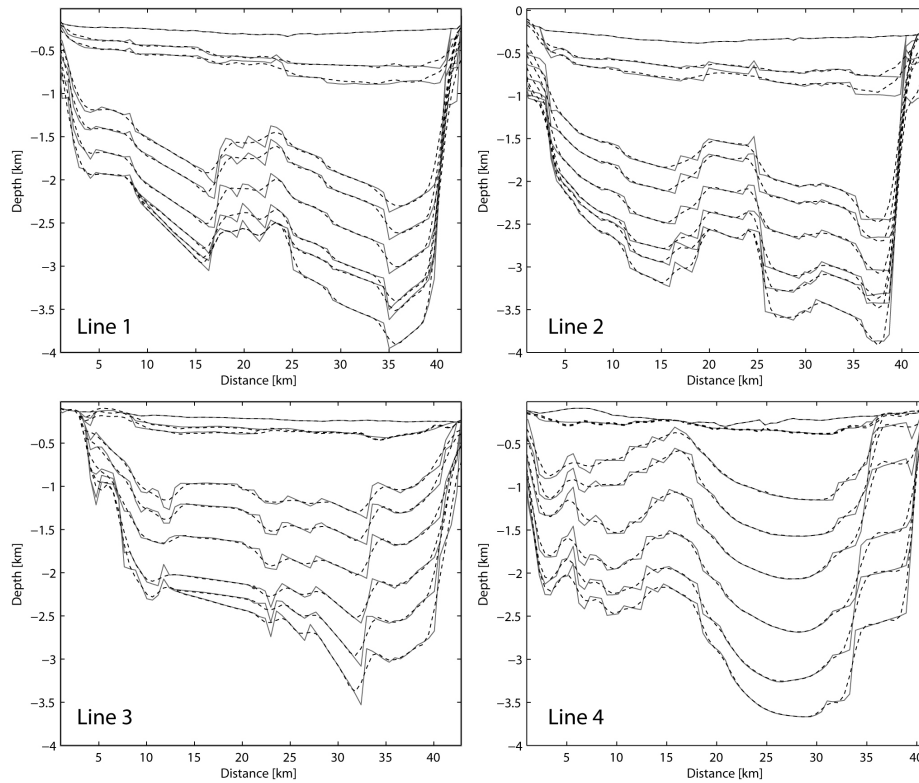


Figure 5.11: Comparison of TTSF-modeled and input stratigraphy. Basin Stratigraphy can be best fitted with two extensional phases spanning 47 - 19.5 Ma and 5 - 0 Ma.

s^{-1} for Plio-Pleistocene extension (5-0 Ma).

5.6 Interpretation and Discussion

5.6.1 Position and meaning of necking level

The magnitude of total crustal extension across the central parts of the URG, as derived from line-length restoration, TTSF-Modeling and especially the assessment of the 'lost-area' is almost the same for all investigated cross-sections. Large differences occur, however, between the various approaches (equations 5.4, 5.5, 5.6, variable EET and necking depth). Variations in 'published' extension values (Tab. 5.1) are, therefore, primarily related to assumed boundary conditions, input parameters and applied methods. For the line-length approach, it is very likely that the extension value derived for a specific cross-section represents a minimum rather than maximum owing to limitations of the reflection-seismic resolving power, particularly of smaller faults. Therefore about 5 km extension

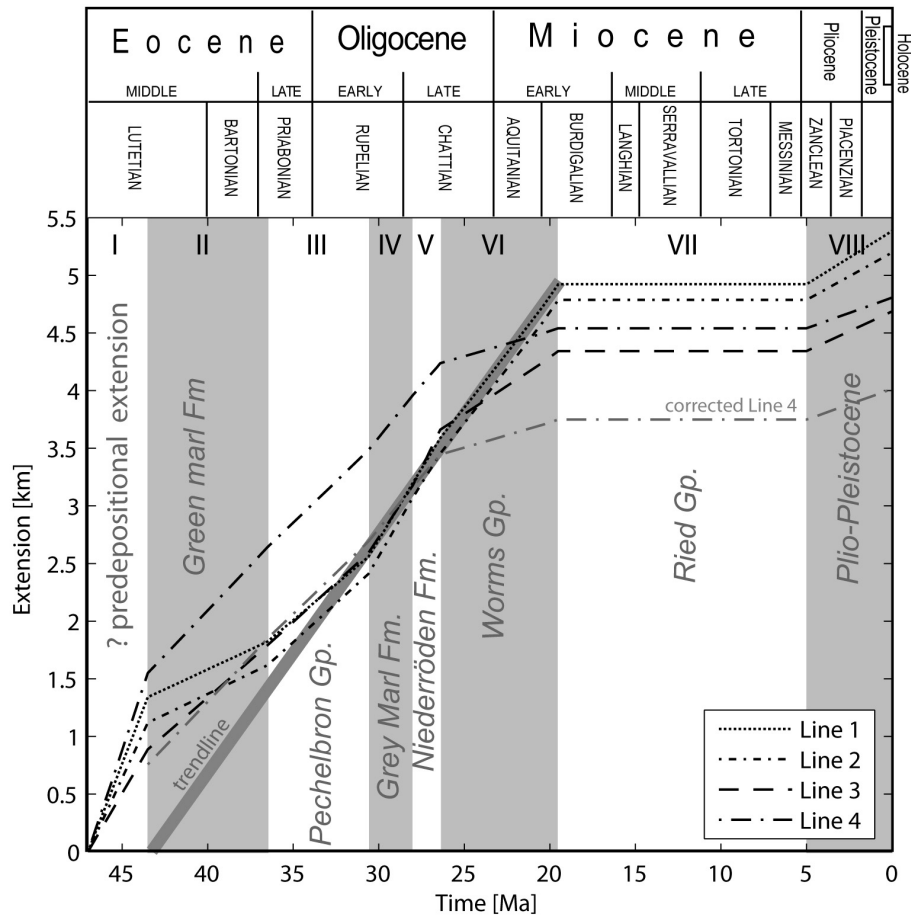


Figure 5.12: 'Best fit' time-extension paths for the investigated cross-sections with EET of 15 km and a necking level at the Moho at an initial depth at 28km. Average extension rate was $1.4 \cdot 10^{-16} \text{ s}^{-1}$ between 47-19.5 Ma and $7.4 \cdot 10^{-17} \text{ s}^{-1}$ between 5-0 Ma. Accumulation of syn-rift sediments was affected by pre- syn- and post- rift flexural uplift.

obtained with equation 5.9 and an 'average' fault plane dip of 60° appears to yield realistic results that match the results obtained by Illies (1967). The total, rift orthogonal component of extension calculated from the 'lost area' or estimated by TTSTF-Modeling depends, however, largely on the assumed position of the necking level and the EET of the lithosphere. The concept of a necking level applies only to pure shear and combined shear rifting models, while in simple shear rifting models a 'mantle shear zone' ought to occur, as suggested for the URG by the DECORP-ECORS crustal profiles (Brun et al., 1992). Nevertheless, the nearly symmetric configuration of the URG, with respect to faulting, shoulder and Moho uplift and gravity anomalies suggests that it evolved essentially by pure shear rifting. Moreover, the listric shape of its crustal faults

indicates that these sole out at a certain depth below which presumably distributed ductile shear prevails and the isostatic response of the lithosphere to its extension is compensated at the so-called necking level (Kooi and Cloetingh, 1992). Being related to the rheological stratification of the lithosphere, the lithospheric necking level may be located in the URG area at three different potential levels. In the upper crust, the highest strength is assumed to coincide with the brittle-ductile transition zone, often referred to a depth of about 15 km, probably representing an absolute minimum. Alternatively, the necking level may be located in the lower crust (20-28 km) or in the uppermost mantle between 28-40 km. Schwarz and Henk (2005) modeled for the URG 8-8.5 km orthogonal extension with border faults soling out at 15-16 km depth, beneath which distributed ductile shear prevails. Assuming a similar necking level, their results can be approximated by TTSF-Modeling (see Fig. 5.9C). By contrast, Groshong (1996) advocated that the URG represents a full graben the border faults of which dip 60° and sole out near the Moho (see also Illies, 1967). According to our analysis, such a deep necking level is indicated by the results of geometrical retro-deformation and TTSF-Modeling (see Tab. 5.3). In the modeled best-fit scenario, the necking level, the base of the brittle-elastic deforming crust and the Moho essentially coincide. This concept is supported by the seismicity of the southern URG where earthquake hypocenters occur in the laminated lower crust almost down to the Moho (Plenefisch and Bonjer, 1997; Meissner and Kern, 2008). This clearly shows that almost the entire crust is deforming in a brittle-elastic manner, while the a-seismic lithospheric mantle probably deforms by distributed ductile shear. The observed amplitude and width of the broad belt of Moho shallowing that is seen in the wider URG area is much too large to be exclusively explained by Cenozoic crustal extension and, thus, suggests probably not uniform crustal thicknesses prior to the onset of Cenozoic rifting (Brun et al., 1992; Dèzes et al., 2004; Ziegler and Dèzes, 2006). The URG developed in an area that was presumably characterized by a relatively thin crust (28-30 km) and therefore by a rheologically strong lithospheric upper mantle. However, the results of our study suggest that in the URG area the lithospheric necking level is located within the crust-mantle transition zone, which raises questions whether in the presence of a relatively thin crust the bulk of the lithospheric strength resided at the onset of rifting indeed in the upper lithospheric mantle (Banda and Cloetingh, 1992; Cloetingh and Burov, 1996; Ziegler and Cloetingh, 2004a). According to thermo-rheological modeling 60% of the present-day lithospheric strength is located in the upper mantle and the remaining 40% in the upper crust (Tesauro et al., 2009a,b). In this context it should be noted that during the latest Cretaceous and Paleocene phase of intraplate compression and injection of melilite dykes, geotherms probably rose gradually in the URG area, causing weakening of the lithospheric mantle (Ziegler and Dèzes, 2005, 2007; Cloetingh et al., 2005). At the Eocene onset of rifting, much of the strength of the lithosphere probably resided within the upper 10 km of the mantle and in the crust that, itself was weakened by pre-existing discontinuities. Under the prevailing stress regime, these discontinuities were reactivated, controlling localization of the URG (Schumacher, 2002; Dèzes et al., 2004). Development

of the URG at the indicated very low extension rates apparently involved deep crustal detachment faulting and deformation of the strong parts of the upper mantle by distributed ductile shear, thus essentially conforming to the model of Gueydan et al. (2008).

5.6.2 Time-extension paths

The time-extension paths derived from the four analyzed cross-sections are very similar but do show some differences which need to be explained (Fig. 5.12). Although syn-rift sedimentation commenced in the southern parts of the URG during the Lutetian, slightly earlier than in its central and northern parts (Fig. 5.2), this does not necessarily mean that in time rifting propagated northward, as suggested by the early Oligocene onset of sedimentation in the Lower Rhine Graben (Sissingh, 2006). Indeed, syn-rift sedimentation commenced in the URG under lacustrine conditions, presumably reflecting the development of local accommodation space, perhaps even above mean sea level. In the area of the modeled cross-sections syn-rift sedimentation commenced during the deposition of the *Green Marl Fm.* (interval II), which onlaps northward the gently S-dipping Mesozoic pre-rift series and ultimately pinches north of cross-section 1 (Fig. 5.3). In the studied area, the record of the initial rifting phase is therefore limited to down-faulting of the pre-rift series (interval I) prior to the diachronous onset of Gray Marl deposition (interval II). The magnitude of crustal extension prior to the onset of syn-rift sedimentation, as indicated by the subcrop pattern of the Mesozoic series beneath the transgressive Eocene deposits (interval II), is poorly constrained but varies between the different cross-sections and appears to increase northward. On the other hand, the slope of the interval II time-extension paths derived from the four cross-sections varies and decreases northward owing to onlap of the Gray Marl Fm (Fig. 5.12). In essence, the combined interval I and II segments of the time-extension paths document the initial rifting phase of the URG and its gradual subsidence beneath the erosional base level which in the investigated area was delayed as compared to its southern parts (Fig. 5.3) presumably owing to its topographic elevation at the onset of rifting. While the modeled Pre-depositional interval in the northern sections can be conclusively explained with such a pre-depositional subsidence the 1.5 km modeled extension in the most southern section 4 appears much too high and most likely results from insufficient data quality or data misinterpretation. Therefore the section 4 was downshifted 'corrected line 4' to fit the other time/ extension paths in most reliable intervals IV and V (Fig. 5.12). For time intervals III to V when the URG had clearly subsided below mean sea level, as indicated by repeated marine transgression, time-extension paths for all four cross-sections are very similar and reflect constant extension rates. These extension rates persisted in the northern cross-section 1 and 2 during time interval VI whilst time-extension paths for the southern cross-sections 3 and 4 indicate a slow-down of extension rates. In the southern cross-sections this is most likely an effect of erosional truncation of interval VI during the development of the mid-Burdigalian unconformity in response to uplift of the Vosges-Black Forest

Arch, involving lithospheric folding (Roll, 1979; Dèzes et al., 2004; Ziegler and Dèzes, 2007). By contrast, the northern cross-sections 1 and 2 are located in the area where the mid-Burdigalian unconformity has disappeared and sedimentation was continuous, albeit at very slow subsidence rates. Lithospheric folding, controlling uplift of the Vosges-Black Forest Arch was obviously not rift-related but can be attributed to increased collisional coupling between the Alpine orogen and its foreland (Ziegler and Dèzes, 2007). On the time-extension paths interval VII is modeled as a post-rift stage. Continuous, though slow sedimentation and subsidence during interval VII could be modeled as being driven by compaction of the graben fill. In Figure 5.12, a best fitting trend line is shown for the Middle Eocene to Early Miocene rift stage. The inclination of this trend line follows the time-extension paths of line 1 and 2 in intervals IV-VI, and of lines 3 and 4 in intervals IV-V. For intervals IV-VI this trend line is deemed very reliable since the corresponding time-extension paths were derived from sedimentary sequences, which are devoid of unconformities and accumulated in a steadily subsiding 'filled - overfilled' basin. Interestingly this trend line confirms a very continuous average strain rate of about $1.7 \cdot 10^{-16} \text{ s}^{-1}$ for the Middle Eocene to Early Miocene rift stage and its projection back in time intersects the maximum age of the *Green Marls Fm.*, documenting in the southern parts of the URG the onset of rapid 'syn-rift subsidence (extension = 0) as 43,5 Ma. Renewed rifting was modeled for the Plio-Pleistocene interval VIII. This is realistic in the face of reflection-seismically documented fault-controlled subsidence of the URG (e.g. Derer et al., 2005; Haimberger et al., 2005; Wirsing et al., 2007). Although the minimum age of the *Ried Group* (interval VII) is poorly constrained and some authors place it into the Middle to Late Pliocene, the onset of renewed rifting coincided with the deflection of the Alpine drainage system into the URG (Ziegler and Fraefel, 2009), indicating that it resumed to subside around 2.8 Ma (see above) (Ziegler and Dèzes, 2005, 2007). In this case a similar strain rate of $1.5 \cdot 10^{-16} \text{ s}^{-1}$ would result for the Plio-Pleistocene subsidence of the URG (sections 1 and 2).

5.7 Conclusions

Extension values obtained from the four investigated cross-sections, applying different methods, are similar and suggest that as a first-order approximation rifting in the URG is compatible with plane strain and, therefore, an orthogonal opening of the investigated rift compartment. Extension values can vary, however, strongly depending on the methods applied and related assumed pre-conditions. These include: (1) the pre-rift and present crustal configuration, and specifically the Moho topography (2) assumptions on the depth of the extensional detachment level, respectively the necking level and (3) the geometry and slip vectors of normal faults. Results of line length balancing indicate extension values in the range of 4 to 6 km. Combined with 'lost area' values of about 125 km^2 a necking depth between 31 km and 21 km is envisaged, implying a rheological strong lower crust and/or upper mantle. Such a deep level of

necking is compatible with the geophysically mapped Moho topography and the observed flexural uplift of the graben shoulders. A best fit between observed and modeled results is obtained with a EET of 15 km and a necking level at (pre-rift) 29 km depth coinciding with the Moho. Under these assumptions, TTSF-Modeling yields an extension value of almost 5 km that is matched by extension values derived from line length balancing, assuming an average of 60° fault dip, and area balancing. Successful modeling of the basin fill was only reached when the Late Miocene *Ried Group* is modeled as a post rift deposit. A northward migration of depocentres in the URG, as also seen in the modeled time-extension paths, can be explained by two phases of flexural uplift. The first uplift phase, affected mainly the northern part of the URG prior to the onset of rifting, can be attributed to the Paleocene phase of intraplate compression (Ziegler, 1990; Ziegler and Dèzes, 2007); it controlled erosional truncation of the Mesozoic strata, and a delay in the subsidence of the northern and central parts of the URG below the erosional base level, and thus the onset of syn-rift sedimentation. The second uplift phase affected the southern parts of the URG during the Early Miocene (Mid-Burdigalian unconformity) and were controlled by lithospheric folding uplift and exhumation of the Vosges-Black Forest Arch, involving about 1-1.5 km differential uplift (Ziegler and Dèzes, 2007). Taking the related unconformities into account the extension history of the four investigated cross-sections is very similar with a nearly constant extension vector of 0.2 mm/a, respectively a strain rate of $1.7 \times 10^{-16} \text{ s}^{-1}$. Such a low and continuous strain rate supports the conclusion that development of the URG involved a high-viscosity lithospheric mantle deforming by distributed ductile shear below a brittle-deforming crust.

5.8 Acknowledgements

This study was carried out under the umbrella of the EUCOR-URGENT Project. We are grateful to GeoModelling Solutions, Zürich, for providing the TECMOD commercial TTSF software.

Chapter 6

Elastic plate bending and shoulder uplift in the (southern) Upper Rhine Graben: new evidence from the sedimentary record and flexural Isostasy modeling

Sebastian Hinsken

Preliminary manuscript, publication planned

6.1 Abstract

Shoulder uplift in the southern Upper Rhine Graben (URG) was studied according to geological evidence and flexural isostasy modeling. The sedimentary record of the URG and North Alpine Foreland Basin (NAFB) indicates at least 2 episodes of flexural uplift in the area of the southern URG separated by a phase of flexural subsidence. The first episode of uplift in the area of the URG predates the Mid Eocene onset of rift basin subsidence. It indicates a higher wavelength and a lower amplitude and is partly compatible with an alpine subduction related 'flexural-forebulge' that initiated broad flexural uplift in the North Alpine Foreland during the Eocene. Additional grabenshoulder uplift of several hundred meters occurred during the Late Eocene and Early Oligocene. Rapid flexural subsidence of ≥ 200 m is indicated during the middle Rupelian when the graben and the rift shoulders were transgressed. Former interpretation of eustasy to account for this transgression are contraindicated by (1) published global sea level curves and (2) by contemporaneous regression in the NAFB. Its timing however coincides with transition from syn-collisional to post-collisional stage of the Alpine orogeny that involved mechanical failure of the subducting slab. Therefore the flexural subsidence might be explained with elastic relaxation of an subduction related flexural forebulge due to post-collisional 'slab breakoff' which is supported by 1D forebulge modeling. During the late Chattian to Aquitanian, renewed establishment of a shorter and higher 'forebulge' initiated the rise of the Vosges-Black Forest Arch (VBFA) that climaxed during the Mid-Burdigalian centering around the mid-Miocene Kaiserstuhl volcano. Its buildup is documented by the diachrone Early Aquitanian to Pleistocene erosional unconformity in the S-URG extending N-S ward into Burdigalian deposits of the northern URG and Molasse Basin, that was during further evolution convergently onlaped from N and S. Neogene Rise of the VBFA occurred mainly during the Mid-Late Miocene post-rift stage and corresponds with build up of compressional stresses and imbrication of the North Alpine Foreland (NAF) that finalized basin evolution in the NAFB. Renewed extension in the URG at the Plio-Pleistocene boundary led to renewed subsidence and deposition of Alpine derived Rhine gravels in the URG. Numerical modeling of Cenozoic rock uplift of the VBFA is highly compatible with flexural isostatic compensation of changes in static loading of a thin elastic plate having an elastic thickness (T_e) of about 15km due to URG rifting and Alpine Orogeny. The changing crustal loads include (1) static unbalanced crustal thinning in the URG (2) the sedimentary fill of URG and Molasse Basin (3) erosion on the graben shoulders and (4) forebulge formation in response to crustal thickening in the Alps. Although the rift related amount of flank uplift can be roughly reproduced, the modeled 'Alpine Forebulge' significantly underestimates the observed height by about factor 2 respectively by about 400 m. Moreover the model provides no explanation for differential uplift of the massives bordering the northern URG. Differences between the modeled and the observed uplift might arise from (1) the simplistic modeling approach (2) additional sub surface loading due to alpine 'slab-pull' or most likely (3) lithospheric folding related to build up of compressional stress

within the foreland lithosphere.

6.2 Introduction

The Vosges and Black Forest Arch (VBFA) represent the southern high elevated graben shoulders of the Cenozoic Upper Rhine Graben (URG), where crystalline basement is exposed at almost 1.5 km above the sea and the dome shaped flexural uplift pattern is reflected by local Moho rise to less than 24 km below its culmination centering around the Palaeogene depo-center of the southern URG and the Kaiserstuhl volcano (Fig. 6.1). Since the onset of rifting in the URG about 50 ma ago the VBFA has been uplifted by approximately 2.5 km (e.g. Illies, 1970; Roll, 1979; Schwarz and Henk, 2005). Recent studies in the URG (Gutscher, 1995; Laubscher, 2001; Bourgeois et al., 2007; Ziegler and Dèzes, 2007) agree the observed uplift of the VBFA is due to large wavelength bending of the lithosphere, that occurred in context of URG rifting and Alpine orogeny. However the origin and orientation of forces ('forebulge' versus 'buckling') amounting for bending are debated and the spatio-temporal patterns of uplift and subsidence remain controversial. To date a quantitative model explaining rift related shoulder uplift in the URG does not exist.

In the easiest assumption uplift of the VBFA might be explained with flexural isostatic response to changes in crustal static loading that came along with Alpine orogenesis and rifting in the URG (Fig. 6.2).

Cross-section balancing in the URG has provided evidence that the level of lithospheric necking (level where material points only move horizontal due to extension) is located at the Moho (Fig. 6.2A Groshong, 1996; Hinsken et al., 2007, ; Chapter 4). In such a case crustal rock volumes that will compensate the extension (gained area in x-section) will be entirely compensated by graben formation (lost area in x-section).

Consequently strong mechanical unloading equating the weight of crust (basin volume x density of crust, $\sim 2700kg/m^3$) will occur. Additional but less strong unloading ($\sim 40kg/m^3$) is expected from 'mechanical' replacement of 'cold' mantle lithosphere with 'hot' asthenosphere. Such strong localized unloading will result in regional isostatic compensation that will be recognized in flexural 'graben shoulder' uplift (Fig. 6.2A).

Unloading related to crustal thinning however will be partly compensated by sediment loading due to filling of the created sediment accommodation space (Fig. 6.2B). In contrast erosion on the exposed graben shoulders will result in further unloading and hence rock uplift. In case of a pre-rift reference horizon the amount of eroded material can be reconstructed and a material balance can be performed. In this light modeling of flexural isostasy appears possible. Fig. 6.2C shows a classic model of flexural forebulge and foreland basin development. elastic plate bending results on the subducting plate due to a bending moment caused by slab pull and/or thrust sheet loading (orogenic wedge). Additionally sediment loading occurs in the foreland basin while erosional unloading is expected due to erosion on the elevated forebulge.

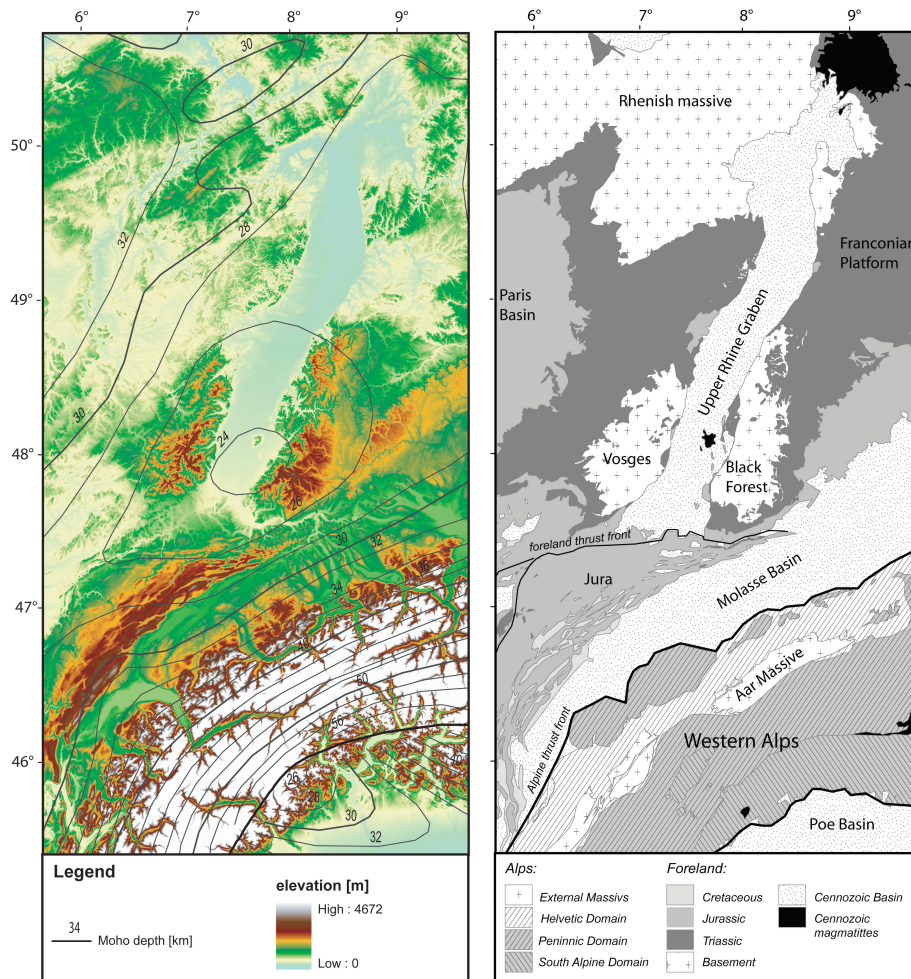


Figure 6.1: Overview about the Alps and their northern foreland including the Upper Rhine Graben and its uplifted shoulders: Left DEM topography superimposed by Moho depth iso-lines (from Dèzes et al., 2004). Right simplified geological Map.

New datations and stratigraphic correlations of URG and the North Alpine Foreland Basin (e.g. Grimm, 2005a; Berger et al., 2005a,b) show lateral base-level changes that imply long wavelength flexural deformations. These flexural deformations appear to have first order controlled the sedimentation in the URG and NAFB and question the widely accepted view of eustatic control on sedimentation in these basins. Next to differential base-level movements, coarse clastic supply from the graben shoulders can be used to reconstruct the history graben shoulder uplift. Timing of those flexural deformations in reference to URG rifting and alpine orogeny appears crucial in understanding of their origin.

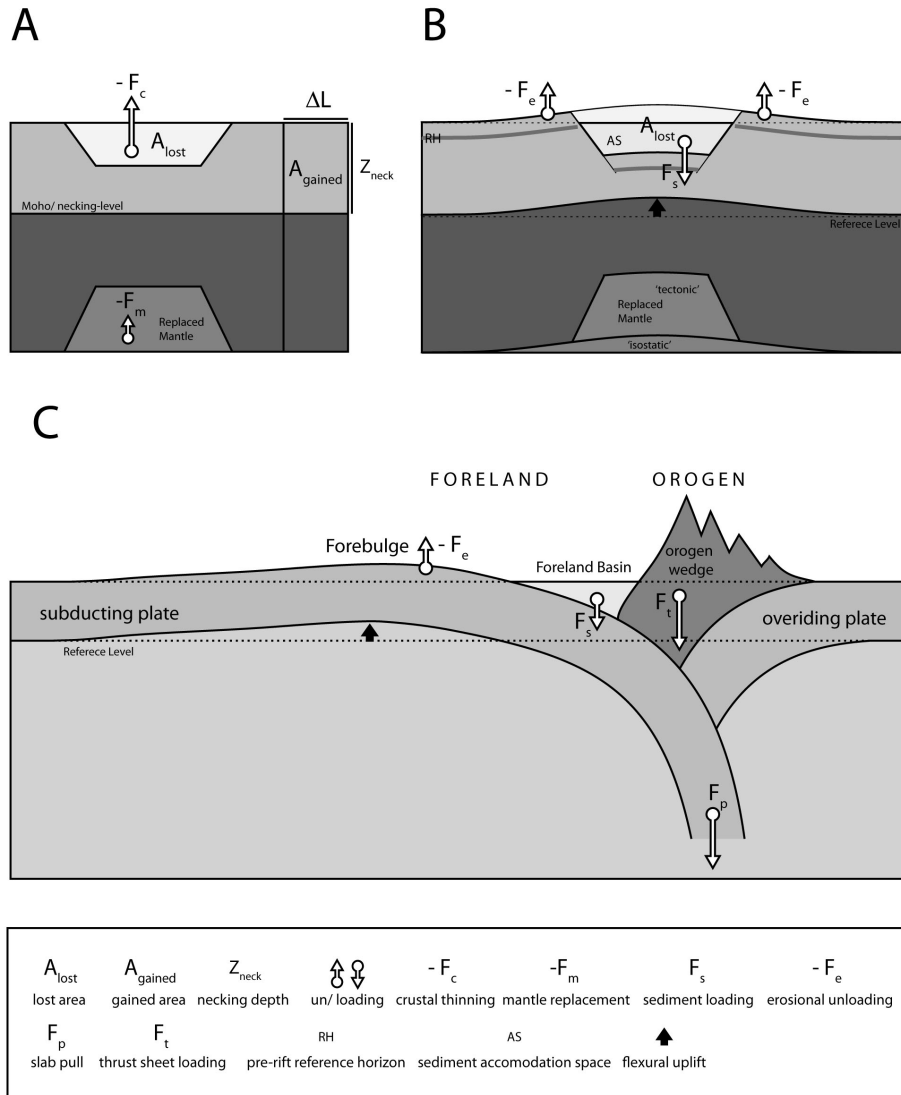


Figure 6.2: Concept of flexural isostasy to account for uplift in the area of the southern URG. A The necking level located at the Moho leads to entire compensation of crustal thinning by graben formation. Thus strong static unloading equating the graben volume times the crustal density will occur. B consequently unloading will result in flexural 'graben shoulder' uplift. However part of the crustal unloading will be compensated by sediment loading, while further unloading will result from erosion on rift shoulders. C concept of an 'alpine' flexural forebulge due to elastic plate bending resulting from slab pull, thrust sheet loading, and sediment loading in the foreland basin. Additional rock uplift is expected due to erosion on the elevated forebulge.

This is the aim of this study in a first part the sedimentary record of the URG and North NAFB is analyzed and signatures of flexural plate bending like lateral variations in Base level development are analyzed. Further up coarse clastic supply is used to reconstruct rock uplift. In the second part flexural isostatic response of the lithosphere to Eocene to Recent changes in crustal static loading was modeled using a 3D solution of a 2D thin plate equation.

6.3 Geologic evidence for elastic plate bending in the URG and North Alpine Foreland

Geological evolution of the Western Alps, the North Alpine Foreland and the URG was investigated along a N-S transect from the northern URG into the Swiss Alps (Fig. 6.3). Focus was next to lateral differences in base-level movements the occurrence of coarse clastic facies and palaeokarst documenting uplift of the rift-shoulders respectively the foreland swell.

6.3.1 Geological context

The study area (Fig. 6.1) involves the URG, the NAFB and the southward adjoining central part of the Swiss Alps.

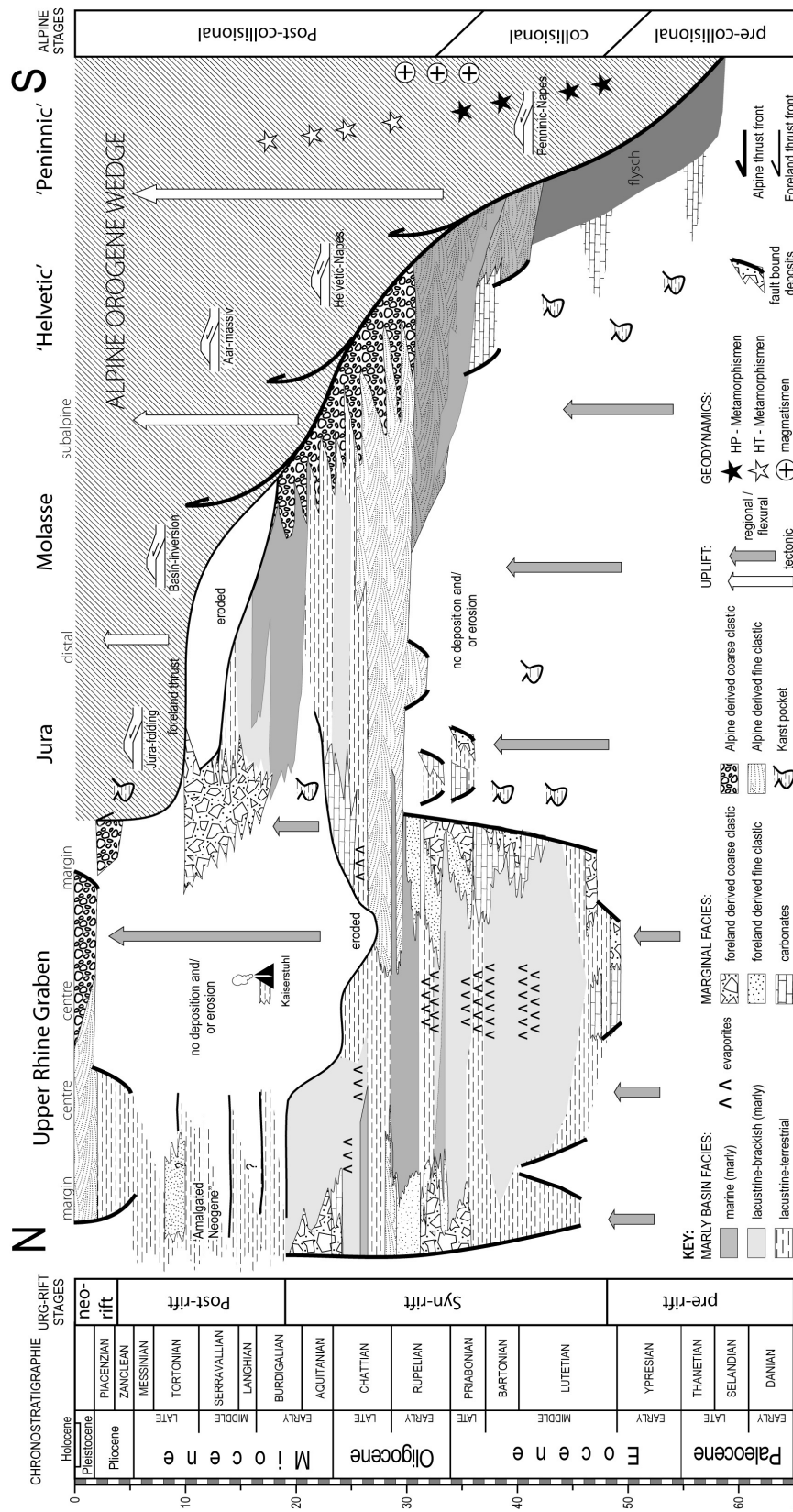


Figure 6.3: Spatial and temporal patterns of Alpine Orogeny and foreland evolution along a N-S transect focusing on sedimentation in the NAFB and URG.

Alps

The Alps result at least from two independent orogenies (e.g. Schmid et al., 2004). The first orogeny led to closure of the Meliata-Hallstatt Ocean during the Late Cretaceous and led to crustal shortening in the East-Alpine and the South Alpine domains. A second orogeny during the Cenozoic led to closure of the Alpine Tethys between Apulia and Europe and the formation of the Western Alps. This Cenozoic Alpine Orogeny can be roughly subdivided into pre-collisional, collisional and post-collisional stage (e.g. Schmid et al., 2004).

Pre-collisional stage During Late Cretaceous to Early Eocene involved subduction of the (1) oceanic lithosphere, (2) the Briançonnais domain and (3) the formation of an accretionary wedge. It was accompanied by subduction related HP-metamorphism.

Collisional stage started during Early Eocene (about 50 my ago) with the collision of the European distal margin with Apulia and terminated at the end of the Eocene with closure of remaining 'flysch' troughs, as well as magmatism, and uplift.

Post collisional stage during the Oligocene and the Neogene led to propagation of the orogene wedge into the southern and northern foreland. In the northern-part of the Western Alps stacking of the Helvetic nappes happened during Oligocene to Early Miocene. Ongoing crustal shortening led to subsequent up-thrusting of the External Massives (e.g. AAr-masiv) during the Middle and Late Miocene along deep-rooted basement-thrusts reaching vertical displacements of up to 10km. In this context the western part of the NAFB got incorporated into the Alpine orogenic wedge leading to internal thrusting and uplift of up to 2km's at its southwestern tip. Folding and thrusting at its NW tip resulted in formation of the Jura Mountains Fold and Thrust Belt between 10 and 5 ma (see below).

North Alpine Foreland Basin

The North Alpine Foreland Basin NAFB developed as a flexural foreland basin in front of the northern Alps between the Palaeocene and Late Miocene (e.g. Allen and Allen, 2005) for detailed palaeogeographic reconstructions see Herb (1988); Kempf and Pfiffner (2004); Kuhlemann et al. (1999). The basin shifted NW ward in front of the approaching orogene while the internal parts got progressively incorporated into the orogene wedge. An Early Flysch stage, Late Molasse stage and post depositional Jura stage of basin evolution can be diminished:

Flysch-stage: Early Basin evolution during Palaeocene to Late Eocene was characterized by deep marine 'flysch'- sedimentation in the internal part of the basin and deposition of shallow water carbonates at its outer margin (e.g. Herb,

1988). Remnants of this early 'Flysch' stage of basin evolution are preserved as Eocene- cover of the Helvetic Naps. There is no evidence for a (high elevated) mountain chain during this time of basin formation - the Alps probably represented an island arc (e.g. Herb, 1988). Exposure and erosion of the Mesozoic platform north of the feather edge (e.g. karstification in the area of the Jura mountains) has been interpreted as an subduction related forebulge (e.g. Herb, 1988). During Late Eocene to Early Oligocene a transitional basin-stage occurred that was characterized by hemi-pelagic sedimentation (Foraminifera Marls).

Molasse-stage: During the Oligocene to Middle Miocene late stage in basin evolution the basin migrated into its present day position (Molasse Basin). The western part of the Basin including the area of the Jura Mountains was overfilled by siliziclastic 'Molasse type' sedimentation. This is evidenced by absence of karstification of this age in the Jura mountains (Engesser, 2006 pers comm.). In contrast the eastern part of the Basin remained under filled. The Basin fill of the western Molasse basin is represented by two large base level fall cycles documenting the transition from a marine into a continental domain.

Jura-stage: During Late Miocene the orogene-wedge pro graded further into the foreland and led to inversion of the western part of the NAFB leading to the post depositional Jura stage. In this context the entire basin got uplifted and up to 2km of basin fill were eroded near the Alps. Folding and thrusting of the Basin on its NW and W outer edge including the Mesozoic substratum above a Triassic evaporite detachment during Late Miocene and Pliocene resulted in formation of the Jura Mountains fold and thrust belt (e.g. Burkhard and Sommaruga, 1998). Uplift and exposure of the Mesozoic platform at that time is documented by frequent occurrence of palaeokarst.

Upper Rhine Graben

The URG forms part of the European Cenozoic Rift System (ECRIS) that developed during the Mid Eocene to the Recent. A post rift stage however occurred during the Late Miocene and (Early) Pliocene.

Syn-rift evolution durated from the Middle Eocene to the Early Miocene. Extension rate was about 0,2 mm/a and amounted to about 5 km rift orthogonal extension (chapter 4). During Mid-Eocene to Early Oligocene the URG was strongly under filled with material that was locally eroded from the rift shoulders. The base-level within the graben was matter of strong fluctuations, rendering sediment volume partitioning an important process. The depositional environment changed repeatedly between lacustrine, brackisch and continental evaporite precipitation (Düringer, 1988; Hinsken et al., 2007). Short term marine incursions happened during the Early Oligocene (Griessemer, 2002; Pirkenseer, 2007, Chapter 1). Alluvial fans that formed at the graben margins

document strong uplift and erosion of the rift shoulders that climaxed during the Late Eocene to Early Oligocene. During the Middle Oligocene a marine transgression flooded the entire URG as well as parts of the rift flanks and the area of the northern Jura. Subsequent a sea-way formed between URG and the 'overfilled' Molasse Basin (Kuhlemann et al., 1999; Hinsken et al., 2007). Thus alpine material was transported into the URG and the basin was filled rapidly leading to an overfilled basin, whereas erosion on the rift-shoulders was drastically reduced (Huber, 1994; Hinsken et al., 2007; Roussé, 2006). By the end of the Oligocene, the URG got disconnected from alpine clastic supply again, that is evident by deposition of lacustrine limestones in the Northern Jura and the southern-most URG. During the Early Miocene a thick brackisch to lacustrine sequence accumulated in the depot-centre of the northern URG. It remains an open question to which extent sedimentation continued in the southern URG during the Early Miocene as most of the higher syn-rift deposits in the southern URG have been removed by erosion. Although Roussé (2006) interpreted the highest marly syn-rift deposits in the Potash Basin (up to 150 m) to represent Early Miocene age there is no direct evidence from biostratigraphy for Early Miocene deposits preserved in the southern URG. Moreover there is some evidence for uplift and reduced sedimentation in compare to the northern URG for the Late Oligocene and Early Miocene. Renewed flank uplift in the Late Oligocene is evident from fan delta deposits in the Northern URG near Heidelberg (Grimm2005a). Early Miocene karstification of Mesozoic limestones, indicative for uplift and weathering, is documented at the southern rim of the URG near Porrentruy (Becker, 2003), alike crystalline pebbles from the Black Forest that are found in marginal deposits of the NAFB.

post rift evolution During the Late Burdigalian strong uplift affected the southern and middle URG and led to deep erosive truncation of the graben fill (Ziegler and Dèzes, 2007) south of the so called 'concordance line' (Roll, 1979) crossing the URG near the city of Speyer. In contrast in the northern part of the URG a thin sequence of fluvial and lacustrine deposits accumulated until the end of the Pliocene testifying to reduced basin subsidence. Early Burdigalian uplift was followed by volcanism during mid-Miocene that led to the formation of the mid-Miocene Kaiserstuhl, Hegau and Vogelsberg volcanoes. Deposits of the Kaiserstuhl rest on erosional truncated Eo-Oligocene deposits and therefore testify uplift and erosion to predate volcanism. Nevertheless uplift and erosion commenced during the Middle and Late Miocene, as indicated by s-ward transported re-sediments from the graben shoulders, that are found in the area of the NW-Jura Mountains and subsumed under the term Jura-Nagelfluh.

Plio- Pleistocene neo-rift stage Thus during the Pliocene the Alpine drainage spread out into the Alpine Foreland and the so called Sundgau Gravel were deposited in the southern URG by rivers following the Jura to the west and draining via Bresse and Rhone Grabens into the Mediterranean, while a drainage

divide was located in the area of the Kaiserstuhl. Renewed extension in the URG in the Pliopleistocene (post 2.8 ma) opened a new 'alpine' drainage pathway through the graben into the North Sea (e.g. Ziegler and Fraefel, 2009).

6.3.2 Reconstruction of graben shoulder uplift in the southern URG

Estimating the syn-rift flank uplift requires evaluation of two data sets; (1) the pre-rift elevation of the palaeo-land surface and (2) the amount of erosion on the rift shoulders since that time.

pre-rift elevation Former workers have claimed a palaeo-land surface at 100-300 metres above the Recent sea level (e.g. Roll, 1979). Erosional patterns and intense karstification of the Mesozoic strata but also coarse clastics found at the base of the URG graben fill testify to intense weathering and erosion and hence an upland elevated between a few tens to some hundred meters above the ancient sea level. Moreover the non marine facies of the Eocene basin fill indicates the early stage rift basin subsidence occurred within an elevated continental domain. However there is some evidence for short incursions during the Lutetian (Grimm, 2005a). According to (HAQ et al., 1987) the Middle Eocene eustatic sea-level was about 200 meter higher than the Recent one. Therefore the postulated 300m elevation represents rather a minimum than a maximum of pre-rift elevation of the Middle Eocene land surface. The idea of an Eocene peneplain (Roll, 1979) is contradicted by the erosional pattern indicating a pre-rift dome shaped uplift below the Potash Basin. Nevertheless erosional amplitudes and elevation higher than 300m above the palaeo sea-level appears to be very unlikely. A palaeo land surface between 300-500 m above the present day sea-level might therefore represent an realistic range.

Early 'Palaeogene' uplift Calculating the amount of erosion on the graben shoulders requires next to knowledge about the pre-rift elevation of the land surface knowledge of the present day elevation of the base of the Mesozoic and the pre-rift thickness of the Mesozoic there.

This is not possible, however the Top Basement/Base Mesozoic interface is still evident from the geomorphology ('Rumpfflächen') and remnants of basal Mesozoic strata occur in wide parts of the VBFA (e.g. Paul, 1955). However in the culmination of BF and Vosges near the break away faults erosion has removed the reference horizon and evidence about its former position is uncertain. Moreover local observations show, that the thickness of the pre-rift strata and the geometry of the Top Basement reference surface are matter of local variations. For instance the arch of the northern Black Forest can be followed as a regional anticlinal rise towards the NW. A similar local high was mapped around the Feldberg (1492m, highest elevation of BF) by Paul (1955) that is moreover assumed to form a local horst. The maximum elevation of the Mesozoic reference horizons is therefore not much higher as the peaks of the highest mountains

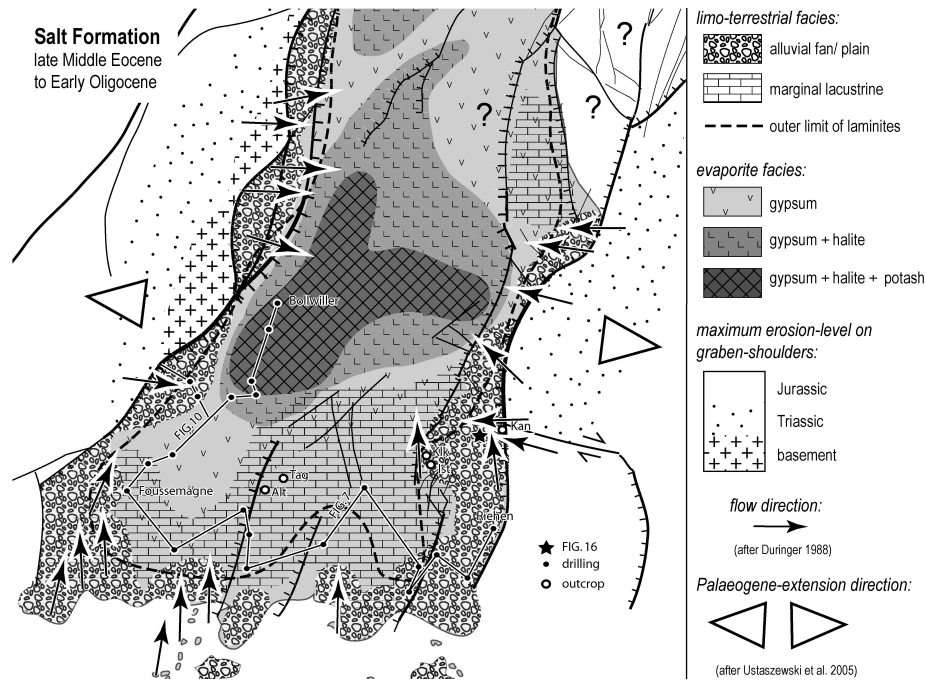


Figure 6.4: Palaeogeography of the Middle Eocene to Early Oligocene Salt Formation in the southern Upper Rhine Graben. Maximum shoulder uplift occurred in the footwall of the master fault near the recent highest elevation of the Vosges (Grand Ballon). Erosion in the area of the northern Jura Mountains however widely remained in the Late Jurassic strata

reaching almost 1500 m, while extrapolation suggests maximum erosion of 300 m close to the break away faults.

Early Oligocene flexural flank uplift with a maximum amplitude around the Potash Basin depot-center is inferred from the pebble petrography of alluvial fan conglomerates at the basin margins indicating a maximum incision of up to 1000 m that occurred in the footwall of the master fault near the recent day highest elevation of the Vosges (Grand Ballon), where the crystalline basement became exposed during the early Rupelian (Fig.6.4 Hinsken et al., 2007). Incision at the southern graben tip however largely remained within the Late Jurassic series.

Translating the observed amount of incision directly into uplift is somehow questionable for the following reasons: (1) The basin formed an enclosed evaporite basin for most of the time and might have been therefore disconnected from the global base-level. (2) Calculation of differential uplift in compare with the deposits at the southern margin (about 800m) might be overestimated as the area to the south forms part of the Rhine Bresse Transform Zone, that was affected by tectonic subsidence too (Hinsken et al., 2007).

Middle Oligocene flexural subsidence? A marine transgression during the middle Rupelian led to rapid base-level raise, that is highly indicative for regional subsidence (Hinsken, 2003; Hinsken et al., 2007; Rotstein et al., 2005; Roussé, 2006; Pirkenseer, 2007). The formerly uplifted graben shoulders subsided and water depths in the area of Basel have been estimated to $\geq 200\text{m}$ according to the micro faunistic evidence (Huber, 1994). Interestingly an opposite regressive trend is indicated at the same time in the adjoining western part of the NAFB - when the basin changed from off-shore pelagic deposition into a marginal marine or even continental domain (Pirkenseer, 2007). Although eustatic sea-level and related base-level were falling toward the end of the Oligocene, and rifting in the URG was proceeding, there is no evidence for flank uplift during this time span (Hinsken, 2003; Roussé, 2006). The dualism of Palaeogene vertical graben shoulder motions is very well documented in the Cenozoic cover of the Heuberg about 1 km from the SW corner of the Black Forest near Kandern and there it appears possible to estimate the amplitude of vertical motions at least for the Early Oligocene flank uplift (Figure 6.5).

The Early Oligocene conglomerates host an inverse sequence ranging from the Late/Middle Jurassic at the base to the Middle Triassic at the top and are covered by pelagic grey marine marls of Late Rupelian age. On top the Neogene Heuberg gravels document erosion of Middle Triassic to Basement rocks. The monomict granitic and rhyolitic basement rocks document a local catchment in the adjacent Blauen Wiesental Block of the Black Forest. 300-400m of Early Oligocene incision can be reconstructed from the Mesozoic pre-rift series that is most likely related to the same amount of flexural flank uplift. On the other hand the absence of an 'incision gap' between the Early Oligocene and Neogene uplift indicates drastic reduced respectively non-erosion during the middle-late Oligocene.

6.3.3 Discussion and interpretation of Palaeogene uplift and subsidence

The existence of a Eocene flexural forebulge north of the NAFB has been proposed by the erosional unconformity below the NAFB. Indeed karstification of the Mesozoic platform confirming uplift and exposure is known from the Eocene of the Forealps and the Jura Mountains. Towards the north these unconformity cuts deeper into Mesozoic strata and reaches its first maximum below the depo-centre of the southern URG. This indicates that the pre-rift uplift seen below the sediments of the southern URG is likely to be related to an Eocene flexural forebulge uplift. However as the feather edge of the Eocene NAFB was related about 200 km south of the recent n-margin of the NAFB, this Eocene forebulge must have had a higher wavelength than the recent observed one. As there is no evidence for a high elevated mountain chain at that time formation of this forebulge must have been related to subduction of the European below the Adriatic Plate which fits with the geodynamic scenario at that time (Fig. 6.3). Carbonate deposition on the feather edge of the NAFB and within the southern URG furthermore indicate a relative shallow swell with low clastic supply.

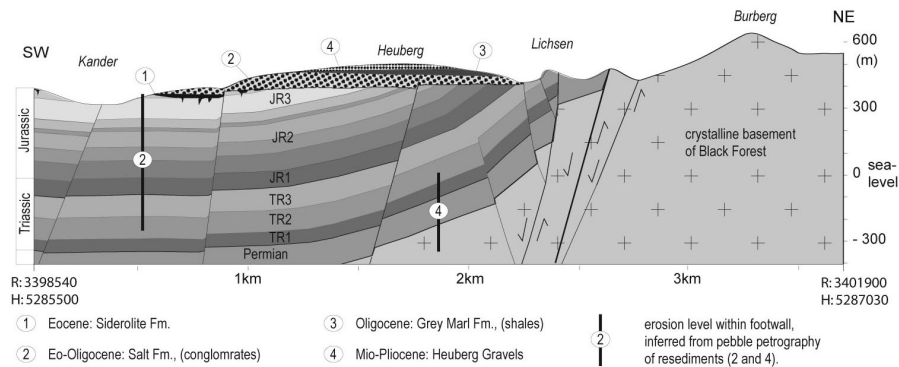


Figure 6.5: Field evidence for diachronous shoulder uplift in the southern URG. 'Palaeokander' gravels at the Heuberg locality documents uplift of the Blauen-Wiesental-Block during the Late Eocene to Early Oligocene and the Middle Miocene. About 300 to 400 m uplift can be estimated for the Late Eocene to Early Oligocene, while Middle to Late Oligocene shales imply regional subsidence at this time.

Additional uplift of the rift shoulders until the end of the Early Oligocene is most likely related to flexural graben shoulder uplift. Within this context it must be added that the Eocene -Early-Oligocene URG represented a closed sedimentary system; sediment loading of the graben was compensated by erosional unloading of the graben shoulders. Nevertheless additional forebulge uplift can not be excluded for this time interval.

A still unresolved problem is the observed flexural subsidence during the Middle Oligocene.

Most Authors regard the so called 2nd Rupelian transgression as a eustatic event and indeed it has been described from a number of other basins in central Europe. However the eustatic sea level curve of (HAQ et al., 1987) shows just a minor sea-level rise of some tens of metres during the middle Oligocene (Fig. 6.6A). A significant sea level rise is however observed during the Early Oligocene (about 100m) and notified as a marine ingression leading to deposition of the Middle Pechelbronn Beds. Nevertheless a sea-level rise of $\geq 200\text{m}$ would be required to transgress the elevated rift shoulders and to explain deposition of 'deepwater' Foraminifera Marls directly on terrestrial variegated marls, as observed in the southern URG. This is far too high to fit into an eustatic context. Alternatively the observations could be explained with rapid subsidence.

Post rift thermal subsidence has been proposed for the drowning of the graben shoulders in the southern URG (Hinsken, 2003; Rotstein et al., 2005; Roussé, 2006). This interpretation is however contraindicated for two reasons: (1) the URG is considered to be a passive rift and due to low strain rates thermal rise appears to be unlikely (2) restoration of cross sections (chapter 4) suggest, that the syn-rift stage lasted from Mid Eocene to Mid Miocene with a nearly

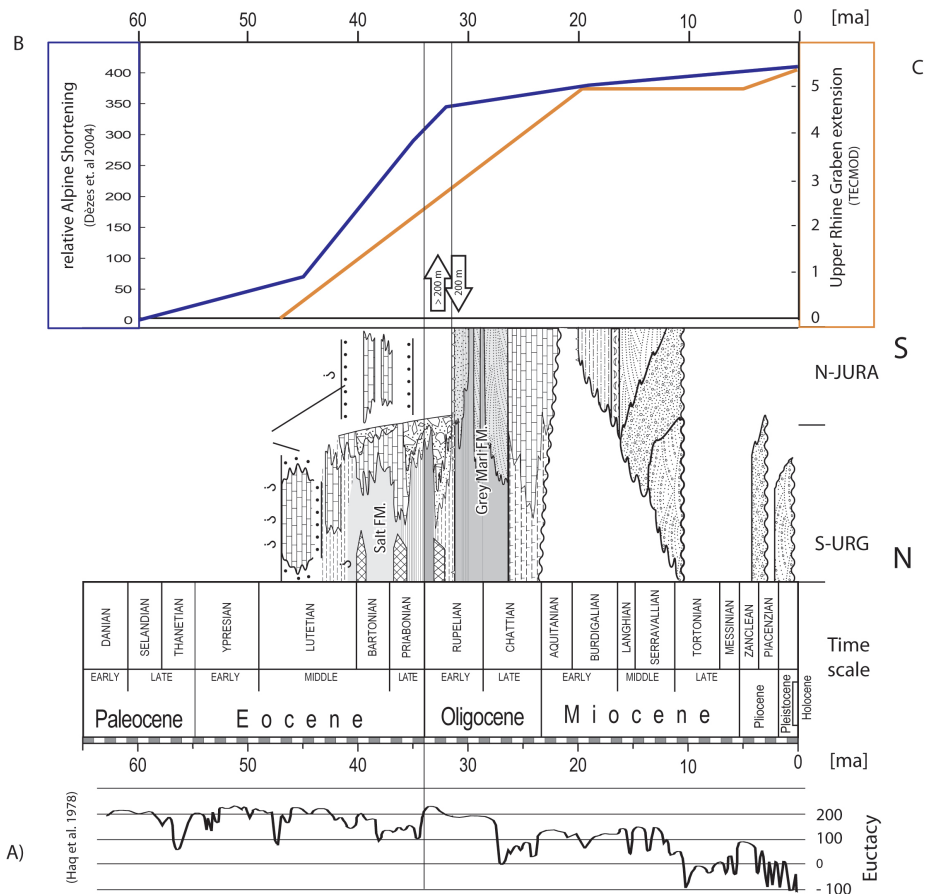


Figure 6.6: correlation of signals with Mid Oligocene observed drowning of graben shoulders. A eustatic curve shows only minor rise during the Middle Oligocene, B Alpine shortening shows a slow down, C extension in the URG did not change. consequently eustatic sea level rise and post-rift subsidence can not account for quick change from graben shoulder uplift to graben shoulder subsidence.

constant extension rate (Fig. 6.6B).

In timing the flexural subsidence correlates with an overall tectonic re-organisation, that happened in context with the transition from syn-collisional to post-collisional stage of the alpine orogeny. This involved (1) a drastic reduction in the shortening rate at the Early-Mid Oligocene transition (Fig. 6.6C) according to reconstructions of Dèzes et al. (2005), and (2) a magmatic event (Bergell-plutonismen) in the central Alps.

(3) Palaeogeographically this time marks the transition from a Thetian to a Parathetian stage respectively the transition from flysch stage to molasse stage during the NAFB-evolution. It moreover corresponds to (4) an episode of strong uplift in the Alps. The turnover from deep water to shallow water /continental deposition in the NAFB and the opposite trend in the URG is best shown by the temporal offset of the Foraminifera Marl deposition in both basins. The Foraminifera Marl of the NAFB was deposited during the early Rupelian, that of the URG dates to the late Rupelian.

In context of the transition from syn-collisional to collisional stage during the alpine orogeny Davies and Von Blanckenburg (1995) and Dèzes et al. (2004) proposed a model of slab break off. However they argue this slab break off was pre-plutonismen and they assume an Late Eocene age. With regards to the model of a subduction related plate bending it should be noticed that a slab pull force can reach up to $5 \times 10^{-15} \text{Nm}^{-1}$ (Stüwe, 2007) and therefore act as an important sub surface load. Such an major sub-surface load will result in an considerable forebulge uplift in the foreland, however in the collision zone it might prevent uplift of previously thickened continental crust.

Fig.6.7 shows reconstructions of two 'hypothetic' Early Oligocene Forebulges modeled with a 1D analytical solution of a thin plate equation, a T_e of 15 km and a point load of 10^{-15}Nm^{-1} respectively $5 \times 10^{-15} \text{Nm}^{-1}$. The forebulge is plotted against the URG and reconstructed NAFB basin fill. A maximum forebulge uplift between 150 and 700 m can be modeled and it can be shown that the northern part of this forebulge would have been located in the area of the southern URG.

Alpine 'slab break off' would have consequently resulted in relaxation and subsidence of an subduction related alpine forebulge while in the collision zone uplift would be expected. Therefore the observed subsidence in the S-URG and uplift in the Alps NAFB might be conclusively explained with slab detachment occurring at the transition from syn-post collisional stage.

With respect to the models of Davies and Von Blanckenburg (1995) and Dèzes et al. (2005) it needs to be notified that slab pull as driving force is a self organizing process driven by subduction of cold and heavy lithosphere. During collision continental crust thickens leading to increased heat production and convergence rate decreases. Both processes are likely to stop or reduce the amount of slab pull. Moreover a thermal event will reduce the mechanical strength of the subducting plate and might lead to mechanical failure. In this light it appears possible that a mechanical slab failure ('slab break off') in the Alps occurred syn-magmatic during the middle Rupelian and not pre-magmatic during the Late Eocene as proposed by the former workers.

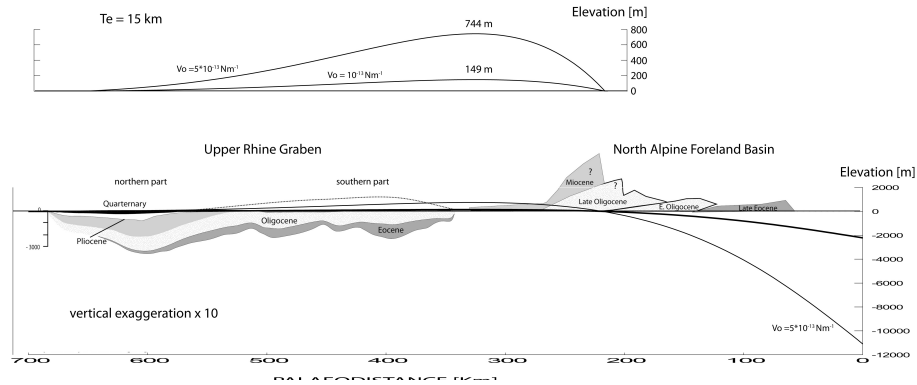


Figure 6.7: Reconstruction of an hypothetical E.-Oligocene Forebulge modeled with a 1D solution of a plate equation, a T_e of 15 km and a point load of 10^{-15}Nm^{-1} respectively $5 \times 10^{-15}\text{Nm}^{-1}$. Maximum modeled forebulge uplift is up 750m and it can be shown that such a forebulge would have reached the southern URG.

A model for the Palaeogene uplift and subsidence of the VBFA is shown in Fig. 6.8A-C.

Fig. 6.8A shows a reconstructed lithospheric section of the pre collisional state of the Alpine orogeny during the Late Cretaceous (modified after Dèzes et al., 2005). Fig. 6.8B shows the situation at the beginning of the collisional stage when the Penninic domain had become partly subducted. The URG develops on an elevated forebulge while flysch sedimentation prevailed in the NAFB. Fig. 6.8C shows the situation at the end of the collisional stage when the last flysch-throughs were closed and pelagic sedimentation widely covered the Alpine domain. Additional flexural shoulder uplift occurred at that time and the URG was dominated by restricted continental sedimentation. It is likely that at that time the geotherm increased due to slowdown of convergence and considerable thickening of the continental crust. Fig. 6.8D shows the proposed mechanical slab failure ('slab break off') at the transition from syn to post collisional stage. This 'slab break off' is assumed to be responsible for relaxation of the Eocene subduction related forebulge resulting in subsidence in the area of the southern URG, while it led to uplift in the area of the Alps. Subsequent sedimentary overstepping in the area of the Jura led to drainage of alpine clastic supply into the URG.

6.4 Numerical modeling of flexural rock uplift

The aim of the modelling approach is to see if the Recent observed graben shoulder uplift in the URG is compatible with elastic plate bending due to loading and unloading effects that appeared in context of URG rifting and Alpine orogeny.

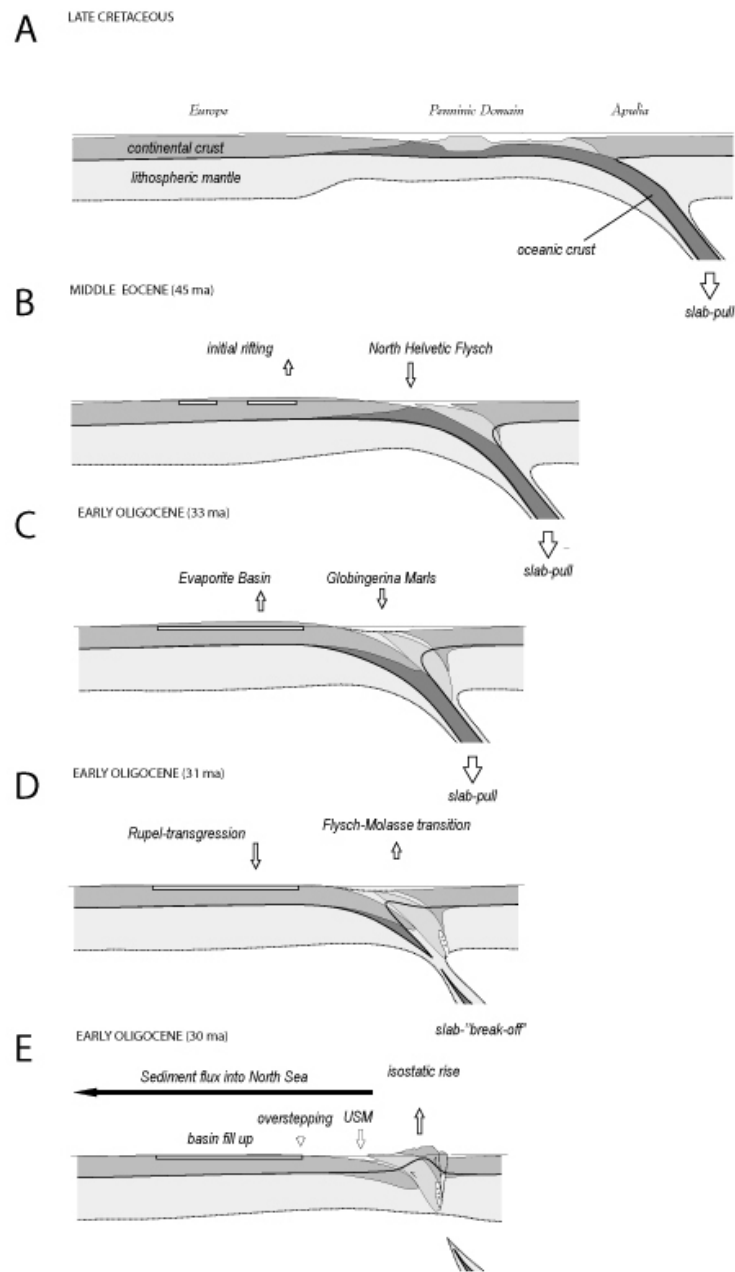


Figure 6.8: Geodynamic model for Palaeogene uplift and subsidence of the VBFA. A Palaeogeographic reconstruction of the pre-collisional stage. B,C Collisional stage resulted in ongoing subduction low relief and flexural forebulge uplift. D increasing geotherm during the Early Oligocene initiates mechanical slab failure leading E subsequent to 'slab break off' isostatic uplift in the Alps and relaxation of the flexural forebulge.

The simple model assumes the area of the southern URG prior to the onset of rifting during the Early Eocene to have represented an elevated peneplain that rested in isostatic equilibrium and that was not affected at this time by the Alpine collision - an outcome that is however contradicted by the first part of this chapter. Changes in crustal static loading resulted from (A) rifting in the URG, (B) Alpine thrust sheet loading and (C) related surface processes. The rock volumes that caused changes in crustal static loading can be mapped in their recent day geometry, and hence distributed net changes in crustal loading can be calculated. Assuming the North European Foreland Lithosphere to represent a fully elastic plate it should be possible to reproduce flexural isostatic rock uplift seen in the VBFA with numerical modeling of the elastic response to these long term load changes. The modeling is however based on several presumptions that result from conclusions of previous studies.

- The Middle European Plate is resting in isostatic equilibrium and behaves mechanically like a thin elastic plate and prior to rifting it was an exposed lowland resting some deca to a few hundred metres above the global base level.
- The lithospheric necking-level in the URG is located at the Moho and the amount of unloading equates the basin volume times the crustal density (Groshong, 1996; Hinsken et al., 2007)
- The subducted alpine mantle slab has been syn-collisional detached (Davies and Von Blanckenburg, 1995; Dêzes et al., 2005) and loading effects of a possible regrown mantle slab are negligible.

6.4.1 Material and Methods

Reference level and thickness mapping

Reference levels thicknesses that were later used for calculation of loads and unloads were mapped and compiled using GIS Software as follows.

Base Mesozoic Topography and URG Basin Volume In order to calculate the basin volume of the URG, the elevation of the Base Mesozoic reference horizon was mapped in the North Alpine Foreland between the Rhenish Massive and the Alps (Fig. 6.9). The approach is very similar to that used by Bourgeois et al. (2007), however more regional data was included. The following methods were applied to map the elevation of the Base Mesozoic Topography:

1. Direct measurements of elevation from well-reports.
2. Compilations of published isopach and isobath maps (URG, Paris Basin, Baden Württemberg, Molasse Basin).
3. Direct altitude measurement (SRTM-DEM) of the outcropping Base Mesozoic reference surface on geological maps

4. Extrapolation of the Base Mesozoic reference surface above the highest peaks in BF and Vosges.
5. Direct altitude measurement (SRTM-DEM) of outcropping Mesozoic stratigraphic contact surfaces on geological maps and depth conversion with interpolated strata thickness maps.

After interpolation the basin volume of the URG was calculated. Therefore the rift basin outline defined by the outer break away fault was sliced out of the Base Mesozoic reference horizon and the curvature of the graben shoulders was extrapolated above the rift. The mapped Base Mesozoic Topography was subtracted from this horizon.

Sediment fill of URG and Molasse An isopach map was compiled from published isopach and isobath maps for the URG and Molasse Basin.

URG graben-shoulder erosion The present day elevation of the Graben shoulders (SRTM-DEM) was subtracted from a published map of (Illies, 1970) showing reconstructed altitude of the (eroded) Mesozoic strata on graben shoulders.

Alps crustal thickening within the Alps was calculated from the topography (SRTM-DEM) and the Moho-elevation (Dèzes et al., 2005) assuming a constant pre-collisional plate thickness of (29 km) at Europe's southern palaeo plate margin.

6.4.2 Set up

Rock volumes were mapped and thicknesses were interpolated in ARC GIS based on a WGS84 reference grid. These Thickness maps were rasterized and imported to Matlab where they were projected to a metric grid with cylindrical projection and datum at N47° / E 7°. For calculation the data was interpolated onto a grid with 501x501 nodes and a footprint 4 km² covering an area of 2000x2000 km. Loads were calculated by multiplying the rock volume on each node with the rock densities.

Loads and unloads were calculated with the following specific densities (g/cm³):

- URG basinvolume -2.75
- URG fill 2.4
- URG shoulder erosion - 2.5
- Molasse-fill 2.4
- Forealps 2.5
- southern Alps 2.75

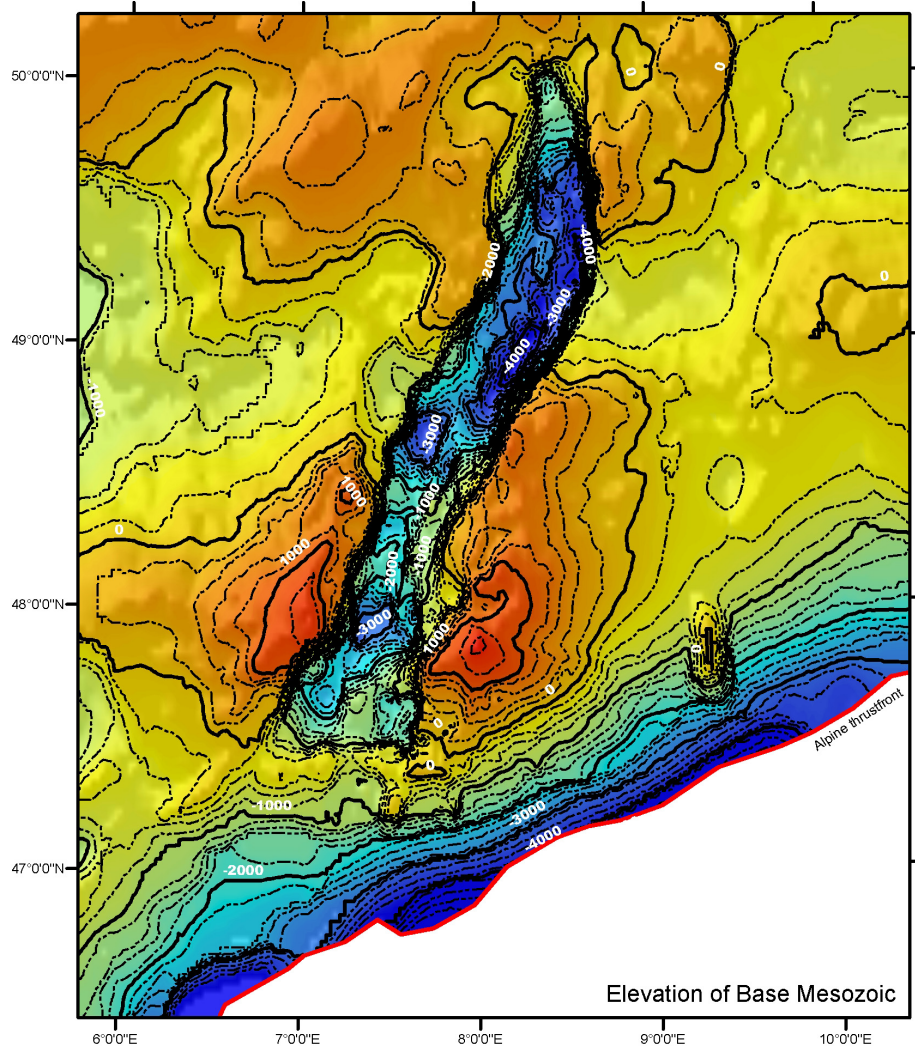


Figure 6.9: Base Mesozoic topography in the North Alpine Foreland displaying the Basin geometries of the Cenozoic URG. The URG basin volume was taken to model the rift induced shoulder uplift.

- Ivrea 3

Density of crust was assumed with 2.7 g/cm³ and mantle with 3.3 g/cm³. Calculation was performed using a FD-numerical 3D-solution (S. Schmalholz, written com.) of an 2D thin-plate equation (Turcotte and Schubert, 2002):

$$D\left(\frac{\delta^4\omega}{\delta x^4}\right) + P\left(\frac{\delta^2\omega}{\delta x^2}\right) + (\rho_{mantle} - \rho_{air})g = 0 \quad (6.1)$$

6.4.3 modelling approach

In a first preliminary run the Te was fitted. In a second step the plate bending effects of the individual loads was investigated and finally the resulting modeled uplift of all loads was compared with the real observed one. For this purpose a few observation points were chosen; the Feldberg (F, 1493 m. MSL) and Grand Ballon (B, 1411 m MSL) represent today the highest elevations in the VBFA while Zürich (Z) and Luzern (L) are located in the Molasse Basin.

6.4.4 Results

URG A Te of ~ 15 km reproduces the observed pattern of uplift in the VBFA best. Fig.6.10 left, displays the modeled elastic regional isostatic response (isolines (m)) due to crustal thinning (modeled with the basin volume x crustal density) in the URG area (figure superposed by the Basin volume of the URG). Oval shaped flexural shoulder uplift reaching about 1000 m uplift near the break away faults can be modeled. South-plunging of the graben shoulders near the southern end of the URG can be reproduced. About 650 m rock uplift in the Feldberg area and 970 m for the Grand Ballon strongly underestimate the real observed rock uplift. Fig.6.10 right, shows modeled rock uplift in response to rifting sediment filling and erosion on the rift shoulders. The modelled uplift pattern with stronger uplift in the south than in the north resembles the graben-shoulder uplift observed in the URG. 1250 m rock uplift for B respectively 950 m rock uplift for F are to low compared with the observed values. Fig.6.11, displays modeled forebulge uplift (written isolines with high in meters) and subsidence in the Molasse Basin (unwritten -1000 m isolines). Left; modelling with Molasse Basin and Alpine thrust sheet loading leads to a forebulge with a local maximum uplift of about 400m centering around the Feldberg area. Comparison with observed topography east of the BF shows that this is about the halve of the observed uplift. Subsidence of the Molasse Basin fits however slightly overestimates the thickness of the Molasse Basin; ~1.5 km observed versus ~2km modeled for Zürich and about ~4km observed versus ~5km modeled thickness for Luzern. Fig.6.11right, shows the 'unrealistic' scenario where the alpine loading has been doubled. Under this circumstances a forebulge with sufficient high can be modeled, however the depth of the Molasse Basin gets much to high.

Fig.6.12 represents the final outcome and shows rock uplift due to URG rifting, Alpine thrust-sheet loading and related surface processes. The modeled

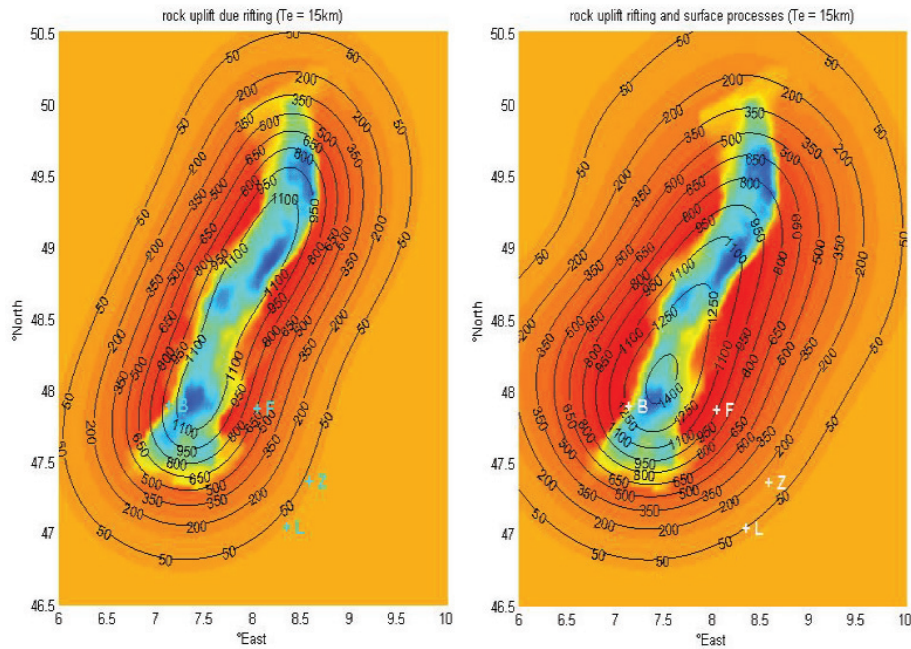


Figure 6.10: Modeled rock uplift for the URG shoulders (contours) superimposed by rift basin volume. Left hand modeling without surface processes results oval shaped flexural rift shoulder uplift. Modeling with sediment fill and erosion on shoulders results to higher rift-shoulders in the south owing to less graben fill and deeper erosion on the shoulders and a broader zone of rift shoulder uplift.

outcome resembles relatively well the shape of the VBFA with broader 'graben-shoulder' uplift in the BF. However Uplift of B and F are still to low. With a pre-rift elevation of ~ 350 m and about ~ 650 (F) - ~ 800 m(B) mesozoic pre-rift overburden (see ?Hinsken et al., 2007) about 1800m-2000m rock uplift can be assumed for F(~ 1800 m) and B(~ 2000 m).

A realistic uplift can however be modeled with the Alps x 2 unrealistic high amount of thrust sheet loading, that however is in conflict with the geological background and leads to to high basin depth in the Molasse Basin.

6.4.5 Discussion and interpretation of modeling results and the Neogene rise of VBFA

The results demonstrate that the Recent day uplift pattern of the VBFA can be to a large part explained with bending of an elastic plate with a T_e of about 15 km due to long term net changes in its static loading. In compare to the 'Alpine Forebulge' graben-shoulder related part of the uplift can be relatively good reproduced and therefore supports the theory of a necking-level respectively compensation depth of faulting at Moho discontinuity. Nevertheless the model fails to

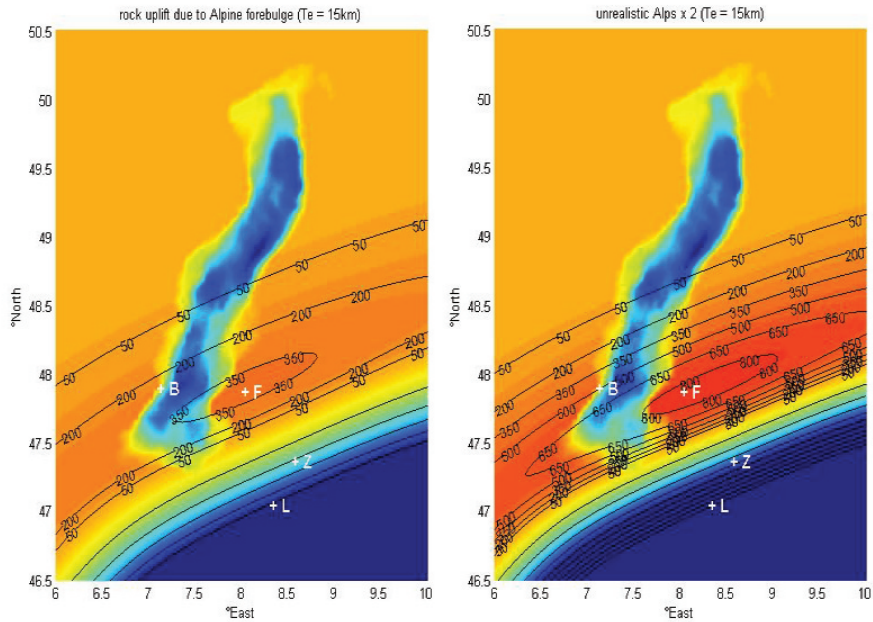


Figure 6.11: Modeled forebulge uplift due to Alpine thrust sheet loading and sedimentary fill of the Molasse Basin. Right; realistic model reproduces Molasse Basin subsidence (unwritten -1000 m isolines) quite well but fails modelling observed forebulge elevation by factor 2. Realistic forebulge uplift is reached when Alpine loading is multiplied by factor 2 and hence resulting in unrealistic high Molasse Basin subsidence.

explain differential rock uplift in the Northern URG like the Saverne-Kraichgau Depression and uplift of the Odenwald and the Rhenish Massif in the north. The modeled Alpine forebulge reaching only 400 m altitude is only the half of what is observed respectively needed to explain the height of the VBFA. In case the area was already uplifted by an Eocene forebulge, this Neogene 'forebulge' uplift is even higher.

Next to a geological reason the outcome could be explained by chosen very simplistic methodology. The chosen plate equation models the behavior of a 15 km fully elastic plate on top of an inviscid fluid, conditions that are not fulfilled in the real world, where in the area of the URG a more than 25km thick 'elastic' crust with most likely regional variable T_e rests on a high viscous 'non elastic' lithospheric mantle probably decoupled within the lower crust (Chapter 4). Moreover modeling temporal changes (in time) would require popper forward modeling. It is very likely that modeling with a thicker viscoelastic plate with local variations in T_e might result in a different outcome especially with respect to the modeled forebulge uplift.

With respect to the plate equation it has to be pointed out, that the pre-

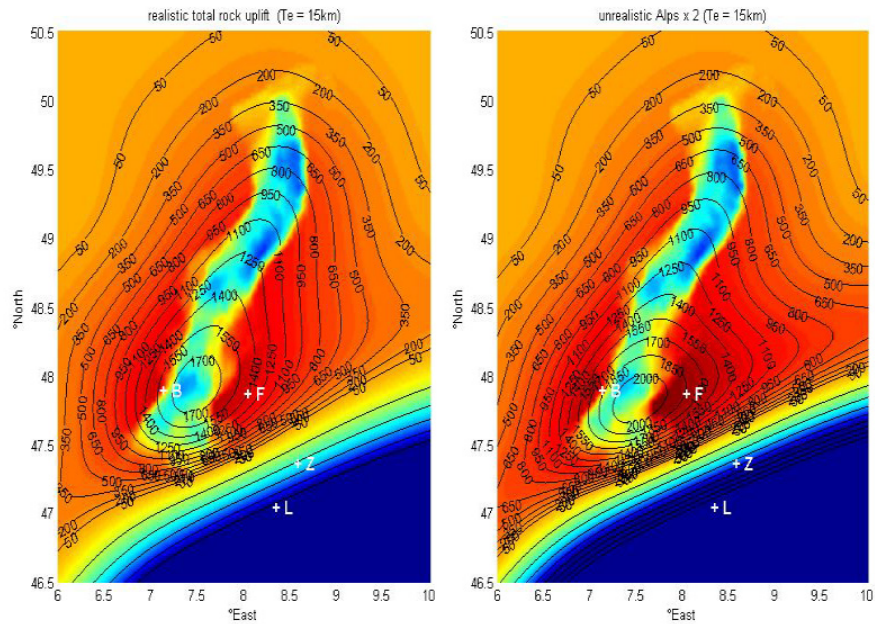
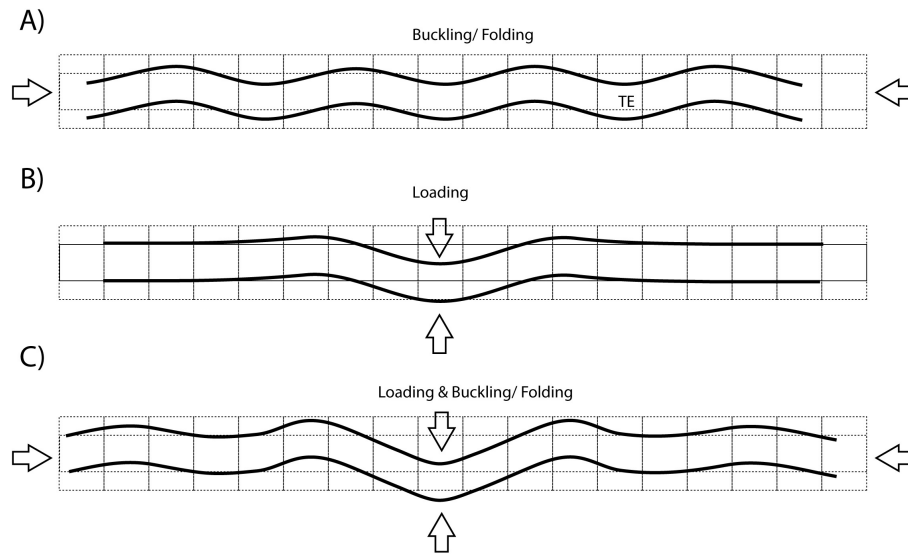


Figure 6.12: Rock uplift of the VBFA due to URG rifting Alpine Forebulge and related surface processes. Left, realistic model fits the observed uplift pattern but underestimates the reconstructed rock uplift. Unrealistic model with Alpine loading $\times 2$ resembles the real uplift pattern best and fits roughly the observed Amplitude.

sented result only invoke the first term of the Plate equation referring to plate bending due to vertical loading and therefore represents a static model. The unresolved second term however describes bending of an elastic plate due to tectonic compressive stress. Fig 6.13 shows the superposition (C) of (A) loading with (B) buckling both related to the T_e and therefore assumed to bend in similar wavelengths. A possible explanation is shown in (D); The Horizontal loading forces of the Alps are assumed to be equilibrated by horizontal stress below the Alps. These high stresses caused by the Adriatic indenter are transmitted to the European Plate where they cause buckling that amplifies pre-existing bulges. Such an outcome would be in agreement with results of Ziegler and Fraeffel (2008subm.) and Bourgeois et al. (2007) and would next to higher uplift in the URG also explain uplift patterns in the northern URG. Moreover the second 'Neogene' uplift phase correlates with buildup of compressive stresses in the NAF as indicated by beginning thrusting of European domains in the Alps and a change from synrift to post-rift stage in the URG (Fig. 6.3) However as an amplification is only seen with respect to uplift and not with respect to NAFB subsidence the elastic nature (buckling) of the controlling processes has to be questioned. Alternatively a base crustal detachment could occur as



D) North Alpine Foreland:

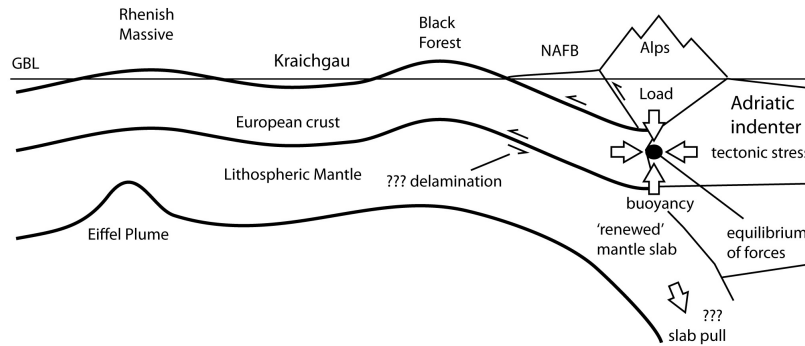


Figure 6.13: Interpretation of Neogene rise of VBFA: elastic plate bending can be due to A tectonic stress (horizontal force), B loading (normal force) or C superposition of both, while the flexural wavelength is scaled by the flexural rigidity respectively T_e . Additional lithospheric folding could explain the differences between modeled and observed topography. Lithospheric folding might be explained with buckling of shear along a base crustal detachment.

the mantle is not involved in the orogenic wedge. This could lead to folding of the crust in the area of the VBFA.

6.5 Final Conclusions

Although the results of this study remain somehow preliminary and further investigation is needed to test the concepts presented here, the following points can be already concluded:

- Uplift of the VBFA is widely compatible with elastic plate bending, however a complex interplay of several events account for uplift and subsidence.
- Pre-rift uplift of the southern URG area is compatible with a wide and shallow elevated alpine subduction related flexural forebulge.
- Early syn-rift uplift can be conclusively explained with rift related unloading, additional 'forebulge' uplift, however, can not be excluded.
- 'Middle' Oligocene flexural subsidence correlates with a change from syn-post collision stage in the Alps and might be explained with mechanical slab failure at that time.
- Numerical modeling with a thin plate equation reproduces the 1st order uplift pattern of the VBFA very well, however it underestimates the height of the 'Alpine forebulge' and provides no information on differential uplift pattern in the N-URG.
- The amount of rift related shoulder uplift appears however realistic and proves therefore the model of a deep level of necking at the Moho.
- Lithospheric folding due to compressive stress might explain the difference between modeled and observed height of the VBFA.
- several observations indicate reduction in flexural rigidity with time that might be explained with viscoelastic relaxation or plate softening in response to URG rifting and Kaiserstuhl volcanism.

Further geological evaluations should focus on the distribution of the 2nd Rupelian transgression and a more detailed reconstruction of shoulder uplift and erosion history i.e. as presented with the Kandern fan here. A next step in numerical modeling should invoke variability of the Te. Further modeling should involve a solution for buckling and finally viscoelastic forward modeling would be required.

Chapter 7

Summary and Conclusions: UPPER RHINE GRABEN; new evidences from the sedimentary record and numerical modeling

The southern parts of the Upper Rhine Graben (URG) form a prominent rift valley the surface of which is largely located above the erosional base-level (Fig. 7.1).

Beginning in the Middle Eocene and persisting into to the Late Oligocene, this rifted basin subsided rapidly and accommodated over 2.5 km syn-rift sediment in its Potash Basin southern depocentre near the city of Mulhouse. A profound erosional unconformity separates these Paleogene syn-rift sediments from a veneer of Pliocene-Quaternary and remnants of Late Miocene alluvial deposits (Fig. 7.2)

7.1 Palaeogene syn-rift Sedimentation in the southern URG

Two different stages can be distinguished in the Paleogene evolution of this basin, namely an under-filled Middle Eocene to Early Oligocene and an over-filled Middle to Late Oligocene stage.

During the Middle Eocene to Early Oligocene the rifted URG basin formed a more or less closed sedimentary system located in an area with a Mediterranean to subtropical seasonal-dry climate (Fig. 7.3). The Basin remained highly under-filled by clastics supplied from the elevated graben shoulders and

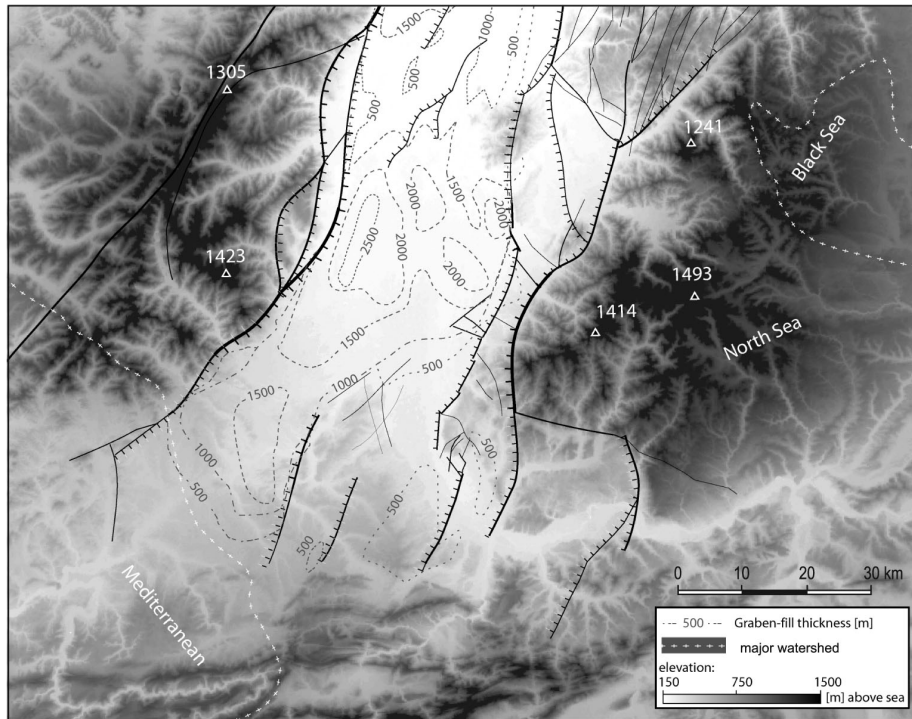


Figure 7.1: DEM of the southern URG superimposed with fault pattern and isopaches of Cenozoic graben fill (Chapter 3).

depositional environments were affected by rapid changes in the physiochemical conditions.

Strong climatically and eustatically controlled base-level fluctuations led to alternating lacustrine-brackish and evaporitic depositional environments, interrupted by short termed marine incursions, rendering sediment volume partitioning an important process. An up to 2 km thick sequence of marls and evaporites accumulated in the quick subsiding Potash Basin, while thin fluvio-terrestrial deposits and shallow water carbonates dominated the sedimentation in the shallow southernmost parts of the URG. Along the basin margins alluvial fans formed testifying to uplift of the graben flanks. Tectonic subsidence exerted a first-order control on the facies patterns of these early stage syn-rift sedimentary sequences that were chosen for analyzing the subsidence history of the southern URG.

During Middle to Late Oligocene the URG rift was affected by supra-regional subsidence and connected to the overfilled flexural foreland basin of the Alps, as reflected by temporary marine incursions. Consequently the URG basin was converted into an open depositional system. Alpine sediment supply to the URG is evidenced by a change in sediment transport directions (Roussé, 2006)

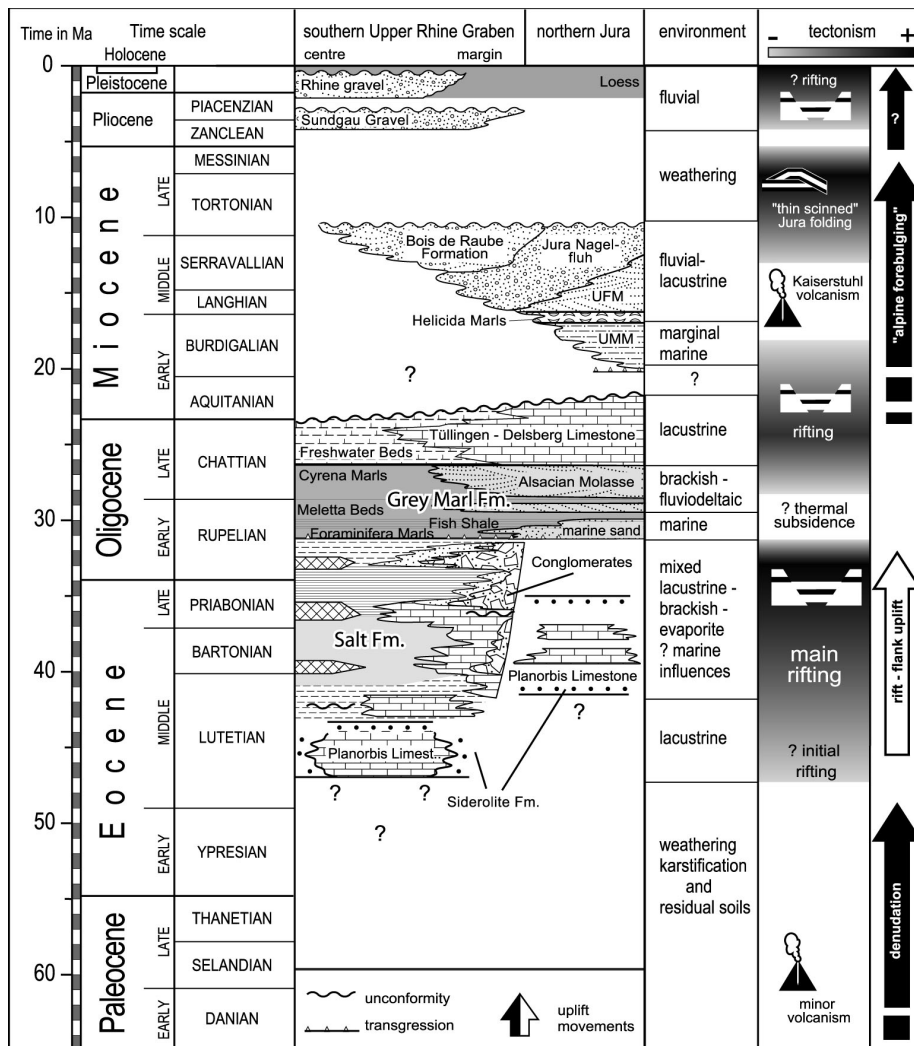


Figure 7.2: Stratigraphic chart showing Cenozoic evolution of the southern URG and adjoining northern Jura Mountains (Hinsken et al., 2007).

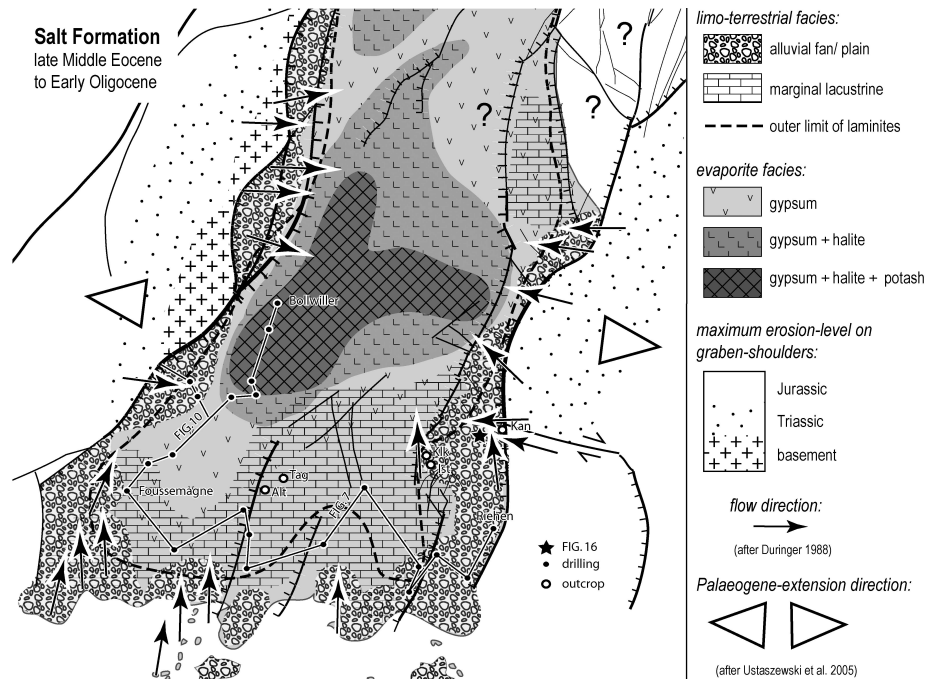


Figure 7.3: Palaeogeographic map illustrating facies distribution of Middle Eocene to Early Oligocene syn-rift deposits in the southern URG (Hinsken et al., 2007). A fluvio-lacustrine facies is dominant in the southernmost graben compartement, while evaporites and marls dominate in the Potash Basin depo-centre of the southern URG.

and the influx of reworked microfossils (Pirkenseer, 2007). Within the URG facies patterns of the Middle to Late Oligocene series were controlled by the influx of Alpine derived sediments, whilst evidence for sediment supply from the graben shoulders is lacking, suggestive of their sedimentary overstepping that is documented by drowning of the Jura-swell. During the latest Oligocene, carbonates were deposited in the southernmost part of the URG and in the southward adjacent area of the future Jura Mountains, indicating interruption of Alpine sediment supply into the URG and implying repeated uplift of the Jura swell. Middle and Late Oligocene sediments preserved in the southern URG beneath a profound Late Pliocene to Quaternary erosional surface, locally attain thicknesses of up to 500 m.

During the Early Miocene (ca. 18 Ma) the southern URG was uplifted above the erosional base level, although crustal extension continued. With this, development of the present-day southern URG rift valley commenced. In the process of this, Palaeogene syn-rift deposits were subjected to deep erosion. The thickness of strata removed is estimated at 500-1000 m (Roll, 1979). Subsidence of the southern URG resumed again during the Late Pliocene and Quaternary, as evidenced by the fault controlled accumulation of up to 240 m thick fluvial

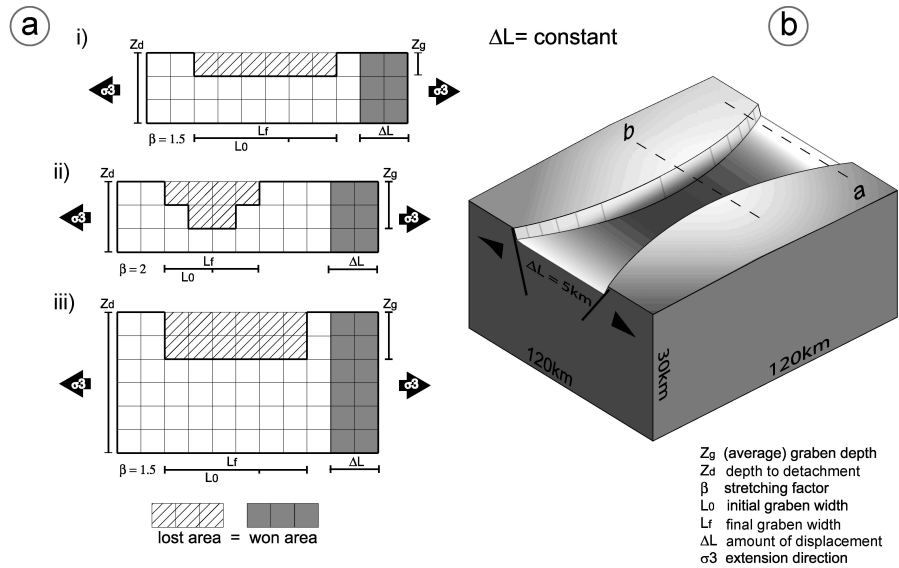


Figure 7.4: Effect of crustal volume balance at constant extensional strain. A) subsidence of rifted basins largely depends on graben width L_f (i versus ii) and depth of the necking-level Z_d at which material points move only horizontally during pure shear extension (i versus iii). B) at constant extensional strain depocentres develop in narrow graben segments owing to strain concentration (b), while shallower grabens develop in broader rift compartments (a).

gravels in the area of the Potash Basin.

7.2 Extension and basin subsidence

Subsidence analyses carried out for the southern URG shown that average subsidence of the different graben segments depended on their width that is defined by the distance between the westernmost and easternmost break away faults (Fig. 7.4). Balancing of published cross-sections and Thermo-Tectono-Stratigraphic modelling yielded similar results indicating across the URG an average extensional strain of about 4.5 km - 5 km, whilst the cross-sectional graben area (lost area) gave average values of about 120 km². It is therefore concluded that (1) the extensional strain across the URG remains constant, despite on-trend variations in its width that ranges between 63 km in the area of Basel, 35 km across the Potash Basin and about 50 km in the Colmar transect. Development of the discrete Potash Basin depot-centre is related to extensional strain concentration in a narrow graben segment that is characterized by a stretching factor of 1.14, which decreases to less than 1.1 in the northward and southward adjacent broader and shallower graben segments.

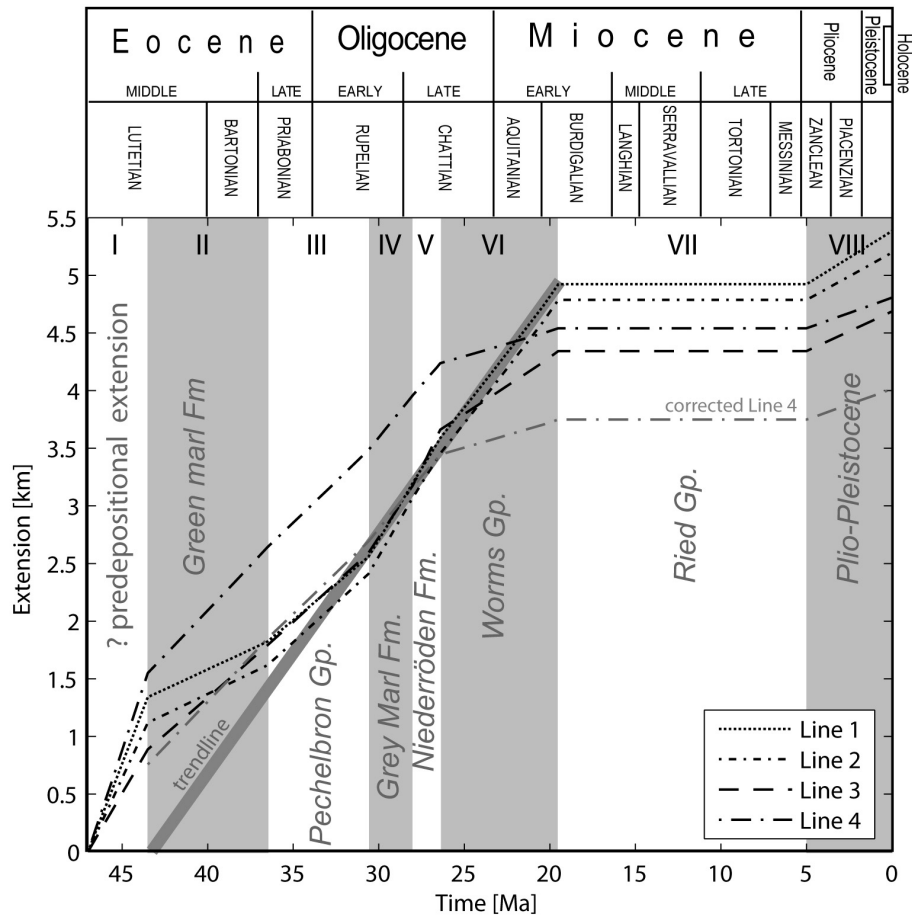


Figure 7.5: TFSM modeled Time Extension paths for the rifting in the central part of the northern Upper Rhine Graben. Results imply very constant extension rates and a post-rift stage during the Late Miocene.

7.3 Necking level and lithospheric strength

The ratio between extensional strain and the 'lost area' suggests a 'compensation-depth' of about 27-28 km depth that coincides with the depth of the Moho discontinuity in the URG area. Assuming pure shear rifting, this 'compensation depth' represents the necking-depth of the lithosphere. Thermo Tectonic Forward (TTFM) Modeling of 4 published cross sections from the central Northern part of the URG provided further evidence that the Necking level that is located at the Moho in coincidence with the brittle ductile transition and, hence represents the compensation level of the extensional faults. In this case formation of the URG can be explained to be a simple process: Lithospheric scale extension with a brittle elastic crust onto of a high viscous mantle.

(TTFM) Modeled extension-time paths imply rifting during Middle Eocene to Early Miocene times, a Late Miocene post-rift stage and renewed rifting during the Pliocene to recent (Fig. 7.5). A northward migration of modeled extension in time can be explained by 'non rift-related' uplift and the development of regional angular unconformities. Correcting for these 'uplift' effects, a very similar extension history is evident for the four modeled cross-sections, suggesting plane strain deformation at very low, strain rates of about $1.7 \times 10^{-16} \text{ s}^{-1}$. These results challenge the hypothesis of a poly-phase rifting stage and argue for a uniform rifting process and a highly viscose upper lithospheric mantle.

7.4 Rift-shoulder uplift and elastic plate bending

Localized crustal thinning with a necking level at the Moho leads to strong mechanical unloading nearly equating the weight of crust (basin volume multiplied by density of crust) that was displaced during extension. The sedimentary record of the URG and North Alpine Foreland Basin (NAFB) indicates at least 2 episodes of flexural uplift in the area of the southern URG separated by a phase of flexural subsidence (Fig 7.6). The first episode of uplift in the area of the URG predates the Mid Eocene onset of rift basin subsidence. It indicates a higher wavelength and a lower amplitude and is partly compatible with an alpine subduction related 'flexural-forebulge' that initiated broad flexural uplift in the North Alpine Foreland during the Eocene. Additional graben-shoulder uplift of several hundred meters occurred during the Late Eocene and Early Oligocene. Rapid flexural subsidence of ≥ 200 m is indicated during the middle Rupelian when the graben and the rift shoulders were transgressed. Former interpretation of eustasy to account for this transgression are contraindicated by (1) published global sea level curves and (2) by contemporaneous regression in the NAFB. Its timing however coincides with transition from syn-collisional to post-collisional stage of the Alpine orogeny that involved mechanical failure of the subducting slab.

Therefore the flexural subsidence might be explained with elastic relaxation of an subduction related flexural forebulge due to post-collisional 'slab breakoff' which is supported by 1D forebulge modeling. During the late Chattian to Aquitanian, renewed establishment of a shorter and higher 'forebulge' initiated the rise of the Vosges-Black Forest Arch (VBFA) that climaxed during the Mid-Burdigalian centering around the mid-Miocene Kaiserstuhl volcano. Its buildup is documented by the diachrone Early Aquitanian to Pleistocene erosional unconformity in the S-URG extending N-S ward into Burdigalian deposits of the northern URG and Molasse Basin, that was during further evolution convergently onlaped from N and S. Neogene Rise of the VBFA occurred mainly during the Mid-Late Miocene post-rift stage and corresponds with build up of compressional stresses and imbrication of the North Alpine Foreland (NAF) that finalized basin evolution in the NAFB.

Renewed extension in the URG at the Plio-Pleistocene boundary led to renewed subsidence and deposition of Alpine derived Rhine gravels in the URG.

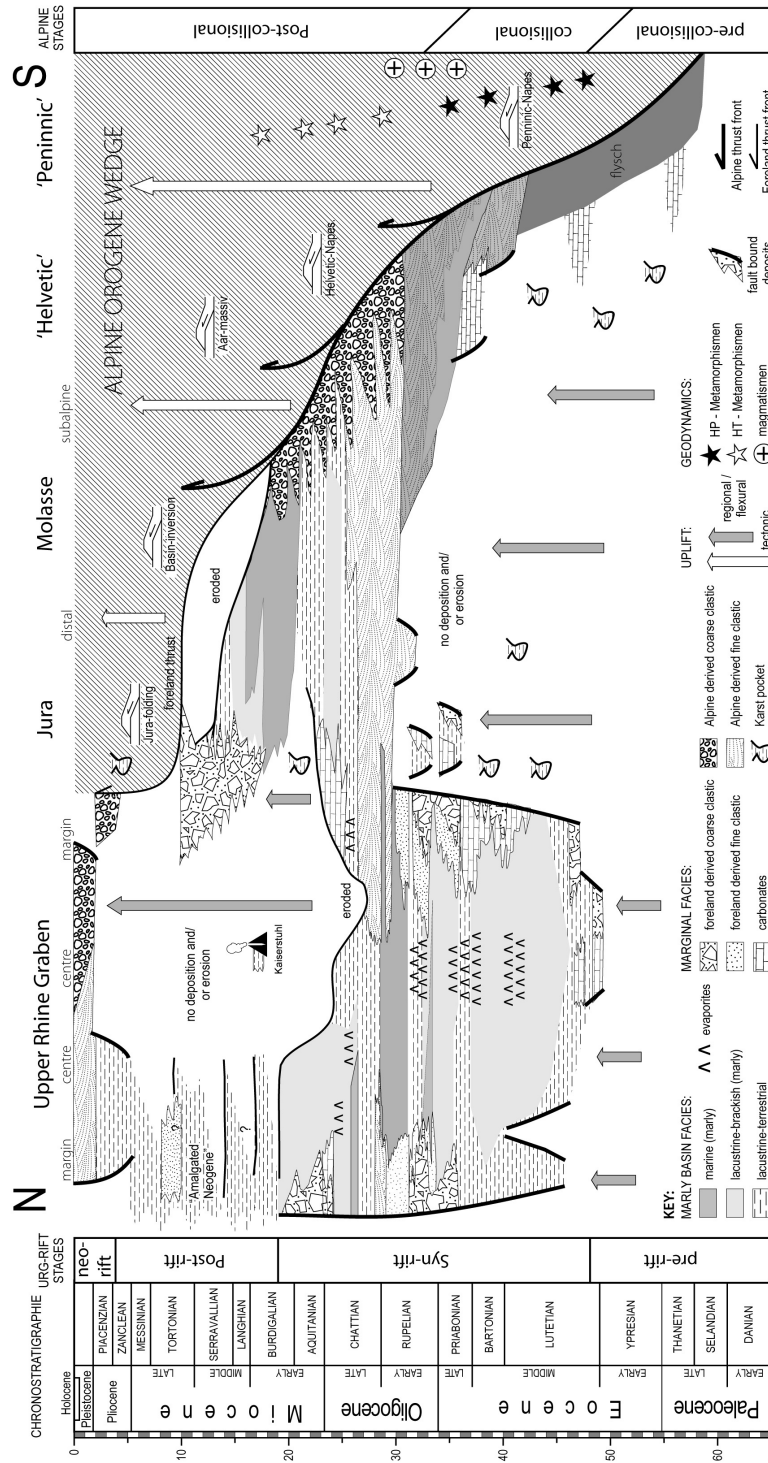


Figure 7.6: Geological Transsect from the N-URG to the central Swiss Alps showing the Cenozoic evolution of the Alps and the North Alpine Foreland Basin and the URG.

Numerical modeling of Cenozoic rock uplift of the VBFA is highly compatible with flexural isostatic compensation of changes in static loading of a thin elastic plate having an elastic thickness (T_e) of about 15km due to URG rifting and Alpine Orogeny (Fig. 7.7).

The changing crustal loads include (1) static unbalanced crustal thinning in the URG (2) the sedimentary fill of URG and Molasse Basin (3) erosion on the graben shoulders and (4) forebulge formation in response to crustal thickening in the Alps.

Although the rift related amount of flank uplift can be roughly reproduced, the modeled 'Alpine Forebulge' significantly underestimates the observed height by about factor 2 respectively by about 400 m. Moreover the model provides no explanation for differential uplift of the massives bordering the northern URG. Differences between the modeled and the observed uplift might arise from (1) the simplistic modeling approach (2) additional sub surface loading due to alpine 'slab-pull' or most likely (3) lithospheric folding related to build up of compressional stress within the foreland lithosphere.

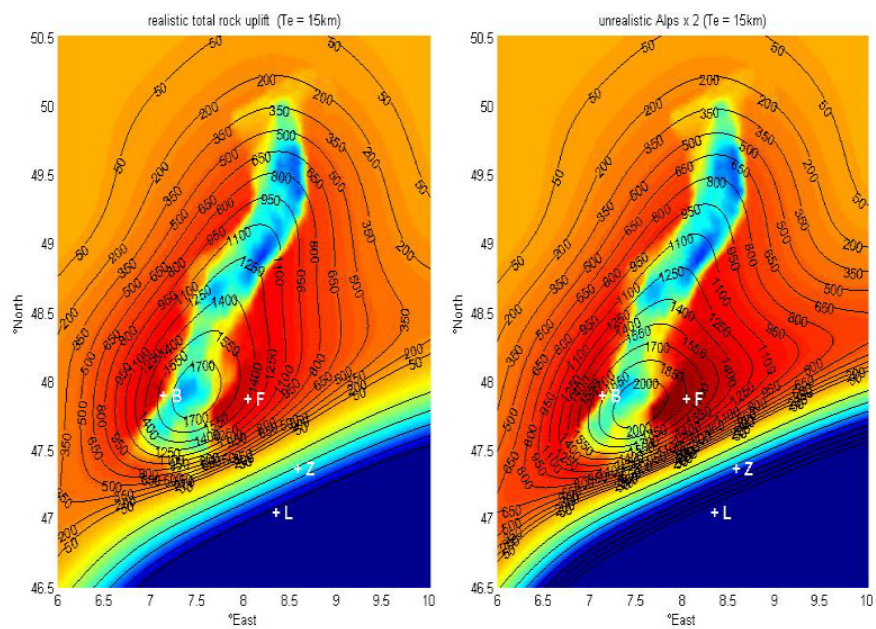


Figure 7.7: Results of Flexural Isostasy modelling (Chapter 5): Uplift of VBFA can be to a large part explained with regional isostatic compensation of changes in Lithospheric loading that occurred due to Alpine Orogeny and URG rifting (left side). However realistic 'forebulge uplift' can only be modeled when Alpine thrust sheet loading is doubled (right side). The misfit could be explained with Lithospheric folding.

Bibliography

- Abe, M., 1988. A biosystematic study of the genus *Athalia* Leach of Japan (Hymenoptera: Tenthredinidae). *Eskia* 26, 91–131.
- Achauer, U., Masson, F., 2002. Seismic tomography of continental rifts revisited: from relative to absolute heterogeneities. *Tectonophysics* 358, 17–37.
- Allen, P. A., Allen, J. R., 2005. *Basin Analysis: Principles and Applications*, 2nd Edition. Blackwell Publishing.
- Allenbach, R., Wetzel, A., 2006. Spatial patterns of Mesozoic facies relationships and the age of the Rhenish lineament: a compilation. *Int. J. Earth Sci.* 95, 803–813.
- Banda, A., Cloetingh, S., 1992. Europe's lithosphere - physical properties. In: Blundell, D., Freeman, R., Mueller, S. (Eds.), *A Continent Revealed - The European Geotraverse*. University Press, Cambridge, pp. 71–109.
- Barnes, R., 1994. *The Brackish Water Fauna of Northwestern Europe*. Cambridge University Press, Cambridge.
- Bartz, J., 1974. Die Mächtigkeit des Quartärs im Oberrheingraben. In: Illies, J., Fuchs, K. (Eds.), *Approaches to Taphrogenesis - Proceedings of an International Rift Symposium held in Karlsruhe April, 13-15, 1972*. Nägeli u. Obermiller, Stuttgart, pp. 78–87.
- Becker, A., 2000. The Jura mountains - an active foreland fold-and-thrust belt? *Tectonophysics* 321, 381–406.
- Becker, D., 2003. Paléocologie et paléoclimats de la molasse du Jura (Oligo-Miocène): apport des Rhinocérotoidea (Mammalia) et des minéraux argileux. *GeoFocus* 9, 327.
- Behrmann, J., Hermann, O., Horstmann, M., Tanner, D. C., Bertrand, G., 2003. Anatomy and kinematics of oblique continental rifting revealed: A three-dimensional case study of the Southeast Upper Rhine Graben (Germany). *American Association of Petroleum Geologists Bulletin* 87 (7), 1–17.
- Benson, R. B., 1962. A revision of the genus *Athalia* (Hymenoptera: Tenthredinidae). *Bull. Brit. Mus. (Nat. Hist.), Entomol.* 2 (7), 333–382.

- Berger, J.-P., Reichenbacher, B., Becker, D., Grimm, M., Grimm, K., Picot, L., Storni, A., Pirkenseer, C., Derer, C., Schaefer, A., 2005a. Paleogeography of the upper rhine graben (urg) and the swiss molasse basin (smb) from eocene to pliocene. *Int. J. of Earth Sci.* 94 (4), 697–710.
- Berger, J.-P., Reichenbacher, B., Becker, D., Grimm, M., Grimm, K., Picot, L., Storni, A., Pirkenseer, C., Schaefer, A., 2005b. Eocene-pliocene time scale and stratigraphy of the upper rhine graben (urg) and the swiss molasse basin (smb). *Int. J. of Earth Sci.* 94 (4), 711–731.
- Bergerat, F., 1987. Stress fields in the european platform at the time of africa-eurasia collision. *Tectonics* 6 (2), 99–132.
- Bertrand, G., Horstmann, M., Hermann, O., Behrmann, J., 2005. Retrodeformation of the southern upper rhine graben: new insights on continental oblique rifting. *Quaternary Science Reviews* 24, 347–354.
- Blanc-Valleron, M.-M., 1991. Les formations Paléogènes évaporitiques du Bassin Potassique de Mulhouse et des Bassins plus septentrionaux d’Alsace. Document du BRGM n° 204. Éditions du BRGM, Orléans.
- Blanc-Valleron, M.-M., Schuler, M., 1997. The salt basins of alsace (southern rhine graben). In: Brusson, G., Schreiber, B. C. (Eds.), *Sedimentary Deposition in Rift and Foreland Basins in France and Spain (Paleogene and Lower Neogene)*. Columbia University Press, New York, pp. 95–135.
- Bohacs, K. M., Carroll, A. R., Neal, J. E., Mankiewicz, P. S., 2000. Lake-basin type, source potential and hydrocarbon character: an integrated sequence-stratigraphic-geochemical-framework. In: Gierlowski-Kordesch, E. H., Kelts, K. R. (Eds.), *Lake Basins Through Space and Time*. Vol. 46. AAPG Studies in Geology, pp. 3–43.
- Boigk, H., Schöneich, H., 1970. Die tiefenlage der permbasis im nördlichen teil des oberrheingrabens. In: Illies, J., Mueller, S. (Eds.), *Graben Problems. Proceedings of an International Rift Symposium held in Karlsruhe 1968, International Upper Mantle Project*. E. Schweitzerbart’sche, Stuttgart, pp. 45–55.
- Bourgeois, O., Ford, M., Diraison, M., Le Carlier de Veslud, C., Gerbault, M., Pik, R., Ruby, N., Bonnet, S., 2007. Separation of rifting and lithospheric folding signatures in the nw-alpine foreland. *International Journal of Earth Science* 96 (6), 1003–1032.
- Boyer, B., 1982. Green river laminites: Does the playa lake model really invalidate the stratified lake model? *Geology* 10, 321–324.
- Braun, G., 1914. Zur morphologie der umgebung von basel. *Verh. d. naturf. Ges. in Basel* 25, Sonderabdruck.

- Braun, J., Beaumont, C., 1989. A physical explanation of the relation between flank uplift and the break up unconformity at rifted continental margins. *Geology* 17, 760–764.
- Brun, J. P., Gutscher, M. A., teams, D.-E., 1992. Deep crustal structure of the rhine graben from dekop-ecors seismic reflection data: a summary. *Tectonophysics* 208, 139–147.
- Buchanan, P., Nieuwland, D., 1996. Modern developments in structural interpretation, validation and modeling. *Geol. Soc. London, Spec. Publ.* 99, 1–369.
- Buchner, F., 1981. Rhinegraben: horizontal stylolithes indicating stress regimes of earlier stages of rifting. *Tectonophysics* 73, 113–118.
- Burkhard, M., Sommaruga, A., 1998. Evolution of the western swiss molasse basin: structural relations with the alps and the jura belt. In: Mascle, A., Puidgefåbregas, C., Luterbacher, H. P., Fernàndez, M. (Eds.), *Cenozoic Foreland Basins of Western Europe*, geological society special publication Edition. Vol. 134. Geological Society, London, pp. 279–298.
- Carpenter, F. M., 1992. Superclass hexapoda. In: Moore, R. C., Kaesler, R. (Eds.), *Treatise on invertebrate paleontology. Part R. Arthropoda 4. Vol. 3-4.* Geol. Soc. Am. Univ. Kansas press, Boulder, Colorado, p. 655.
- Chorowicz, J., Defontaine, B., 1993. Transfer faults and pull-apart model in the rhinegraben from analyses of multisource data. *Journal of Geophysical Research* 98 (B8), 14,339–14,351.
- Cloetingh, S., Burov, E., 1996. Thermomechanical structure of european continental lithosphere: constraints from rheological profiles and eet estimates. *Geophysical Journal International* 124, 695–723.
- Cloetingh, S., Ziegler, P., Beekman, F., Andriessen, P., Hardenbold, N., Dèzes, P., 2005. Intraplate deformation and 3d rheological structure of the rhine rift system and adjacent areas of the northern alpine foreland. *International Journal of Earth Sciences*, 94, 758–778.
- Cloos, H., 1939. Hebung-spaltung-vulkanismus. *Geol. Rundschau* 30, 401–527.
- Cockerell, T., 1906. Fossil saw-flies from florissant, colorado. *Bull. Am. Mus. Nat. Hist.* 22, 499–501.
- Cockerell, T., 1927. Hymenoptera and a caddis larva from the miocene of colorado. *Ann. Mag. Nat. Hist.* 20 (9), 429–435.
- Cole, R. D., Pickard, M. D., 1981. Sulfur-isotope variations in marginal lacustrine rocks of the green river formation, colorado and utah. *Recent and Ancient nonmarine Depositional Environments: Models for Exploration* 31.

- Collinson, M., 1992. Vegetational and floristic changes around the eocene/oligocene boundary in western and central europe. In: Prothero, D. R., Berggren, W. A. (Eds.), *Eocene-Oligocene Climatic and Biotic Evolution*. University press, Princeton, NJ, pp. 437–450.
- Courtot, C., Gannat, E., Wendling, E., 1972. Le bassin potassique de mulhouse et ses environs. Étude du tertiaire. *Sci. Géol., Bull.* 25 (2-3), 69–91.
- Cross, T. A., Lessenger, M. A., 1998. Sediment volume partitioning: rationale for stratigraphic model evaluation and high-resolution stratigraphic correlation. In: Gradstein, F. M., Sandvik, K. O., Milton, N. J. (Eds.), *Sequence Stratigraphy - Concepts and Applications*. Vol. 8. NOF Spec. Publ. (Elsevier), Amsterdam, pp. 171–195.
- Davies, J., Von Blanckenburg, F., 1995. Slab breakoff: A model of lithosphere detachment and its test in the magmatism and deformation of collisional orogens. *Earth and Planetary Science Letters* 129, 85–102.
- Derer, C., Kosinowski, M., Luterbacher, H. P., Schäfer, A., Süss, M. P., 2003. Sedimentary response to tectonics in extensional basins: the pechelbronn formation (late eocene to early oligocene) in the northern upper rhine graben, germany. In: McCann, T., Saintot, A. (Eds.), *Tracing Tectonic Deformation Using the Sedimentary Record*. Vol. 208. Geol. Soc. London, Spec. Publ., London, pp. 55 – 69.
- Derer, C., Schumacher, M., Schäfer, A., 2005. The northern upper rhine graben: basin geometry and early syn-rift tectono-sedimentary evolution. *Int. J. Earth Sci* 94, 640–679.
- Doehl, F., 1967. The tertiary and pleistocene sediments of the northern and central part of the upper rhine graben. *Abh. geol. L.-Amt Baden Württ.* 6, 48–54.
- Doehl, F., 1970. Die tertiären und quartären sedimente des südlichen rhein-grabens. In: Illies, J. H., Mueller, S. (Eds.), *Graben Probleme. Proceedings of an International Rift Symposium held in Karlsruhe October, 10-12, 1968*. Vol. International Upper Mantle Project. E. Schweizerbart'sche, Stuttgart, pp. 56–66.
- Doehl, F., Teichmüller, R., 1979. Zur geologie und heutigen geothermik im mittleren oberrhein-graben. *Fortschr. Geol. Rheinl. Westfalen* 27, 1–27.
- Dohr, G., 1957. Zur reflexionsseismischen erfassung sehr tiefer unstetigkeitsflächen. *Erdöl und Kohle* 10, 278–281.
- Downes, H., 1993. The nature of the lower continental crust of europe: petrological and geochemical evidence from xenoliths. *Phys. Earth Planet. Int.* 76, 195–218.

- Duncan, 2003. Decay and disarticulation of the cockroach: Implications for preservation of the blattoids of writhlington (upper carboniferous), uk. *Palaios* 18, 256–265.
- Duringer, P., 1988. Les conglomérats des bordures du rift cénozoïque rhénan. dynamique sédimentaire et contrôle climatique. Ph.D. thesis, Université Louis Pasteur.
- Duringer, P., Gall, J.-C., 1994. Morphologie des constructions microbiennes en contexte de fan-delta oligocène. exemple du rift rhénan (europe occidentale). *Palaeogeography, Palaeoclimatology, Palaeocology*, 107, 35–47.
- Durst, H., 1991. Aspects of exploration history and structural style in the rhine graben area. In: Spencer, A. e. (Ed.), *Generation, accumulation and production of Europe's hydrocarbons*. Vol. 1. European Association of Petroleum Geoscientists, Spec. Publ., pp. 247–261.
- Dèzes, P., Schmid, S. M., Ziegler, P. A., 2004. Evolution of the european cenozoic rift system: interaction of the alpine and pyrenean orogens with their foreland lithosphere. *Tectonophysics* 389, 1–33.
- Dèzes, P., Schmid, S. M., Ziegler, P. A., 2005. Reply to comments by l. michon and o. merle on "evolution of the european cenozoic rift system: interaction of the alpine and pyrenean orogens with their foreland lithosphere" by p. dèzes, s. m. schmidt and p. a. ziegler, *tectonophysics* 389 (2004) 1-33. *Tectonophysics* 401, 257–262.
- Echtler, H. P., Chauvet, A. C., 1992. Carboniferous convergence and subsequent crustal extension in the southern schwarzwald (sw germany). *Geodinamica Acta* 5 (1-2), 37–49.
- Eisbacher, G. H., Lüschen, E., Wickert, F., 1989. Crustal-scale thrusting and extension in the hercynian schwarzwald and vosges. *Tectonics* 8 (1), 1–21.
- Etter, W., 1994. *Palökologie: Eine methodische Einführung*. Birkhäuser-Verlag, Basel.
- Eugster, H. P., Surdam, R., 1973. Depositional environment of the green river formation of wyoming: A preliminary report. *Geol Soc Am Bull* 84, 1115–1120.
- Fischer, H., 1969. Geologischer Überblick über den südlichen oberrheingraben und seine weitere umgebung. *Regio Basiliensis* 10 (1), 57–84.
- Fontes, J.-C., Filly, A., Gaudant, J., Duringer, P., 1991. Origine continentale des évaporites paléogènes de haute alsace: arguments paléoécologiques, sédimentologiques et isotopiques. *Bull. Soc. géol. France* 162 (4), 725–737.
- Franke, W., 1989. Tectostratigraphic units in the variscan belt of central europe. *Geol Soc Am Spec Pap* 230, 67–90.

- Franzen, J. L., 1968. Revision der gattung palaeotherium cuvier 1804 (palaeotheriidae, perissodactyla, mammalia). Ph.D. thesis, Univ. Freiburg.
- Frodge, J., Li, K., 1997. August 1997 lake washington fish kill. <http://dnr.metrokc.gov/wlr/waterres/lakes/fishkill.htm>.
- Förster, B., 1891. Die insekten des plattigen steinmergels von brunstatt. Abh. zur geol. Spezialkarte von Elsass Lothringen 3 (5), 336–593.
- Förster, B., 1892. Geologischer Führer für die Umgebung von Mülhausen i. E. Vol. 3 (4) of Mittheilungen der geologischen Landesanstalt von Elsass-Lothringen. Strassburger Druckerei und Verlagsanstalt.
- Förster, B., 1913. Die versteineringen aus den tiefbohrungen auf kali im oligocän des oberelsass. Mitt. d. Geol. Landesanstalt v. Elsass-Lothr. 8 (1), 1–47.
- Gale, H. S., 1920. The potash deposits of alsace. UGS Bull. 715 (B), 17–55.
- Gaudant, J., 1979. Sur la présence de gobiidae (poissons téléostéens) dans l'oligocene inferieur de roufach (haut-rhin). Sciences Géologiques 32 (2), 131–137.
- Gaudant, J., 1984. Un nouveau cyprinodontidae (poisson téléostéen) de l'oligocène inferieur de kleinkembs (pays de bade, allemagne) : Prolebias rhenanus nov. sp. erratum et corrigendum. Sciences Géologiques 37 (2), 173–174.
- Gaudant, J., 1988. Mise au point sur l'ichthyofaune oligocène de rott, stösschen et orsberg (allemagne). C. R. Acad. Sci. Paris Ser II 306, 831–834.
- Gaudant, J., Burkhardt, T., 1984. Sur la découverte de poissons fossiles dans les marnes grises rayées de la zone fossilifère (oligocène basal) d'altkirch (haut-rhin). Sciences Géologiques 37 (2), 137–152.
- Gaup, R., Nickel, B., 2001. Die pechelbronnschichten im raum eich-stockstadt (nördlicher oberrheingraben; blatt 6216 gernsheim). Geol. Jb. Hessen 128, 19–27.
- Genser, H., 1959. Stratigraphie und tektonik der vorbergzone am südwestlichen schwarzwaldrand zwischen staufen und badenweiler. Ber. Naturf. Ges. Freiburg i. Br. 49, 59–112.
- Geyer, O. F., Gwinner, M. P., 1986. Geologie von Baden-Württemberg. E.Schweizerbart'sche Verlagsbuchhandlung (Nägele und Obermiller), Stuttgart.
- Giamboni, M., Ustaszewski, K., Schmid, S. M., Schumacher, M. E., Wetzell, A., 2004. Plio-pleistocene transpressional reactivation of paleozoic and paleogene structures in the rhine-bresse transform zone (northern switzerland and eastern france). International Journal of Earth Sciences 93, 207–223, DOI: 10.1007/s00531-003-0375-2.

- Gradstein, F. M., Ogg, J., Smith, A., 2004. A geologic time scale. University press, Cambridge.
- Griessemer, T., Uffenorde, H., Radtke, G., 2007. Die ostrakoden der mittleren pechelbronn-schichten (unter-oligozän) in der bohrung wallau b98-bk5. Geol. Abh. Hessen 116, 7–36.
- Griessemer, T. W., 2002. The bolboforma signal – a distinctive level for correlating lower oligocene deposits (np22), the melania clay formation of northern hesse (hessian depression) with the middle pechelbronn formation of the mainz basin (rhineland-palatinate, germany). In: Proceeding of the 8th Biannual Meeting Northern European Cenozoic Stratigraphy. Landesamt für Natur und Umwelt des Landes Schleswig-Holstein, Flintbek, p. 57–66.
- Grimaldi, D., Engel, M. S., 2005. Evolution of the insects. Cambridge University Press, New York.
- Grimm, K., Grimm, M., 2003. Die fossilen wirbellosen des mainzer tertiärbeckens, teil 1-1. geologischer führer durch das mainzer tertiärbecken. Mainzer Naturwissenschaftliches Archiv 26, 180.
- Grimm, M., 2005a. Beiträge zur lithostratigraphie des paläogens und neogens im oberrheingebiet (oberrheingraben, mainzer becken, hanauer becken). Geol. Jb. Hessen 132, 79–112.
- Grimm, M., Hottenrott, M., 2005b. Das tertiär des oberrheingrabens in der stratigraphischen tabelle von deutschland 2002. Newsl. Stratigr. 41 ((1-3)), 351–358.
- Groshong, R. H., 1996. Construction and validation of extensional cross sections using lost area and strain, with the application to the upper rhine graben. In: Buchanan, P. G., Nieuwland, D. (Eds.), Modern developments in structural interpretation. Vol. 99. Geol. Soc. Spec. Pub., pp. 79–87.
- Gueydan, F., Morency, C., Brun, J.-P., 2008. Continental rifting as a function of lithosphere mantle strength. Tectonophysics 460, 83–93.
- Gutscher, M., 1995. Crustal structure and dynamics in the rhine graben and the alpine foreland. Geophys. J. Int. 122, 617–636.
- Hagedorn, E.-M., Boenik, W., 2008. The pliocene and quaternary sedimentary and fluvial history in the upper rhine graben based on heavy mineral analyses. Netherlands J. Geosci 87 (21-32).
- Haimberger, R., Hoppe, A., Schäfer, A., 2005. High-resolution seismic survey on the rhine river in the northern upper rhine graben. Int. J. Earth Sci. 94, 657–668.
- Hallam, A., 1972. Models involving population dynamics. In: Schopf, T. (Ed.), Models in Paleobiology. Freeman, Cooper and Company, San Francisco, pp. 62–80.

- HAQ, B. U., HARDENBOL, J., VAIL, P. R., 1987. Chronology of fluctuating sea levels since the triassic. *Science* 235 (4793), 1156 – 1167.
- Hauber, L., 1991. Ergebnisse der geothermiebohrungen riehen 1 und 2 sowie reinach 1 im südosten des rheingrabens. *Geol. Jb.* E48, 167–184.
- Heiskanen, W. A., Vening-Meinesz, F. A., 1958. *The earth and its gravity field.* McGraw-Hill, New York.
- Herb, R., 1988. Eocaene paläogeographie und paläotektonik des helvetikums. *Eclogae geol. Helv.* 81 (3), 611–657.
- Hessler, R. R., 1969. Peracardia. In: Moore, R. C. (Ed.), *Treatise of invertebrate Paleontology.* Vol. 4 (1). GSA and University of Kansas, pp. R360–R393.
- Hinsken, S., 2003. Geologische untersuchungen an syn-rift sedimenten des südlichen oberrheingrabens. unpublished msc-thesis, Universität Basel.
- Hinsken, S., Ustaszewski, K., Wetzel, A., 2007. Graben-width controlling synrift sedimentation: The palaeogene southern upper rhine graben as an example. *International Journal of Earth Sciences* 96 (6), 979–1002.
- Hofmann, P., Huc, A. Y., Carpentier, B., Schäffer, P., Albrecht, P., Keely, B., Maxwell, J. R., Sinninghe Damsté, J. W., De Leeuw, J. W., Leythaeuser, D., 1993. Organic matter of the mulhouse basin, france: a synthesis. *Org. Geochem.* 20 (8), 1105–1123.
- Hooker, J. J., 1992. British mammalian palaeocomunities across the eocene-oligocene transition and their environmental implications. In: Prothero, D. R., Berggren, W. A. (Eds.), *Eocene-Oligocene Climatic and Biotic evolution.* University press, Princeton, NJ, pp. 449–515.
- Hottenrott, M., Pross, J., 2007. Terrestrische und aquatische mikrofloren aus den mittleren pechelbronn-schichten der bohrungen w07 und b98 bei wallau. *Geol. Abh. Hessen* 116, 127–139.
- Huber, B., 1994. Rupelian foraminifera in the southern rhinegraben and their paleoecological significance. Phd, Universität Basel.
- Illies, J. H., 1967. An attempt to model the rhinegraben tectonics. *Abh. geol.-L.A. Baden-Württemberg* 6, 10–12.
- Illies, J. H., 1970. Graben tectonics as related to crust mantle interaction. In: Illies, J., Mueller, S. (Eds.), *Graben Problems. Proceedings of an International Rift Symposium held in Karlsruhe 1968, International Upper Mantle Project.* E. Schweitzerbart'sche, Stuttgart, pp. 4–27.
- Illies, J. H., 1981. Mechanisms of graben formation. *Tectonophysics* 73, 249–266.
- Illies, J. H., Greiner, G., 1978. Rhine graben and alpine system. *Geological Society of America Bulletin* 89, 770–782.

- Jordan, T. E., 1981. Thrust loads and foreland basin evolution, cretaceous, western united states. *Bull Am. Assoc. Petrol. Geol.* 65, 2506–2520.
- Juengst, H., 1938. Fischsterben im kurischen haff. *Geologie der Meere und Binnengewässer* 1 (352-356).
- Keller, J., Kramel, M., Henjes-Kunst, F., 2002. $^{40}\text{Ar}/^{39}\text{Ar}$ single crystal laser dating of early volcanism in the upper rhine graben and tectonic implications. *Schweiz. Min. u. Pet. Mitt.* 82, 1–10.
- Kempf, O., Pfiffner, A. O., 2004. Early tertiary evolution of the north alpine foreland basin and adjoining areas. *Basin Research* 16, 549–567.
- Kessler, P., 1909. Die tertiären küstenkonglomerate in der mittlrheinischen mit besonderer berücksichtigung der elsässischen vorkommen. *Mitt. d. Geol. Landesanstalt v. Elsass-Lothr.* 7, 167–290.
- Kiefer, H., 1928. Das tertiär der breisgauer vorberge zwischen freiburg i. br. und badenweiler. *Ber. Naturf. Ges. Freiburg i. Br.* 28, 1–98.
- Kälin, D., 1997. Litho- und biostratigraphie der mittel- bis obermiozänen bois de raube-formation (nordwestschweiz). *Eclogae Geologicae Helvetiae* 90 (1), 97–114.
- Kock, S., Huggenberger, P., Preusser, F., Rentzel, P., Wetzel, A., 2009a. Formation and evolution of the lower terrace of the rhine river in the area of basel. *Swiss J. Geosci.* 102, 307–321.
- Kock, S., Kramers, J., Preusser, F., Wetzel, A., 2009b. Dating of late pleistocene terrace deposits of the river rhine using uranium series and luminescence methods: Potential and limitations. *Quat. Geochronology* 29 (1-11).
- Kooi, H., Cloetingh, S., 1992. Lithospheric necking and regional isostasy at extensional basins 2. stress-induced vertical motions and relative sea level changes. *J. Geophys. Res.* 97 (B12), 17,537–17,591.
- Kuhlemann, J., Spiegel, C., Dunkl, I., Frisch, W., 1999. A contribution to the paleogeography of central europe: New evidence from fission track ages of the southern rhine-graben. *N. Jb. Geol. Paläont. Abh.* 214 (3), 415–432.
- Lacombe, O., Angelier, J., Byrne, D., Dupin, J., 1993. Eocene-oligocene tectonics and kinematics of the rhine-saone continental transform zone (eastern france). *Tectonics* 12 (4), 874–888.
- Larroque, J., Laurent, P., 1988. Evolution of the stress field pattern in the south of the rhine graben from the eocene to the present. *Tectonophysics* 148, 41–58.
- Laubscher, H., 1970. Grundsätzliches zur tektonik des rheingrabens. In: Illies, J., Mueller, S. (Eds.), *Graben Problems. Proceedings of an International Rift Symposium held in Karlsruhe 1968, International Upper Mantle Project.* E. Schweitzerbart'sche, Stuttgart, pp. 79–86.

- Laubscher, H., 1998. Der ostrand des laufenbeckens und der knoten von grellingen: die verwickelte begegnung von rheingraben und jura. *Eclogae Geologicae Helvetiae* 91, 275–291.
- Laubscher, H., 2001. Plate interactions at the southern end of the rhine graben. *Tectonophysics* 343, 1–19.
- Laubscher, H., 2004. The southern rhine graben: A new view of the initial phase. *International Journal of Earth Science* 93, 341–347.
- Le Carlier de Velsud, C., Bopurgeois, O., Diraison, M., Ford, M., 2005. 3d stratigraphic and structural synthesis of the dannemarie basin (upper rhine graben). *Bull. Soc. géol. Fr.* 176 (5), 433–442.
- Leeder, M. R., Gathrope, R. L., 2002. Sedimentary models for extensional tilt-block/ half-graben basins. In: Holdsworth, R. E., Turner, J. P. (Eds.), *Extensional Tectonics: Regional-scale Processes*. Vol. 2. The Geological Society, Key Issues in Earth Sciences, London, pp. 171–184.
- Lopes Cardozo, G. G., Behrmann, J. H., 2006. Kinematic analysis of the upper rhine graben boundary fault system. *Journal of Structural Geology* 28, 1028–1039.
- Löschke, J., Güldenpfennig, M., Hann, H. P., Sawatzki, G., 1998. Die zone von badenweiler-lenzkirch (schwarzwald): Eine variskische suturzone. *Zeitschr. d. Deutsch. Geol. Gesellschaft* 149 (2), 197–212.
- Lutz, H., 1984a. Beitrag zur kenntnis der unteroligozänen insektenfauna von ceresté (süd-frankreich). *Documenta naturae* 21, 1–26.
- Lutz, H., 1985a. Eine fossile stechmücke aus dem unter-oligozän von céreste, frankreich (diptera: Culicidae). *Paläont. Z.* 59 (3/4), 269–275.
- Lutz, H., 1985b. Eine fossile stielaugenfliege aus dem unter-oligozän von chéreste, frankreich (diptera: Diopsidae). *Paläont. Z.* 59 (1/2), 75–78.
- Lutz, H., 1990. Systematische und palökologische untersuchungen an insekten aus dem mittel-eozän der grube messel bei darmstadt. *Courier Forsch.-Inst. Senckenberg* 124, 1–159.
- Lutz, H., 1996. Die fossile insektenfauna von rott. In: Koenigswald, W. (Ed.), *Fossilagerstätte Rott bei Hennef am Siebengebirge*. Rheinlandia, Siegburg, pp. 41–56.
- Lutz, H., 1997. Taphozönosen terrestrischer insekten in aquatischen sedimenten - ein beitrag zur rekonstruktion des paläoenvironments. *N. Jb. Geol. Paläont. Abh.* 203 (2), 173–210.
- Lutz, H., Uwe, K., 2006. A dynamic modell for the lake eckfeld maar (middle eocene, germany). *Z. dt. Ges. Geowiss.* 157 (3), 433–450.

- Lutz, M., Cleintuar, M., 1999. Geological results of a hydrocarbon exploration campaign in the southern upper rhine graben. *Bull. appl. Geol.* 4, 3–80.
- MacGillivray, A., 1906. A study on the wings of the tenthredinoidea, a superfamily of hymenoptera. *Proc US Nat Mus* 29 (1438), 569–654.
- Magyar, I., 2002. Palaecological study of lake pannon, a long-lived brackish lake from the neogene of the parathetys. In: Berger, J.-P. (Ed.), *Workshop on Freshwater and Brackish (Paleo) Ecosystems*. Fribourg, pp. 42–52.
- Mai, D., 1995. *Tertiäre Vegetationsgeschichte Europas*. G. Fischer, Jena, Germany.
- Maikovsky, V., 1941. Contribution à l'étude paléontologique et stratigraphique du bassin potassique d'alsace. Ph.D. thesis, Faculté des Sciences de l'Université de Strasbourg.
- Manz, O., 1934. Die ur-aare als oberlauf und gestalterin der pliozänen oberen donau (teil 1). *Hohenzoller Jh* 1, 113–160.
- Martini, E., 1972. Die gattung eosphäroma (isopoda) im europäischen alttertiär. *Senckenbergiana lethaea* 53 (1/2), 65–79.
- Martini, E., 1995. Kalkiges nannoplankton aus dem unter-oligozän von morvillars, territoire de belfort, frankreich. *Jber. Mitt. oerrh. geol. Ver.* NF77, 265–269.
- Martini, E., Radtke, G., 2007. Die bohrung wallau im nordöstlicher mainzer becken (rotliegend, pechelbronn-gruppe, bodenheim formation) einföhrung und synthèse. *Geol. Abh. Hessen* 116, 7–36.
- Martínez-Delclós, X., Martinell, J., 1993. Insect taphonomy experiments. their application to the creataceous outcrops of lithographic limestones from spain. *Kaupia* 2, 133–144.
- Maurin, J.-C., 1995. Drapage et décollement des séries jurassiques sur la faille de détachement majeure du rift rhénan sud: implications sur la géometrie des dépôts syn-rifts oligocènes. *C.R. Acad. Sci. Paris* 321 (11), 1025–1032.
- McAllister, 1984. Osmeridae. In: Whitehead, P. P., Bauchot, M.-L., Hureau, J.-C., Nielsen, J., Tortonese, E. (Eds.), *Fishes of the North-eastern Atlantic and the Mediterranean*. UNESCO, Paris, pp. 399–403.
- McKenzie, D. P., 1978. Some remarks on the developement of sedimentary basins. *Earth and Planetary Science Letters* 40, 25–32.
- Meier, L., Eisenbacher, G. H., 1991. Crustal kinematics and deep structure of the northern rhine graben, germany. *Tectonics* 10 (3), 621–630.

- Meissner, R., Berckhemer, H., Wilde, R., Poursadeg, M., 1970. Interpretation of seismic refraction measurements in the northern part of the rhinegraben. In: Illies, J. H., Mueller, S. (Eds.), Graben Problems. Proceedings of an International Rift Symposium held in Karlsruhe 1968, International Upper Mantle Project. E. Schweitzerbart'sche, Stuttgart, pp. 184–189.
- Meissner, R., Kern, H., 2008. Earthquakes and strength in the laminated lower crust - can they be explained by the "corset model"? *Tectonophysics* 448 (49–59).
- Mengel, K., 1992. Evidence from xenoliths for the composition of the lithosphere. In: Blundell, D., Freeman, R., Mueller, S. (Eds.), A continent revealed - the European geotraverse. University Press, Cambridge, pp. 91–101.
- Merle, O., 2001. The formation of the west european rift: A new model as exemplified by the massiv central area. *Bull Soc géol France* 172 (2), 213–221.
- Merz-Preiss, M., Riding, R., 1999. Cyanobacterial tufa calcification in two fresh-water streams: ambient; chemical treshholds and biological processes. *Sedimentary Geology* 126 (103–124).
- Metz, R., 1970. Dehnungsstrukturen im grundgebirge des schwarzwalds vor beginn der grabentektonik. In: Illies, J., Mueller, S. (Eds.), Graben Problems. Proceedings of an International Rift Symposium held in Karlsruhe 1968, International Upper Mantle Project. E. Schweitzerbart'sche, Stuttgart, pp. 79–86.
- Meyer, H. W., 2003. The fossils of Florissant. Smithsonian Books, Washington.
- Michon, L., Merle, O., 2000. Crustal structures of the rhinegraben and the massiv central grabens: An experimental approach. *Tectonics* 19 (5), 896–904.
- Michon, L., Merle, O., 2001. The evolution of the massiv central rift: spatio-temporal distribution of the volcanism. *Bull Soc géol France* 172 (2), 201–211.
- Michon, L., Merle, O., 2005. Discussion on "evolution of the european cenozoic rift system: interaction of the alpine and pyrenean orogens with their foreland lithosphere". *Tectonophysics* 401, 251–256.
- Michon, L., Van Balen, R., Merle, O., Pagnier, H., 2003. The cenozoic evolution of the roer valley rift system integrated at a european scale. *Tectonophysics* 367, 101–126.
- Mieg, M., Bleicher, G., Fliche, P., 1892. Note complémentaire sur le gisement de roppenzwiller et le gisement à insectes et à plantes de kleinkembs. *Bull. Soc. géol. France* 20, 375–385.
- Moore, L., Burne, R., 1994. The modern thrombolites of lake cliffton, western australia. In: Monty, C., Bertrand-Sarfati, J. (Eds.), Phanerozoic Stromatolites. Vol. 2. Kluwer Academic Publishers, Dordrecht, Boston, London, pp. 3–29.

- Mueller, S., 1977. A new model of the continental crust. In: Heacock, J. G. (Ed.), *Geophysical Monograph*. Vol. 20. Amer. Geophys. Union, Washington, pp. 289–317.
- Mueller, W., Naef, H., Graf, H., 2002. Geologische entwicklung der nordschweiz, neotektonik und langzeitszenarien zürcher weinland. In: NAGRA (Ed.), *Technischer Bericht*, 99-08. NAGRA, Wettingen, p. 237.
- Nel, A., 1991. *Analyses d'entomofaunes cenoziques : intérêts de la paléontologie pour les sciences de la terre et de la vie.* unpublished thesis, Univ. Paris.
- Nel, A., 1997. The probabilistic inference of unknown data in phylogenetic analysis. In: Grancolas, P. (Ed.), *The origin of Biodiversity in insects: phylogenetic tests on evolutionary scenarios*. *Mém. Mus. natl Hist. Nat.* 173, p. 305–327.
- Nel, A., Nel, J., Balme, C., 1993. Un nouveau lépidoptère satyrinae fossile de l'Éoligocène du sud-est de la France (insecta, lepidoptera, nymphalidae). *Linn. Belg* 14 (1), 20–36.
- Neugebauer, H., 1978. Crustal doming and mechanisms of rifting: Part 1. rift formation. *Tectonophysics* 45, 159–186.
- Paul, W., 1955. Zur morphogenese des schwarzwalds. *Jh. geol. Landesamt Baden-Württemberg* 1, 395–427.
- Pawlowski, J., Holzmann, M., 2002. Molecular phylogeny of foraminifera - a review. *Erop. J. Protistol.* 38, 1–10.
- Pflug, R., 1982. *Bau und Entwicklung des Oberrheingrabens*. Wissenschaftl. Buchges, Darmstadt.
- Pfretzschner, H. U., 1998. Ein weiteres exemplar von *lethe? corbieri* nel 1993 (lepidoptera, satyridae) aus dem unter-oligozän von céreste (süd-frankreich). *Paläont. Z.* 72 (1-2), 56–64.
- Pirkenseer, C., 2007. *The southern upper rhine graben paleogene: Microfossil assemblages (focus on ostracoda and foraminifera) and their palaeoecologic, biostratigraphic and palaeogeographic implications in reference to reworked planktonic foraminifera*. Phd-thesis, Université.
- Plenefisch, T., Bonjer, K.-P., 1997. The stress field in the rhine graben area inferred from earthquake focal mechanisms and estimations of frictional parameters. *Tectonophysics* 275, 71–97.
- Prezant, R. S., Chalermwat, K., 1984. Flotation of the bivalve *corbicula fuminea* as a means of dispersal. *Science* 225, 1492–1493.
- Prodehl, C., Mueller, S., Haak, V., 1995. The european cenozoic rift system. In: Olsen, K. (Ed.), *Continental Rifts: Evolution, Structure, Tectonics*. *Developments in Geotectonics* 25. Elsevier, Amsterdam, pp. 133–212.

- Prothero, D. R., 1994. The Eocene–Oligocene Transition. Columbia University press, New York.
- Rasnitsyn, A. P., Martínez-Delclòs, X., 2000. Wasps (insecta: Vespida = hymenoptera) from the early cretaceous of spain. *Acta Geol Hist* 35, 65–95.
- Rasnitsyn, A. P., Quicke, D. L. J., 2002. History of insects. Kluwer Academic Publisher, Dordrecht, The Netherlands.
- Rauscher, M., Schuler, M., Sittler, C., 1988. Les dinokystes dans le paléogène d'alsace: le problème de l'origine du sel. *C. R. Acad. Sci. Paris II* (307), 175–178.
- Reichenbacher, B., 2000. Das brackisch lakustrine oligozän und untermiozän im mainzer becken und hanauer becken: Fischfaunen, paläoökologie, biostratigraphie, paläogeographie. *Courier Forschung Senkenberg* 222 (1-143).
- Rochy, J.-M., 1997. Continental rift system of western europe: Location of basins, paleogeographic and structural framework, and the distribution of evaporites. In: Busson, G., Schreiber, B. C. (Eds.), *Sedimentary Deposition in Rift and Foreland Basins of France and Spain (Palaeogene and Lower Neogene)*. Columbia University Press, New York, pp. 45–94.
- Roll, A., 1979. Versuch einer volumenbilanz des oberrheintalgrabens und seiner schultern. *Geol. Jb.* A52, 3–82.
- Rollier, L., 1911. Revision de la stratigraphie et de la tectonique de la molasse au nord des alpes en général et de la molasse subalpine suisse en particulier. *Neue Denkschriften d. Schweiz. Naturf. Ges.* 46 (1), Abh.
- Roth, J. L., Dilcher, D. L., 1987. Some considerations in leaf size and leaf margin analyses of fossil leaves. *Courier Forschung Senkenberg* 30, 165–171.
- Rotstein, Y., Behrmann, J., Lutz, M., Wirsing, G., Lutz, A., 2005. Tectonic implications of transpression and transtension: Upper rhine graben. *Tectonics* 24 (doi:10.1029/2005TC001797).
- Rotstein, Y., Edel, J.-B., Gabriel, G., Boulanger, D., Schaming, M., Munsch, M., 2006. Insight into the structure of the upper rhine graben and its basement from a new compilation of bouguer gravity. *Tectonophysics* 425 (55-70).
- Roussé, S., 2006. Architecture et dynamique des séries marines et continentales de l'oligocène moyen et supérieur du sud du fossé rhénan : Evolution des milieux de dépôt en contexte de rift en marge de l'avant-pays alpin. Phd-thesis, Strasbourg.
- Ruepke, L. H., Schmalholz, S. M., Schmid, D. W., Podladchikov, Y. Y., 2008. Automated thermotectonostratigraphic basin reconstruction: Viking graben case study. *AAPG Bulletin* 92 (3), 309–326.

- Rust, J., 1999. Biologie der Insekten aus dem ältesten Tertiär Nordeuropas. Habilitation, Univ. Göttingen.
- Rust, J., 2000. Fossil record of mass moth migration. *Nature* 405, 530–531.
- Schäfer, A., 2005. Klastische Sedimente: Fazies und Sequenzstratigraphie. Spektrum Verlag, München.
- Schmid, S., Fügenschuh, B., Kissling, E., Schuster, R., 2004. Tectonic map and overall architecture of the alpine orogen. *Eclogae geol. Helv.* 97, 93–117.
- Schmidt, C., Braun, L., Paltzer, G., Mühlberg, M., Christ, P., Jacob, F., 1924. Bohrungen von Buix bei Pruntrut und Allschwil bei Basel. Beiträge zur Geologie der Schweiz. Geotechnische Serie, X. Lieferung, 74.
- Schmidt-Kittler, N., 1987. International symposium on mammalian biostratigraphy and palaeoecology of the European Paleogene. *Münchener Geowiss. Abh.* 10, 312pp.
- Schmidt-Kittler, N., Storch, G., 1985. Ein vollständiges Theridomyiden-Skelett (Mammalia: Rodentia) mit Rennmaus-Anpassungen aus dem Oligozän von Céreste, Frankreich. *Senckenb. Lethaea* 66 (1/2), 89–109.
- Schnarrenberger, C., 1925. Kalisalz und Erdöl im Rheintal. Niederschrift über die Versammlung der Direktoren der geol. L.-Anst. d. Deutsch. Reiches u. Deutsch-Österreichs. Preuss. geol. L.-Anst., Berlin.
- Schreiner, A., 1977. Tertiär. In: Baden-Württemberg, G. L. (Ed.), Erläuterungen zur Geologischen Karte von Freiburg und Umgebung (1:50000). Landesvermessungsamt Baden-Württemberg, Stuttgart, pp. 133–153.
- Schuler, M., 1990. Environments et Paléoclimats Paléogènes: Palynologie et biostratigraphie de l'Eocène et l'Oligocène inférieur dans les Fossés Rhénan, Rhodanien et de Hesse. Document du BRGM n° 190. BRGM, Orleans.
- Schulmeister, S., 2003a. Review of morphological evidence on the phylogeny of basal Hymenoptera (Insecta), with a discussion of the ordering of characters. *Biol J Linn Soc* 79, 209–243.
- Schulmeister, S., 2003b. Genitalia and terminal abdominal segments of male basal Hymenoptera (Insecta): morphology and evolution. *Org Divers Evol* 3 (4), 253–279.
- Schumacher, M. E., 2002. Upper Rhine Graben: Role of preexisting structures during rift evolution. *Tectonics* 21(1), 6–16–17.
- Schwarz, M., Henk, A., 2005. Evolution and structure of the Upper Rhine Graben: insights from three-dimensional thermomechanical modelling. *International Journal of Earth Science*, 44.

- Sissingh, W., 1998. Comparative tertiary stratigraphy of the rhine graben, bresse graben and molasse basin: correlation of alpine foreland events. *Tectonophysics* 300, 249–284.
- Sissingh, W., 2006. Kinematic sequence stratigraphy of the european cenozoic rift system and alpine foreland basin: correlation with mediterranean and atlantic plate-boundary events. *Netherlands J. Geosci.* 85, 77–129.
- Sittler, C., 1969. Le fossé rhénan en alsace. aspect structural et histoire géologique. *Revue de Géographie physique et de Géologie dynamique* (2) 11 (5), 465–494.
- Stehlin, H. G., 1909. Remarques sur les faunules de mammifères des couches éocènes et oligocènes du bassin de paris. *Bull Soc géol France* 9, 488–520.
- Storni, A., 2002. Etude paléontologique et sédimentologique de la carrière d’altkirch (alsace, paléogène). Diploma-thesis, Fribourg.
- Stucky, A., 2005. Der melanienkalk im südlichen oberrheingraben: Sedimentationsdynamik pedogenetisch alterierter karbonate (tagolsheim, elsass). Diplomarbeit, unpubliziert., Universität Basel.
- Sturmfels, E., 1943. Das kalisalzager von buggingen (südbaden). *N. jhrb. Miner. Geol. Paleont. Abh.* A78, 131–216.
- Stüwe, K., 2007. *Geodynamics of the Lithosphere*. Springer Verlag.
- Talbot, M. R., Allen, P. A., 1998. Lakes. In: *Sedimentary Environments: Processes, Fazies and Stratigraphy*. Blackwell Science.
- Tappan, H., 1980. *The Paleobiology of Plant Protists*. W.H. Freeman and Co.
- Tesauro, M., K., K. M., A.P.L., C. S., 2009b. A new thermal and rheological model of the european lithosphere. *Tectonophysics* 476, 478–495.
- Tesauro, M., K., K. M., Cloetingh, S. A., 2009a. How rigid is europe’s lithosphere. *Geophys. Res. Lett.* 36 (L16303), doi:10.1029/2009GL039229.
- Théobald, N., 1937. Les insectes fossiles des terrains oligocènes de france. Ph.D. thesis, Université Nancy.
- Timar-Geng, Z., Fügenschuh, B., Wetzel, A., Dresmann, H., 2006. Low-temperature thermochronology of the flanks of the southern upper rhine graben. *International Journal of Earth Sciences* 95, 685–702.
- Tischlinger, H., 2001. Bemerkungen zur insekten taphonomie der solnhoener plattenkalke. *Archaeopterix* 19, 29–44.
- Todorov, I., Schegg, R., Wildi, W., 1993. Thermal maturity and modelling of mesozoic and cenozoic sediments in the south of the rhine graben and the eastern jura (switzerland). *Eclogae Geologicae Helvetiae* 86, 667–692.

- Turcotte, D., Schubert, G., 2002. Geodynamics, second edition Edition. Cambridge University Press, Cambridge.
- Ustaszewski, K., 2004. Reactivation of pre-existing crustal discontinuities: the southern upper rhine graben and the northern jura mountains - a natural laboratory. Phd, University of Basel.
- Ustaszewski, K., Schumacher, M., Schmid, S., Nieuwland, D., 2005b. Fault reactivation in brittle-viscous wrench systems - dynamically scaled analogue models and application to the rhine-bresse transfer zone. *Quaternary Science Reviews* 24, 363–380.
- Ustaszewski, K., Schumacher, M. E., Schmid, S. M., 2005a. Simultaneous normal faulting and extensional flexuring during rifting: an example from the southernmost upper rhine graben. *International Journal of Earth Sciences* 94 (4), 680–696, DOI: 10.1007/s00531-004-0454-z.
- Vilhelmsen, L., 2001. Phylogeny and classification of the extant basal lineages of the hymenoptera. *Zool J Linn Soc* 131, 393–442.
- Villemin, T., Alvarez, F., Angelier, J., 1986. The rhinegraben: Extension, subsidence and shoulder uplift. *Tectonophysics* 128, 47–59.
- Villinger, E., 1999. Freiburg im breisgau- geologie und stadtgeschichte. *LGRB Info*. 12, 8–13.
- Von Eller, J.-P., Sittler, C., 1974. Les vosges et la fossé rhénan. In: Debelmas, J. (Ed.), *Géologie de la France Vol. 1, Vieux massifs et grand basins sédimentaires*. Doin, Paris, pp. 63–104.
- Vonderschmitt, L., 1942. Die geologischen ergebnisse der bohrungen von hirtzbach bei altkirch (ober-elsass). *Eclogae Geologicae Helvetiae* 35 (1), 67–99.
- Wagner, W., 1924. Woher und wann trat das tertiärmeer zum erstenmal in die rheintalsenke ein. *Notizblatt des Vereins für Erdkunde und der Hessischen geologischen Landesanstalt zu Darmstadt für das Jahr 1924* 5 (7), 56–89.
- Wagner, W., 1938. Das unteroligozän (sannoisien) im rheinalgraben unter berücksichtigung seiner lagerstätten. *Notizbl. d. Hess. Geol. Landesanstalt* 5 (19), 120–149.
- Wappler, T., 2003a. Die insekten aus dem mittel-eozän des eckfelder maares, vulkaneifel. *Mainzer Naturwissenschaftliches Archiv* 27, 1–234.
- Wappler, T., 2003b. Systematik, phylogenie, taphonomie und paläoökologie der insekten aus dem middle-eozän des eckfelder maares, vulkaneifel. *Clausthaler Geowiss* 2, 1–241.

- Wappler, T., 2004. The first lace bug (insecta: Heteroptera: Tingidae) from the lower oligocene deposits near céreste, france. *N Jahrb Geol Paläont Mh* 5, 277–287.
- Wappler, T., Hinsken, S., Brocks, J. J., Wetzel, A., Meyer, C. A., 2005. A fossil sawfly of the genus *athalia* (hymenoptera: Tenthredinidae) from the eocene - oligocene boundary of altkirch, france. *C. R. Palevol* 4, 7–16.
- Ward, J. V., 1991. *Aquatic Insect Ecology, Part I, Biology and Habitat*. John Wiley and Sons.
- Wenzel, F., Brun, J. P., group, E.-D. w., 1991. A deep reflection seismic line across the northern rhine graben. *Earth and Planetary Science Letters* 104, 140–150.
- Wernicke, B., 1985. Uniform sense normal simple shear of the continental lithosphere. *Canadian Journ. earth Sci.* 22 (108-125).
- Wetzel, A., 1991. Stratification in black shales: Depositional models and timing - an overview. In: Einsele, G., Ricken, W., Seilacher, A. (Eds.), *Cycles and Events in Stratigraphy*. Springer Verlag, pp. 508–523.
- Wetzel, A., Allenbach, R., Allia, V., 2003. Reactivated basement structures affecting the sedimentary facies in a tectonically "quiescent" epicontinental basin: an example from nw switzerland. *Sedimentary Geology* 157, 153–172.
- Wilson, M. V. H., 1980. Eocene lake environments: depth and distance-from-shore variations in fish, insect, and plant assemblages. *Palaeogeography, Palaeoclimatology, Palaeoecology* 32 (21-44).
- Wilson, M. V. H., 1982. Early cenozoic insects: paleoenvironmental biases and evolution of the north american insect fauna. *Proceedings of the 3rd North American Paleontological Convention* 2, 585–588.
- Wilson, M. V. H., 1988a. Reconstruction of ancient lake environments using both autochthonous and allochthonous fossils. *Palaeogeography, Palaeoclimatology, Palaeoecology*, 62, 609–623.
- Wilson, M. V. H., 1988b. Taphonomic processes: Information loss and information gain. *Geoscience for Canada* 15, 131–148.
- Wimmenauer, W., 1977. Junger vulkanismus. In: Baden-Württemberg, G. L. (Ed.), *Erläuterungen zur Geologischen Karte von Freiburg und Umgebung (1:50000)*. Landesvermessungsamt Baden-Württemberg, Stuttgart, pp. 133–153.
- Wirsing, G., Luz, A., Engesser, W., Koch, A., 2007. Hochauflösende reflexionssismik auf dem rhein und rheinseitenkanal zwischen mannheim und rheinfeldern. *Regierungspräsidium Freiburg. LGRB-Fachbericht* 1/07, 1–60.

- Wirth, R., 1962. Die erdöllagerstätten badens. Abh. geol. L.-Amt Baden Württ. 4, 63–80.
- Wittenberg, A., Vellmer, C., Kern, H., Mengel, K., 2000. The variscan lower continental crust: evidence for crustal delamination from geochemical and petrological investigations. In: Franke, W., Haak, V., Oncken, O., Tanner, D. (Eds.), *Orogenic Processes: Quantification and Modelling in the Variscan Belt*. Vol. 179. Geol. Soc., London, Spec. Publs, pp. 401–414.
- Wittmann, O., 1952. Erläuterungen zu Blatt Lörrach und Blatt Weil. Kommissionsverlag von Herder u. CO, Feriburg Brsg.
- Wolfe, J. A., 1992. Climatic, floristic, and vegetational changes near the eocene/oligocene boundary in north america. In: Prothero, D. R., Berggren, W. A. (Eds.), *Eocene–Oligocene climatic and biotic evolution*. University press, Princeton, p. 421–436.
- Woodward, N. B., Boyer, S. E., Suppe, J. (Eds.), 1987. *Balanced Geological Cross-Sections: An Essential Technique in Geological Research and Exploration*. Vol. 6 of Short Course in Geology. American Geophysical Union.
- Wright, V. P., Platt, N. H., 1995. Seasonal wetland carbonate sequences and dynamic catenas: a re-appraisal of palustrine limestones. *Sedimentary Geology* 99 (2), 65–71.
- Zeis, S., Gajewski, D., Prodehl, C., 1990. Crustal structure of southern germany from seismic refraction data. *Tectonophysics* 176, 59–86.
- Zhelochovtzev, A. N., Rasnitsyn, A. P., 1972. On some tertiary sawflies (hymenoptera, symphyta) from colorado. *Psyche* 79, 315–327.
- Ziegler, P., 1994. Cenozoic rift system of western and central europe an overview. *Geologie en Mijnbouw* 73, 99–127.
- Ziegler, P., Bertotti, G., Coething, S., 2002. Dynamic processes controlling foreland development: the role of mechanical (de)coupling of orogenic wedges and forelands. In: Bertotti, G., Schulmann, K., Cloetingh, S. (Eds.), *Continental Collision and the Tectono-Sedimentary Evolution of Forelands*. Vol. 1. Europ. Geophys. Soc. Stephan Mueller Spec. Publ., pp. 29–91.
- Ziegler, P., Cloetingh, S., 2004a. Dynamic processes controlling evolution of rifted basins. *Earth-Sci. Reviews* 64, 1–50.
- Ziegler, P., Dèzes, P., 2005. Evolution of the lithosphere in the area of the rhine rift system. *Int. J. Earth Sci.* 94, 594–614.
- Ziegler, P., Dèzes, P., 2006. Crustal evolution of western and central europe. In: Gee, D. G., Stephenson, R. A. (Eds.), *European Lithosphere Dynamics*. Vol. 32. Geological Society (Memoirs), London, pp. 43–56.

- Ziegler, P., Fraefel, M., 2009. Response of drainage systems to neogene evolution of the jura fold-thrust belt and upper rhine graben. *Swiss J. Earth Sci* 102, 57–75.
- Ziegler, P., Schumacher, M., Dèzes, P., Van Wees, J.-D., Cloetingh, S., 2004b. Post-variscan evolution of the lithosphere in the rhine graben area: constraints from subsidence modeling. In: Wilson, M., Neumann, E.-R., Davies, G., Timmerman, M., Heeremans, M., Larsen, B. (Eds.), *Permo-Carboniferous Magmatism and Rifting in Europe*. Vol. 223. Geol. Soc., London, Spec. Publ., pp. 289–317.
- Ziegler, P. A., 1990. *Geological Atlas of Western and Central Europe*. Shell Internationale Petroleum Maatschappij B.V. Den Haag, Geological Society Publishing House, Bath.
- Ziegler, P. A., 1992. European cenozoic rift system. *Tectonophysics* 208, 91–111.
- Ziegler, P. A., Dèzes, P., 2007. Cenozoic uplift of the variscan massifs in the alpine foreland: Timing and controlling mechanisms. *Global and Planetary Change* 58, 237–269.
- Ziegler, P. A., Fraeffel, M., 2008subm. Response of drainage systems to neogene evolution of the jura fold and thrust belt and the urg. *Swiss journ. of earth Sci*.

Curriculum Vitae

Name: Sebastian Hinsken

Date of birth: March 11th 1977

Place of birth: Lörrach (Germany)

Citizenship: German

December 2003 - 2008 PhD in Earth Sciences (Geology) at the University of Basel Supervised by: Prof, Dr. A. Wetzel

October 1998 - December 2003 Diploma of Earth Sciences at the University of Basel; Diplomathesis: Geologische Untersuchungen an syn-rift Sedimenten des südlichen Oberrheingrabens. Geologische Kartierung am südwestlichen Schwarzwaldrand, zwischen Kandern, Sitzenkirch und der Scheideckhöhe. Supervised by: Prof, Dr. A. Wetzel and PD. Dr. C. Meyer. Subsidiary subject: Geophysics at the ETH-Zürich.

December 1997- October 1998 Jobbing and traveling in Asia and Scandinavia.

October 1996 - December 1997 Alternative service in Hospital (Kreiskrankenhaus Husum/ Nordfriesland).

July 1996 Allgemeine Hochschulreife (Abitur), Ernährungswissenschaftliches Gymnasium Lörrach. Main subjects: Organic chemistry and dietetics, biology